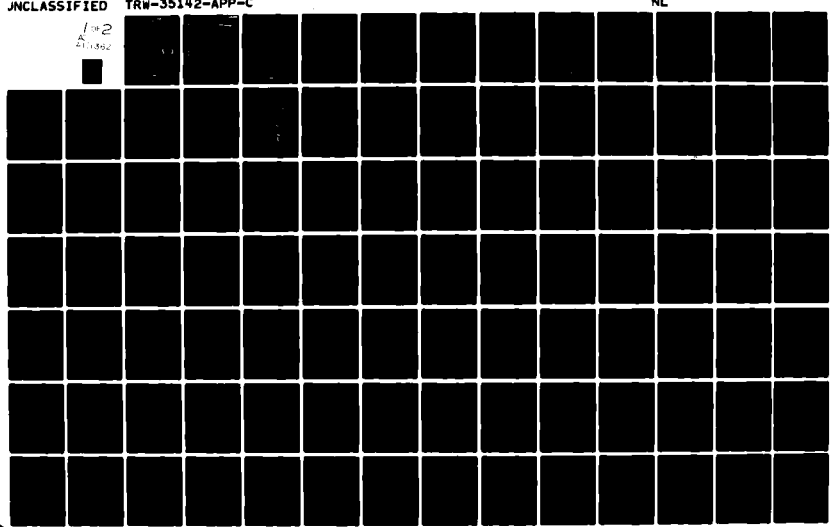


AD-A101 362 TRW DEFENSE AND SPACE SYSTEMS GROUP REDONDO BEACH CA F/G 17/2.1
EVALUATION OF DCS III TRANSMISSION ALTERNATIVES. PHASE 1A REPORT--ETC(U)
MAY 80 T M CHU DCA100-79-C-0044
JNCLASSIFIED TRW-35142-APP-C NL

1-12
L11392



AD A101362

AP 101361

(12)

LEVEL II

EVALUATION OF DCS III
TRANSMISSION ALTERNATIVES
PHASE 1A REPORT

APPENDIX C
REGIONAL CONSIDERATIONS
AND CHARACTERIZATION

26 MAY 1980

DTIC
ELECTED
S JUL 14 1981 D
B

Prepared for
Defense Communications Agency
Defense Communications Engineering Center
Reston, Virginia 22090

Contract No. DCA 100-79-C-0044

DISTRIBUTION STATEMENT A

Approved for public release;
Distribution Unlimited

TRW
DEFENSE AND SPACE SYSTEMS GROUP

ONE SPACE PARK . REDONDO BEACH, CALIFORNIA 90278

81608081

+ DMIC FILE COPY

UNCLASSIFIED

SECURITY CLASSIFICATION OF THIS PAGE (When Data Entered)

(2) Final Report

14. REPORT DOCUMENTATION PAGE		READ INSTRUCTIONS BEFORE COMPLETING FORM
1. REPORT NUMBER TRW 35142 APT-C	2. GOVT ACCESSION NO. AD-A101 362	3. RECIPIENT'S CATALOG NUMBER [REDACTED]
4. TITLE (and Subtitle) EVALUATION OF DCS III TRANSMISSION ALTERNATIVES - PHASE 1A REPORT Regional Considerations and Characteristics		5. TYPE OF REPORT & PERIOD COVERED Final Phase 1A Report
6. AUTHOR(S) T. M. Chu		7. PERFORMING ORG. REPORT NUMBER [REDACTED]
8. CONTRACT OR GRANT NUMBER(s) DCA 100-79-C-0044		
9. PERFORMING ORGANIZATION NAME AND ADDRESS TRW, Inc.; Defense and Space Systems Group One Space Park Redondo Beach, CA 90278		10. PROGRAM ELEMENT, PROJECT, TASK AREA & WORK UNIT NUMBERS N/A
11. CONTROLLING OFFICE NAME AND ADDRESS Defense Communications Engineering Center Transmission Engineering Division, R200 1860 Wiehle Ave., Reston, VA 22090		12. REPORT DATE 26 May 1980
13. MONITORING AGENCY NAME & ADDRESS (if different from Controlling Office) N/A		14. NUMBER OF PAGES 1044
		15. SECURITY CLASS. (of this report) Unclassified
		15a. DECLASSIFICATION/DOWNGRADING SCHEDULE N/A
16. DISTRIBUTION STATEMENT (of this Report) Approved for public release; distribution unlimited		
17. DISTRIBUTION STATEMENT (of the abstract entered in Block 20, if different from Report) N/A		
18. SUPPLEMENTARY NOTES Four Volumes: Main and Appendixes A, B, and C.		
19. KEY WORDS (Continue on reverse side if necessary and identify by block number) Defense Communications System EHF Satellite System Digital Transmission System Airborne Relay Platform Millimeter Wave LOS System Cable/Optical Fiber System		
20. ABSTRACT (Continue on reverse side if necessary and identify by block number) This report covers DCS III requirements, transmission media characteristics, regulatory factors, and DCS III transmission system alternatives. Appendix A documents results of transmission-media investigations. Appendix B presents a detailed review of rules, procedures, regulations, standards, and recommendations established by national/international organizations. Appendix C provides a description of topographic and climatic conditions in Germany, Turkey, and Hawaii.		

35142

EVALUATION OF DCS III TRANSMISSION ALTERNATIVES PHASE 1A REPORT

APPENDIX C REGIONAL CONSIDERATIONS AND CHARACTERIZATION

26 MAY 1980

Prepared by

T. M. Chu

Dr. T.M. Chu
Manager
DCS III Project

Approved by

N. Estersohn

N. Estersohn
Manager
Communications Architecture

Prepared for

Defense Communications Agency
Defense Communications Engineering Center
Reston, Virginia 22090

Contract No. DCA 100-79-C-0044

TRW.
DEFENSE AND SPACE SYSTEMS GROUP

ONE SPACE PARK . REDONDO BEACH, CALIFORNIA 90278

THIS PAGE INTENTIONALLY LEFT BLANK

FOREWORD AND ACKNOWLEDGEMENT

This Appendix C, Regional Considerations and Characterization, is one of the four-volume report on Evaluation of DCS III Transmission Alternatives. These four volumes are:

1. Phase IA Report, Evaluation of DCS III Transmission Alternatives
2. Appendix A, Transmission Media
3. Appendix B, Regulatory Barriers
4. Appendix C, Regional Consideration and Characterization

The three above appendices present additional information which is intentionally omitted in the main report for clarity and balance.

This Appendix C includes topographic and climatic descriptions of Turkey, West Germany, Hawaii, and seven supplements which provide additional background information.

Project work, as documented in the above noted Phase IA Report Evaluation of DCS III Transmission Alternatives and three appendices, has been performed by Defense and Space Systems Group, TRW Inc. and by TRW subcontractor, Page Communications Engineers, Inc., Northrop Corp, for the Defense Communications Engineering Center, Defense Communications Agency, under Contract No. DCA 100-79-C-0044.

This project has been managed by Dr. T. M. Chu and is supported by Messrs. G. J. Bonelle, and S. H. Cushner; Dr. T. W. Kao; Mr. S. H. Lin; Drs. A. J. Mallinckrodt, E. W. Rahneberg, and R. A. Smith; Mr. C. Y. Yoon; and by other TRW personnel on an as-required basis. Subcontracted work has been managed by Mr. J. C. Elliott and is supported by Messrs. I. Benoliel, G. Dalyai, P. Ege, R. S. Graver, and R. Sadler.

Gratefully acknowledged are the many helpful discussions, suggestions, and guidance offered by Messrs., J. R. Mensch (Current COR) and J. L. Osterholz (Previous COR) of the Defense Communications Engineering Center throughout the course of this study.

THIS PAGE INTENTIONALLY LEFT BLANK

TABLE OF CONTENTS

	<u>Page</u>
FOREWORD AND ACKNOWLEDGEMENT	
C.1 TOPOGRAPHIC AND CLIMATIC CONDITIONS OF TURKEY	C-2
C.1.1 Location and Political Boundaries	C-2
C.1.2 Population	C-2
C.1.3 Commercial Telecommunications	C-5
C.1.4 General Topographic Conditions for the Sparsely Netted DCS	C-5
C.1.5 General Climatic Conditions for the Sparsely Netted DCS	C-6
C.1.6 Natural Geographic Regions of Turkey	C-14
C.1.6.1 The Aegean Coastlands and Turkish Straits	C-14
C.1.6.2 The Black Sea Region	C-15
C.1.6.3 The Mediterranean Coastland	C-15
C.1.6.4 Anatolia	C-16
C.1.6.5 The Eastern Highlands	C-16
C.1.7 Vegetation and Soils	C-17
C.1.8 Available Topographic Maps of Turkey from the DoD . . .	C-18
C.2 TOPOGRAPHIC AND CLIMATIC CONDITIONS OF GERMANY	C-19
C.2.1 Location and Political Boundaries	C-19
C.2.2 Population Centers	C-20
C.2.3 Commercial Telecommunications	C-20
C.2.4 Natural Topographic Regions of West Germany	C-20
C.2.5 General Topographic Conditions for the Densely Netted DCS	C-24
C.2.6 General Climatic Conditions for the Densely Netted DCS	C-25
C.2.7 Available Topographic Maps of West Germany from the DoD	C-26
C.3 TOPOGRAPHIC AND CLIMATIC CONDITIONS OF HAWAII	C-26
C.3.1 Location and Distribution of the Hawaiian Islands . . .	C-29
C.3.1.1 The Leeward Islands	C-29
C.3.1.2 The Major Islands	C-30
C.3.2 Population	C-30
C.3.3 General Topographic Conditions for the Densely Netted DCS	C-30
C.3.4 General Climatic Conditions for the Densely Netted DCS	C-32
C.3.5 Available Topographic Maps of Hawaii from the DoD . . .	C-37

SUPPLEMENTS TO APPENDIX C

- | | | |
|---|--|--------|
| I | SYNOPSIS OF TOPOGRAPHIC CONSIDERATIONS FOR THE DCS (See
Supplement I for Detailed Contents) | CI-1 |
| II | SYNOPSIS OF CLIMATIC CONSIDERATIONS FOR THE DCS (See
Supplement II for Detailed Contents) | CII-1 |
| III | REPRINT OF "CUMULATIVE TIME STATICS OF SURFACE-POINT
RAINFALL RATES", RICE AND HOLMBERG, 1973 (Facsimile
Reprint) | CIII-1 |
| IV | REPRINT OF "ESTIMATING YEAR-TO-YEAR VARIABILITY OF RAINFOAL
OR MICROWAVE APPLICATIONS", DOUGHERTY AND DUTTON,
1978 (Facsimile Reprint) | CIV-1 |
| V | REPRINT OF "YEAR-TO-YEAR VARIABILITY OF RAINFALL FOR
MICROWAVE APPLICATIONS IN THE U.S.A.", DUTTON AND
DOUGHERTY, 1979 (Facsimile Reprint) | CV-1 |
| VI | REPRINT OF "PRESENT STATE AND FUTURE OF TELECOMMUNICA
TIONS IN TURKEY", BAYRAKTAR AND ABUT, 1976 (Facsimile
Reprint) | CVI-1 |
| VII | REPRINT OF "PRESENT STATE AND TRENDS OF PUBLIC COMMUNI
CATIONS IN THE FEDERAL REPUBLIC OF GERMANY", DINGELDEY,
1974 (Facsimile Reprint) | VII-1 |
| SOURCE OF FIGURES FOR APPENDIX C AND SUPPLEMENTS I AND II | | CR-1 |
| SOURCE OF TABLES FOR APPENDIX C AND SUPPLEMENTS I AND II | | CR-3 |
| BIBLIOGRAPHY FOR APPENDIX C AND SUPPLEMENTS I AND II | | CR-5 |

RE: DISTRIBUTION STATEMENT.
EVALUATION OF DCS III TRANSMISSION
ALTERNATIVES.
STATEMENT A PER JANET ORNDORF
DCA TECHNICAL LIBRARY CODE 312
WASHINGTON D. C. 20305

Accession For	
NTIS GRA&I	<input checked="" type="checkbox"/>
DTIC TAB	<input type="checkbox"/>
Unannounced	<input type="checkbox"/>
Justification	
By _____	
Distribution/	
Availability Codes	
Dist	Avail and/or Special
A	

LIST OF FIGURES

	<u>Page</u>
C-1 The Republic of Turkey	C-3
C-2 Major Geographic Features of Turkey	C-6
C-3 Mean Annual Rainfall for Turkey	C-7
C-4 West Germany with Outline of DCS Area of Interest	C-21
C-5 Rhine River with Outline of DCS Area of Interest	C-22
C-6 Major Hawaiian Islands	C-31
C-7 Sketch of Oahu	C-31
C-8 Effects of Trade Winds on a Mountain Summit	C-36
C-9 Mean Precipitation (in/yr) on Oahu	C-38

LIST OF TABLES

	<u>Page</u>
C-1 Temperature, Relative Humidity, and Precipitation Data at 17 Turkish Locations	C-8
C-2 Available Map Coverage of Turkey from the DoD	C-19
C-3 Weather Conditions in or near the DCS Area of Interest in West Germany	C-27
C-4 Available Topographic Maps of West Germany from the DoD	C-26
C-5 Average Temperatures and Honolulu	C-34
C-6 Honolulu Weather Station Locations	C-34
C-7 Precipitation (in) at Honolulu	C-38
C-8 Weather Conditions at Honolulu for 1978	C-39
C-9 Normal, Mean, and Extreme Weather Conditions at Honolulu	C-39
C-10 Available Topographic Maps of the Major Hawaiian Islands from the DoD	C-37

THIS PAGE INTENTIONALLY LEFT BLANK

APPENDIX C

REGIONAL CONSIDERATIONS AND CHARACTERIZATION

The purpose of Appendix C is to provide a description of the general topographic and climatic conditions which may affect telecommunications in the sparsely netted DCS throughout the Republic of Turkey and the densely netted DCS in parts of the Federal Republic of Germany and part of the State of Hawaii.

Various modes of radio propagation are available for use by the DCS. These modes may be characterized as:

- Line-of-sight (Includes terrestrial, referred to as LOS, and active platforms and satellites)
- Reflection (Includes passive devices such as platforms and satellites)
- Diffraction (Over smooth earth, knife-edge, rounded obstacles, and irregular terrain)
- Refraction (Ionospheric)
- Scatter (Tropospheric and Ionospheric).

Each of these propagation modes is affected differently by operating frequency, ground terrain characteristics, atmospheric structure, and weather. Therefore, topographic and climatic conditions were collected and used for alternative system designs for the various regions.

Regional considerations and characterization for each of the three regions considered, namely, Turkey, Germany and Hawaii, is presented in Sections C.1, C.2, and C.3 respectively. Supplements I and II provide a synopsis of topographic and climatic considerations which may affect radio propagation, with emphasis placed on the modes pertinent to and areas highlighted by the DCS III Study, and Supplements III through VII contain reprints of literature relevant to climatic considerations or the state of commercial telecommunication in the areas of interest mentioned above.

Sources of figures and tables, as well as a bibliographic listing of all references applicable to Appendix C and Supplements I and II thereto also are included in this document.

C.1 TOPOGRAPHIC AND CLIMATIC CONDITIONS OF TURKEY

This section provides a general description of topographic and climatic conditions of the Republic of Turkey. The information presented here was used either as basis or reference for DCS III alternative system designs.

C.1.1 Location and Political Boundaries

The Republic of Turkey is situated in the eastern Mediterranean region with a land area of about 767,000 sq. km (296,000 sq. mi.), slightly smaller than Texas and Louisiana combined. The Republic shares common borders with Bulgaria and Greece to the northwest, the U.S.S.R. and Iran to the east, and Iraq and Syria to the south. Turkey is adjacent to the Black Sea to the north, the Mediterranean Sea to the south, and the Aegean Sea to the west.

About three percent of Turkey's land is in Europe. This section, known as Thrace, is separated from the Asian portion by the Bosporus Strait, the Sea of Marmara, and the Dardanelles Strait. They are known collectively as the Turkish Straits and connect the Black and Mediterranean Seas. The Asian portion is known by a variety of names: Asia Minor, Asiatic Turkey, the Anatolian Plateau, and Anatolia.

Internally, the Republic of Turkey is divided into 67 provinces. The official designation of these divisions is "il" but the more traditional term, "vilayet", is extensively used.

Figure C-1 shows the international boundaries, major cities, railroads, roads, and international airports of the Republic of Turkey.

C.1.2 Population

Urban areas have experienced tremendous growth since 1950 as a result of the movement of villagers to the cities. Today, about 65 percent of the populace are villagers.

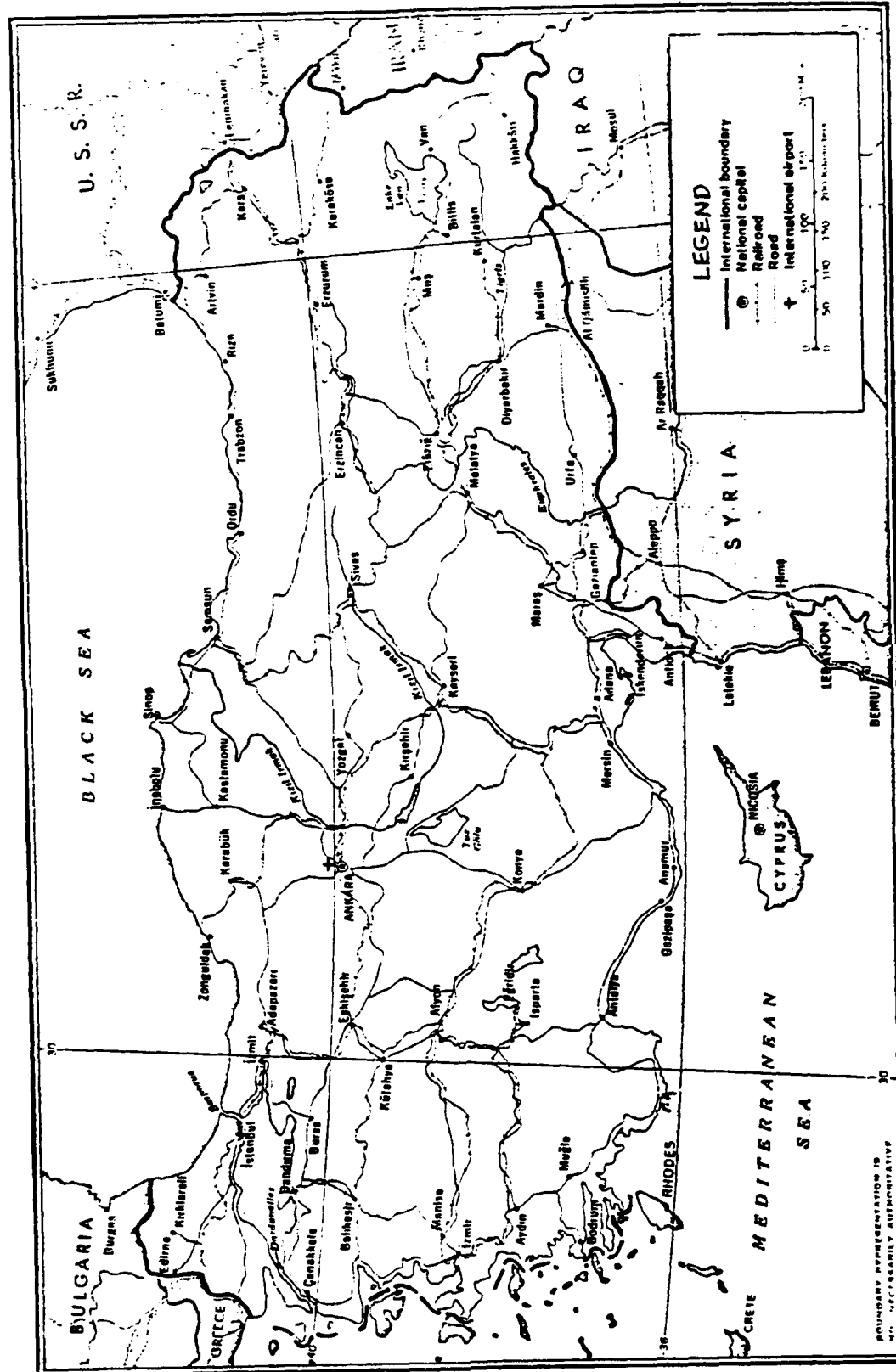


Figure C-1. The Republic of Turkey

Population is more dense along the coastal regions where climate and soil conditions are more favorable to agriculture and in the western half of the country. The most sparsely populated areas are the central highlands and the eastern and southeastern mountain regions.

In 1970, the population totaled 35.7 million with an annual growth rate of almost 2.7 percent. Based on this rate, the population is expected to double by 1995. The relatively high growth rate is reflected in the age structure with 80 percent under the age of 40 and over 40 percent under 15 years of age.

Istanbul, on the European side of the Bosphorus Strait, is the most populated city in Turkey. The capital city of Ankara, in central Turkey, has the second largest population among Turkish cities.

C.1.3 Commercial Telecommunications

Supplied in Supplement VI.

C.1.4 General Topographic Conditions for the Sparsely Netted DCS

Except for a relatively small segment along the Syrian Border, which is a continuation of the Arabian Platform, Turkey is part of the great Alpine-Himalayan mountain belt. The intensive folding and uplifting of the mountain belt during the Tertiary Period of geographic history was accompanied by strong volcanic activity and intrusions of igneous rock material, followed by extensive faulting in the Quarternary (most recent) Period. This faulting is still in progress, making Turkey one of the ranking earthquake regions of the world.

The structural complexity is reflected in relief as well as drainage. Wedged between two folded mountain ranges that converge in the east (the Pontic Mountains along the Black Sea and the Taurus Mountains bounding the Mediterranean Sea), the massif of central Turkey is structurally a very complex region composed of uplifted blocks and downfolded troughs covered by recent deposits, that give the appearance of a plateau with rough terrain.

True lowland is confined to Thrace, extending along rivers that discharge into the Aegean Sea or the Sea of Marmara, and to a few narrow coastal strips along the Black and Mediterranean Sea coasts. Moderately sloping land surface is limited almost entirely to Thrace and to the hill-land of the Arabian Platform along the border with Syria.

Over 80 percent of the Turkish land surface is rough, broken, and mountainous, and therefore of limited agricultural value. Nearly 85 percent of the country lies above 460 meters (1,500 ft.) and the median elevation is 1,130 meters (3,700 ft.). These features are augmented in the eastern part of the country where the Taurus and Pontic ranges converge into a lofty mountain region with a median elevation of over 1,525 meters (5,000 ft.), reaching its highest elevation along the border with the Soviet Union and Iran. Turkey's highest mountain peak is Mount Ararat at 6,087 meters (19,966 ft.), situated near the location where the three countries meet. Figure C-2 shows the major geographic features of Turkey.

C.1.5 General Climatic Conditions of the Sparcely Netted DCS

Turkey is a focal point of contrasting climates. The pressure systems of all the adjacent regions affect the climate of the country, yet the landforms are high enough to minimize the outside influences. The climate is continental temperate, with some Mediterranean and maritime temperate influences.

In the interior plateau, there is a wide range of temperature. Winters are cold with January temperatures averaging -1°C (30°F), and frost may occur more than 100 days during the year. Summers are warm, with high daytime temperatures and cool nights. The mean for July, the warmest month, lies between $20 - 23^{\circ}\text{C}$ ($68 - 73^{\circ}\text{F}$). Between 254 and 432 millimeters (10 and 17 in.) of rainfall are received annually on the plateau, the precise amount depending on elevation. May is generally the wettest month, and July and August are the driest months.

Figure C-2. Major Geographic Features of Turkey

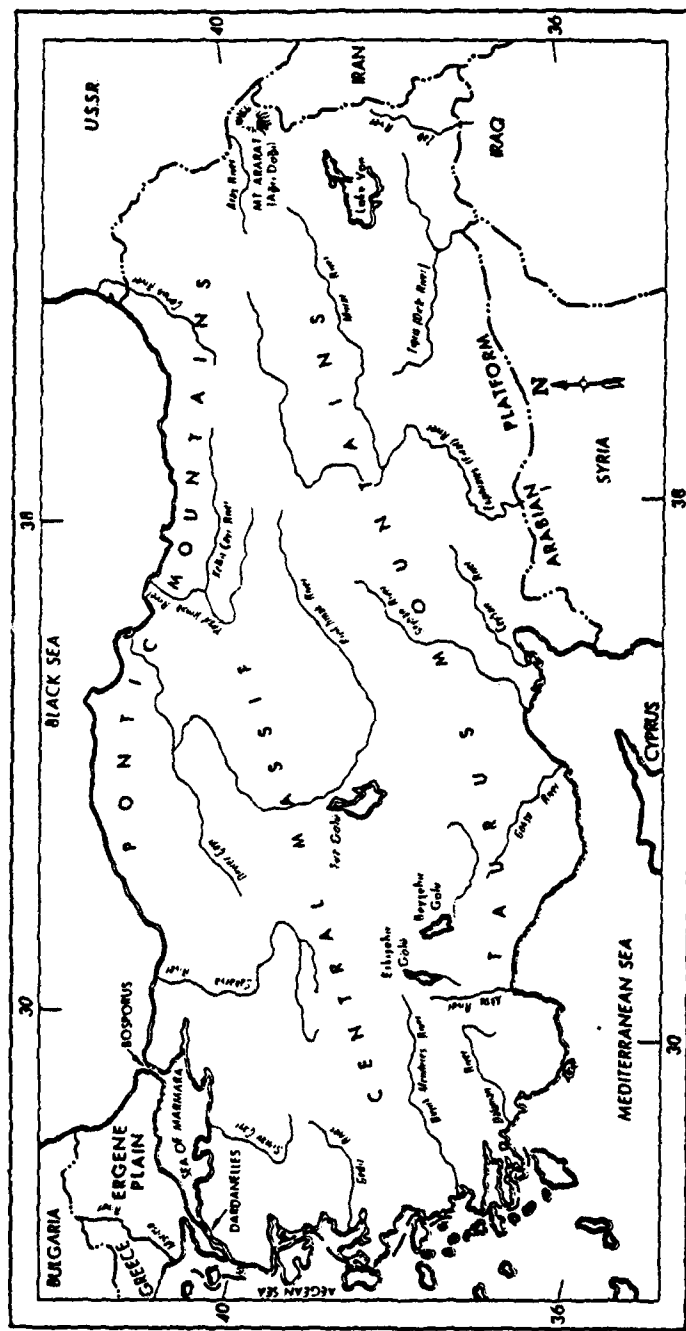


Figure C-3. Mean Annual Rainfall for Turkey

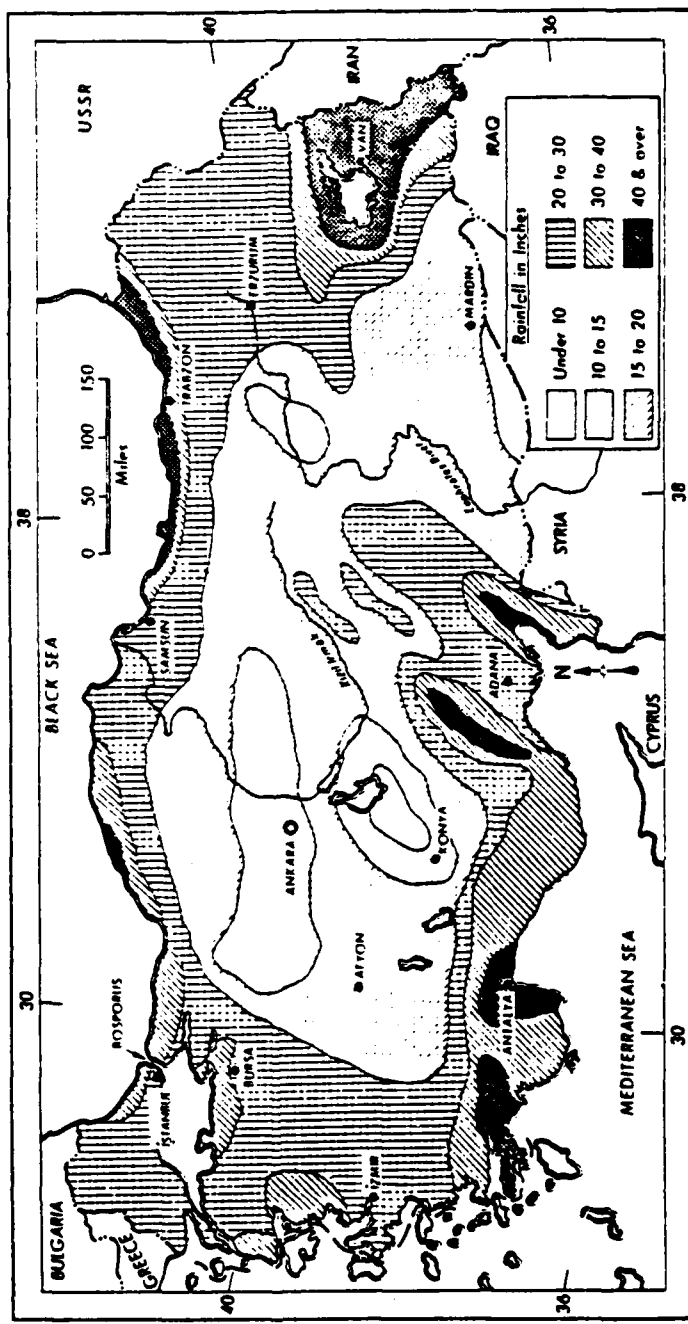


Table C-1. Temperature, Relative Humidity, and Precipitation at 17 Turkish Locations

BURSA 40°11'N, 29°05'E 528 ft

Period 1932-1949	Temperature				Relative humidity		Precipitation		
	Average daily	Average of highest each month	Average of lowest each month	Absolute	Average of observations at all hours	Average monthly fall	Maximum fall in 24 h	Average No. of days with 0.04 in or more	
	Max. Min.			Max. Min.	per cent	inches			
degrees Fahrenheit									
January	48	35	64	23	71	9	76	2.5	2.5
February	50	36	65	23	72	- 3	74	2.5	2.1
March	55	38	76	25	81	15	69	2.9	1.5
April	66	45	83	33	94	29	68	2.4	1.5
May	73	53	90	43	99	35	68	2.4	1.9
June	82	59	95	50	105	43	62	1.3	1.7
July	87	63	98	56	106	47	58	2.0	8.2
August	87	63	97	55	109	46	50	0.9	3.2
September	80	57	93	48	101	41	65	1.9	4.1
October	72	51	85	41	96	32	69	2.4	1.5
November	62	46	78	23	87	17	75	3.1	1.7
December	52	38	67	24	75	6	74	3.8	1.9
Year	68	48	100	16	108	- 3	68	20.1	8.2
No. of years	18	18	18	18	18	18	18	18	18

IZMIR (SMYRNA) 39°27'N, 27°15'E 82 ft

Period 1864-1883 1890-1918 1924-1949	Temperature				Relative humidity		Precipitation		
	Average daily	Average of highest each month	Average of lowest each month	Absolute	Average of observations at 0700 1400	Average monthly fall	Maximum fall in 24 h	Average No. of days with 0.04 in or more	
	Max. Min.			Max. Min.	per cent	inches			
degrees Fahrenheit									
January	55	39	66	28	73	12	78	4.4	3.3
February	57	40	67	28	73	12	75	3.3	3.0
March	63	43	75	32	84	19	72	3.0	2.0
April	70	49	81	38	91	30	69	1.7	3.2
May	79	56	92	47	106	37	65	1.3	1.7
June	87	63	97	55	105	50	56	0.6	1.8
July	92	69	101	61	108	52	53	0.2	1.1
August	92	69	101	61	107	53	57	0.2	1.7
September	85	62	96	53	103	42	64	0.8	3.3
October	76	55	88	45	98	31	71	2.1	9.1
November	67	49	78	37	88	19	77	3.3	3.2
December	58	42	69	21	79	20	77	4.8	4.6
Year	73	53	103	34	108	12	68	25.5	9.1
No. of years	39	39	39	39	35	39	10	28	29

USAK 38°40'N, 29°45'E 3022 ft

Period 1932-1949	Temperature				Relative humidity		Precipitation		
	Average daily	Average of highest each month	Average of lowest each month	Absolute	Average of observations at all hours	Average monthly fall	Maximum fall in 24 h	Average No. of days with 0.04 in or more	
	Max. Min.			Max. Min.	per cent	inches			
degrees Fahrenheit									
January	42	28	53	11	58	- 4	78	3.1	1.3
February	45	29	57	15	65	- 8	76	2.8	1.5
March	51	32	68	18	73	7	69	2.5	1.5
April	62	39	77	28	80	23	63	1.3	0.7
May	72	47	84	38	92	30	60	1.7	2.0
June	79	53	90	43	97	35	53	0.9	1.6
July	85	57	95	49	99	37	66	0.2	0.6
August	86	58	94	49	99	44	65	0.5	1.1
September	70	51	89	41	95	22	49	0.5	2.0
October	69	46	80	34	91	24	61	1.4	1.3
November	68	39	70	27	79	11	72	2.3	1.4
December	47	33	57	18	64	- 9	78	3.9	1.7
Year	65	43	85	8	99	- 9	63	21.1	2.0
No. of years	15	15	15	15	15	15	15	15	15

Table C-1 Temperature, Relative Humidity, and Precipitation at 17 Turkish Locations (Continued)

ADANA 36°59'N, 35°18'E 82 ft

Period 1899-1902 1908-1911 1920-1949	Temperature				Relative humidity Average of observations at 0730 and 1430 per cent	Precipitation		
	Average daily	Average of highest each month	Average of lowest each month	Absolute		Average monthly fall in 24 h	Average maximum fall in 24 h	Average No. of days with 0.04 in or more
	Max. Min.			Max. Min.		inches	inches	inches
degrees Fahrenheit								
January	57 29	65	28	72 19	70 49	4.3	6.2	8
February	59 41	69	30	76 20	70 47	4.0	2.7	7
March	66 45	78	33	87 23	67 44	2.5	3.2	6
April	74 51	87	40	93 32	72 46	1.6	2.6	5
May	83 59	96	51	106 45	72 45	2.0	2.6	4
June	89 66	100	57	109 49	74 47	0.7	1.7	2
July	93 77	99	64	106 57	74 46	0.2	1.4	0.5
August	94 72	101	66	109 59	75 44	0.2	1.2	0.7
September	91 66	98	57	106 52	70 39	0.7	2.5	1
October	84 58	95	50	107 38	64 34	1.9	2.3	4
November	73 51	85	39	94 32	62 37	2.4	3.7	5
December	61 43	71	32	80 24	69 50	3.8	4.8	7
Year	77 55	104	25	106 19	70 44	24.5	4.8	51
No. of years	21 21	23	23	23 24	5	5	31	35

ANKARA 39°57'N, 32°53'E 2825 ft

Period 1916-1949	Temperature				Relative humidity Average of observations at 0700 and 1400 per cent	Precipitation		
	Average daily	Average of highest each month	Average of lowest each month	Absolute		Average monthly fall in 24 h	Average maximum fall in 24 h	Average No. of days with 0.04 in or more
	Max. Min.			Max. Min.		inches	inches	inches
degrees Fahrenheit								
January	39 24	51	8	56 -13	85 70	1.3	0.8	8
February	42 26	54	10	64 -12	84 67	1.2	0.8	8
March	51 31	70	18	80 3	81 52	1.3	1.1	7
April	63 40	78	27	89 20	72 40	1.3	1.1	7
May	73 49	85	38	94 31	68 38	1.9	1.5	7
June	78 53	91	44	98 35	64 34	1.0	1.6	5
July	86 59	98	50	100 44	57 28	0.5	1.6	3
August	87 50	96	48	100 40	54 25	0.4	1.0	1
September	78 52	91	39	96 29	62 31	0.7	0.9	3
October	69 44	81	39	89 27	72 37	0.9	0.8	5
November	57 37	71	23	78 0	62 52	1.2	1.1	6
December	43 29	54	14	63 -13	65 71	1.9	2.7	9
Year	64 42	88	2	100 -13	72 45	13.6	2.7	68
No. of years	26 26	26	26	26 26	16	16	24	22

ANTALYA 36°53'N, 30°42'E 131 ft

Period 1931-1949	Temperature				Relative humidity Average of observations at all hours per cent	Precipitation		
	Average daily	Average of highest each month	Average of lowest each month	Absolute		Average monthly fall in 24 h	Average maximum fall in 24 h	Average No. of days with 0.04 in or more
	Max. Min.			Max. Min.		inches	inches	inches
degrees Fahrenheit								
January	59 43	65	33	69 24	70	10.2	9.2	11
February	60 44	67	35	72 24	69	8.9	3.8	9
March	64 46	73	57	81 30	65	3.1	3.1	6
April	70 52	81	43	81 38	67	3.5	3.1	4
May	78 60	91	52	102 43	68	1.3	4.7	3
June	86 67	99	59	107 53	64	0.5	2.6	1
July	93 73	106	66	110 59	60	0.1	0.7	0.2
August	92 72	104	68	108 57	61	0.1	0.3	0.4
September	87 67	98	59	109 51	59	0.6	3.5	1
October	80 59	92	51	102 46	64	2.1	3.0	4
November	71 52	82	43	97 32	68	4.7	7.2	5
December	62 46	69	36	73 29	70	10.5	11.5	11
Year	75 57	106	31	110 24	65	41.7	11.5	56
No. of years	18 19	19	19	18 19	18	21	19	19

Table C-1. Temperature, Relative Humidity, and Precipitation at
17 Turkish Locations (Continued)

ERZURUM 39°54'N, 41°16'E 6402 ft

Period 1932-1949	Temperature						Relative humidity	Precipitation		
	Average daily		Average of highest each month	Average of lowest each month	Absolute	Average of observations at 0800 1500		Average monthly fall	Maximum fall in 24 h	Average No. of days with 0.04 in or more
	Max.	Min.			Max. Min.	per cent		inches		
degrees Fahrenheit										
January	24	8	37	-11	42 -22	78 74	1-4	1-6		8
February	28	12	40	-8	49 -17	77 71	1-6	0-9		8
March	35	18	49	-1	64 -13	80 69	2-0	1-0		8
April	50	32	65	16	71 -1	75 51	2-5	1-6		10
May	62	41	73	31	78 22	71 45	3-1	0-9		11
June	70	46	80	27	86 34	66 27	2-1	1-6		9
July	78	53	87	44	93 37	58 28	1-3	1-7		5
August	80	53	88	45	93 34	60 28	0-9	1-0		4
September	72	46	83	34	89 25	66 30	1-1	1-5		4
October	59	37	71	26	79 10	71 29	2-3	1-4		8
November	45	29	59	12	68 -10	78 55	1-8	1-1		8
December	31	16	45	-2	54 -14	78 64	1-1	1-4		6
Year	53	33	89	-14	93 -22	71 40	21-2	1-7		89
No. of years	16	16	16	16	16 16	8 8	16	16		16

KARS 40°36'N, 43°05'E 5741 ft

Period 1932-1949	Temperature						Relative humidity	Precipitation		
	Average daily		Average of highest each month	Average of lowest each month	Absolute	Average of observations at 0800 1500		Average monthly fall	Maximum fall in 24 h	Average No. of days with 0.04 in or more
	Max.	Min.			Max. Min.	per cent		inches		
degrees Fahrenheit										
January	21	1	36	-22	41 -32	85	3-1	0-6		7
February	25	3	38	-20	44 -35	68	1-1	1-3		7
March	34	12	46	-11	66 -29	71	1-1	0-6		8
April	50	28	65	13	75 -9	70	1-7	1-1		9
May	63	38	74	28	80 19	69	3-4	1-8		15
June	70	43	80	34	85 30	67	2-9	1-0		12
July	77	49	87	39	94 33	63	2-1	1-6		8
August	79	49	87	40	94 33	60	2-1	2-8		7
September	71	40	83	31	90 24	61	1-2	1-1		5
October	59	32	71	20	77 1	69	1-6	0-9		7
November	44	23	59	8	70 -12	72	1-2	0-7		6
December	29	9	43	-14	52 -31	71	1-0	0-7		7
Year	52	27	89	-27	94 -35	67	20-5	2-8		98
No. of years	16	16	16	16	16 16	10	16	16		16

KASTAMONU 41°22'N, 33°46'E 2592 ft

Period 1932-1949	Temperature						Relative humidity	Precipitation		
	Average daily		Average of highest each month	Average of lowest each month	Absolute	Average of observations at 0800 1500		Average monthly fall	Maximum fall in 24 h	Average No. of days with 0.04 in or more
	Max.	Min.			Max. Min.	per cent		inches		
degrees Fahrenheit										
January	27	22	50	3	56 -16	79	1-0	0-8		6
February	42	24	51	7	63 -7	76	1-1	0-8		6
March	50	29	59	15	62 6	68	1-2	1-0		6
April	61	37	70	24	83 19	65	1-8	1-0		7
May	71	45	85	32	92 27	66	2-9	1-2		10
June	76	60	88	40	95 35	64	2-3	1-4		8
July	81	53	93	46	100 41	59	1-3	1-8		4
August	82	53	94	46	100 34	59	1-1	1-2		3
September	75	47	87	37	96 32	65	1-0	1-4		4
October	66	41	80	30	88 19	72	1-3	1-4		6
November	52	23	68	20	73 -3	80	1-3	1-3		6
December	41	26	54	9	64 -11	83	1-2	1-1		6
Year	61	38	85	0	100 -16	70	17-4	1-8		72
No. of years	16	16	16	16	16 16	16	16	16		16

Table C-1. Temperature, Relative Humidity, and Precipitation at
17 Turkish Locations (Continued)

KONYA 37°51'N 32°30'E 3363 ft

Period 1832-1949	Temperature						Relative humidity	Precipitation		
	Average daily		Average of highest each month	Average of lowest each month	Absolute	Average of observations at all hours		Average monthly fall in	Maximum fall in	Average No. of days with 0.04 in or more
	Max. Min.	Max. Min.	Max. Min.	Max. Min.	Max. Min.	per cent		inches	24 h	
degrees Fahrenheit										
January	39	23	54	6	61 -19	76	1-8	1-1	1-1	7
February	44	25	58	10	67 -9	72	1-3	2-9	1-1	6
March	52	29	69	16	78 3	62	1-1	1-3	1-1	5
April	62	38	78	26	87 20	55	1-3	1-1	1-1	5
May	72	47	85	36	93 31	53	1-4	1-3	1-3	6
June	80	53	89	43	95 35	48	0-8	1-9	0-8	3
July	86	59	95	50	100 44	41	0-3	0-7	0-7	1
August	85	58	95	48	98 41	39	0-1	0-6	0-6	1
September	78	50	89	39	95 32	47	0-5	1-2	1-2	2
October	69	42	80	30	89 17	58	1-3	2-2	2-2	4
November	56	34	71	19	78 -2	70	1-4	1-7	1-7	4
December	43	27	57	12	68 -15	78	1-6	1-1	1-1	7
Year	64	40	86	- 1	100 -19	58	12-9	2-9	2-9	50
No. of years	18	18	18	18	18 18	18	18	18	18	18

SAMSUN 41°17'N, 38°19'E 131 ft

Period 1880-1891 1911-1914 1929-1949	Temperature						Relative humidity	Precipitation		
	Average daily		Average of highest each month	Average of lowest each month	Absolute	Average of observations at all hours		Average monthly fall in	Maximum fall in	Average No. of days with 0.04 in or more
	Max. Min.	Max. Min.	Max. Min.	Max. Min.	Max. Min.	per cent		inches	24 h	
degrees Fahrenheit										
January	50	38	66	27	72 20	69	2-9	2-6	2-6	10
February	51	38	68	28	77 20	72	2-6	3-1	3-1	10
March	54	40	76	30	80 20	75	2-7	1-7	1-7	11
April	59	45	82	36	94 28	77	2-3	1-6	1-6	9
May	67	53	85	44	99 36	79	1-8	3-1	3-1	8
June	74	60	85	59	95 48	75	1-5	3-6	3-6	6
July	79	65	87	59	103 51	73	1-3	3-6	3-6	4
August	80	65	87	60	102 49	72	1-3	2-6	2-6	4
September	75	61	85	52	94 44	74	2-4	3-0	3-0	6
October	69	56	86	46	95 38	75	3-2	3-3	3-3	7
November	62	49	80	39	90 27	72	3-5	7-5	7-5	8
December	55	43	69	32	76 23	68	3-4	3-9	3-9	9
Year	65	51	83	24	103 20	73	28-1	3-9	3-9	92
No. of years	24	24	22	22	22 22	18	27	21	21	18

EDINOP 42°02'N, 35°10'E 82 ft

Period 1901-1946	Temperature						Relative humidity	Precipitation		
	Average daily		Average of highest each month	Average of lowest each month	Absolute	Average of observations at 0700 and 1300		Average monthly fall in	Maximum fall in	Average No. of days with 0.04 in or more
	Max. Min.	Max. Min.	Max. Min.	Max. Min.	Max. Min.	per cent		inches	24 h	
degrees Fahrenheit										
January	48	37	62	26	65 21	61 72	3-3	1-3	1-3	13
February	49	38	64	29	72 22	63 71	2-2	1-2	1-2	10
March	49	38	67	29	85 17	84 71	1-9	1-4	1-4	10
April	56	43	72	36	80 32	85 71	1-6	0-9	0-9	8
May	65	51	81	43	91 36	83 72	1-5	2-4	2-4	7
June	73	58	81	51	87 35	76 69	1-6	5-1	5-1	5
July	79	65	87	59	94 56	89 66	1-2	3-7	3-7	3
August	79	66	85	60	99 56	72 64	1-7	2-9	2-9	4
September	74	61	82	52	91 44	78 67	2-8	2-6	2-6	7
October	67	53	80	46	85 33	83 70	2-1	3-6	3-6	9
November	60	48	72	39	77 30	84 71	4-1	1-3	1-3	11
December	53	42	67	31	72 25	82 73	4-9	2-2	2-2	13
Year	63	50	88	24	94 17	80 70	28-1	5-1	5-1	100
No. of years	8	19	8	19	8 19	7 7	20	20	20	34

Table C-1. Temperature, Relative Humidity, and Precipitation at 17 Turkish Locations (Continued)

SIVAS 39°44'N, 38°59'E 3888 ft

Period 1932-1949	Temperature						Relative humidity Average of observations at all hours	Precipitation		
	Average daily		Average of highest each month	Average of lowest each month	Absolute	Average monthly fall		Average maximum fall in 24 h	Average No. of days with 0.04 in or more	
	Max. Min.				Max. Min.					
degrees Fahrenheit										
January	31	15	43	-8	51	-24	77	3.6	1.0	10
February	34	19	46	-2	56	-30	77	2.6	0.8	8
March	43	25	61	7	76	-11	72	2.6	0.8	8
April	58	35	73	22	78	17	64	2.0	1.5	9
May	67	42	79	31	86	22	61	2.3	1.5	9
June	74	46	86	38	94	31	57	1.2	1.3	5
July	81	50	91	42	98	37	53	0.3	0.7	1
August	82	50	93	41	97	38	52	0.7	0.4	1
September	75	44	87	33	93	27	54	0.8	1.6	3
October	65	38	77	27	84	16	62	1.6	2.1	6
November	51	33	66	16	75	-5	72	1.7	1.6	7
December	38	22	51	3	60	-22	78	1.6	1.1	9
Year	58	35	93	-15	90	-30	65	16.6	2.1	76
No. of years	18	18	18	18	18	18	18	18	18	18

TRABZON 41°00'N, 39°43'E 354 ft

Period 1880-1891 1926-1949	Temperature						Relative humidity Average of observations at all hours	Precipitation		
	Average daily		Average of highest each month	Average of lowest each month	Absolute	Average monthly fall		Average maximum fall in 24 h	Average No. of days with 0.04 in or more	
	Max. Min.				Max. Min.					
degrees Fahrenheit										
January	50	40	65	30	71	21	73	2.8	3.1	10
February	50	39	67	28	74	19	73	2.7	1.6	9
March	52	40	73	30	88	22	75	2.3	0.9	10
April	58	46	82	37	89	31	77	2.2	1.6	9
May	66	55	86	46	101	40	80	1.7	2.6	8
June	73	62	92	55	92	50	79	1.9	1.3	8
July	78	67	94	62	91	59	77	1.8	2.4	7
August	79	68	96	62	101	56	78	1.6	1.8	5
September	74	63	82	54	90	45	76	2.7	2.0	8
October	69	58	83	49	90	40	74	3.2	3.8	8
November	61	51	77	41	91	32	74	4.0	2.7	10
December	54	43	69	34	79	26	70	3.0	1.7	10
Year	64	53	92	36	101	19	73	26.9	3.8	102
No. of years	14	14	19	19	17	17	14	19	16	16

URFA 37°07'N, 38°48'E 1772 ft

Period 1932-1949	Temperature						Relative humidity Average of observations at all hours	Precipitation		
	Average daily		Average of highest each month	Average of lowest each month	Absolute	Average monthly fall		Average maximum fall in 24 h	Average No. of days with 0.04 in or more	
	Max. Min.				Max. Min.					
degrees Fahrenheit										
January	48	34	57	23	63	13	71	4.7	2.1	12
February	53	36	63	25	69	10	67	2.8	2.2	8
March	60	41	76	29	84	22	60	2.2	1.9	8
April	71	58	84	36	92	29	53	1.6	2.4	8
May	84	55	95	46	103	39	41	0.6	0.7	3
June	95	67	104	57	106	47	26	<0.1	0.3	0.4
July	102	74	109	64	115	48	26	<0.1	0.2	0.3
August	101	73	107	65	109	63	30	<0.1	<0.1	0
September	93	66	101	57	107	50	34	0.1	0.3	0.3
October	80	57	91	45	96	35	45	0.9	1.2	3
November	67	47	78	35	87	28	38	1.8	1.8	6
December	53	38	63	27	69	23	68	3.0	2.7	7
Year	76	53	100	39	115	30	49	17.3	2.7	53
No. of years	13	13	13	13	13	13	13	13	13	13

Table C-1. Temperature, Relative Humidity, and Precipitation at 17 Turkish Locations (Concluded)

VAN 38°28'N, 43°21'E 5682 ft

Period 1940-1949	Temperature						Relative humidity	Precipitation		
	Average daily Max. Min.	Average of highest each month	Average of lowest each month	Absolute	Average of observations at all hours	Average monthly fall in fall		Maximum fall in 24 h	Average No. of days with 0.04 in or more	
	degrees Fahrenheit						per cent	inches		
January	34 18	43	1	47 -11	73	2.2	1.2	9		
February	35 17	47	1	56 -9	73	1.6	1.1	6		
March	40 23	52	6	63 -4	73	2.0	0.9	9		
April	52 34	63	20	69 14	69	2.3	0.9	10		
May	65 43	77	33	80 26	60	1.4	0.9	8		
June	75 50	65	41	92 37	51	0.6	0.7	2		
July	83 57	91	49	93 45	45	0.2	0.7	1		
August	83 57	91	48	95 41	41	0.1	0.3	1		
September	76 49	87	42	81 39	43	0.3	0.7	1		
October	62 41	75	28	82 7	61	2.0	1.4	7		
November	52 33	61	22	67 3	69	1.5	1.5	7		
December	38 22	49	5	55 -5	70	1.3	0.8	7		
Year	58 37	82	- 5	85 -11	61	15.5	1.5	70		
No. of years	9 10	9	10	9 10	10	10	10	10	10	

ZONGULDAK 41°27'N, 31°48'E 138 ft

Period 1931-1946	Temperature						Relative humidity	Precipitation		
	Average daily Max. Min.	Average of highest each month	Average of lowest each month	Absolute	Average of observations at all hours	Average monthly fall in fall		Average Maximum fall in 24 h	Average No. of days with 0.04 in or more	
	degrees Fahrenheit						per cent	inches		
January	48 38	65	24	80 18	78	5.7	1.4	15		
February	49 38	65	27	70 27	78	3.8	1.8	12		
March	49 38	71	28	80 24	77	4.1	1.3	11		
April	54 44	76	34	84 33	80	3.3	4.9	9		
May	65 52	85	42	98 37	79	2.0	1.1	7		
June	72 58	86	51	105 49	81	2.1	3.7	5		
July	77 62	88	57	99 54	78	1.8	1.8	5		
August	76 62	85	55	104 50	78	2.6	2.7	6		
September	72 57	81	50	87 48	79	3.3	2.8	7		
October	67 53	60	44	85 38	80	3.6	3.2	10		
November	60 47	76	37	82 32	80	6.0	3.0	12		
December	52 40	69	29	76 19	78	8.2	1.6	14		
Year	62 49	84	23	105 18	79	40.4	4.9	110		
No. of years	8 8	8	8	8 8	8	9	9	19		

Along the coastal regions, winters are mild and summers moderately hot. Along the Black Sea, August is the hottest month with a mean temperature of 22°C (72°F). Along the Aegean Sea, August temperatures often exceed 32° C (90° F). Winters generally contain the wettest months on this coast. The western coastal areas do not experience frost, but in the east snow may remain on the ground for as long as four months of the year. Rainfall averages 508 - 762 millimeters (20 - 30 in.) annually along the Aegean and Mediterranean Seas to over 2,540 millimeters (100 in.) along the Black Sea, which is the only region of Turkey with a moisture surplus throughout the year. Along the southern coasts the summers are very hot.

The climate of eastern Turkey is most extreme. Summers are hot and extremely dry; winters are bitterly cold. Spring and autumn are both subject to sudden hot and cold spells.

Figure C-3 shows the mean annual rainfall for Turkey. Table C-1 shows temperature, relative humidity, and precipitation information for seventeen stations located throughout Turkey.

C.1.6 Natural Geographic Regions of Turkey

The topographic and climate conditions of the Republic of Turkey lend themselves to divide the country into five natural geographic regions. Each of these regions will be briefly discussed.

C.1.6.1 The Aegean Coastlands and Turkish Straits. The western portion of the region consists mainly of rolling hill-land that is well suited for agriculture, receiving a mean annual rainfall of 635 millimeters (25 in.). The region includes the city of Istanbul and is densely populated. Its land frontier with Bulgaria and Greece is an artificial one that has varied considerably over the last century.

The Bosphorus Strait is 26 km (16 mi.) long and averages 1.6 km (1 mi.) in width but narrows to less than 460 meters (1,500 ft.) in places. Both banks rise steeply from the water and form a succession of cliffs, coves, and nearly landlocked bays. Most of the shores are densely wooded and are marked by numerous small towns and villages. The Dardanelles Strait is 40 km (25 mi.) long and increases in width toward the south. Unlike the Bosphorus, there are few settlements of any kind along the shores of the Dardanelles, the region being used primarily for grazing.

The Aegean region in Asia has fertile soils and a typically Mediterranean climate with mild, rainy winters and hot, dry summers. The lowlands of the region contain about half of the country's agricultural wealth in broad, cultivated valleys.

C.1.6.2 The Black Sea Region. The region has a steep and rocky coast, and rivers cascade through gorges of the coastal ranges. A few larger rivers that have cut back through the Pontic Mountains have tributaries that flow in broad elevated basins. Access inland from the coast is limited to a few narrow valleys, and the coast has therefore always been isolated from the interior. The eastern part of the region is heavily forested.

The narrow coastal ribbon running between the cities of Zonguldak and Rize is an area of concentrated cultivation. All available areas, including mountain slopes wherever they are not too steep, are put to use. The mild, damp climate favors commercial farming.

C.1.6.3 The Mediterranean Coastland. The plains of the Mediterranean coast are rich in agricultural resources with fertile, humid soils and warm climate. Summers are hot and droughts are not uncommon.

The plains around Adana in the east are largely reclaimed floodlands. In the western part of the Mediterranean coastal region, rivers have not cut valleys to the sea making inland movement restricted. The backland is mainly karst and rises suddenly along the coast to elevations of 2,750 meters (9,000 ft.). There are few major cities along this coast, but the triangular plain of Antalya is extensive enough to support the rapidly growing city and port of the same name, which is an important trading center.

C.1.6.4 Anatolia. The plateau-like highlands of Anatolia are considered the heartland of the country. Like the steppes of the Soviet Union, the region varies in elevation from 610 - 1,220 meters (2,000 - 4,000 ft.) west to east. It is arid and supports little plant or animal life. Wooded areas are confined to the northwest and northeast, and cultivation is restricted to the river valleys that are sufficiently wide. Although irrigation is practiced wherever water is available, the deeply entrenched river courses make it difficult to raise water to the surrounding agricultural land. For the most part, the region is bare and monotonous and is used for grazing.

Rainfall is limited and in Ankara amounts to less than 254 millimeters (10 in.) annually. Overgrazing has caused soil erosion in the plateau, and during the frequent duststorms of summer a fine yellow powder blows across the plains. In bad years there are severe losses of stock. Locusts may ravage the eastern area in April and May. An area of extreme heat and virtually no rainfall in summer, the central plateau is cold in winter with heavy, lasting snows and villages may be isolated by severe snowstorms.

A structural line, or fault, of major importance runs inland from the Sea of Marmara in the general direction of Ankara. The fault underlies a densely populated region that is a major transportation and communication corridor. However, the most devastating earthquakes in recent years occurred in the eastern part of the country.

C.1.6.5 The Eastern Highlands. Eastern Turkey is rugged country with higher elevations, a more severe climate, and more precipitation than the central plateau. In the extreme east at Kars, winter temperatures have been known to fall as low as -40°C (-40°F).

From the highlands in the north, sometimes called "Turkey's Siberia", to the mountains of Kurdistan in the south that descend toward the Mesopotamian Plain in Iraq, vast stretches of this eastern region consist only of wild or barren wasteland. Many of the peaks are extinct volcanoes reaching about 3,000 - 4,400 meters (10,000 - 14,500 ft.) in height. Fertile basins lie at the foot of the lofty ranges. Here are the

headwaters of the Tigris and Euphrates. In the easternmost part of this region, the surface consists of lava deposits, and the soil cover is often thin or absent. Government efforts in the 1940s to resettle sections of the thinly inhabited eastern highland region resulted in significant population increases in some agricultural areas. Along the Murat and Tigris river valleys, rich alluvial soils containing decomposed lava make possible intensive crop cultivation. The entire eastern third of Turkey, however, remains sparsely settled. Its southeastern segment is inhabited largely by nomadic and seminomadic tribesmen.

The northern mountains are covered with deciduous and coniferous forests up to the timberline. In many areas of this region, the villagers have cleared substantial tracts of forest land and have thus added to the erosion problem. The government has sought to prevent further destruction by resettling some of the mountain villages.

C.1.7 Vegetation and Soils

Both the natural vegetation and the cultivated crops are closely related to climate. The constantly warm and moist coastal regions, especially on the north coast, are forested unless they have been cleared for cultivation. The coastal forests, which cover over 13 percent of the land, are mainly on the mountain slopes facing the seas. Because of the climate, mixed evergreen, coniferous, and deciduous woodlands cover the slopes along the north and southeast. Evergreen oaks generally grow on the lower slopes up to 915 meters (3,000 ft.). Cedars, maple, juniper, fir, and valonia oak are found at the higher elevations.

The mountain peaks near the Sea of Marmara and Izmir in the west have humid grassland near the snowline. The landscape below the snowline is covered by conifers, and below this the slopes are covered with broadleaf trees that remain green year round. Broadleaf trees include the poplar, sycamore, and mulberry. Along the west and southwest coastal regions, shrubs and evergreens flourish, particularly on the thinner soils. Walnut and poplar trees grow extensively in the damper areas, and cactus plants flourish in the more arid areas of the coast. In the eastern highlands mixed forests predominate, but the higher ridges and peaks have alpine vegetation.

In the drier interior of the plateau, steppe vegetation is common. Typical vegetation is a combination of short grasses and bush, with lines of stunted willow trees along the watercourses.

There are wide differences in the kinds of soils. In the narrow coastal regions of the west, north and south, terra rossa is found. Formed from limestone, it is strongly weathered and leached. Although this kind of soil is low in humus content, it is enriched by iron and silica and is fertile and suitable for vines and citrus crops. The high iron content gives the terra rossa a red color that becomes yellowish in areas of higher rainfall. Rich alluvium, with marl and clay, and some swampy or saline patches prevail in the few delta areas.

Vast areas of the country are covered by gray-brown acidic soil, occurring primarily in the mountain regions, which are stony and generally lack cropping possibilities. Dense stands of deciduous and coniferous trees grow on these soils in the higher elevations. Large areas of the east and some parts of the central plateau are covered with hardened lava and are almost entirely devoid of vegetation.

The interior plateau regions have brown and reddish-brown soils that are deficient in nitrogen and phosphorus. Where the grass areas have been removed, erosion has stripped off the hillside soils.

C.1.8 Available Topographic Maps of Turkey from the DoD

The Department of Defense has two series of topographic maps which cover the Republic of Turkey, as printed by the Army Map Service, Corps of Engineers. Also, city plans of three Turkish cities are available. These maps are tabulated in Table C-2.

Although it is desirable to use maps scaled at 1:50,000 or larger for path profiling purposes, the map coverages listed above are the largest scale maps known to be available from the Department of Defense.

Table C-2. Available Map Coverage of Turkey from the DoD

Area	Series No.	Scale
Federal Republic of Turkey	1404	1:500,000
Federal Republic of Turkey	K 502	1:250,000
City Plans of:		
Mersin	K 911	1:5,000
Adana	K 911	1:10,000
Iskenderun	K 911	1:10,000

C.2 TOPOGRAPHIC AND CLIMATIC CONDITIONS OF GERMANY

This section presents a general description of topographic and climatic conditions of the Federal Republic of Germany. The information contained here was used either as basis or reference for DCS III alternative system designs.

C.2.1 Location and Political Boundaries

Strategically located in north-central Europe, the Federal Republic of Germany (F.R.G., West Germany) has an area of about 248,460 sq. km (95,930 sq. mi.), about the same size as the United Kingdom or the State of Wyoming. Its northern and southern borders are relatively fixed by natural topographic features, bounded on the north largely by the North and Baltic Seas and on the south by the Rhine River, Baden (See Lake Constance), and the Austrian Alps. Politically, it is bounded by Denmark to the north and Switzerland and Austria to the south. Because the country is in the center of the northern European Plain, its eastern and western borders do not follow natural formations. It is bounded by the Netherlands, Belgium, Luxembourg, and France to the west and by the German Democratic Republic (G.D.R., East Germany) and Czechoslovakia to the east.

Internally, the F.R.G. consists of 10 states, or Lander. West Berlin is located 177 km (110 mi.) inside of East Germany and is entirely surrounded by its territory. Although not a part of the Federal Republic and not governed by it, West Berlin has developed strong ties with West Germany, and has been treated increasingly as the eleventh Land by the Federal Republic.

The portion of West Germany which is of particular interest to the DCS is approximately bounded by $50^{\circ} 05'$ north latitude on the north, 49° north latitude to the east and the French border to the west and the south, $7^{\circ} 15'$ east longitude on the west, and $8^{\circ} 45'$ east longitude on the east. Figure C-4 is a map of West Germany indicating this region. A map of the Rhine River is provided in Figure C-5 which also outlines the DCS area of interest.

C.2.2 Population Centers

In West Germany there are two belts of high population density. One is along or near the Rhine River (which includes the densely-netted DCS area of interest) and the other is in the Borderland (which separates the Northern Plains from the Central Uplands). The two meet at the Ruhr, a tributary of the Rhine, which contains the largest concentration of big cities and industries. Outside the Ruhr area, the high-density areas are usually associated with a large number of towns and medium-sized cities rather than big cities. The principal exceptions are the three great metropolises: Bremen, Hamburg, and West Berlin. The former are both seaports, and West Berlin has a unique political status.

C.2.3 Commercial Telecommunications

Supplied in Supplement VII.

C.2.4 Natural Topographic Regions of West Germany

Broadly speaking, the terrain in the Federal Republic of Germany rises from the coastal lowlands in the north to the Alps along the southern border. The country is generally flat in the north and hilly in the central and western areas, rising in the southwest to more than 1,220

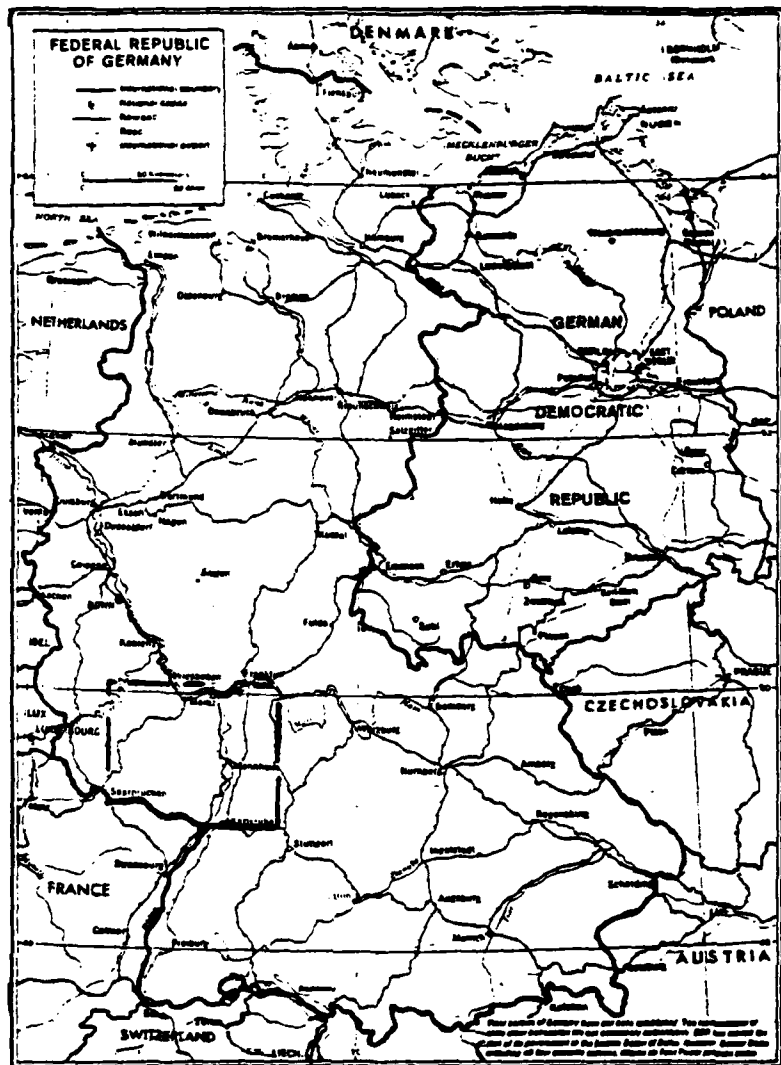


Figure C-4. West Germany with Outline of DCS Area of Interest

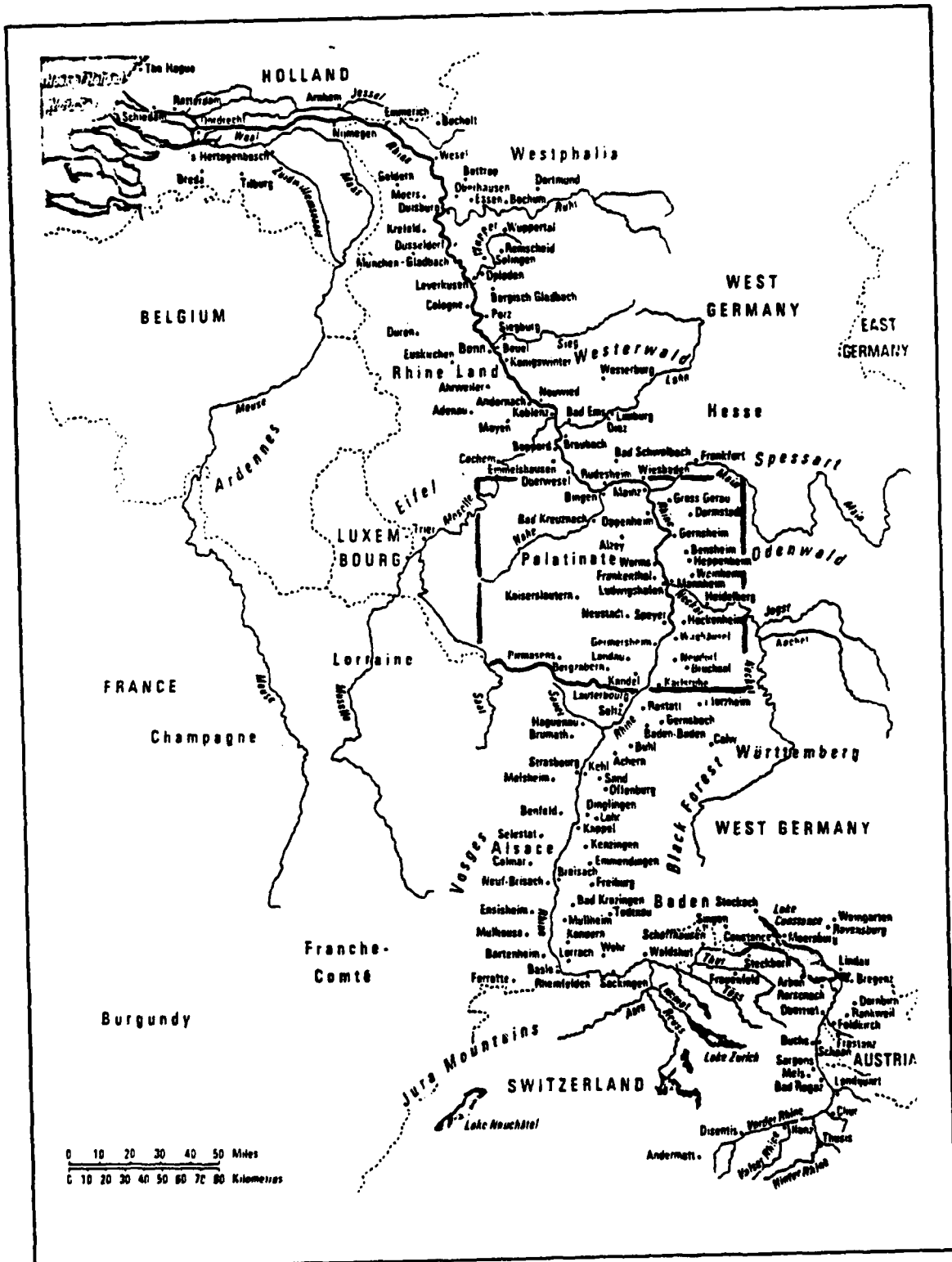


Figure C-5. Rhine River with Outline of DCS Area of Interest

meters (4,000 ft.) above sea level in the Black Forest. The highest elevation is the Zugspitze in the Bavarian Alps at 2,970 meters (9,740 ft.) above sea level. Three major topographic regions, like three east-west bands, can be distinguished.

The North German Plain or Lowland occupies approximately the northern third of West Germany and forms part of the European Plain extending from northern France to the Ural Mountains of the Soviet Union. The West German portion rises very gradually southward from the North the Baltic Seas. Most of it is less than 90 meters (300 ft.) above sea level and only in a few places does it exceed 180 meters (600 ft.). Along the southern edges of the Plain, the rise in elevation to the Central Uplands is gradual in most places. This threshold zone is a strip of land called the Borde or Borderland. It curves northeast from Bonn to Hannover and then southeast toward Leipzig in East Germany.

The Central Uplands of West Germany occupies the central third of the country and is composed of rolling hills and mountain ranges interlaced with innumerable valleys and gorges. The mountain ranges, separated largely by river and stream valleys are rounded and of no great height. Most of them are less than 1,000 meters (3,300 ft.) in elevation. This region occupies the area east of the Rhine River in West Germany and north of the Main River, up to the Borderland.

The southern third of the country is known as the Southern German Uplands. The area lacks no one specific characteristic to distinguish it from the Central Uplands. In its topography, it is rather similar to the central region. Its mountains, however, are derived from different systems from those in central Germany. Its mean elevation, even in plateau regions, is considerably higher. The plateau region, sometimes called the Bavarian Plateau, rises gradually from about 305 meters (1,000 ft.) at the Danube River to about 915 meters (3,000 ft.) at the Alpine Foothills. The Bavarian Alps, the most northern folds of the Alps, lie in a narrow belt along the southern border of West Germany from Baden (See Lake Constance) in the west to Salzburg, just inside East Germany, in the east.

C.2.5 General Topographic Conditions for the Densely Netted DCS

The area of interest to the DCS is outlined in Figures C-4 and C-5. The region is dominated by the Rhine River as it winds west from Mainz to Bingen after having meandered north from Karlsruhe. This portion of the Rhine lies in the northern part of the Upper Rhine Valley or Rift. (The southern part of the Upper Rhine Rift extends from Basle in the south, where the river comes from the east and turns northward, to Karlsruhe. It is a natural frontier between France and West Germany between Basle to just southwest of Karlsruhe.)

The northern part of the valley near Darmstadt is about 24 km (15 mi.) wide and is about 40 km (25 mi.) wide at Karlsruhe, the transition taking place near Mannheim. On the east bank of the Rhine, Mannheim is one of the busiest river ports and manufacturing towns in the entire Rhine Rift. The valley is at about 100 meters (330 ft.) above sea level with little variation in elevation throughout.

East of the valley, around and above Darmstadt, the land is at about 150 meters (490 ft.) and contains trees and low vegetation. Between Darmstadt and Heidelberg, the land rises quickly from the Rhine Rift to about 300 meters (980 ft.). This region contains the western part of the heavily forested Odenwald. Between Heidelberg and Karlsruhe, there are gently rolling hills which reach heights of 250 meters (820 ft.). The soils east of the valley are rich and fertile, containing belts of limestone and crystalline rocks.

To the west of the Rhine Rift in the area of interest, the region is known as Palatinate (Pfalzerbergland). The terrain is quite hilly, and is laced with rich coal seams and dense forests which extend in a southwest-to-northeast direction. The most notable of these is Palatinate Forest (Pfalzerwald), located northwest of Karlsruhe, with an average elevation of about 460 meters (1,500 ft.). North and west of here, up to the Nahe River, the area is slightly lower in elevation and forested areas are more sparse. North of the Nahe, several dense forest regions are again found and the land elevation again averages about 460 meters up to the Mosel (Moselle) River where the area of interest ends.

C.2.6 General Climatic Conditions for the Densely Netted DCS

The Federal Republic of Germany lies entirely in the temperate zone and westerly winds prevail throughout. Although its southern border is on approximately the same latitude as the Canadian border of the western United States, its climate is not as cold as that of the northwestern United States because of the warming effect of the Gulf Stream. Except for the Alpine Region on its southern border, the country does not experience extreme climatic differences. Variations in pressure and temperature are not extreme because the usual differences between a colder north and warmer south are offset by higher land elevation in the south. However, the climate is subject to quick variations when the warm westerly climate of the Gulf Stream collides with the more extreme climate from northeastern Europe.

The highest average monthly temperature 20°C (68°F) occurs in the Rhine-Main Plain and is slightly lower in the Rhine Valley. Spring comes first to the Rhine Valley, it and the North Sea Coast having the longest frost-free period of 7 months or more. The Rhine Rift is reported to have the best climate in all of Germany, mainly because the spring comes earlier and summers are longer.

The prevailing winds are influenced by depressions which come inland, north from the Atlantic. They generally move from the south, west, or northwest and rarely from the north or northeast. The windiest season is early spring for the Rhine Rift. The spring and winter winds, known as Fohn, are an important feature of south German weather. They occur when warm winds, drawn across the Alps, lose moisture and descend on the German side as dry currents warmed by compression during their descent. The low pressures associated with the Fohn are reported to have a depressing psychological effect upon the inhabitants.

Surface elevation and relief are the most important determinants in amount of precipitation. The Central Uplands averages a yearly amount of rainfall between 685 and 1,524 millimeters (27 - 60 in.) with the Rhine Rift being near the lower limit. The maximum rainfall for this region

occurs in summer, July being the wettest month. Snow may begin falling in October above 460 meters (1,500 ft.) and about a month later at lower elevations. It occurs throughout the country into mid-April and into May at the higher elevations. The least amount of snow occurs in the Rhine area (and along the North Sea coast), which may receive rain instead.

Table C-3 is provided to show temperature, relative humidity, precipitation, and sunshine values for locations in or near the DCS area of interest.

C.2.7 Available Topographic Maps of West Germany from the DoD

The Department of Defense has a variety of topographic maps which cover West Germany, as printed by the Army Map Service, Corps of Engineers. Table C-4 shows the series and scales of these maps.

Table C-4. Available Topographic Maps of West Germany from the DoD

Series	Scale
6401	1:500,000
M 501	1:250,000
M 642	1:100,000
M 745	1:50,000
M 841	1:25,000

Additionally, city plans of various large scales are available for a great number of West German cities.

C.3 TOPOGRAPHIC AND CLIMATIC CONDITIONS OF HAWAII

The purpose of this section is to present a brief description of topographic and climatic conditions of the state of Hawaii. The information provided here was used either as a basis or reference for DCS III alternative systems designs.

Table C-3. Weather Conditions in or Near the DCS Area of Interest in West Germany

Frankfurt am Main 50°07'N 8°39'E 103 m

Period 1931-60	Temperature						Relative humidity per cent at 0630 1330	Precipitation			Bright sunshine				
	Average daily		Average monthly		Absolute			Average monthly fall	Maximum fall in 24 h	Average No. of days with 0.1 mm or more	Average monthly duration	Average per cent of possible	Maximum duration in one day	Average No. of days with no sun	
	Max.	Min.	Max.	Min.	Max.	Min.									
January	3.3	-1.6	10.3	-8.6	14.1	-23.0	85	77	58	34	17	45	—	15	
February	8.0	-1.2	11.6	-8.6	18.1	-18.3	86	70	44	20	16	63	—	12	
March	10.8	1.0	18.2	-6.1	23.7	-8.4	84	87	38	36	12	129	36	8	
April	15.7	5.7	24.3	0.0	30.6	-3.6	78	81	44	27	14	184	37	—	
May	20.3	9.3	28.7	2.6	34.2	-1.6	78	80	55	55	14	206	43	—	
June	23.3	12.6	31.4	7.4	38.2	4.0	78	82	73	55	14	227	47	—	
July	24.8	14.5	32.7	10.1	38.1	7.8	81	83	70	48	14	228	47	—	
August	24.4	13.9	32.2	9.1	37.6	6.9	85	84	76	46	14	204	46	—	
September	20.7	10.9	28.3	4.7	34.3	0.8	88	80	57	34	13	145	36	2	
October	14.3	6.6	21.1	0.1	28.7	-4.0	91	88	82	28	14	84	26	—	
November	8.1	3.2	14.6	-2.6	18.6	-7.0	89	77	65	41	16	36	12	15	
December	3.9	-0.2	10.8	-7.4	13.6	-17.6	88	81	84	41	16	31	13	19	
Year	14.5	8.3	34.0*	-12.2*	38.2	-23.8	86	83	876	56	172	1803	32	—	
No. of years	29	29	29	29	29	29	29	29	29	29	29	29	29	29	

Freiburg im Breisgau. 48°01'N 7°50'E 259 m

Period 1931-60	Temperature						Relative humidity per cent at 0630 1330	Precipitation			Bright sunshine				
	Average daily		Average monthly		Absolute			Average monthly fall	Maximum fall in 24 h	Average No. of days with 0.1 mm or more	Average monthly duration	Average per cent of possible	Maximum duration in one day	Average No. of days with no sun	
	Max.	Min.	Max.	Min.	Max.	Min.									
January	4.1	-1.8	12.2	-10.4	17.6	-23.0	85	78	61	34	17	45	—	13	
February	8.0	-2.0	13.3	-10.2	21.1	-22.4	85	72	53	28	14	82	39	4	
March	10.7	1.3	18.7	-8.6	23.6	-12.6	83	80	62	23	13	153	42	—	
April	14.8	4.8	23.6	-1.0	29.3	-8.0	80	84	66	40	15	173	42	4	
May	19.6	8.7	27.7	2.1	31.7	-2.0	91	87	79	44	14	228	49	—	
June	22.4	11.8	30.6	8.6	36.1	3.2	91	88	117	57	16	233	49	2	
July	24.4	12.6	32.2	8.6	38.5	4.6	80	82	106	47	15	247	51	—	
August	24.0	13.3	31.6	7.6	37.4	3.2	84	88	100	50	14	224	50	—	
September	20.4	10.7	28.6	3.7	33.6	-0.1	88	83	86	51	14	174	48	3	
October	14.2	8.8	22.4	-1.1	27.0	-4.6	80	70	67	42	14	123	57	7	
November	8.4	-2.4	18.2	-4.6	20.6	-8.4	88	76	88	38	16	93	38	12	
December	4.6	-0.7	12.0	-8.0	16.3	-20.6	88	78	87	57	17	61	10	14	
Year	14.4	8.7	34.7*	-13.7*	38.6	-23.0	84	86	822	62	177	1800	36	—	
No. of years	27	27	27	27	27	27	24	24	27	27	27	29	29	29	

Table C-3. Weather Conditions in or Near the DCS Area of Interest in West Germany (Concluded)

Stuttgart 48°42'N 9°12'E 401 m

Period 1931-60	Temperature						Relative humidity Average of observations at 0630 & 1230	Precipitation			Bright sunshine				
	Average daily		Average monthly		Absolute			Average monthly fall	Maximum fall in 24 h	Average No. of days with 0.1 mm or more	Average monthly duration	Average per cent. of possible	Maximum duration in one day	Average No. of days with no sun	
	Max.	Min.	Max.	Min.	Max.	Min.									
January	3.2	-2.6	10.9	-11.6	15.0	-25.0	95	74	44	51	16	53	19	—	13
February	4.9	-2.2	12.3	-10.3	18.8	-24.9	94	88	39	50	14	80	29	—	7
March	10.1	0.8	18.6	-8.5	22.8	-13.0	95	67	37	34	12	139	56	—	5
April	14.4	4.7	23.2	-1.5	28.3	-7.2	81	64	48	40	14	157	41	—	4
May	18.8	8.4	27.0	1.6	32.5	-4.3	80	63	73	58	15	213	45	—	4
June	22.0	11.7	30.0	8.4	36.5	2.6	80	66	86	68	15	241	80	—	1
July	23.9	12.6	31.7	8.7	36.2	4.0	81	66	79	64	15	264	86	—	1
August	23.6	13.1	31.4	7.7	36.3	3.7	85	65	75	64	14	225	61	—	1
September	20.3	10.2	28.2	3.9	33.4	-0.6	89	59	82	40	13	157	44	—	3
October	14.2	8.6	22.6	-1.0	28.2	-5.8	91	66	49	32	13	112	34	—	8
November	8.3	2.0	19.8	-4.3	22.8	-11.2	90	74	47	37	14	86	25	—	9
December	3.4	-1.6	11.6	-9.4	17.1	-19.0	88	78	36	26	14	46	18	—	13
Year	14.0	5.3	22.8*	-14.8*	30.2	-25.0	85	62	89	60	100	1778	37	—	69
No. of years	29	29	29	29	29	29	29	29	29	29	29	14	16	—	14

C.3.1 Location and Distribution of the Hawaiian Islands

Officially admitted to the Union in 1959, Hawaii became the 50th State with a land area of about 16,680 sq. km (6,440 sq. mi.), ranking it 47th in size. Located approximately 3,540 km (2,200 mi.) southwest of San Francisco and about a third of the way from San Francisco to Australia, it is the only State which is not on the North American continent. Hawaii consists of 124 small islets and 8 major islands which form an archipelago strung out over 2,400 km (1,500 mi.) of the central Pacific Ocean. No other land lies between Hawaii and the United States mainland. Figure C-6 shows the major islands of Hawaii.

The Hawaiian Islands are in a strategic position on shipping routes between the Americas and Japan, China, the Philippines, and other southwest Pacific areas. Hawaii's location has made it a valuable stopping-place for trans-Pacific air routes. In addition to these obvious peacetime advantages for ships and planes, the Hawaiian Islands provide an ideal location from which control of the Central Pacific can be exercised in time of war. Naval and air bases there were of prime importance during World War II and have been vital links in U.S. Defense Plans since the end of that war. Its military importance in the U.S. Defense system is considered unmatched by any other area in the country.

The Hawaiian Islands include all islands in the chain which extends from the small island of Kure, sometimes called Ocean Islands, in the northwest to the Island of Hawaii, known as the "Big Island", in the southwest, with the exception of the Midway Islands which are under the administration of the U.S. Navy. All of the islands are actually the peaks of a chain of mountains that rise from the Pacific Ocean floor. In centuries past, they were built by volcanoes, inch by inch. There is still some volcanic activity in a few peaks, but it is not very extensive.

C.3.1.1 The Leeward Islands. This chain of small islands, rocks, shoals, and coral atolls extends for about 2,000 km (1,250 mi.) approximately northwest of the Major Islands. Some of the islets are composed of lava rock, some of coral and sand. The chain is bounded by the islands of Kure at the western end and Nihoa in the east.

Because the land mass of the combined Leeward Islands is only 8.3 sq. km (3.2 sq. mi.), the animals and plants on these islets are potentially more endangered than they would be on a larger land mass. For this reason in 1909 President Theodore Roosevelt proclaimed the islands from Kure to Nihoa the Hawaiian Islands Bird Reservation. It is known today as the Hawaiian Islands Wildlife Refuge. All of the islands are uninhabited with the exception of military installations on Kure, Midway, and French Frigate Shoal.

C.3.1.2 The Major Islands. From west to east, the Major Islands are Niihau, Kauai, Oahu, Molokai, Lanai, Kahoolawe, Maui, and Hawaii. Of these, Oahu will be highlighted due to the densely-netted DCS locations on this island. The island is centered about 21° 30' north latitude and 158° west longitude. A sketch of Oahu is given in Figure C-7.

C.3.2 Population

Hawaii ranks 40th among the United States in population with over three-quarters of a million inhabitants. The eight islands positioned at the eastern end of the archipelago are the center of population and activity.

The State is obviously unevenly settled. The capital city, Honolulu, on Oahu, has the largest population of any in the state with about 325,000 residents. It is the center of a metropolitan area which has over 80 percent of the Hawaiian Islands' population.

C.3.3 General Topographic Conditions for the Densely Netted DCS

The Hawaiian Islands may be characterized as having some coasts which are low, sandy, and vulnerable to tidal waves, and some bold cliffs that rise abruptly from the ocean. The sandy beaches lead to low vegetation and flowering trees which quickly give way to rocky, mountainous volcanic peaks.

Oahu Island is the third largest of the Hawaiian Islands (behind Hawaii and Maui) with an area of over 1,550 sq. km (600 sq. mi.). The island is marked by two important land elevations. The Koolau Range, at an

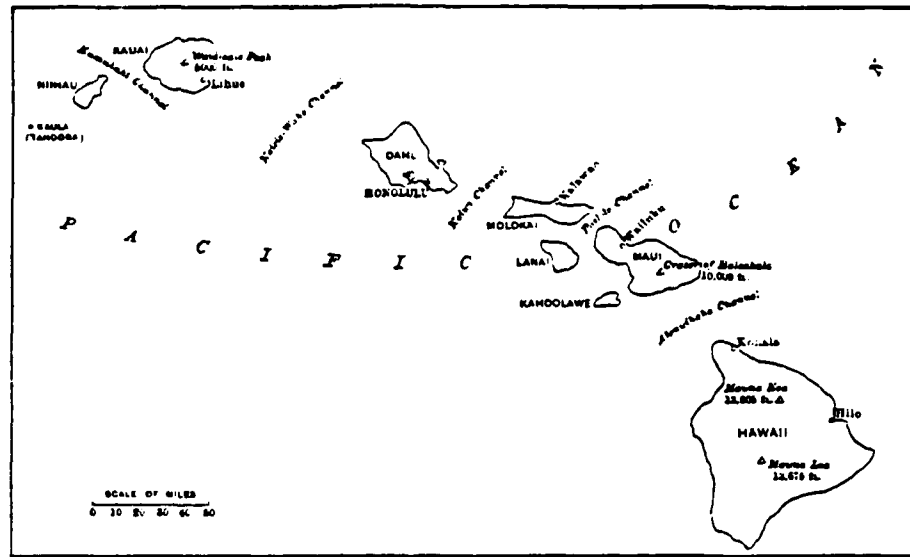


Figure C-6. Major Hawaiian Islands

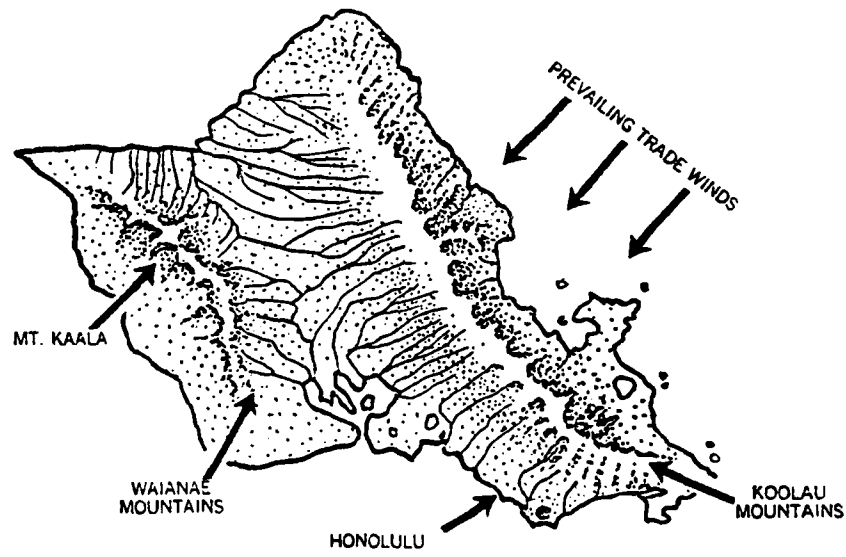


Figure C-7. Sketch of Oahu

average elevation of 610 meters (2,000 ft.) parallels the entire northeastern coast. Its highest peak is konahuanui, reaching an elevation of 946 meters (3,105 ft.). The Waianae Range is somewhat higher in elevation and parallels the western coast. Mt. Kaala is its highest peak at 1,228 meters (4,030 ft.). Both ranges are eroded with deep ravines and gorges and are indented with bays. Few lakes and rivers characterize the surface; streams are chiefly short mountain torrents. Vegetation is most abundant on the northeastern side of the highlands. Between these ranges is a large irrigated plateau at an elevation of about 240 - 305 meters (800 - 1,000 ft.) from the northwest coast to the southern coast. The plateau consists of volcanic ash, gravel, vegetation, crumbling lava, and wind blown sand and dust. Oxidation of iron causes a red soil and rock strata. The iron content is insufficient for smelting, and there are no coal or oil deposits on Oahu or any of the Hawaiian Islands.

In many ways, Oahu is the most important of the Hawaiian Islands. Besides having most of the state's population, the island has an international airport, the capital city of Honolulu, and Pearl Harbor on its southern coast. Pearl Harbor, located about 9.5 km (6 mi.) west of Honolulu, forms a landlocked harbor used by the United States as a naval base and surrounds Ford Islands. Hickman Air Force Base rests on the east side of the Pearl Harbor entrance.

C.3.4 General Climatic Conditions for the Densely Netted DCS

The maritime climate of Oahu is unusually pleasant for the tropics. The most notable of Oahu's climatic features are the extremely equable temperature conditions from day-to-day and season-to-season, the persistent trade wind flow from the northeast, the sunniness of the leeward lowlands in contrast to the persistent cloudiness over nearby crests, the remarkable variability of rainfall over short distances, and infrequency of severe storms.

The Hawaiian chain lies roughly along 20° north latitude and displays tropical to subtropical conditions as expected. At this latitude day length varies only two and a half hours between the summer and winter solstice. This relatively uniform amount of sunlight dictates the temperatures do not vary much throughout the year at any particular location. Another factor which tempers the climate is the effect of the surrounding ocean. Like a vast insulator, the ocean moderates temperatures near the coasts. (Only on the islands of Maui and Hawaii do large mountain masses exert an effect which markedly counters the maritime influence.) Table C-5 presents the average monthly and annual temperatures for 1947 to 1978 at Honolulu. The table also includes the long-term mean, maximum, and minimum temperatures recorded for each month and annually. Table C-6 displays the weather station locations at Honolulu where weather data were collected.

Wind and cloud cover modify the temperatures considerably as well as topography. Deep, shady canyons can be cool while nearby ridges are warm and steamy. Extremes in temperatures tend to occur mostly on leeward coasts or leeward slopes of mountains, where the absence of trade winds permits heat or cold to accumulate. Within the city limits of Honolulu there are both warm and cool sections.

The pattern of trade winds tends to follow the sun. During the summer months when the sun has moved north relative to the earth, the Hawaiian Islands lie midway in the trade belt. During a typical summer month such as August, trade winds come from north-northeast to east 90 percent of the time and half the time they exceed 21 kilometers per hour (13 mph). As these winds traverse vast stretches of the Pacific, they pick up considerable moisture. This affects both cloud cover and rainfall. Completely cloudless skies are quite rare at higher elevations. On the average, it is reported that two-thirds of the sky is covered by clouds during the daylight hours except for the leeward lowlands, where it is generally sunny. Six of the major islands, instead of receiving 635 millimeters (25 in.) of rain per year as do the Leeward Islands, average 1,145 millimeters (45 in.) per year over the entire surface.

Table C-5. Average Temperatures at Honolulu

Table C-6. Honolulu Weather Station Locations

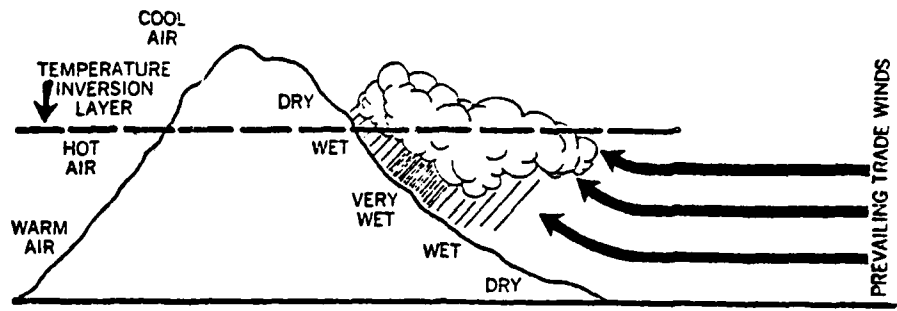
Note: The hygrothermometer exposure was poor beginning about 1965 due to a progressively larger efflorescence around the site that caused maximum temperatures to be too high to be representative for the environment. The instrument was removed from the enclosure in 1970 and reconditioned (Solar 2) against the site's background conditions. It has been operating satisfactorily ever since.

Observatory Annex is located 300 feet SW of USCGS Disk marked "ARP 1936". Requests for information concerning solar radiation data or instrumentation should be made to the Director, National Climatic Center, Federal Building, Asheville, NC 28801.

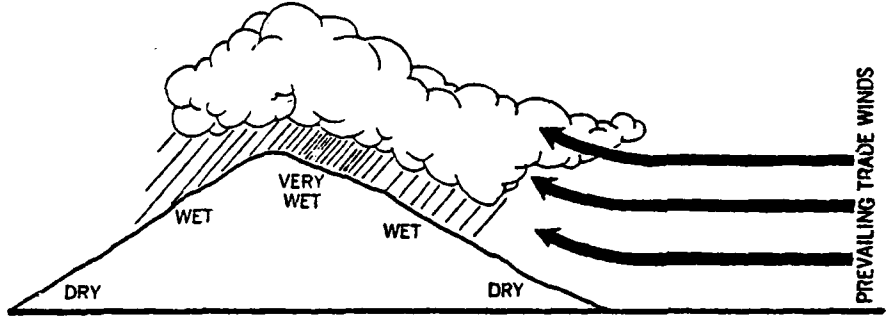
Although temperature on the average decreases with altitude, islands tend to absorb heat, leading to the creation of inversion layers with temperatures increasing slightly with altitude to about 1.5 - 2.1 km (5 - 7 thousand ft.), above which cool air lies. The warm (or hot) air below a temperature inversion layer tends to be held between the cool air above and the less warm air near the ground. In the Hawaiian Islands, an inversion layer of this sort is reported to occur 50 to 70 percent of the time.

When a mountain summit lies above a temperature inversion layer and trade winds force moist air up the windward side of the mountain mass, the trade winds penetrate the cool air at the upper limit of the inversion layer and condense into rainfall on the windward side of the mountain. This phenomenon is demonstrated in Figure C-8a. A rounded mountain summit near the inversion layer will condense rainfall on its windward side, and this precipitation will continue onto the leeward side of the summit until the clouds have lost all of their excess moisture, as in Figure C-8b.

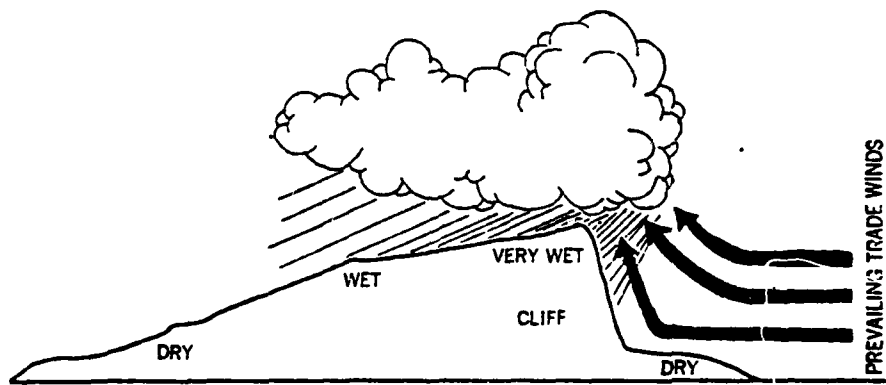
The shape of a mountain range may alter the normal patterns described above, such as on Oahu. The Koolau Mountains form a chain normal to the prevailing direction of the trade winds. The windward side of this range consists of a long, sharp cliff. When the trade winds reach this cliff, they are forced upward suddenly and swiftly. So sudden is this updraft that condensation triggered by the rise is carried over the summit and most of it falls just on the leeward side of the summit, as in Figure C-8c. Rainfall exceeds 6,350 millimeters (250 in. on the leeward side, while at the base of the northeast cliff, amounts are 1,270 - 1,905 millimeters (50 - 75 in.) of rain per year. As rain showers build up over the Koolau Mountains, they may be carried by strong trade winds far over the summit areas. In Honolulu there are often a few very light showers in the afternoon.



a. Mountain Summit Above an Inversion Layer



b. Mountain Summit Near an Inversion Layer



c. Mountain Summit with a Long, Sharp Cliff

Figure C-8. Effects of Trade Winds on a Mountain Summit

Figure C-9 shows the extreme variability of rainfall (in./yr.) over short distances. It should be noted that as the Koolau Mountains trigger rain showers from the trade winds, rainfall decreases on the leeward side and a "rain shadow" is created. The Waianae Mountains are shadowed by the Koolaus and receive very little rainfall by comparison. Table C-7 shows the monthly and annual amount of precipitation received at Honolulu from 1947 to 1978 along with the mean monthly and annual amounts for this 32 year period. Table C-8 and C-9 show the weather conditions at Honolulu for 1978 and long-term normal, mean, and extreme values.

Hurricanes and other severe storms are quite rare on Oahu. Strong winds do occur at times in connection with storm systems moving through the Islands, but seldom cause extensive damage. When the trade winds diminish or give way to southerly winds, a situation known locally as "Kona weather" or "Kona storms" occur, and the humidity may become oppressively high. This is in marked contrast to the persistently moderate humidity experienced during even the warmest months due to the northeasterly trade winds.

C.3.5 Available Topographic Maps of Hawaii from the DoD

The Department of Defense has two series of topographic maps which cover the Major Islands of Hawaii, as printed by the Corps of Engineers, Army Map Service. These maps are tabulated in Table C-10:in

Table C-10. Available Topographic Maps of the Major Hawaiian Islands from the DoD

Series No.	Scale
W 532	1:250,000
W 833	1:25,000

The latter series provides an excellent source for path profiling purposes.

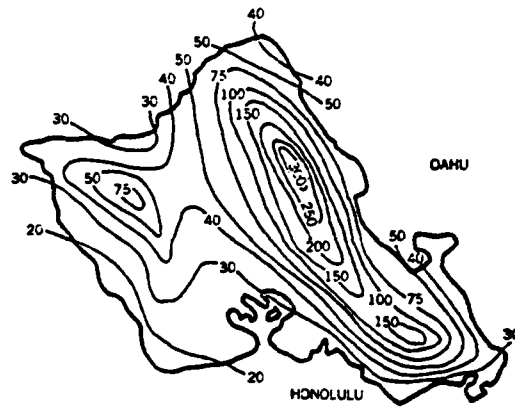


Figure C-9. Mean Precipitation (in/yr) on Oahu

Table C-7. Precipitation (in) at Honolulu

Year	Jan	Feb	Mar	Apr	May	June	July	Aug	Sept	Oct	Nov	Dec	Annual	
1947	1.77	0.93	0.66	0.23	0.15	0.08	0.15	0.79	2.74	0.35	1.55	1.86	30.66	
1948	1.59	1.05	0.67	1.04	0.17	0.15	0.19	1.07	1.17	0.32	1.24	1.43	39.76	
1949	14.76	3.65	0.66	0.16	0.05	0.17	0.37	0.65	0.18	0.39	0.09	2.48	25.89	
1950	13.24	1.04	0.65	3.74	0.18	0.07	0.03	1.00	0.49	0.07	1.92	0.59	31.66	
1951	1.71	2.95	20.79	0.49	0.13	0.24	0.13	0.54	0.14	0.91	1.83	0.23	9.36	30.73
1952	0.43	0.48	0.36	0.37	0.13	0.13	0.07	0.05	0.27	2.35	1.21	0.30	10.65	
1953	1.25	2.97	1.54	0.24	0.16	0.02	0.23	0.03	0.71	0.00	0.82	1.79	9.97	
1954	1.49	3.97	2.34	1.99	0.16	0.20	1.72	0.19	0.34	1.86	9.30	4.06	27.30	
1955	2.74	13.04	4.36	0.85	0.76	0.04	0.23	0.59	0.23	0.37	1.09	11.00	37.66	
1956	2.58	3.36	0.51	0.51	0.15	0.15	0.15	0.53	0.14	1.01	1.26	2.35	21.83	
1957	12.33	1.08	0.61	1.93	0.12	0.12	0.12	0.37	0.07	0.31	0.42	0.54	24.82	
1958	0.50	5.15	14.91	0.60	0.26	0.21	0.08	0.07	0.45	0.05	0.00	2.04	23.02	
1959	3.76	2.23	0.10	0.33	0.07	0.07	0.29	0.00	0.35	0.04	1.00	0.39	16.16	
1960	6.48	0.31	1.46	0.81	0.35	0.16	0.73	0.49	0.31	1.16	0.22	2.24	12.07	
1961	0.37	0.93	0.45	0.71	0.15	0.07	0.09	0.47	0.04	2.40	2.05	1.56	19.35	
1962	2.20	1.97	2.10	1.07	0.32	0.11	0.11	0.32	0.04	0.70	2.05	3.04	23.85	
1963	12.58	1.07	0.24	0.97	0.20	0.12	0.05	0.03	1.97	1.07	0.23	1.03	24.83	
1964	2.01	3.32	0.46	0.66	0.05	0.05	0.34	0.07	0.36	0.04	0.57	0.57	20.12	
1965	7.02	0.60	0.40	1.44	7.23	0.25	1.37	0.87	0.37	2.86	16.72	9.77	41.75	
1966	1.30	3.71	0.36	0.43	0.11	0.04	0.03	0.82	0.10	2.73	9.44	2.70	23.18	
1967	2.79	2.39	0.70	1.20	2.12	1.03	1.21	2.33	0.42	1.83	2.73	0.73	34.54	
1968	6.17	2.71	2.40	3.16	1.12	0.29	0.29	0.10	1.30	2.15	3.04	0.83	27.35	
1969	8.20	0.44	3.00	0.10	0.11	0.22	0.03	0.11	0.37	0.07	1.77	1.00	22.30	
1970	1.81	0.77	0.67	0.70	0.21	0.23	0.01	0.21	0.36	1.00	2.00	1.03	19.09	
1971	6.19	2.37	3.87	2.19	0.43	2.66	0.06	0.26	1.07	2.27	0.93	2.00	26.64	
1972	5.28	3.00	2.65	3.13	0.12	0.79	0.20	0.46	0.93	2.30	0.59	2.90	26.94	
1973	0.67	0.68	0.47	0.72	0.09	0.09	0.04	0.33	0.64	1.76	2.73	1.94	14.24	
1974	0.21	1.25	2.05	4.18	0.82	1.32	0.04	1	2.00	2.77	2.00	0.89	26.02	
1975	0.82	1.34	2.07	0.31	0.19	0.03	0.03	0.07	0.11	0.38	11.50	0.90	26.37	
1976	1.20	6.09	2.87	0.71	0.26	0.18	0.14	0.17	0.30	0.49	0.66	0.66	22.76	
1977	0.52	0.42	2.34	1.01	0.76	0.11	0.14	0.06	0.20	0.19	0.51	1.03	12.36	
1978	0.84	0.73	1.37	2.07	1.20	1.00	0.20	0.03	0.20	11.15	1.55	2.00	23.05	
RECORD MEAN	4.23	2.39	3.29	1.30	1.14	0.62	0.51	0.64	0.70	1.80	2.43	3.20	28.56	

Table C-8. Weather Conditions at Honolulu for 1978

Month	Honolulu, Hawaii # 21791		HONOLULU INTERNATIONAL AIRPORT		Standard time zone	Altitude feet	Latitude 21° 10' N	Longitude 157° 56' W	Elevation 1971-96 - ft	Flotation (specie)	7 days	Year 1978
	Temperature °F	Humidity %	Precipitation in inches	Wind								
ANNUAL												
JAN	66.1	70.1	1.8	1.8	66.1	70.1	1.8	1.8	1.8	1.8	1.8	1.8
FEB	68.0	72.0	2.1	2.1	68.0	72.0	2.1	2.1	2.1	2.1	2.1	2.1
MAR	69.8	73.7	2.4	2.4	69.8	73.7	2.4	2.4	2.4	2.4	2.4	2.4
APR	71.6	75.5	2.7	2.7	71.6	75.5	2.7	2.7	2.7	2.7	2.7	2.7
MAY	73.4	77.3	3.0	3.0	73.4	77.3	3.0	3.0	3.0	3.0	3.0	3.0
JUN	75.2	79.1	3.3	3.3	75.2	79.1	3.3	3.3	3.3	3.3	3.3	3.3
JUL	76.9	80.8	3.6	3.6	76.9	80.8	3.6	3.6	3.6	3.6	3.6	3.6
SEP	78.7	82.5	3.9	3.9	78.7	82.5	3.9	3.9	3.9	3.9	3.9	3.9
OCT	80.5	84.2	4.2	4.2	80.5	84.2	4.2	4.2	4.2	4.2	4.2	4.2
NOV	82.3	85.9	4.5	4.5	82.3	85.9	4.5	4.5	4.5	4.5	4.5	4.5
DEC	84.1	87.6	4.8	4.8	84.1	87.6	4.8	4.8	4.8	4.8	4.8	4.8
YEAR	80.2	82.9	3.1	3.1	80.2	82.9	3.1	3.1	3.1	3.1	3.1	3.1

Month	Honolulu, Hawaii # 21791		HONOLULU INTERNATIONAL AIRPORT		Standard time zone	Altitude feet	Latitude 21° 10' N	Longitude 157° 56' W	Elevation 1971-96 - ft	Flotation (specie)	7 days	Year 1978
	Temperature °F	Humidity %	Precipitation in inches	Wind								
ANNUAL												
JAN	66.1	70.1	1.8	1.8	66.1	70.1	1.8	1.8	1.8	1.8	1.8	1.8
FEB	68.0	72.0	2.1	2.1	68.0	72.0	2.1	2.1	2.1	2.1	2.1	2.1
MAR	69.8	73.7	2.4	2.4	69.8	73.7	2.4	2.4	2.4	2.4	2.4	2.4
APR	71.6	75.5	2.7	2.7	71.6	75.5	2.7	2.7	2.7	2.7	2.7	2.7
MAY	73.4	77.3	3.0	3.0	73.4	77.3	3.0	3.0	3.0	3.0	3.0	3.0
JUN	75.2	79.1	3.3	3.3	75.2	79.1	3.3	3.3	3.3	3.3	3.3	3.3
JUL	76.9	80.8	3.6	3.6	76.9	80.8	3.6	3.6	3.6	3.6	3.6	3.6
SEP	78.7	82.5	3.9	3.9	78.7	82.5	3.9	3.9	3.9	3.9	3.9	3.9
OCT	80.5	84.2	4.2	4.2	80.5	84.2	4.2	4.2	4.2	4.2	4.2	4.2
NOV	82.3	85.9	4.5	4.5	82.3	85.9	4.5	4.5	4.5	4.5	4.5	4.5
DEC	84.1	87.6	4.8	4.8	84.1	87.6	4.8	4.8	4.8	4.8	4.8	4.8
YEAR	80.2	82.9	3.1	3.1	80.2	82.9	3.1	3.1	3.1	3.1	3.1	3.1

Table C-9. Normal, Mean, and Extreme Weather Conditions at Honolulu

Month	Honolulu, Hawaii # 21791		HONOLULU INTERNATIONAL AIRPORT		Standard time zone	Altitude feet	Latitude 21° 10' N	Longitude 157° 56' W	Elevation 1971-96 - ft	Flotation (specie)	7 days	Year 1978
	Temperature °F	Humidity %	Precipitation in inches	Wind								
ANNUAL												
JAN	66.1	70.1	1.8	1.8	66.1	70.1	1.8	1.8	1.8	1.8	1.8	1.8
FEB	68.0	72.0	2.1	2.1	68.0	72.0	2.1	2.1	2.1	2.1	2.1	2.1
MAR	69.8	73.7	2.4	2.4	69.8	73.7	2.4	2.4	2.4	2.4	2.4	2.4
APR	71.6	75.5	2.7	2.7	71.6	75.5	2.7	2.7	2.7	2.7	2.7	2.7
MAY	73.4	77.3	3.0	3.0	73.4	77.3	3.0	3.0	3.0	3.0	3.0	3.0
JUN	75.2	79.1	3.3	3.3	75.2	79.1	3.3	3.3	3.3	3.3	3.3	3.3
JUL	76.9	80.8	3.6	3.6	76.9	80.8	3.6	3.6	3.6	3.6	3.6	3.6
SEP	78.7	82.5	3.9	3.9	78.7	82.5	3.9	3.9	3.9	3.9	3.9	3.9
OCT	80.5	84.2	4.2	4.2	80.5	84.2	4.2	4.2	4.2	4.2	4.2	4.2
NOV	82.3	85.9	4.5	4.5	82.3	85.9	4.5	4.5	4.5	4.5	4.5	4.5
DEC	84.1	87.6	4.8	4.8	84.1	87.6	4.8	4.8	4.8	4.8	4.8	4.8
YEAR	80.2	82.9	3.1	3.1	80.2	82.9	3.1	3.1	3.1	3.1	3.1	3.1

Normal and extreme values are from existing and comparable sources. Normal extremes have been measured at other sites in the locality of Honolulu. Maximum precipitation is 24 hours 17.1 in March 1959 at the City Office. Temperature extreme for period January 1975 through August 1976 excluded as non-representative due to poor exposure of hygrothermometer. See station location table on back page.

(a) Length of record, years, through the year 1970 except for the first or last 5 years of an extreme.

(b) Average of 10 years of record, through the year 1970 except for the first or last 5 years of an extreme.

(c) Based on 10 years of record, through the year 1970 except for the first or last 5 years of an extreme.

Normal = Based on record for the 1961-1970 period. The most recent 5 years of an extreme.

Extreme = Based on record for the 1961-1970 period. The first or last 5 years of an extreme.

Extremes = Based on record for the 1961-1970 period. The first or last 5 years of an extreme.

Normal = Based on record for the 1961-1970 period. The first or last 5 years of an extreme.

Extreme = Based on record for the 1961-1970 period. The first or last 5 years of an extreme.

Extremes = Based on record for the 1961-1970 period. The first or last 5 years of an extreme.

Normal = Based on record for the 1961-1970 period. The most recent 5 years of an extreme.

Extreme = Based on record for the 1961-1970 period. The first or last 5 years of an extreme.

Extremes = Based on record for the 1961-1970 period. The first or last 5 years of an extreme.

Normal = Based on record for the 1961-1970 period. The most recent 5 years of an extreme.

Extreme = Based on record for the 1961-1970 period. The first or last 5 years of an extreme.

Extremes = Based on record for the 1961-1970 period. The first or last 5 years of an extreme.

Normal = Based on record for the 1961-1970 period. The most recent 5 years of an extreme.

Extreme = Based on record for the 1961-1970 period. The first or last 5 years of an extreme.

Extremes = Based on record for the 1961-1970 period. The first or last 5 years of an extreme.

Normal = Based on record for the 1961-1970 period. The most recent 5 years of an extreme.

Extreme = Based on record for the 1961-1970 period. The first or last 5 years of an extreme.

Extremes = Based on record for the 1961-1970 period. The first or last 5 years of an extreme.

Normal = Based on record for the 1961-1970 period. The most recent 5 years of an extreme.

Extreme = Based on record for the 1961-1970 period. The first or last 5 years of an extreme.

Extremes = Based on record for the 1961-1970 period. The first or last 5 years of an extreme.

Normal = Based on record for the 1961-1970 period. The most recent 5 years of an extreme.

Extreme = Based on record for the 1961-1970 period. The first or last 5 years of an extreme.

Extremes = Based on record for the 1961-1970 period. The first or last 5 years of an extreme.

Normal = Based on record for the 1961-1970 period. The most recent 5 years of an extreme.

Extreme = Based on record for the 1961-1970 period. The first or last 5 years of an extreme.

Extremes = Based on record for the 1961-1970 period. The first or last 5 years of an extreme.

Normal = Based on record for the 1961-1970 period. The most recent 5 years of an extreme.

Extreme = Based on record for the 1961-1970 period. The first or last 5 years of an extreme.

Extremes = Based on record for the 1961-1970 period. The first or last 5 years of an extreme.

Normal = Based on record for the 1961-1970 period. The most recent 5 years of an extreme.

Extreme = Based on record for the 1961-1970 period. The first or last 5 years of an extreme.

Extremes = Based on record for the 1961-1970 period. The first or last 5 years of an extreme.

THIS PAGE INTENTIONALLY LEFT BLANK

SUPPLEMENT I SYNOPSIS OF TOPOGRAPHIC
CONSIDERATIONS FOR THE DCS

THIS PAGE INTENTIONALLY LEFT BLANK

TABLE OF CONTENTS

	<u>Page</u>
I.1 GENERAL	CI-2
I.2 ELECTRICAL CHARACTERISTICS OF THE SURFACE OF THE EARTH	CI-2
I.3 TERRAIN ROUGHNESS CONSIDERATIONS	CI-5
I.4 CLUTTERED TERRAIN CONSIDERATIONS	CI-5
I.5 PATH GEOMETRY	CI-6

LIST OF FIGURES

	<u>Page</u>
I-1 Conductivity and Permitivity	CI-3
I-2 Ground Conductivities for Europe and Darts of Asia	CI-4
I-3 Penetration Depth	CI-7
I-4 Additional Attenuation Through Woods	CI-7
I-5 Terrestrial Line-of-Sight (LOS Path Geometry)	CI-9
I-6 Additional Attenuation Through Woods	CI-10
I-7 Tropospheric Scatter Path Geometry	CI-11

LIST OF TABLES

	<u>Page</u>
I-1 Typical Ground Parameters	CI-2

SUPPLEMENT I
SYNOPSIS OF TOPOGRAPHIC CONSIDERATIONS FOR THE DCS

I.1 GENERAL

When radio waves are propagated over the earth, the primary topographic considerations for point-to-point services are the electrical characteristics and the physical structure of the earth's surface along the great circle path.

The electrical characteristics are especially important for the propagation of radio waves near the surface of the earth (i.e., diffraction modes and terrestrial line-of-sight (LOS) modes when ground reflections are likely). For other modes it is prudent to consider the electrical characteristics whenever ground reflections may occur.

The structural characteristics of the earth's surface are also especially important for diffraction and LOS paths but are significant for all other propagation modes because these characteristics include the natural structures of terrain elevation and vegetation and of man-made obstacles. The structural characteristics set the path geometry for several modes of propagation and may cause radio waves to be diffracted or attenuated.

I.2 ELECTRICAL CHARACTERISTICS OF THE SURFACE OF THE EARTH

The surface conductivity, σ (mhos per meter, S/m), of the earth and the permittivity, or ratio of the surface dielectric constant to that of air, ϵ , are important parameters when a radio wave is reflected or diffracted by the surface of the earth. For LOS paths, these ground parameters may be used to determine the magnitude of the theoretical coefficient and phase shift for reflection of a plane wave from a smooth plane surface; for diffraction paths, an estimate of the diffraction loss is a function of these parameters. Their values are not merely determined by the nature of the soil, but also by its moisture content and temperature, by the radio operating frequency, and by the penetration depth and lateral spread of the radio wave.

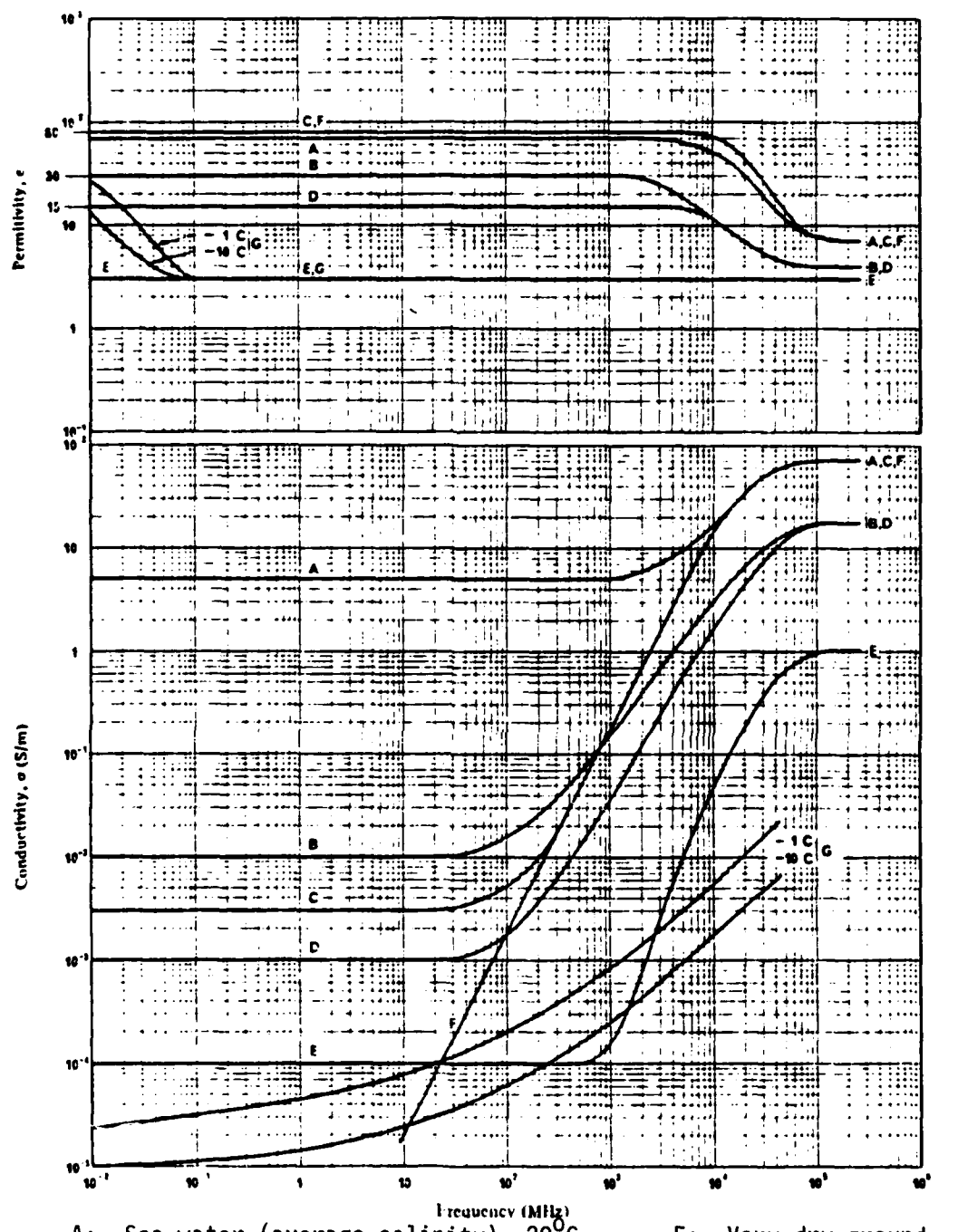
If the values of conductivity and permittivity are not known and cannot be measured, Figure I-1 may be used to determine the approximate range of values for seven different types of earth surfaces as a function of frequency. As a note of caution, values outside of these ranges can occur.

If a rough estimate of these parameters is required, independent of frequency, Table I-1 may be used as an approximation for values of surface conductivity, σ , and permittivity, ϵ .

Table I-1. Typical Ground Parameters

Type of Surface	σ (S/m)	ϵ
Poor Ground (Dry)	0.001	4
Average Ground	0.005	15
Good Ground (Wet)	0.02	25
Sea Water	5.0	81
Fresh Water	0.01	81

Figure I-2 is a map of Europe and parts of Asia which forms part of the first stage in the presentation of a world atlas of ground conductivities called for in paragraph 4 of Decision 3-2 in Reports and Recommendations of the CCIR, 1978. The map is subject to several conditions; the most notable is that they are "limited in application, at least for the time being, to the VLF part of the spectrum (i.e., up to 30 kHz)". From this figure it can be seen that all of Turkey is reported to have a surface conductivity value of between 3×10^{-3} and 1×10^{-2} S/m with the exception of Lake Van, which has a value of 4 S/m. The densely-netted DCS in Germany is reported to have a value of 1×10^{-2} S/m. Unfortunately, areas of interest in Hawaii have been deleted from the available figures.



A: Sea water (average salinity), 20°C
 B: Wet ground
 C: Medium dry ground
 E: Very dry ground
 F: Pure water, 20°C
 G: Ice (fresh water)

Figure I-1. Conductivity and Permittivity

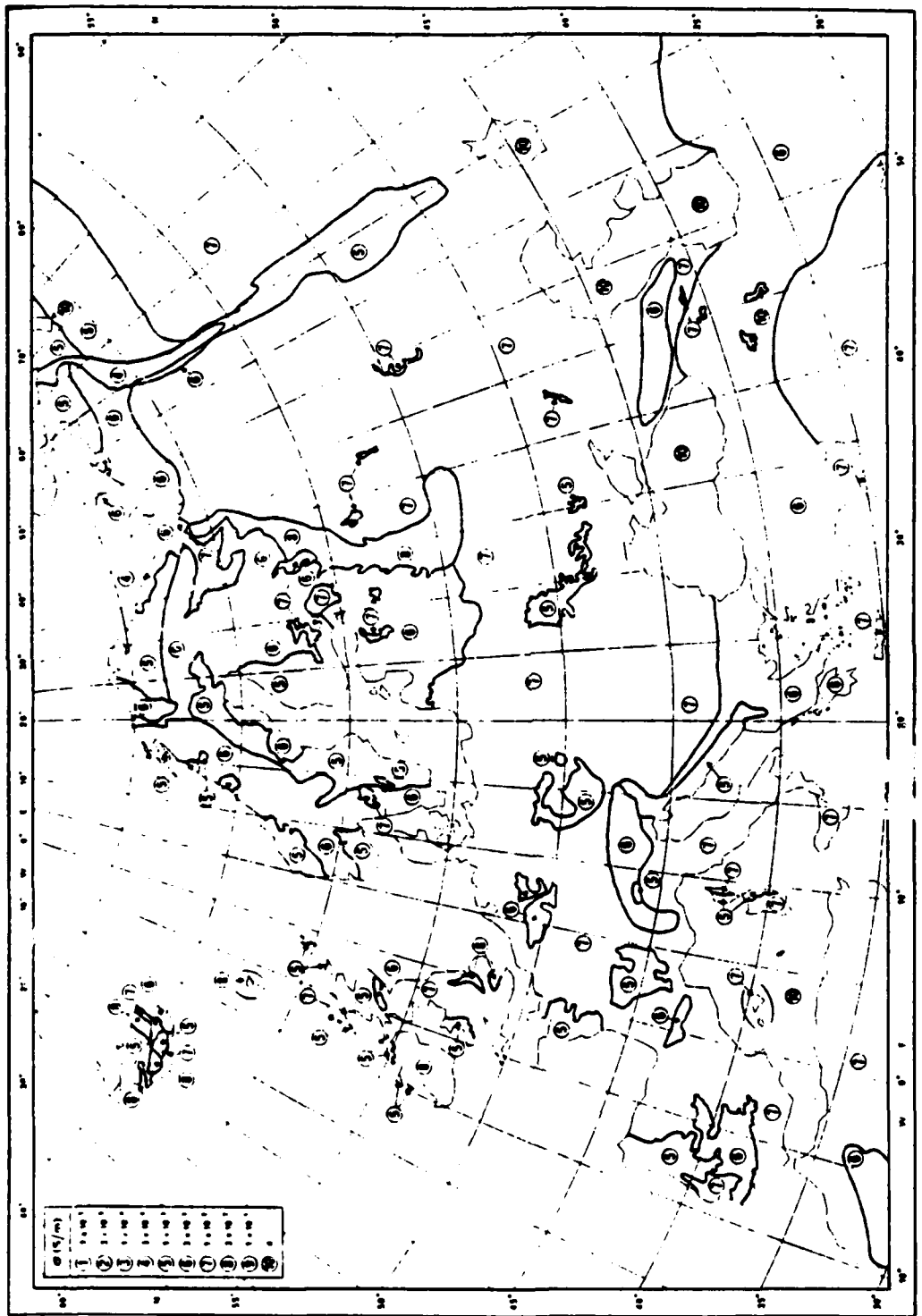


Figure I-2. Ground Conductivities for Europe and Darts of Asia

Figure I-3 shows the penetration depth of radio waves, δ , as a function of frequency for five types of earth surfaces. This parameter is of particular importance when the upper ground layers are of lower conductivity and the electromagnetic wave energy can penetrate more readily to the lower layers. Examples of this are ice-covered lakes and ocean areas. Examination of the figure will reveal that this parameter may be neglected for higher operating frequencies.

I.3 TERRAIN ROUGHNESS CONSIDERATIONS

In addition to the parameters mentioned above which are important factors for use in determining the effective reflection coefficient, the terrain roughness factor, σ_h , is a significant factor for radio paths with ground reflections. The terrain roughness factor is used to estimate multipath fading and also to determine the proportion between the specular (smooth) and diffused (scattered) components of a radio wave reflected from the terrain.

The roughness factor is the root-mean-square deviation of the terrain from an imaginary smooth curve representing the real terrain. For LOS, the terrain roughness factor within the first Fresnel zone is of significant importance for prediction of link performance. The first Fresnel zone is defined as the first ellipsoid containing every point for which the sum of the distances from that point to the two ends of the path is exactly one-half wavelength longer than the direct end-to-end path. Neglecting climatic effects, if no obstacles intercept the first Fresnel zone it may be assumed that the transmission loss for the direct LOS path equals the free space value.

I.4 CLUTTERED TERRAIN CONSIDERATIONS

The effects of diffraction and absorption by trees, hills, and manmade obstacles are often important, especially if a receiving installation is low or is surrounded by obstacles. Absorption of radio energy is probably the least important of these factors except in cases where the only path for radio energy is directly through some building material or where a radio path extends for a long distance through trees.

Studies made at 3 GHz indicate that stone buildings and groups of trees so dense that the sky cannot be seen through them should be regarded as solid objects around which diffraction takes place. It is reported that at 3 GHz the loss through a 23-centimeter-thick dry brick wall was 12 dB and increased to 46 dB when the wall was thoroughly soaked with water. A loss of 1.5 dB through a dry sash window and 3 dB through a wet one were reported to be usual values. Studies also report that the only objects encountered which showed a loss of less than 10 dB at 3 GHz were thin screens of leafless branches, the trunk of a single tree at a distance exceeding 30 meters (100 ft.), wood-framed windows, tile or slate roofs, and the sides of light wooden huts. Field strengths obtained when a thick belt of leafless trees was between transmitter and receiver were within 6 dB of those computed, assuming Fresnel diffraction over an obstacle slightly lower than the trees. Loss through a thin screen of small trees rarely exceeded 6 dB if the transmitting antenna could be seen through their trunks. If sky could be seen through the trees, 15 dB was the greatest expected loss.

One source states the empirical relationship for the rate of attenuation directly through woods to be:

$$A_w = d (0.244 \log f - 0.422), \text{ for } f > 100 \text{ MHz} \quad (1)$$

where A_w is the absorption in dB through d meters of trees in full leaf with the frequency, f , expressed in MHz.

The CCIR reports that in the 30-MHz to 3-GHz range, the average additional attenuation through wooded terrain is given by Figure I-4. Considerable variation can be expected in these values due to the density of the vegetation, the moisture content of the leaves, and the presence of snow on the branches. An increase of 0.1 dB/m has been observed for the higher-frequency part of the curve.

Other sources state that trees intercepting the first Fresnel zone in the vertical plane tend to produce a loss of close to 6 dB. In order to minimize losses, it is suggested that LOS paths should have better than grazing clearance even under the most adverse atmospheric (refractive) conditions.

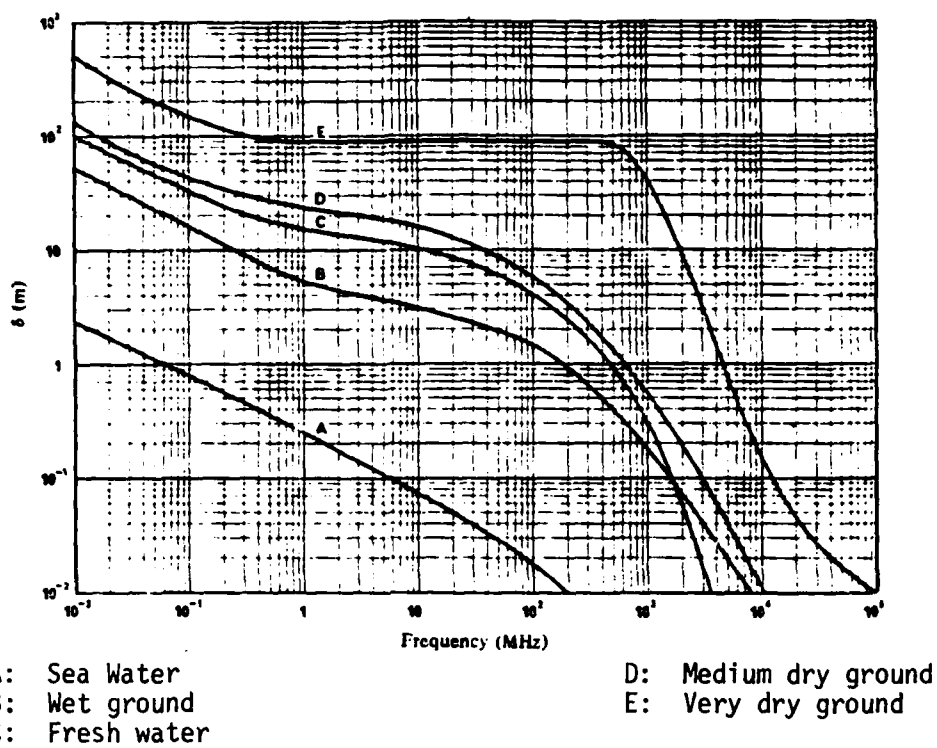


Figure I-3. Penetration Depth

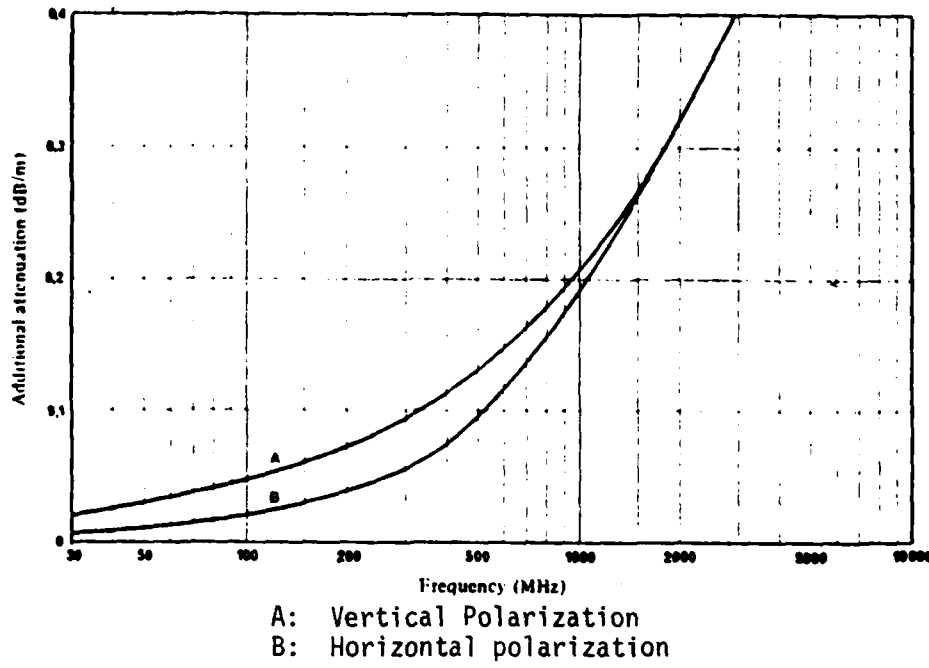


Figure I-4. Additional Attenuation Through Woods

I.5 PATH GEOMETRY

Several figures have been included for the path geometry of several propagation modes which are influenced by the terrain. Figures I-5 through I-7 provide the path geometries and associated symbols for the LOS, diffraction, and troposcatter modes of radio propagation along the great-circle path.

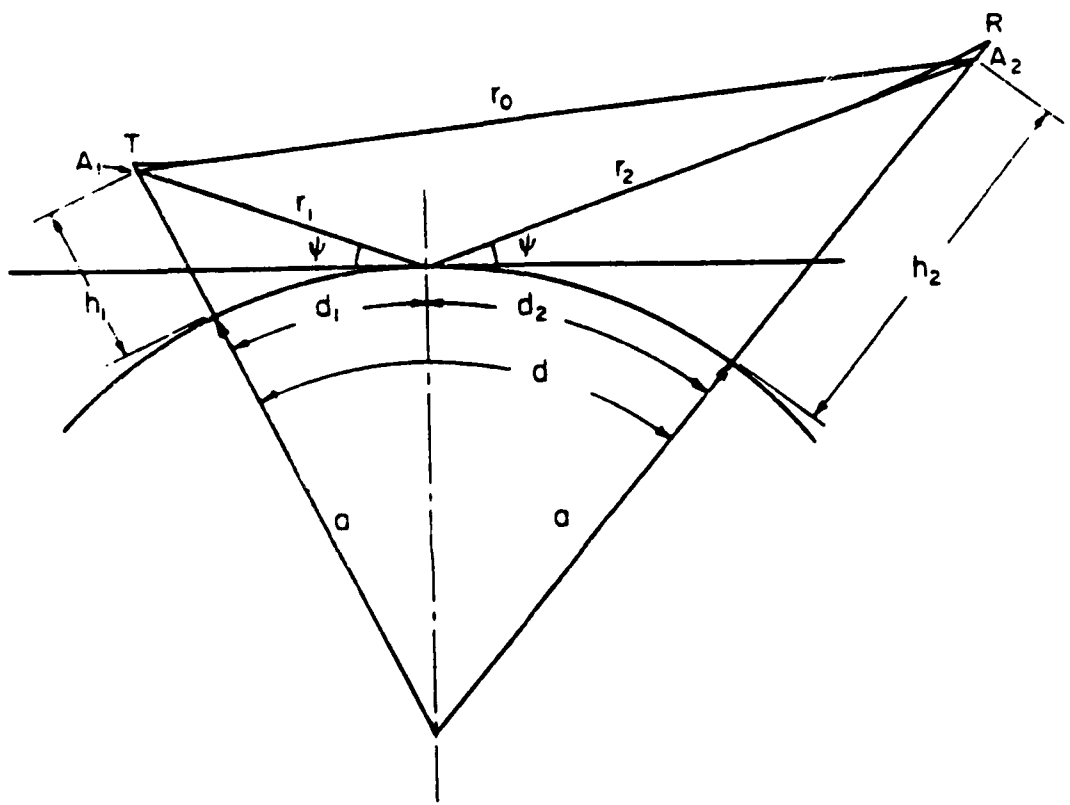
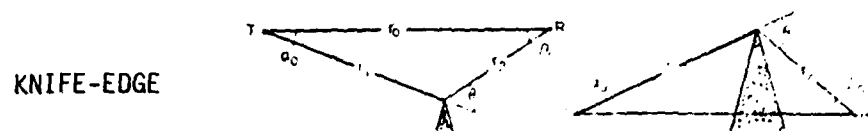
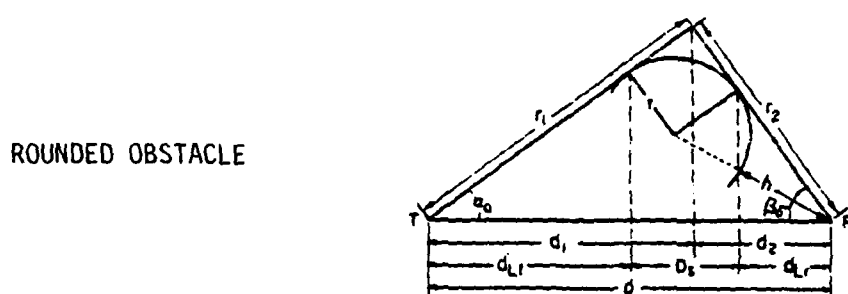


Figure I-5. Terrestrial Line-of-Sight (LOS) Path Geometry



KNIFE-EDGE



ROUNDED OBSTACLE

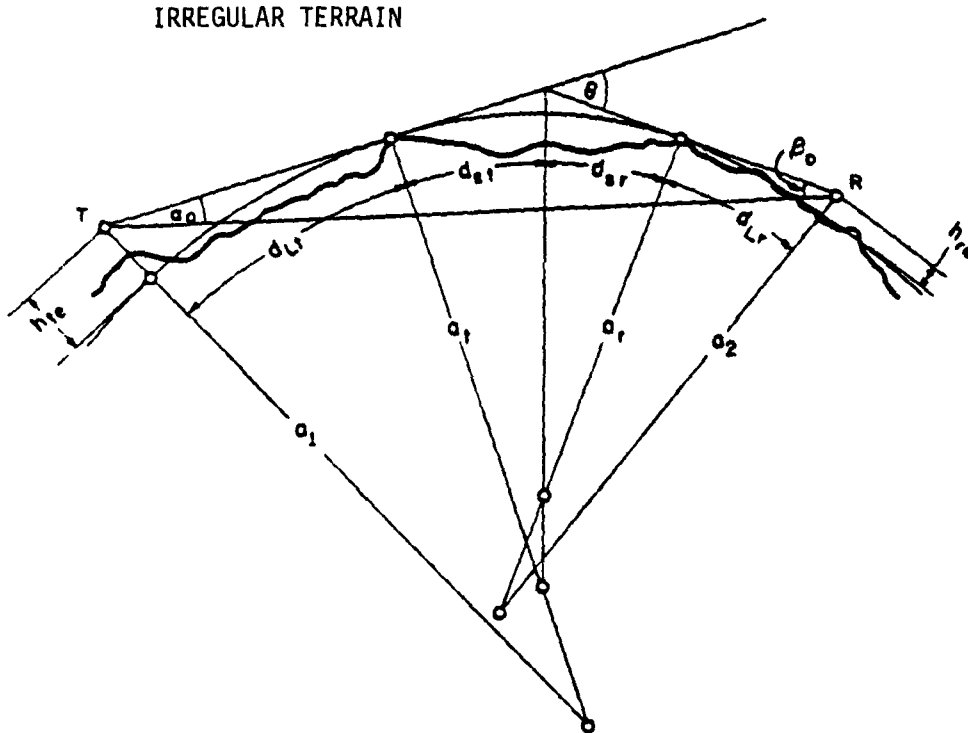


Figure I-6. Additional Attenuation Through Woods

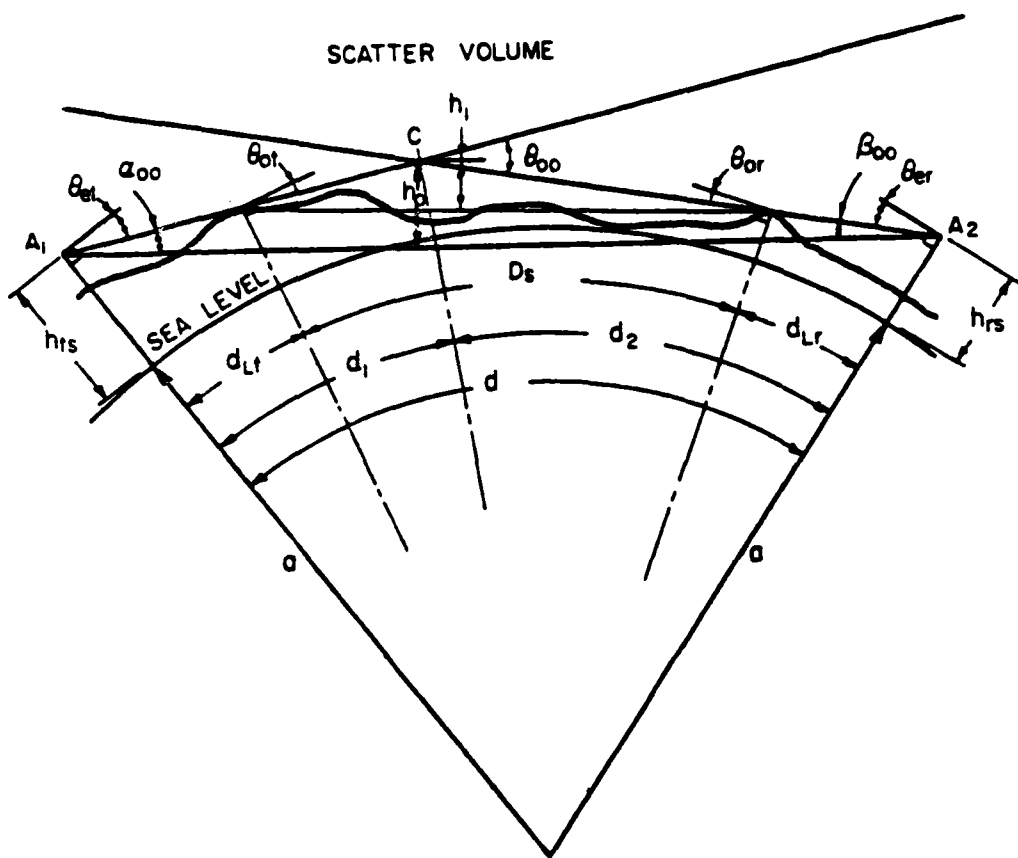


Figure I-7. Tropospheric Scatter Path Geometry

THIS PAGE INTENTIONALLY LEFT BLANK

SUPPLEMENT II SYNOPSIS OF CLIMATIC
CONSIDERATIONS FOR THE DCS

THIS PAGE INTENTIONALLY LEFT BLANK

TABLE OF CONTENTS

	<u>Page</u>
II.1 GENERAL	II-1
II.2 STRATIFICATION OF THE EARTH'S ATMOSPHERE	II-1
II.3 TROPOSPHERIC REFRACTION CONSIDERATIONS	II-8
II.3.1 The Refractive Index, Refractivity, and Refractive Gradient	II-9
II.3.2 Effective Earth Radius in an Exponential Atmosphere	II-11
II.3.3 The Effective Earth Radius Factor	II-11
II.3.4 Variations in "k" and the Refractive Gradient	II-13
II.3.5 Clearance Criteria	II-20
II.3.6 Ducting	II-21
II.3.7 Climate Type Considerations	II-22
II.3.8 Ray-Bending for Earth-Space Paths	II-39
II.4 ATTENUATION BY RAINFALL AND OTHER HYDROMETEORS	II-40
II.4.1 Statistical Characteristics of Rainfall at a Point	II-40
II.4.2 Spatial Characteristics of Rainfall	II-43
II.4.3 Attenuation and Scattering by Hydrometeors	II-50
II.5 CONSIDERATIONS OF ATMOSPHERIC GASES	II-59
II.6 ATTENUATION AND USE OF THE SPECTRUM	II-66

LIST OF FIGURES

	<u>Page</u>
II-1 Stratification of the Earth's Atmosphere	II-2
II-2 Mean Altitude (km) of the Tropopause, February	II-4
II-3 Mean Altitude (km) of the Topopause, May	II-4
II-4 Mean Altitude (km) of the Tropopause, August	II-5
II-5 Mean Altitude (km) of the Tropopause, November	II-5
II-6 Mean Values of N_o , February	II-8
II-7 Mean Values of N_o , August	II-9
II-8 Minimum Monthly Values of N_o	II-10
II-9 Minimum Effective "k" for 99.9 Percent of Time	II-12
II-10 Refractivity Gradient and "k" at Samsun, Turkey	II-14
II-11 Refractive Gradient and "k" at Bitburg, West Germany . .	II-15
II-12 Refractivity Gradient and "k" at Gross Rohrheim, West Germany	II-16
II-13 Refractivity Gradient and "k" at Stuttgart, West Germany	II-17
II-14 Refractivity Gradient and "k" at Wiesbaden, West Germany	II-18
II-15 Refractivity Gradient and "k" at Lihue, Kauai, Hawaii	II-19
II-16 Percent of Time Trapping Frequency is less than 300 MHz, February	II-23
II-17 Percent of Time Trapping Frequency is less than 300 MHz, May	II-24
II-18 Percent of Time Trapping Frequency is less than 300 MHz, August	II-25
II-19 Percent of Time Trapping Frequency is less than 300 MHz, November	II-26

LIST OF FIGURES (Continued)

II-20	Percent of Time Trapping Frequency is less than 1 GHz, February	II-27
II-21	Percent of Time Trapping Frequency is less than 1 GHz, May	II-28
II-22	Percent of Time Trapping Frequency is less than 1 GHz, August	II-29
II-23	Percent of Time Trapping Frequency is less than 1 GHz, November	II-30
II-24	Percent of Time Frequency is less than 3 GHz, February	II-31
II-25	Percent of Time Trapping Frequency is less than 3 GHz, May	II-32
II-26	Percent of Time Trapping Frequency is less than 3 GHz, August	II-33
II-27	Percent of Time Trapping Frequency is less than 3 GHz, November	II-34
II-28	Rain-Climate Zones of the CCIR	II-41
II-29	Percent of Average Year Rainfall Rate is Exceeded for Rain Climates	II-42
II-30	Rainfall-Rate Distribution for Darmstadt, West Germany	II-44
II-31	Rainfall-Rate Distribution for Freiburg, West Germany . .	II-45
II-32	Rainfall-Rate Distribution for Karlsruhe, West Germany	II-46
II-33	Rainfall-Rate Distribution for Koblenz, West Germany . .	II-47
II-34	Average Rain Cell Sizes	II-48
II-35	Rain Attenuation Coefficient for Various Rain Rates . . .	II-49
II-36	Rain Attenuation Coefficient Nomograph	II-51
II-37	Reduction Coefficient for Precipitation Intensities . . .	II-53
II-38	Effective Path Length Through a Rainstorm	II-54
II-39	Specific Attenuation Coefficient for Clouds and Fog . . .	II-55

LIST OF FIGURES (Continued)

	<u>Page</u>
II-40 Rain Scatter Distance for 0.01 Percent of Time, Rain-Climate Zone 1	II-56
II-41 Rain Scatter Distance for 0.01 Percent of Time, Rain-Climate Zone 3	II-57
II-42 Rain Scatter for 0.01 Percent of Time, Rain-Climate Zone 5	II-58
II-43 Specific Attenuation Coefficient for Atmospheric Gases	II-60
II-44 Water Vapor Concentration (g/m^3), February	II-61
II-45 Water Vapor Concentration (g/m^3), August	II-62
II-46 Equivalent Path Length (km) for Oxygen Absorption	II-63
II-47 Equivalent Path Length (km) for Water Vapor Absorption	II-64
II-48 Effective Path Distance (km) for Oxygen Absorption . . .	II-65
II-49 Effective Path Distance (km) for Water Vapor Absorption	II-65
II-50 Total One-Way Zenith Attenuation Through the Atmosphere	II-67
II-51 Theoretical Vertical One-Way Attenuation from Specified Heights to the Top of a Moderately Humid Atmosphere	II-68
II-52 Attenuation Due to Rainfall and Gases in the Atmosphere .	II-69

LIST OF TABLES

	<u>Page</u>
II-1 CCIR Climate Types Summary	II-35
II-2 Locations of Data Collection for CCTR Climate Types . . .	II-38
II-3 Ray Bending for Earth/Space Paths	II-39
II-4 Characteristic Values of Parameters for CCIR Rain-Climates Zones (0.01 Percent of Time)	II-43
II-5 Maximum Rain-Cell Heights for CCIR Rain Climate Zones . .	II-50

THIS PAGE INTENTIONALLY LEFT BLANK

SUPPLEMENT II
SYNOPSIS OF CLIMATIC CONSIDERATIONS FOR THE DCS

II.1 GENERAL

When radio waves are propagated horizontally or vertically through the atmosphere, the primary climatic consideration is the structure of the atmosphere within the troposphere. Tropospheric effects include the bending of radio waves due to refraction, attenuation due to hydrometeors (especially rainfall) and atmospheric gases, and scattering due to these constituents.

For the bending of radio waves due to tropospheric refraction, two models of the refractive gradient are presented. The linear model where the refractive gradient is constant with height and the exponential model. The former applies to propagation near the surface of the earth (i.e., terrestrial line-of-sight (LOS) and diffraction paths). The latter model is more appropriate for tropospheric scatter paths where propagation occurs at greater altitudes. For earth-space paths, the refractive gradient is not as significant because propagation is generally in a more vertical direction.

The attenuation and scattering due to tropospheric constituents is significant for all radio propagation modes mentioned above. Methods of predicting their effects are discussed in this supplement.

II.2 STRATIFICATION OF THE EARTH'S ATMOSPHERE

Many of the varied phenomena occurring in the total atmospheric envelope of the earth can generally be grouped by type and altitude. Strong correlations exist between the physical (and optical) properties and altitude. This natural stratification of the atmosphere is illustrated in Figure II-1, wherein the strata are actually spherical shells which surround the earth. The interfaces, designated by the suffix "pause", separating the strata are not sharply defined, particularly at higher altitudes.

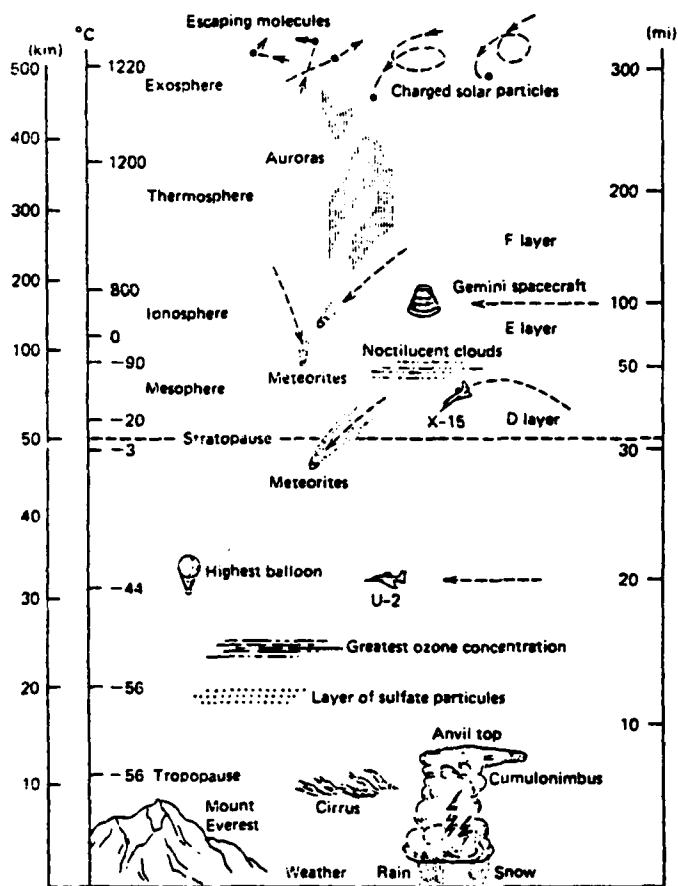


Figure II-1. Stratification of the Earth's Atmosphere

Throughout much of the atmospheric envelope, air pressure and density decrease nearly exponentially as altitude increases whereas temperature generally decreases linearly. Because the main heat source for the lower atmosphere is the sun-heated land-water surface, it is understandable why normally the air is colder with increasing distance from that surface.

Within the troposphere, which extends from the earth's surface to an altitude of about 17 km (10 mi.) over the equator and 9 km (6 mi.) at polar regions, is the turbulent convective layer in which it is concentrated a large percentage of the atmosphere's dust, water vapor, and clouds. Due to the fact that these constituents are essential for weather-making processes, nearly all of the weather phenomena occur in the troposphere.

The layer surrounding the troposphere is the tropopause. The altitude of the summer tropopause is between 15 and 18 km (9 - 11 mi.) over the equator and 8 - 10 km (5 - 6 mi.) at the poles. Figures II-2 through II-5 are world maps showing the mean altitude, in kilometers, of the tropopause for the seasonal months of February, May, August, and November. A nominal altitude of 11 km (7 mi.) may be assumed. The tropopause represents a boundary separating the troposphere (or mixing layer), below which vertical air movement is widespread from the stratosphere (or stratified layer) and above which vertical movement is almost absent.

In the stratosphere, at heights between 24 and 50 km (15 - 31 mi.) where the atmosphere's small amount of ozone is concentrated, temperature rises with altitude. This is because a small fraction of the incoming solar radiation is almost completely absorbed at the top of the ozone layer. Thus, at an altitude of about 50 km (31 mi.), air temperature reaches a second maximum - one which is nearly as high as that of the surface. Although air density in the middle of the stratosphere at about 32 km (52 mi.) is only one-hundredth of its sea level value, manned balloons have ascended to this altitude, which is the usual ceiling for such vehicles. The stratosphere extends to the stratopause located at about 50 km (31 mi.), where air density and pressure are one-thousandth of their sea level values and the temperature is about 0°C (32°F).

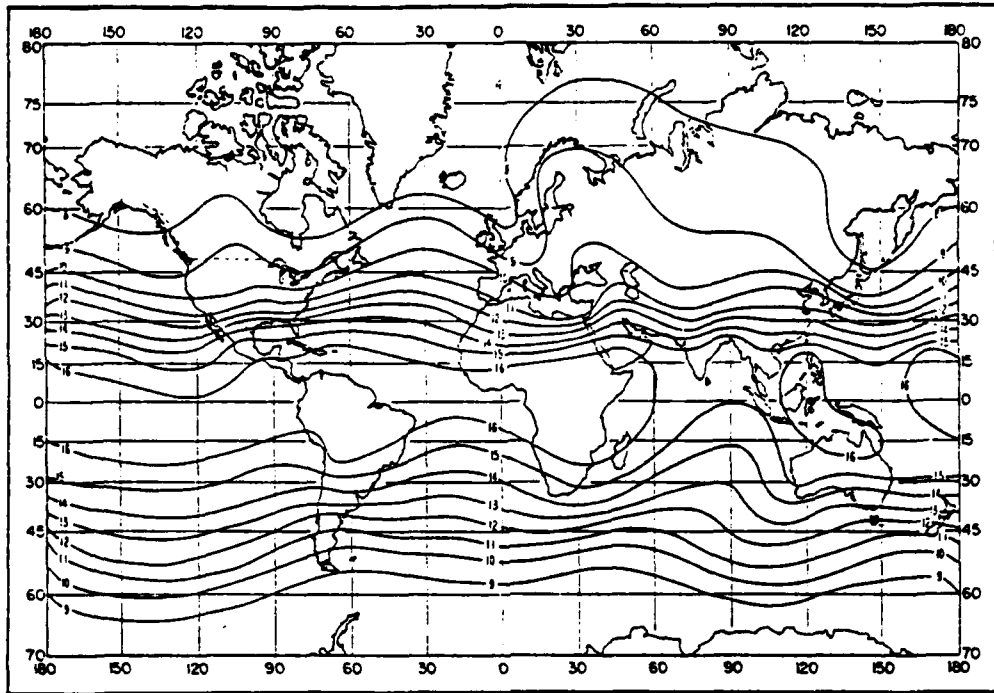


Figure II-2. Mean Altitude (km) of the Tropopause, February

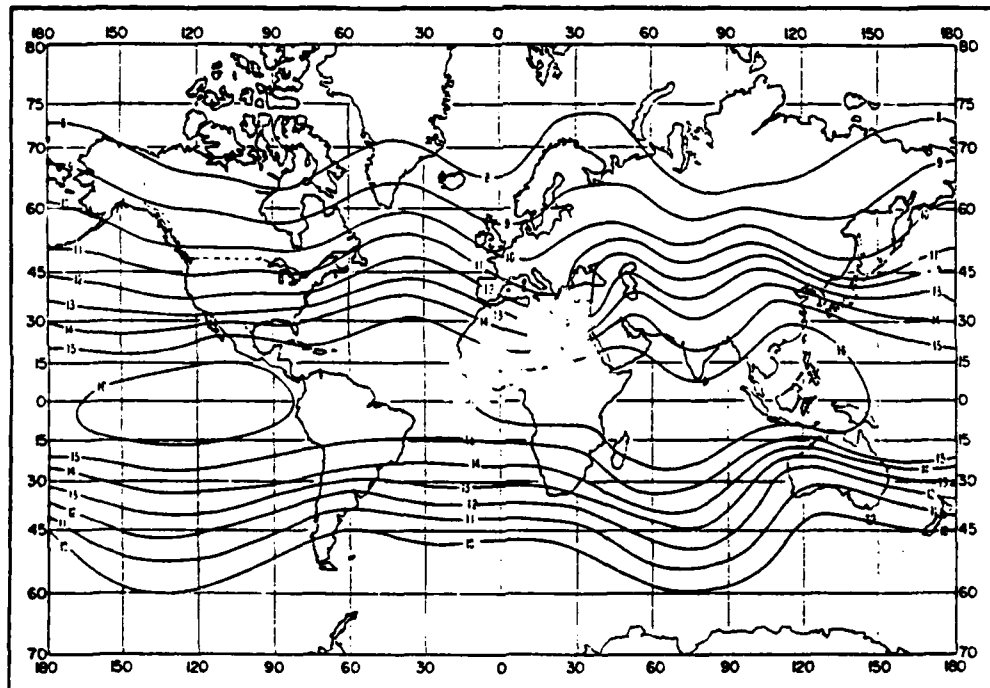


Figure II-3. Mean Altitude (km) of the Tropopause, May

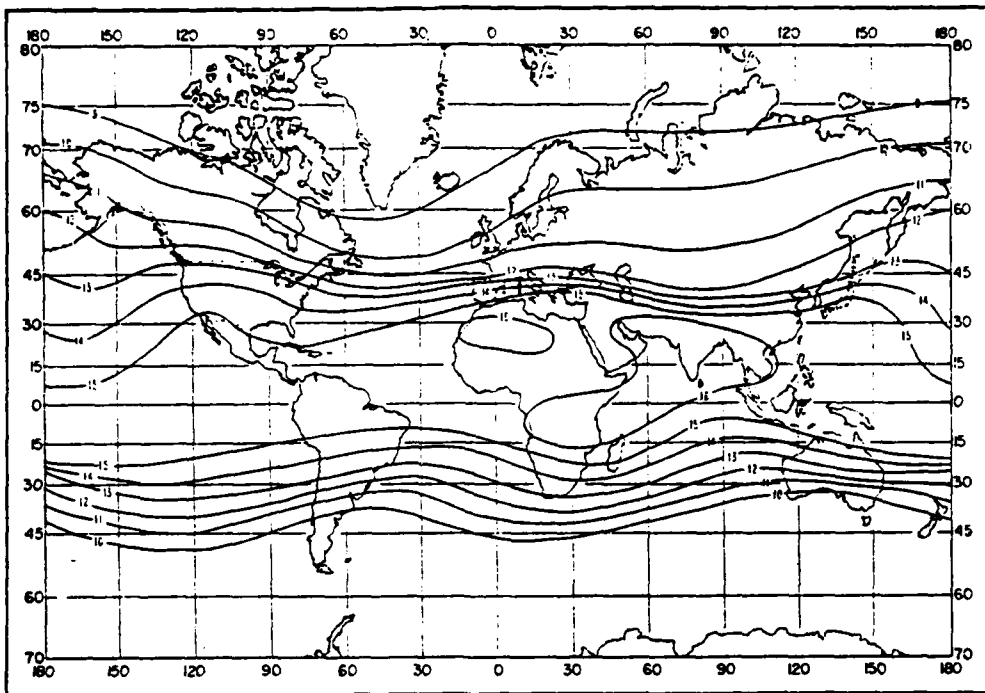


Figure II-4. Mean Altitude (km) of the Tropopause, August

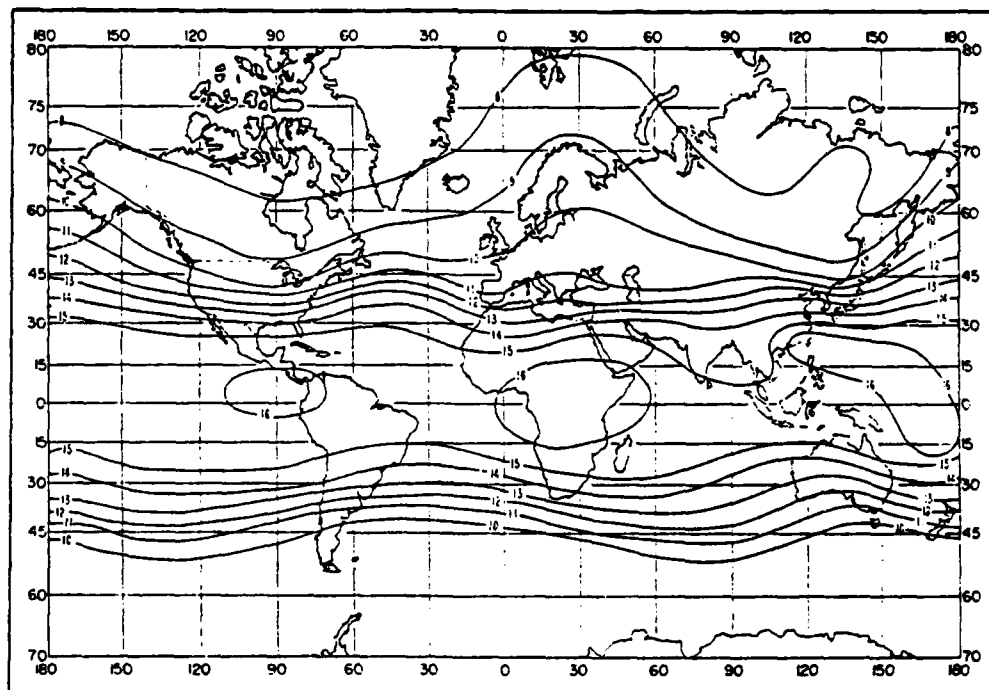


Figure II-5. Mean Altitude (km) of the Tropopause, November

Above is the mesosphere, extending from the stratopause up to 80 km (50 mi.) where the temperature has decreased to about -90°C (-130°F). Most of the meteors that survive swift passage through the outer atmosphere are completely vaporized in this region.

The next layer is the ionosphere, overlapping the upper mesosphere and extending to about 400 km (250 mi.). Lacking the protection of a sensitive layer overhead, the ionosphere is strongly irradiated by solar energy at very short ultraviolet wavelengths and by electrons and protons in the streaming solar winds. Many ionospheric molecules are thereby ionized and dissociated, so that free electrons and atomic oxygen and nitrogen are present. Spectacular auroral displays, or northern lights, occur when bombardment by solar particles is severe. The ionosphere is marked by several identifiable layers of electrons which provide refraction and scattering of radio waves of certain wavelengths.

Above is the thermosphere with temperatures exceeding 1000°C (1800°F) and the exosphere, with the upper exosphere gradually merging into the interplanetary environment.

II.3 TROPOSPHERIC REFRACTION CONSIDERATIONS

Light visually demonstrates how high-frequency radiant energy is refracted (or bent) when it passes from one medium to another having a different density, approaching the more dense medium at an angle other than normal.

This effect may be realized for a radio wave propagating in a horizontal direction as it passes through the troposphere when the atmospheric density is reduced with altitude. (Actually, the atmospheric density is a function of the atmospheric pressure, water vapor pressure, and temperature.) When the top of the wavefront travels in a less dense atmosphere than the bottom of the wavefront, the top travels faster than the bottom, causing the radio wave to bend downward instead of propagating in a straight line, thereby increasing the radio horizon.

II.3.1 Refractive Index, Refractivity, and Refractive Gradient

A 1978 recommendation of the CCIR is that the atmospheric radio refractive index, n , be given by the following formula:

$$n = 1 + (N \times 10^{-6}) \quad (1)$$

where N is the radio refractivity expressed by

$$N = \frac{77.6}{T} \left(P + 4810 \frac{e}{T} \right) \quad (2)$$

where P = atmospheric pressure (mb)

e = water vapor pressure (mb)

T = absolute temperature ($^{\circ}$ K)

Near the ground, up to several hundred meters, the variation of radio refractivity, N , with altitude, h , may be assumed to be linear (i.e., the gradient N is constant). For higher altitudes, an exponential variation of N with h is reported to be statistically more appropriate. The empirical relationship that has been established between the mean value of refractivity at the earth's surface, N_s , and the mean refractive gradient, N , in the first kilometer above the surfaces,

$$N/km = -7.32 \exp (0.005577 N_s) \quad (3)$$

A normal gradient is equivalent to a gradient of about -40 N-units/km over a specified interval, usually assumed to be 100 meters (330 ft.).

For tropospheric scatter propagation, a correlation has been found between the hourly median propagation loss and the monthly mean value of surface refractivity at the altitude of the horizon obstacles. Therefore, N_s may be used to characterize world climatic regions for the purpose of estimating tropospheric scatter losses.

The sea-level value of refractivity, N_0 , may be used to eliminate a height dependence. Worldwide mean values of N_0 for February and August are presented in Figures II-6 and II-7 respectively. Figure II-8 shows the worldwide minimum monthly values of N_0 . The relation between N_s and N_0 is reported to have the form

$$N_s = N_0 \exp (-0.1057 h_s) \quad (4)$$

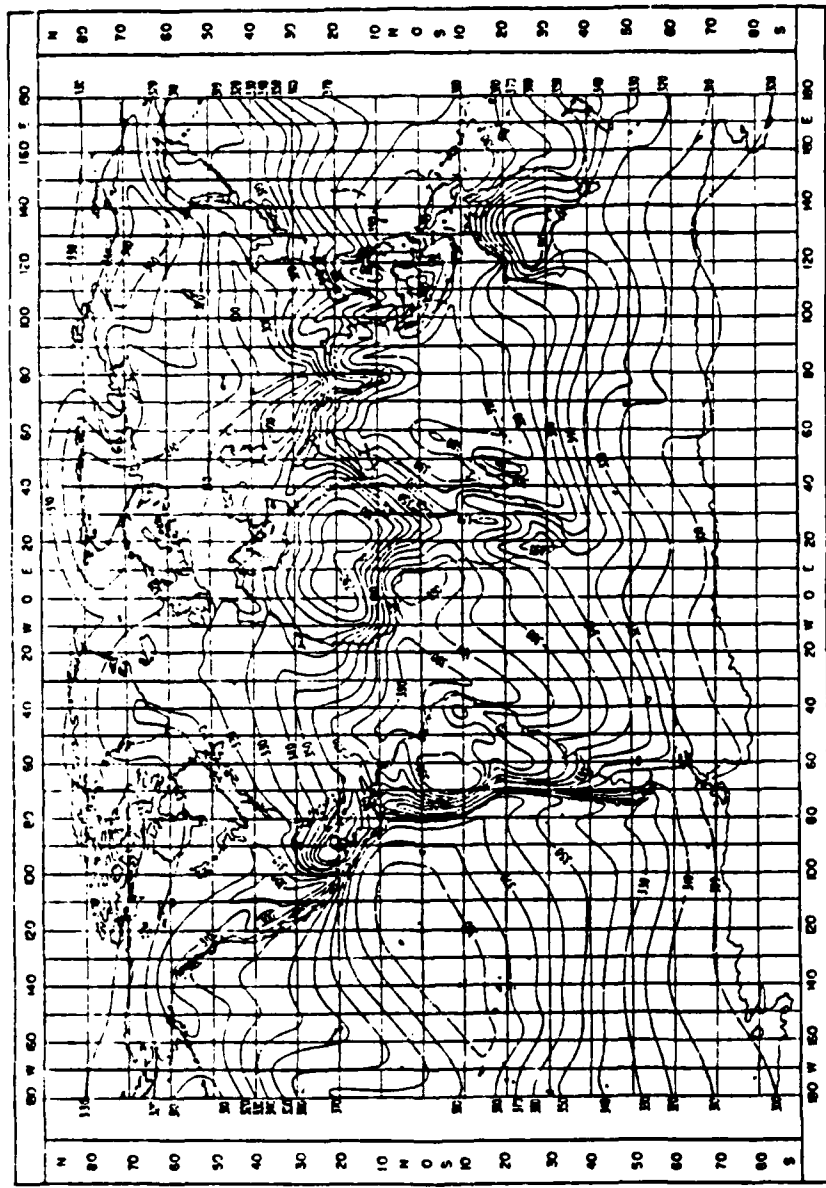
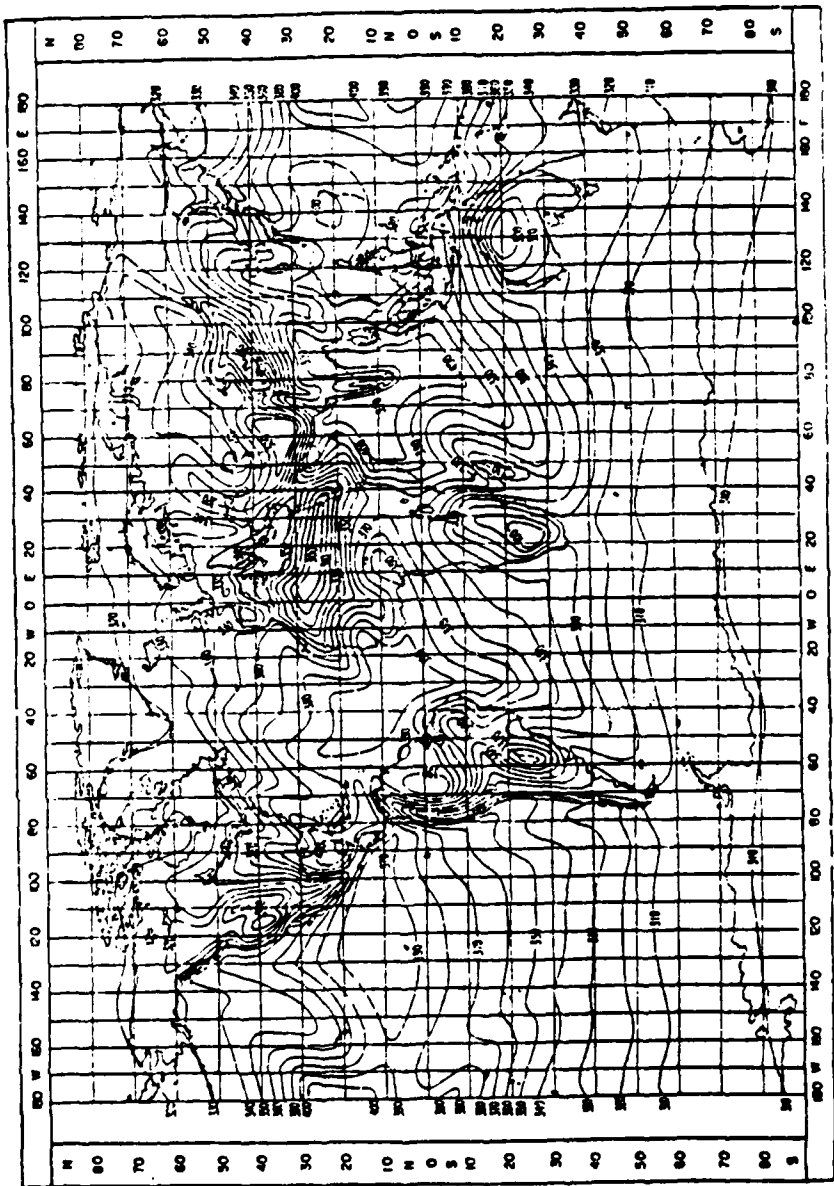


Figure II-6. Mean Values of N_0 , February

Figure II-7. Mean Values of N_o , August



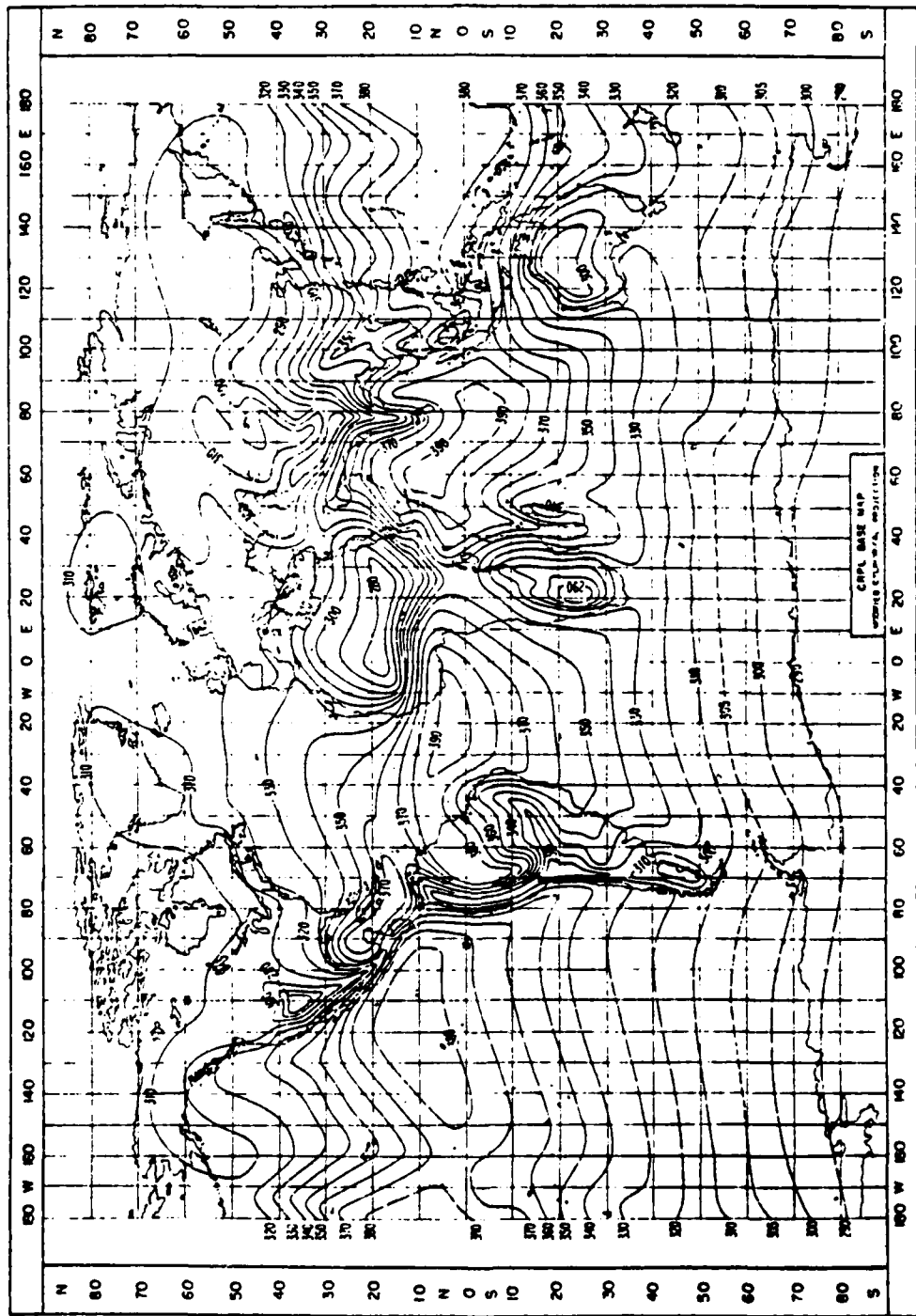


Figure III-8. Minimum Monthly Values of N_0

where h_s is the elevation of the surface of the earth above mean sea level, in kilometers and N_0 is taken from Figure II-8. The latter figure indicates that Turkey has a minimum monthly mean value of N_0 ranging from 300 to 320 N-units, the area of interest in Germany has an approximate value of 320 N-units, and 350-N units is the value for Hawaii. In the northern temperature zones in such as Turkey and Germany field strengths and values of N_s reach minimum values during winter afternoons.

II.3.2 Effective Earth Radius in an Exponential Atmosphere

The concept of the effective earth radius is to alter the radius of the earth on path profiles so that radio waves which normally bend downward in the atmosphere may be represented as radio rays by straight lines. The effective earth radius, a , for an exponential atmosphere is given by the expression

$$a = a_0 \left[1 - 0.04665 \exp (0.005577 N_s) \right]^{-1} \quad (5)$$

where a_0 is the true earth radius in kilometers. Generally, 6370 km is used as the true radius of the earth.

Most of the refraction of a radio wave takes place at low elevations, so it is appropriate to determine N_0 and h_s (or N_s if that value is known) for locations corresponding to the lowest elevation of the radio wave's most important propagation path, normally the great-circle path.

II.3.3 The Effective Earth Radius Factor

If the gradient N is constant (i.e., a linear atmospheric model) a radio wave will bend with a constant curvature. For this condition the effective earth radius is given by the expression

$$a = k a_0 \quad (6)$$

where a_0 is the true earth radius in kilometers and k is the effective earth radius factor given by the expression

$$k \approx \left[1 + a_0 \frac{N}{h} \times 10^{-6} \right]^{-1} \quad (7)$$

with h in kilometers and other parameters as previously defined.

The value of k defined above from measured parameters taken at a point may not necessarily be the same for another point along the great-circle path. Source statistical analysis is available to provide a cumulative distribution of k for the path from the measured parameters defining k at a point. The CCIR reports a curve of the minimum effective value of k as a function of path length for a continental temperate climate, such as that which is dominant in Germany and most of Turkey, exceeded for approximately 99.9 percent of the time. This curve is presented in Figure II-9.

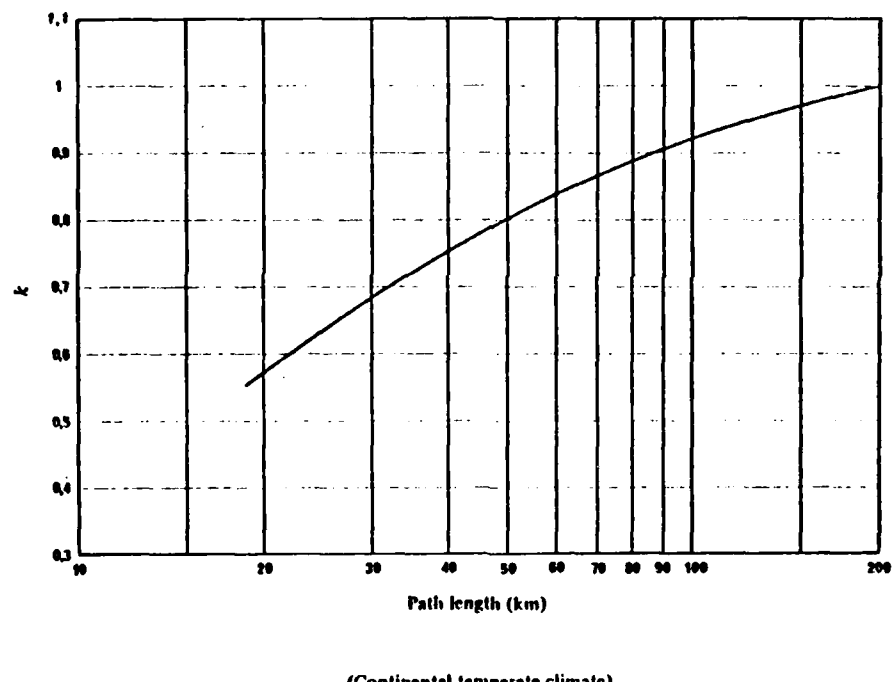
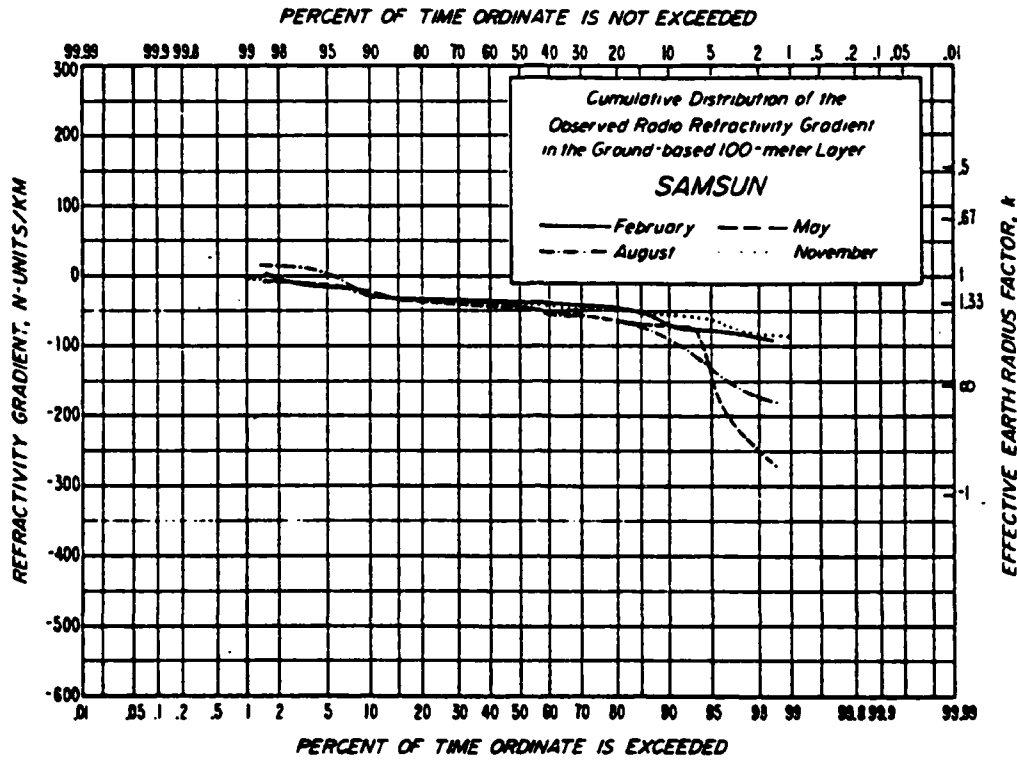


Figure II-9. Minimum Effective "k" for 99.9 Percent of Time

C. A. Samson has provided curves of the cumulative probability distribution based on measured parameters of refractivity at a 100-meter (330 ft.) altitude above the ground. The curves have dual scales to show both the refractivity gradient in N-units/km and the effective earth radius factor, k . The only station within Turkey used to obtain refractivity data was located in Samsun. The resulting curve, shown in Figure II-10, may be representative of the Black Sea coastal region where a maritime climate is dominant, but it is recommended that this curve not be used for other regions of the country. For Germany, several data-gathering stations were located in or near the area of interest. Figures II-11 through II-14 present curves for Bitburg, Gross Ruhrheim, Stuttgart, and Wiesbaden. A curve available for Hanover has not been included because it is in a different geographic region than the area of interest in Germany. Two stations in Hawaii were used to collect weather data, one in Hilo on the island of Hawaii and the other in Lihue on the island of Kauai. A curve from the latter station is presented in Figure II-15 because it is thought to be more representative of the climatic conditions experienced in the area of interest in Hawaii.

II.3.4 Variations in "k" and the Refractive Gradient

As defined by equation (7) above, the point value of k may be determined by the vertical refractive gradient at that point. In usual conditions the refractive gradient is negative, about -40 N-units/km, the radio wave is bent toward the earth, and the radio horizon is increased. This is reflected in the effective earth radius factor $k \approx 4/3$ and defines the condition called normal gradient. Conditions resulting in $k > 4/3$ are said to be superrefractive, with a larger than normal gradient (more negative) causing the radio wave to be bent more downward than with a normal gradient. This condition may be defined as having a gradient of -50 to -100 N-units/km or more. The condition of subrefraction is an increase in refractivity, N , with height (positive gradient) that causes the radio wave to be bent upward. This results in $k < 1$ and is known as an earth-bulge condition. It may result in a decrease of the available clearance above the ground (or obstacles), with fading due to diffraction loss by the earth-bulge.



Samsun, Turkey

41° N, 36° 20' E

44 meters msl

Data: Radiosonde

0300Z (0500 LST): 5/53 - 11/15-53

0200Z (0400 LST): 11/16/53 - 2/57

0000Z (0200 LST): 5/57 - 11/60

Temperature (°F):

January 50/38; July 79/65

Mean Dewpoint (°F):

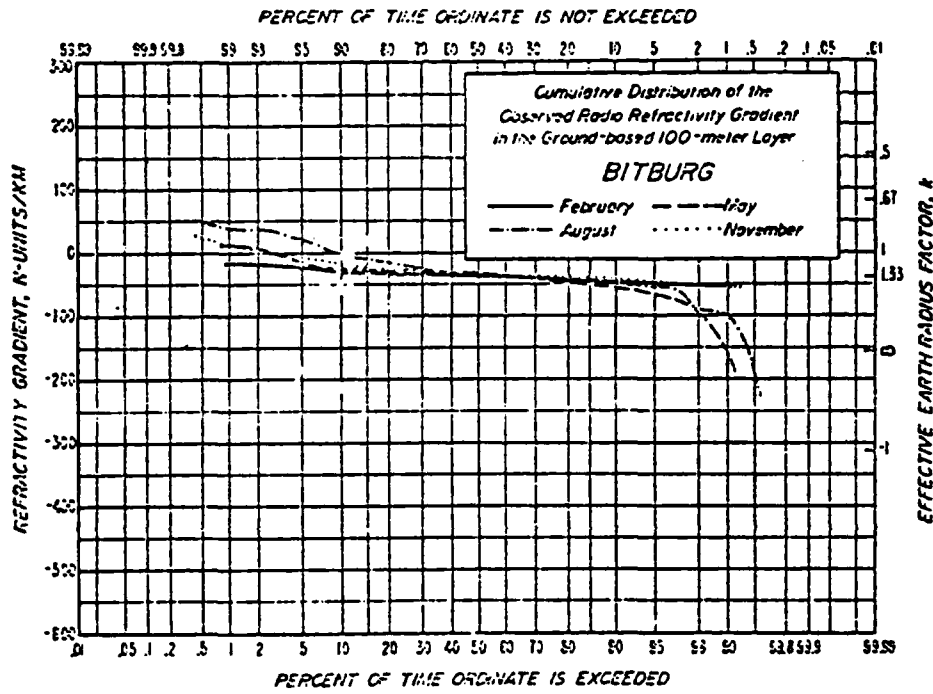
January 33; July 63

Precipitation (inches):

Annual 29.1; November 3.50; August 1.30

Located in an agricultural and forested area on the south shore of the Black Sea; Canik Mountains to the south. A relatively mild predominantly maritime climate.

Figure II-10. Refractivity Gradient and "k" at Samsun, Turkey



Bitburg, Germany (Federal Republic)

49-57 N. 06-31 E 374 meters msl

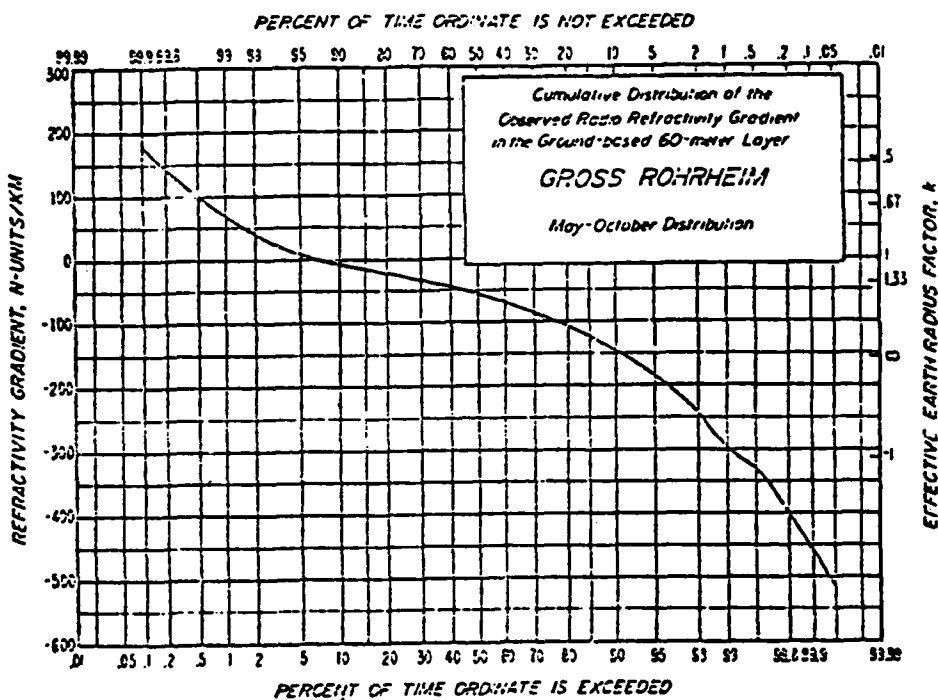
Data: Radiosonde 0300 and 1500Z (0300 and 1500 LST) 12/54 -
Temperature ($^{\circ}$ F): 12/55
January 35/27; July 69/53

Mean Dewpoint ($^{\circ}$ F): January 27; July 53

Precipitation (inches): Annual 24.9; July 2.77; April 1.48

Located in rolling terrain of westert Germany, about 15 miles from
the Moselle River. A cool continental climate modified by frequent
exposure to maritime air masses.

Figure II-11. Refractive Gradient and "k" at Bitburg, West Germany



Gross Rohrheim, Germany (Federal Republic)

49-43 N, 08-28 E

90 meters msl

Data:

60 meter gradients based on 3 hourly dry-
and wet-bulb temperature measurements on a
65-meter tower 20 km southwest of Darmstadt.
June - October 1966; May - October 1967

Analyzed by:

Dr. L. Fehlhaber, Fermeldeotechnisches
Zentralamt, Darmstadt

Temperature ($^{\circ}$ F):

January 38/19; July 75/56

Mean Dewpoint ($^{\circ}$ F):

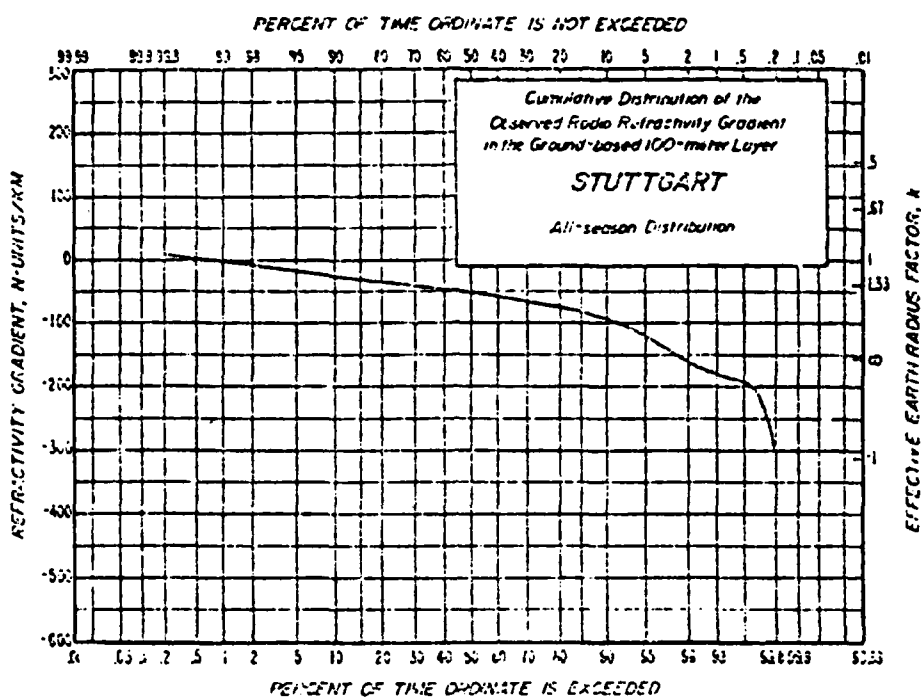
January 29; July 54

Precipitation (inches):

Annual 25.0; July 2.80; February 1.58

Located in the Rhine Valley. A continental climate modified by exposure to maritime air masses.

Figure II-12. Refractivity Gradient and "k" at Gross Rohrheim,
West Germany



Stuttgart, Germany (Federal Republic)

48-50 N, 09-12 E

325 meters msl

Data: Radiosonde

0000 and 2000Z (0100 and 1300 LST) 1961 and 1962

Analyzed by:

Dr. L. Pehlhaber, Fernmeldetechnisches Zentralamt, Darmstadt

Temperature ($^{\circ}$ F):

January 38/28; July 75/57

Mean Dewpoint ($^{\circ}$ F):

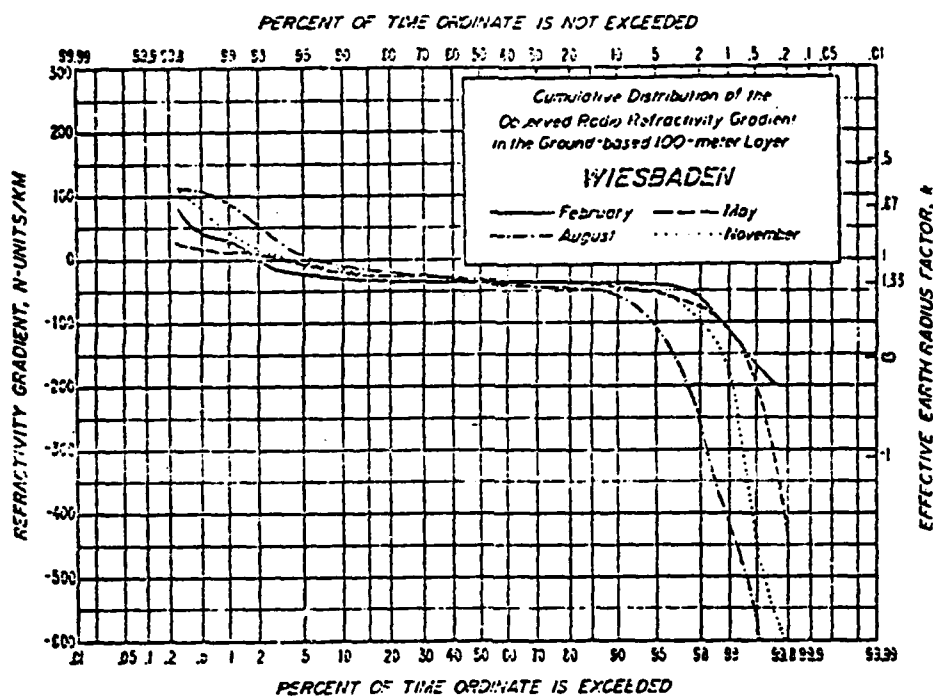
January 27; July 53

Precipitation (inches):

Annual 26.5; June 3.30; February 1.30

Located in the valley of the Neckar River; woods, orchards, and vineyards in vicinity. A continental climate modified by the exposure to maritime air masses.

Figure II-13. Refractivity Gradient and "k" at Stuttgart, West Germany



Wiesbaden, Germany (Federal Republic)

50-03 N, 08-20 E 140 meters ms¹

Data: Radiosonde 0300 and 1500Z (0400 and 1600 LST) 8/50 - 5/57

Analyzed by: Stan Doran, Telecom, Inc., McClean, Virginia

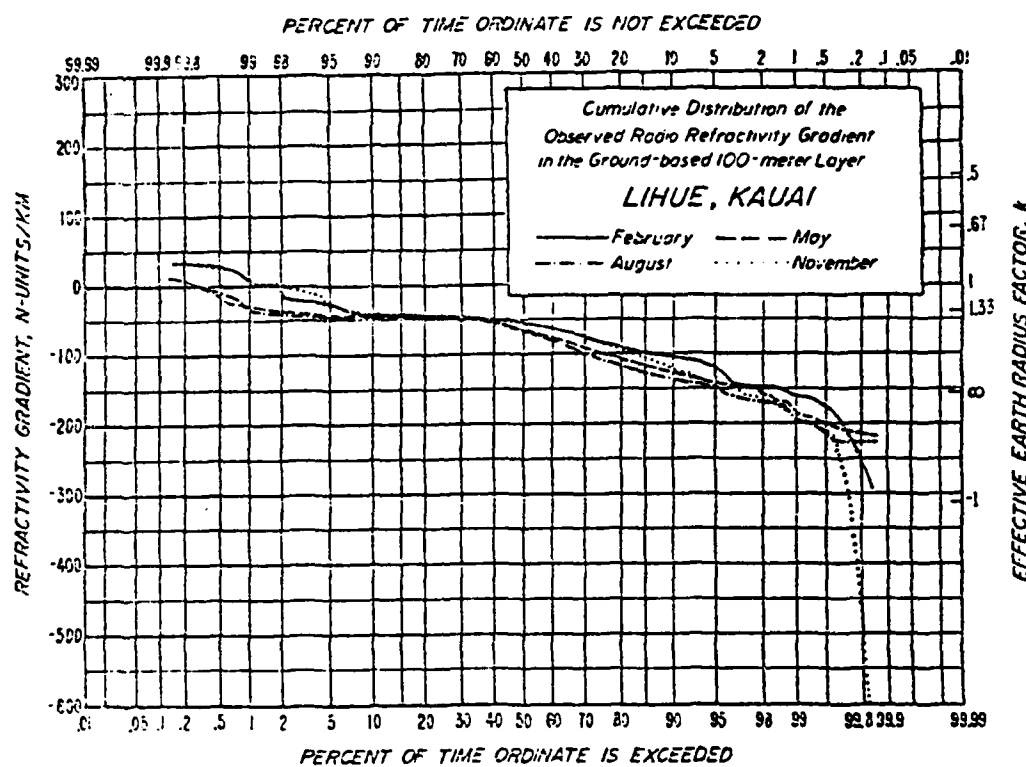
Temperature (⁰F): January 37/28; July 74/57

Mean Dewpoint (⁰F) January 27; July 54

Precipitation (inches): Annual 18.5; August 2.52; April 0.91

Located on the north side of the Rhine Valley, just below the junction of the Rhine with the Main River. A continental climate modified by exposure to maritime air masses.

Figure II-14. Refractivity Gradient and "k" at Wiesbaden, West Germany



Lihue, Kauai, Hawaii

21° 59' N, 159° 21' W

36 meters msl

Data: Radiosonde

0300 and 1500Z (1600 and 0400 LST): 1/51 -

5/57

0000 and 1200Z (1300 and 0100 LST): 6/57 -
12/57

Temperature (°F):

January 78/64; July 83/72

Mean Dewpoint (°F):

January 63; July 68

Precipitation (inches):

Annual 43.0; January 5.51; June 1.46

Located near the eastern shore of a mid-ocean island 53 km long and 40 km wide; in the trade wind belt. Mild maritime climate with small diurnal and annual temperature ranges.

Figure II-15. Refractivity Gradient and "k" at Lihue, Kauai, Hawaii

II.3.5 Clearance Criteria

In order to account for the variation of k and minimize diffraction fading, a standard engineering practice is to establish conditional clearance criteria.

The publication Engineering Considerations for Microwave Communication Systems, 1975, states that in terms of the first Fresnel zone, F_1 (defined in A.3 of this report), the following are typical clearance criteria:

- For "Heavy Route", Highest-Reliability Systems

At least $0.3 F_1$ at $k = 2/3$ and $1.0 F_1$ at $k = 4/3$, whichever is greater. In areas of very difficult propagation, it may be necessary also to ensure a clearance of at least grazing at $k = 1/2$. (For 2-GHz paths above 36 miles, substitute $0.6 F_1$ at $k = 1.0$.)

- For "Light-Route" Systems with Slightly Less Stringent Reliability Requirements

At least $0.6 F_1 + 10$ feet at $k = 1.0$.

The publication Design Objectives for DCS LOS Digital Radio Links, 1977, suggests the following criteria:

- Antenna tower heights on each radio link shall be determined such that the antennas are unobstructed and have a clearance above path terrain and obstacles on the link. The antenna beam path shall meet or exceed the following conditions:

a. For space diversity systems, all top-to-bottom antenna beam paths shall have a 0.3 Fresnel zone clearance for $k = 2/3$, where k is the effective earth's radius factor

b. For non-diversity radio links, the beam path between the single antennas at each end of the link shall have a 0.3 Fresnel zone clearance for $k = 2/3$

c. If year-round refractive index statistics are available for the particular geographic area of concern, all top-to-top antenna beam paths must meet or exceed grazing conditions for 99.99 percent of the year.

II.3.6 Ducting

Ducting is an intensified form of superrefraction (defined in B.3.4) that tends to trap radio waves as though in a waveguide, greatly extending the radio horizon. With a refractive gradient in excess of (more negative than) -157 N-units/km, k becomes negative and radio energy may be refracted to such a degree that it follows the curvature of the earth. If a radio wave is elevated above a minimum angle, reported to range from less than two degrees to less than one-half degree, the radio wave may penetrate or escape the duct.

A duct may be "ground-based" with the ground serving as the ducting base, or may be an "elevated duct." Elevated ducts are usually less important than ground-based ones for tropospheric propagation. The more common ground-based ducts may be caused by subsidence or be formed by the passage of a cold front over a warm, moist ground or body of water at any time of the day or night, but tend to occur most often during clear, calm, cool evenings and early mornings; they seldom occur during the afternoon with its accompanying warmth, low humidity, atmospheric mixing, and air turbulence.

Ducting is characterized by the thickness of the ducting layer and trapping frequency. When the radio operating frequency exceeds the trapping frequency, the mechanism of fading is associated with reflections in the upper and lower bounds of the duct. If both antennas are located above the duct and the bending of the radio wave occurs above it, the radio path clearance may be referred to the top of the duct. With only one antenna inside the duct or interception of the radio wave by it there will be shadow zones resulting in a strong power fading. With both antennas inside the duct, radio energy at frequencies above the trapping frequency will be guided, resulting in a strong, steady received signal.

If economically feasible, in areas of frequent ducting the antenna heights may be designed with enough clearance above the duct. Vertical space diversity may be useful if one of the receive antennas is illuminated while the other is in a shadow zone. Frequency diversity may not be useful unless one of the frequencies is well below the trapping frequency.

Figures II-16 through II-27 show the percent of time ground-based ducts may occur for the seasonal months of February, May, August and November for frequencies of 300 MHz, 1 GHz, and 3 GHz. The figures indicate that trapping may occur 20 percent of the time in Turkey for all three frequencies in August and 10 percent or less for all other months; trapping may occur 2 percent of the time for all four seasonal months in Germany but only during summer months at 3 GHz; trapping may occur for 5 percent of the time in Hawaii in August at 1 and 3 GHz and is less than this value for all other conditions.

II.3.7 Climate Type Considerations

For scattering in the troposphere, statistical data have been correlated with the annual mean value of N_s and the annual range of monthly mean N_s for long-term power fading. Both the long-term median transmission loss and the variability about the long-term median loss are correlated with measured data.

The nine types of climate based on measured data and classified by the CCIR are listed in Table II-1 with a description of each type. Table II-2 defines the location from which the measured data was collected.

Turkey's climate type is predominately temperate. However, due to the contrasting climates found in Turkey, it is not obvious if the appropriate classification for the country is continental temperate or maritime temperate, overland. Turkey experiences prevailing winds which traverse a large land mass, and the terrain is rugged. Therefore, the region more closely fits the classification of continental temperate with some Mediterranean and maritime temperate influences. The climate type for the area of interest in Germany is clearly continental temperate with some of the data for this climate type having been collected in West Germany. For the area of interest in Hawaii, maritime temperate is the appropriate classification.

AD-A101 362

TRW DEFENSE AND SPACE SYSTEMS GROUP REDONDO BEACH CA
EVALUATION OF DCS III TRANSMISSION ALTERNATIVES. PHASE 1A REPORT--ETC(U)
MAY 80 T M CHU
TRW-35142-APP-C

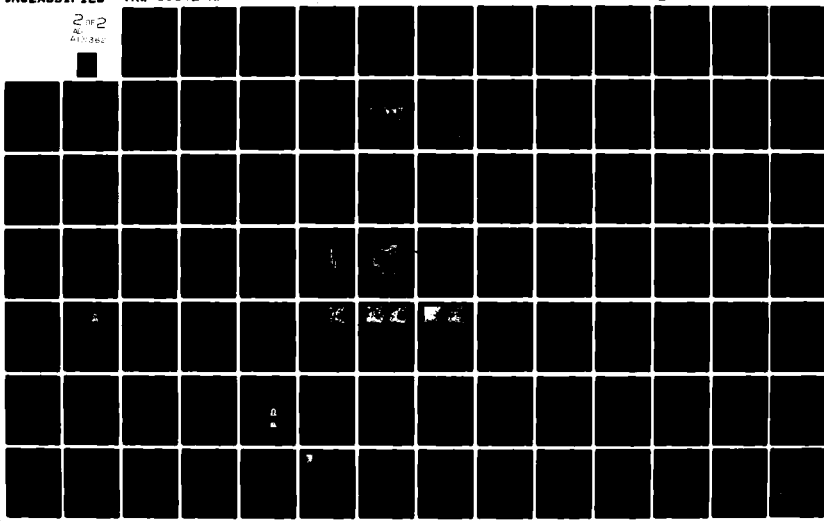
F/G 17/2.1

DCA100-79-C-0044

NL

JNCLASSIFIED

2 of 2
41-362



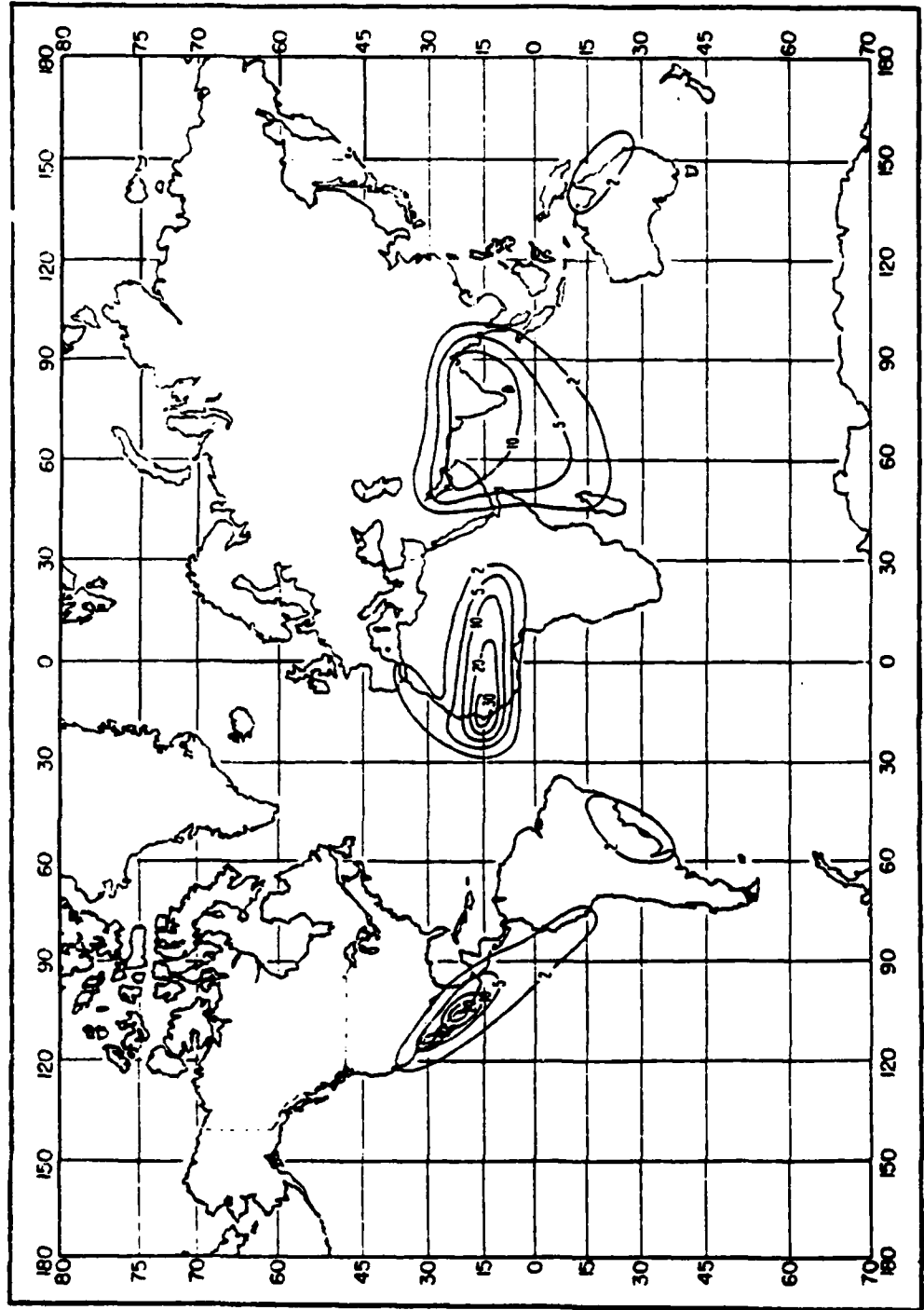


Figure II-16. Percent of Time Trapping Frequency is Less Than 300 MHz, February

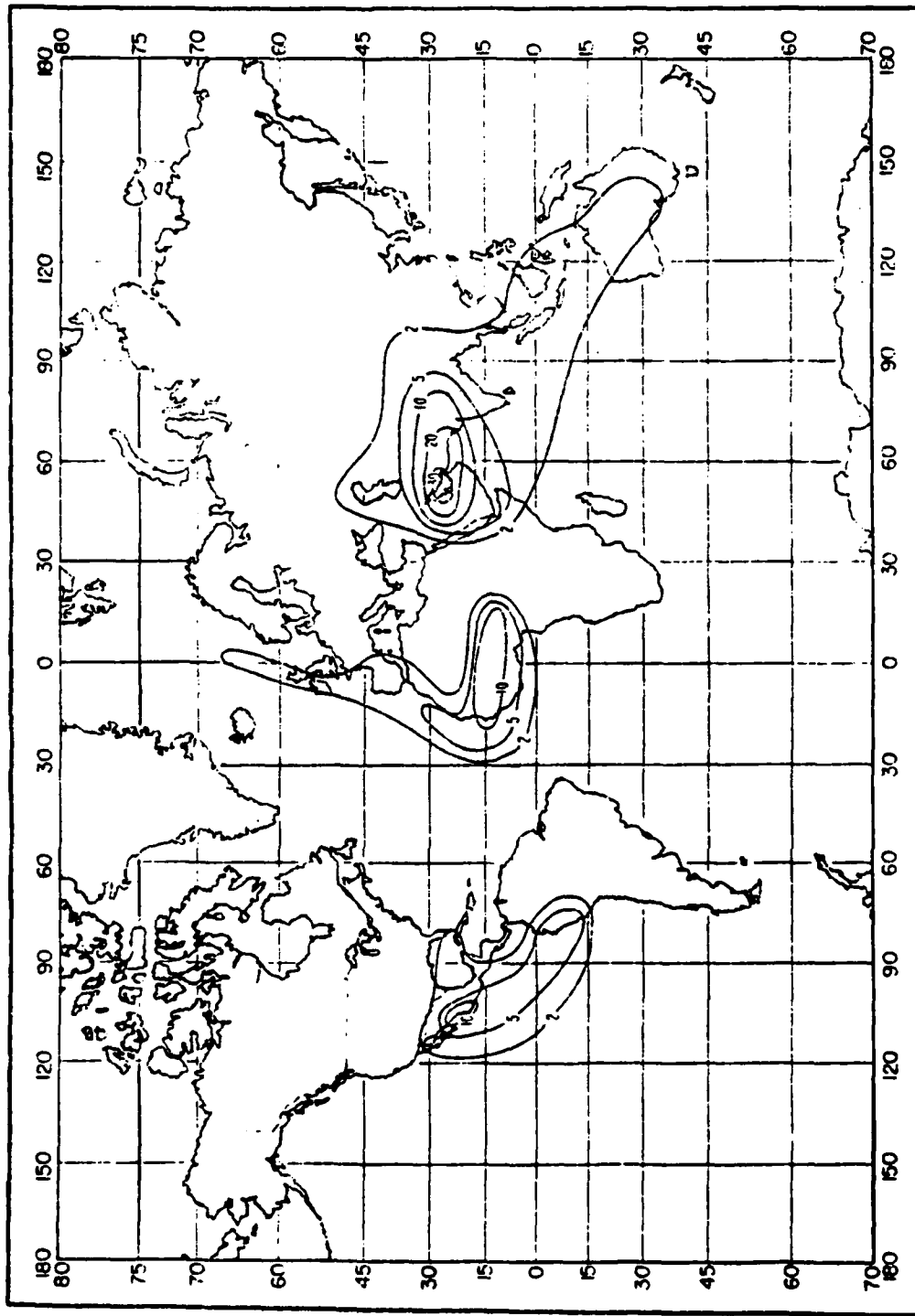


Figure II-17. Percent of Time Trapping Frequency is Less Than 300 MHz, May

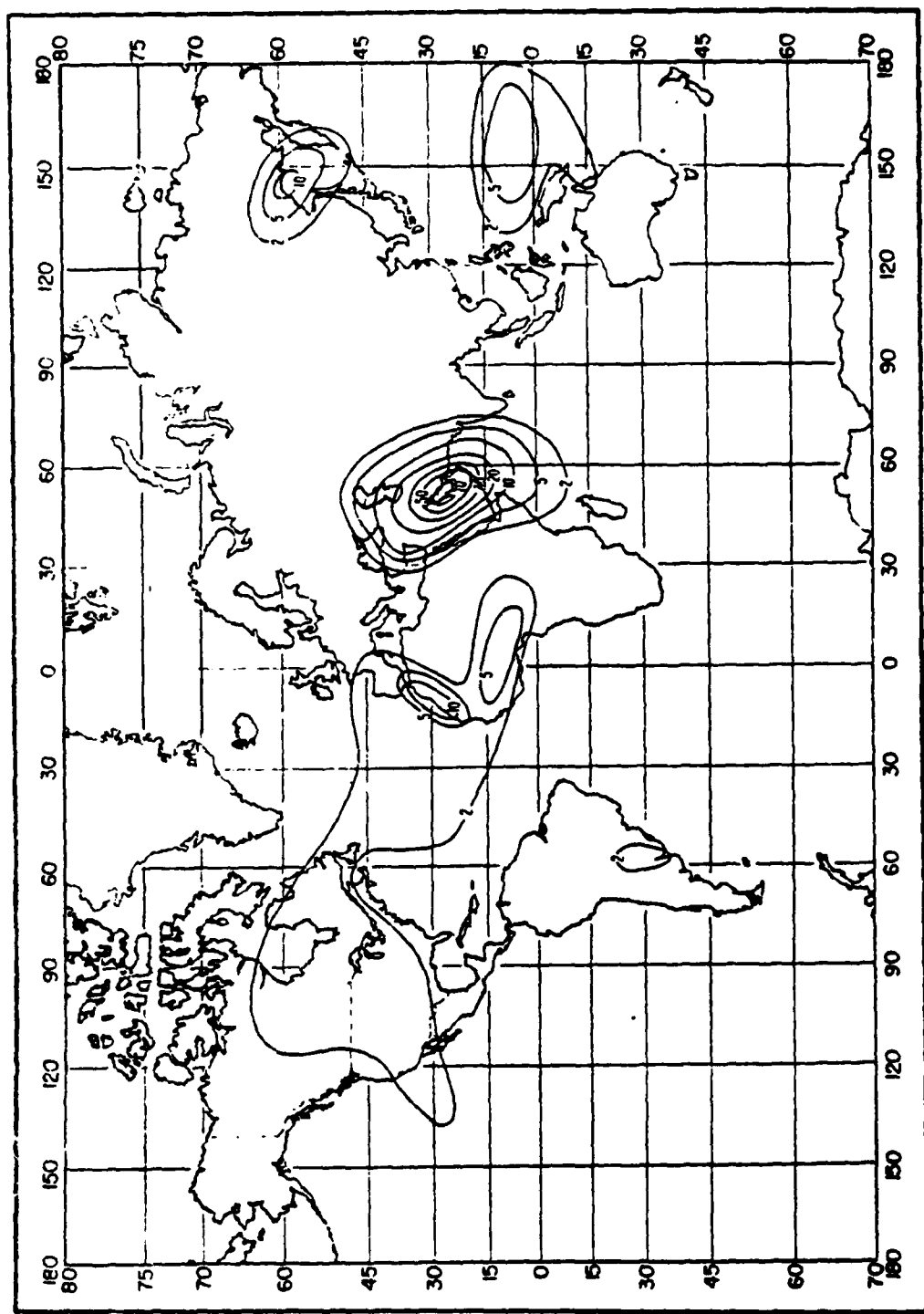


Figure 11-18. Percent of Time Trapping Frequency is Less Than 300 MHz, August

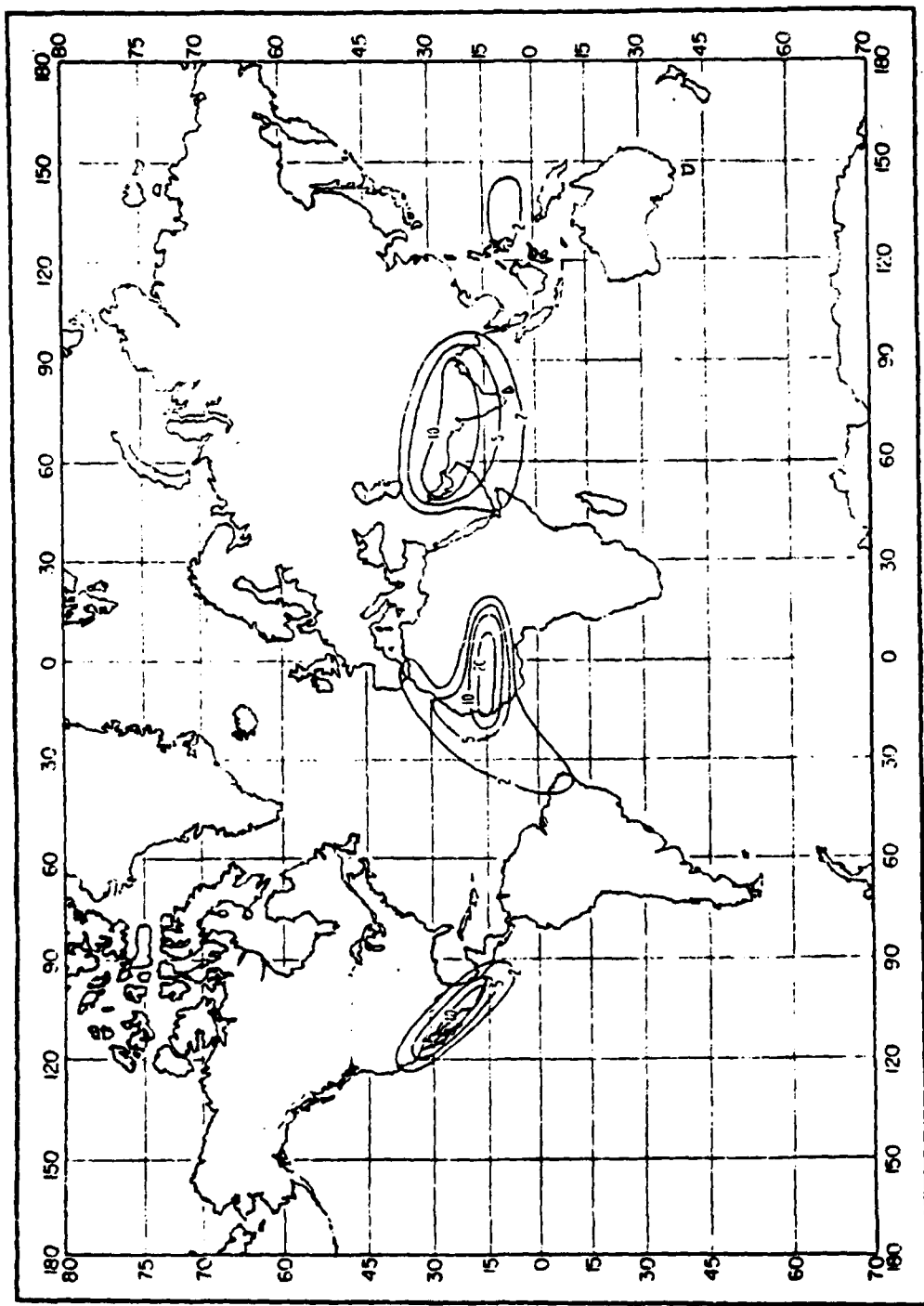


Figure III-19. Percent of Time Trapping Frequency is Less Than 300 MHz, November

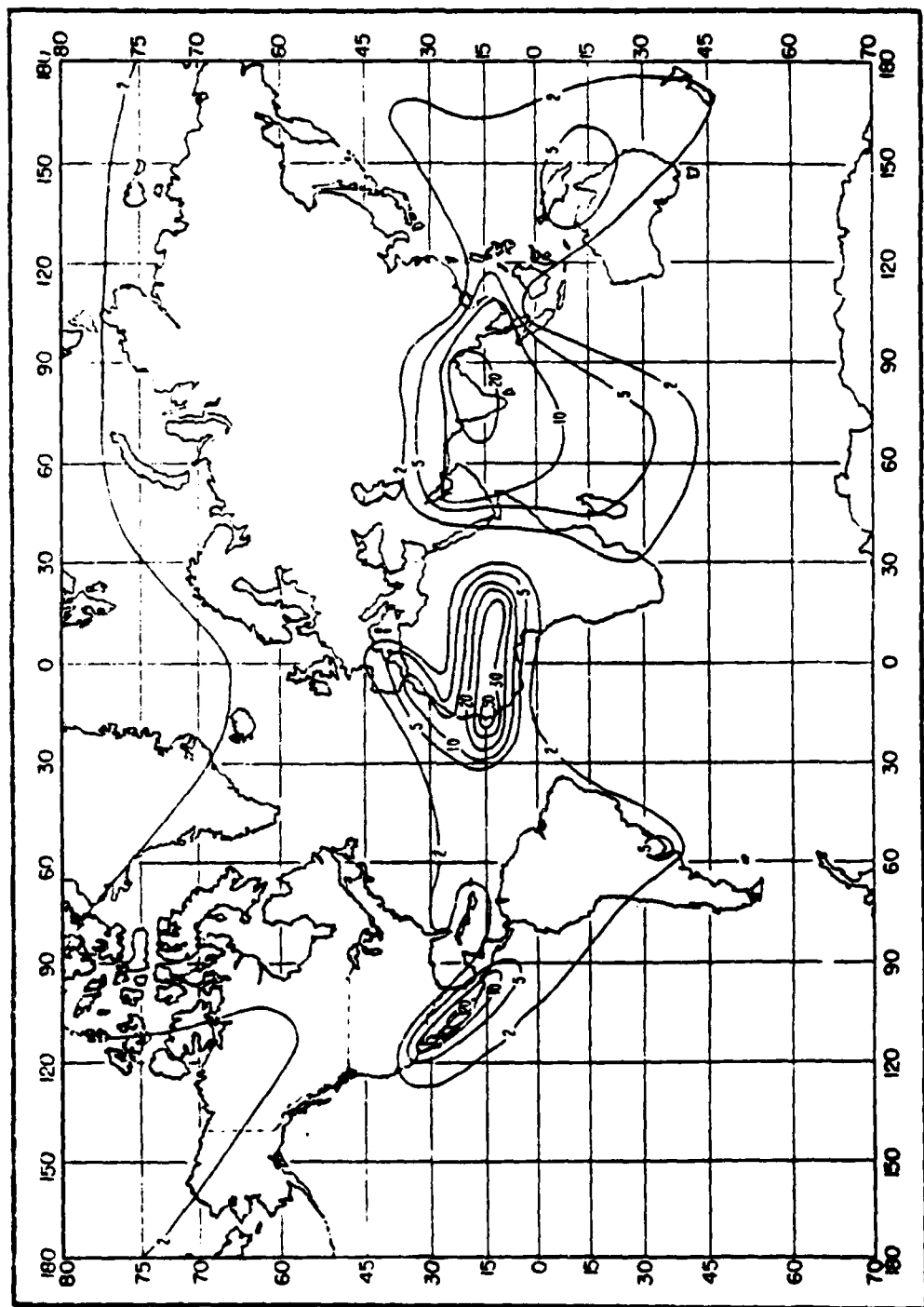


Figure 11-20. Percent of Time Trapping Frequency is Less Than 1 GHz, February

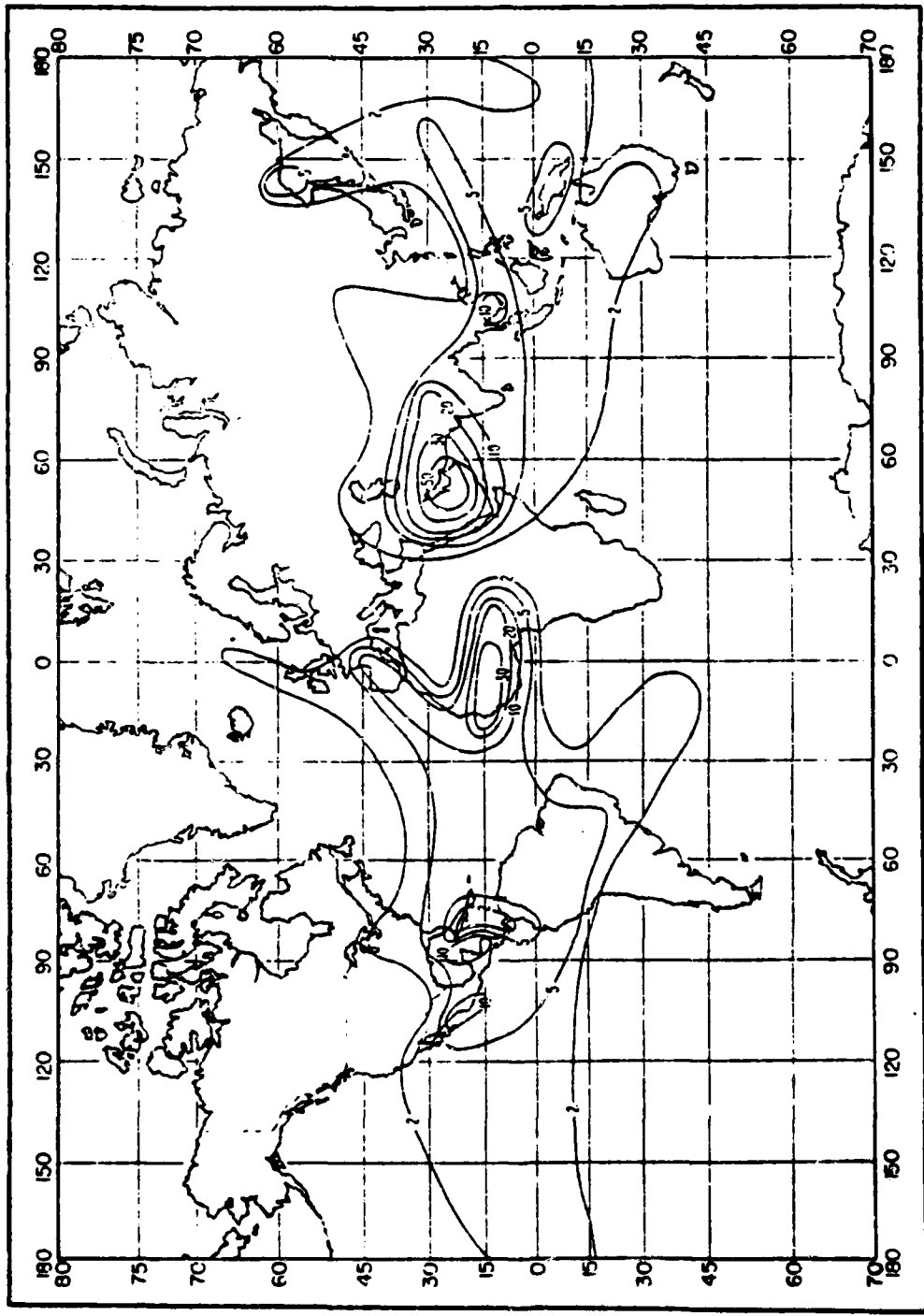


Figure II-21. Percent of Time Trapping Frequency is less Than 1 GHz, May

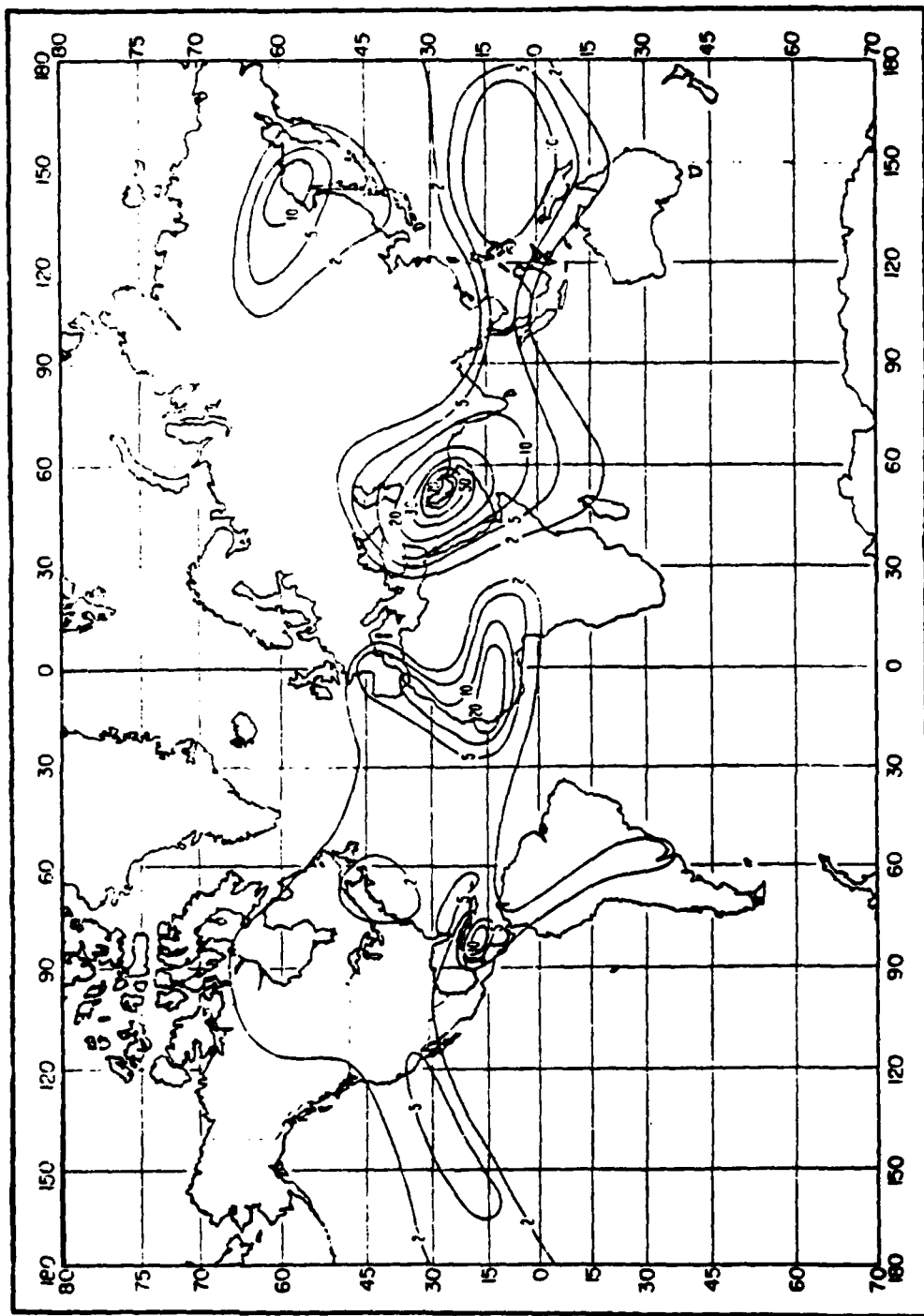


Figure 11-22. Percent of Time Trapping Frequency is Less Than 1 GHz, August

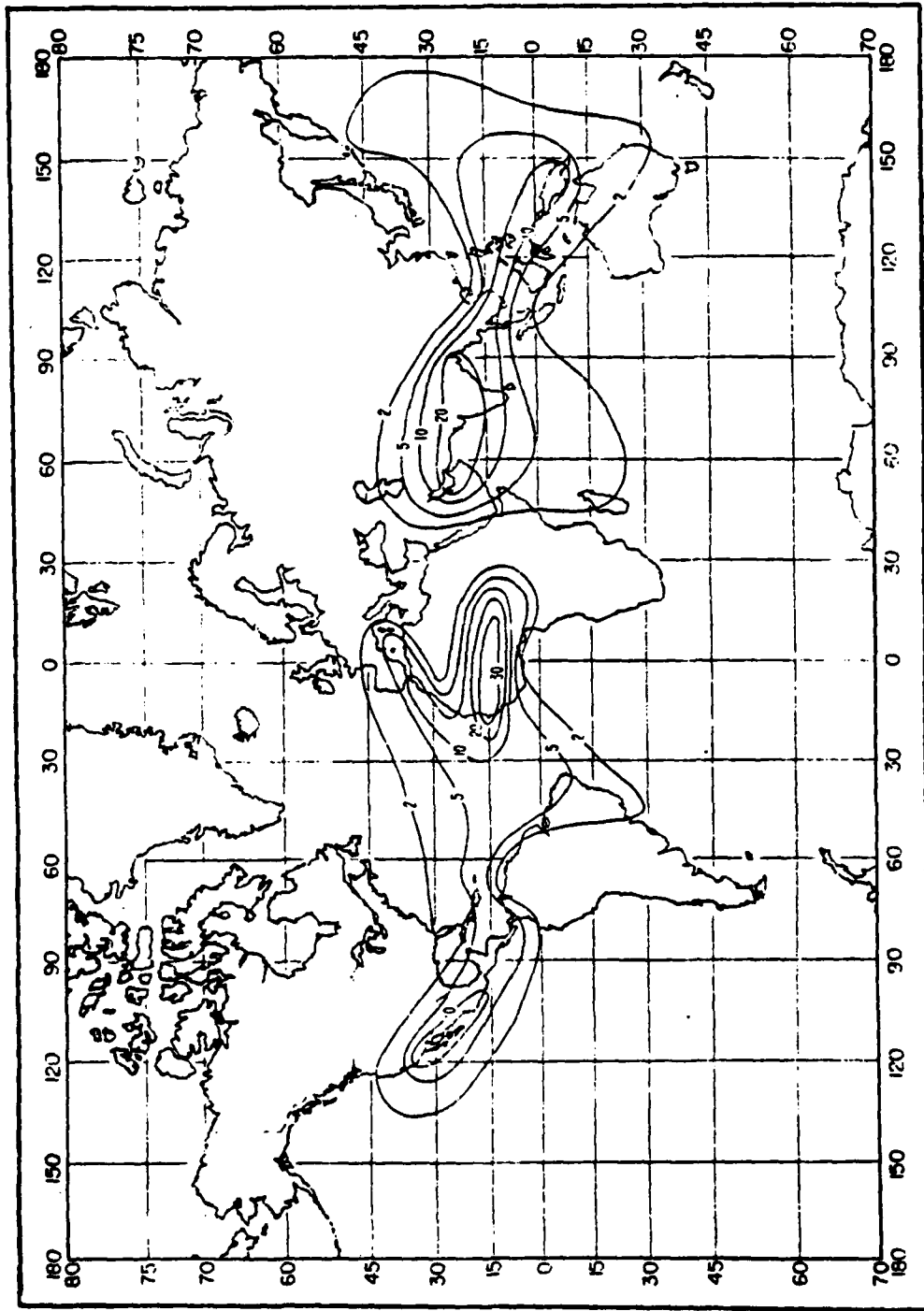


Figure II-23. Percent of Time Trapping Frequency is Less Than 1 GHz, November

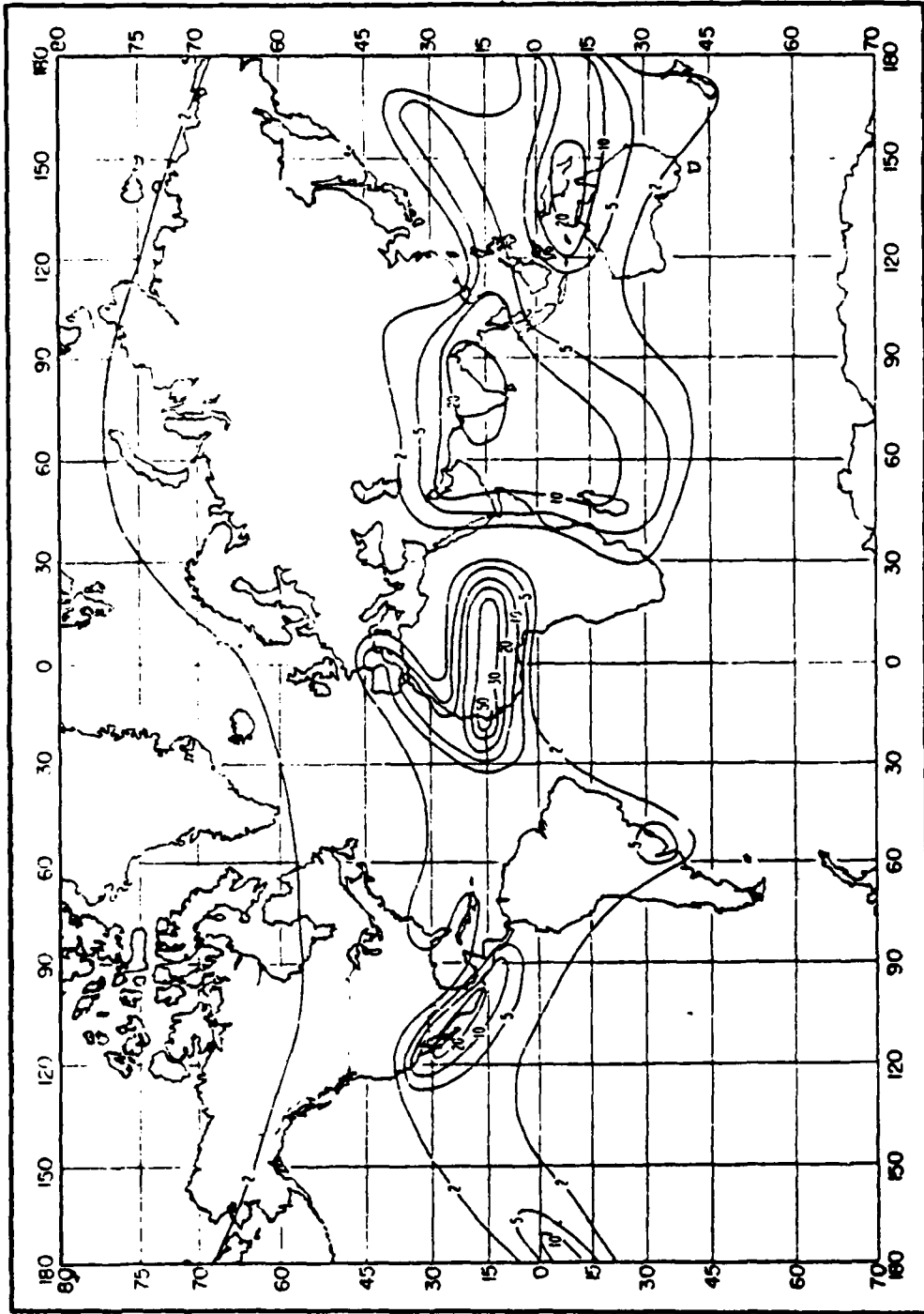


Figure II-24. Percent of Time Trapping Frequency is Less Than 3 GHz, February

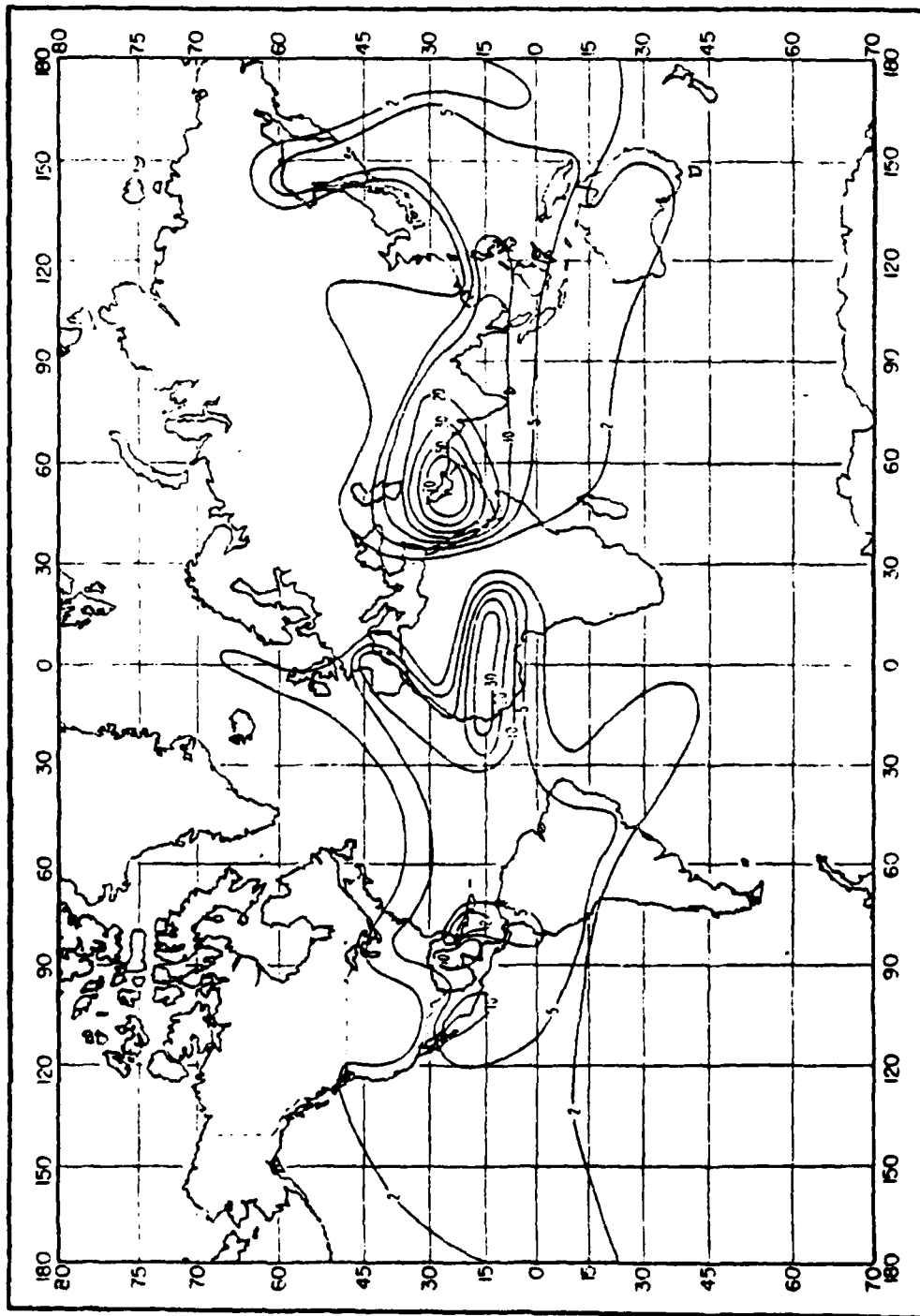


Figure II-25. Percent of Time Trapping Frequency is Less Than 3 GHz, May

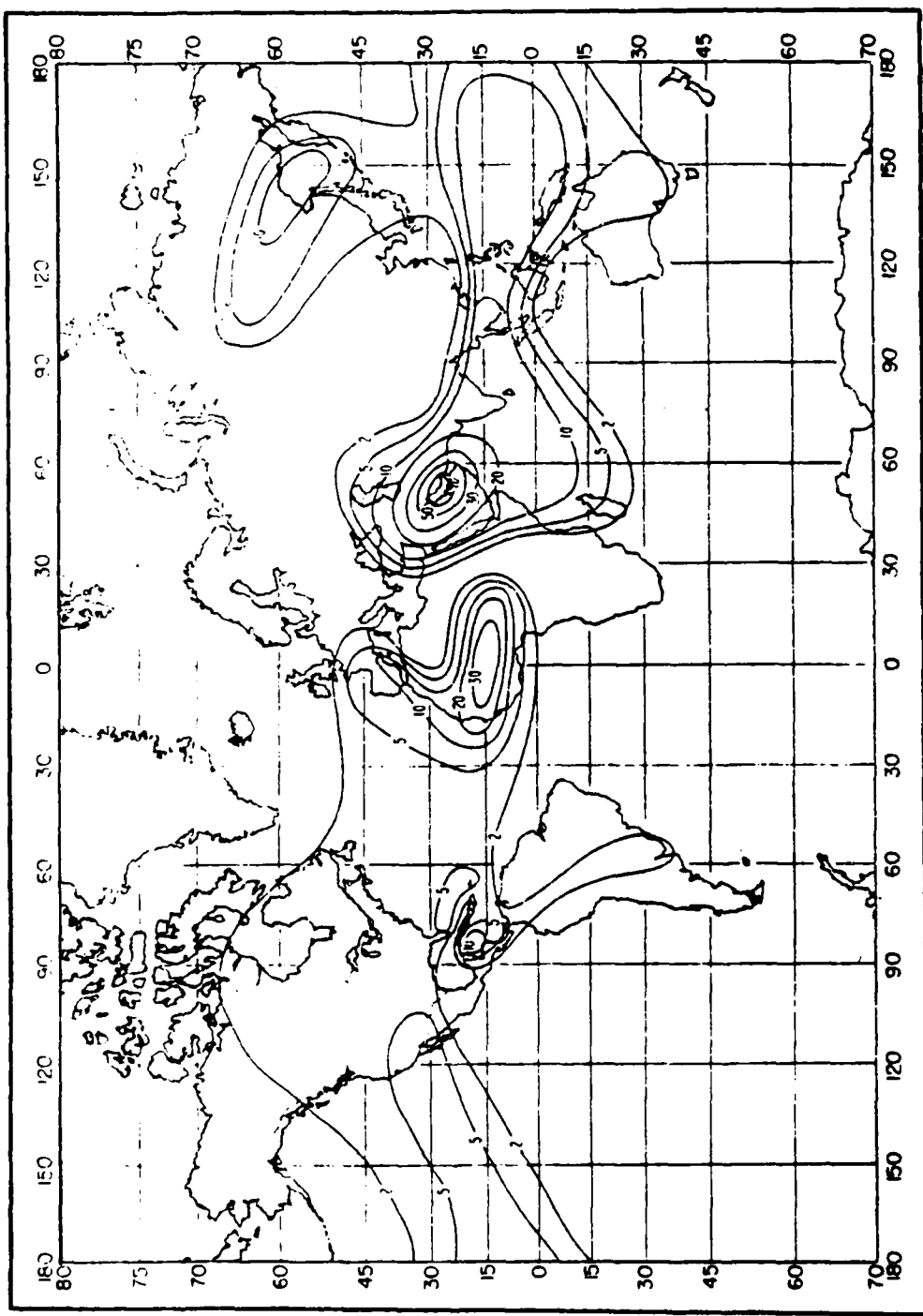


Figure II-26. Percent of Time Trapping Frequency is Less Than 3 GHz, August

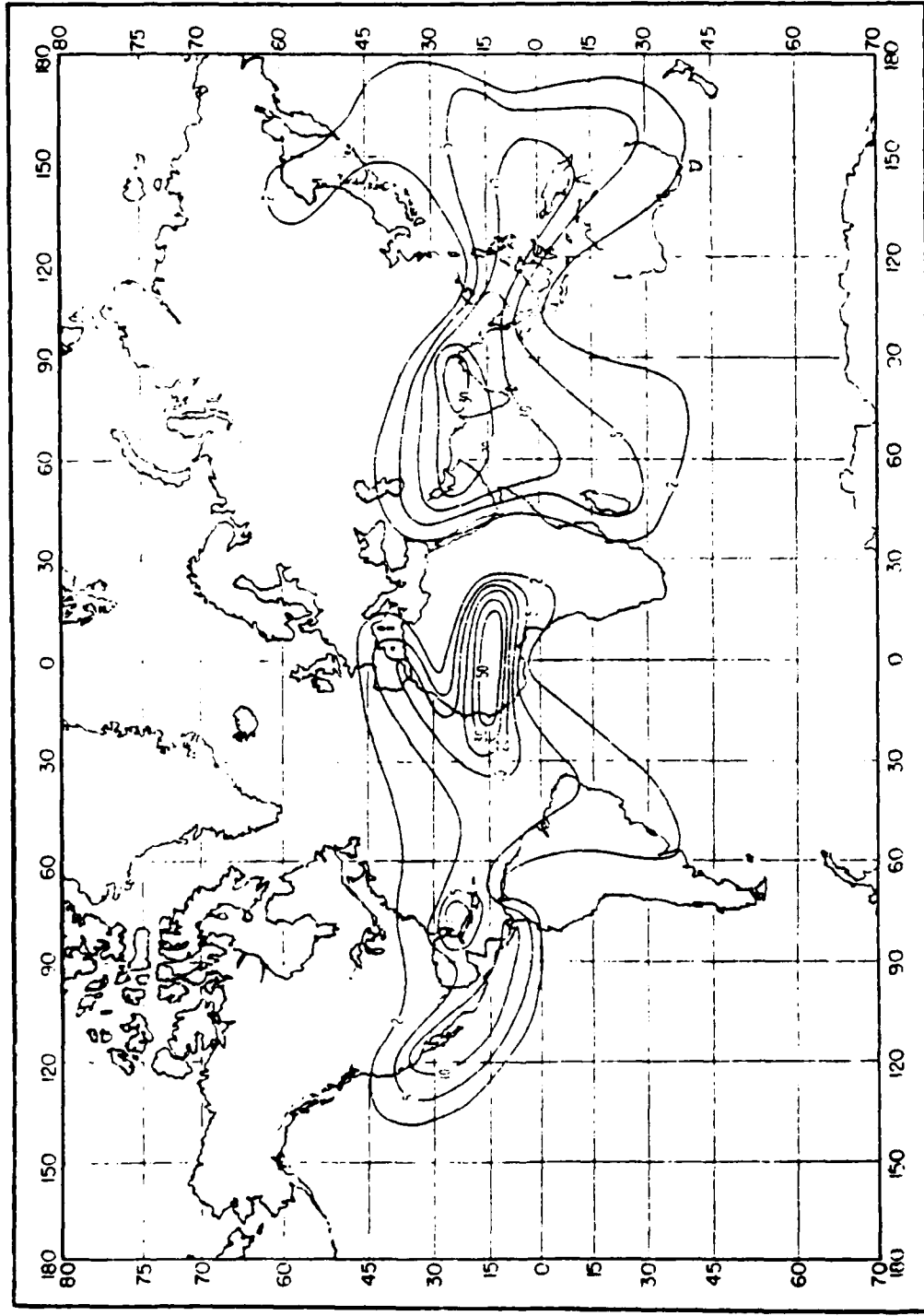


Figure II-27. Percent of Time Trapping Frequency is Less Than 3 GHz, November

Table II-1. CCIR Climate Types Summary

CCIR Climate Type	Description
1. Equatorial	Corresponds to the region between latitudes 10° N and 10° S. The climate is characterized by a slightly varying high temperature and by monotonous heavy rains which sustain a permanent humidity. The annual mean value of N, (refractivity at the surface of the earth = $(n-1) 10^6$ where n is the refractive index of the air) is about 360 N-units and the annual range of variation is 0 to 30 N-units.
2. Continental Subtropical	Corresponds to the regions between latitudes 10° and 20° . The climate is characterized by a dry winter and rainy summer. There are marked daily and annual variations of radio propagation conditions, with least attenuation in the rainy season. Where the land area is dry, radio ducts may be present for a considerable part of the year. The annual mean value of N, is about 320 N-units and the range of variation, throughout the year, of monthly mean values of N, is 60 to 100 N-units.
3. Maritime Subtropical	Also corresponds to the regions latitudes 10° and 20° and is usually found on lowlands near to the sea. It is strongly influenced by the monsoon. The summer monsoon, which blows from sea to land, brings high humidity into the lower layers of the atmosphere. Although the attenuation of radio waves is relatively low at both the beginning and end of the monsoon season, during the middle of the monsoon the atmosphere is uniformly humid to great heights and the radio attenuation increases considerably despite a very high value of N. There is an annual mean N, of about 370 N-units with a range of variation over the year of 30 to 60 N-units.

Table II-1. CCIR Climate Types Summary (Cont.)

CCIR Climate Type	Description
4. Desert	<p>Corresponds to two land areas which are roughly situated between latitudes 20° and 30°. Throughout the year there are semi-arid conditions and extreme diurnal and seasonal variations of temperature. This climate is very unfavorable for forward-scatter propagation, particularly in summer. There is an annual mean value of N_s, of about 280 N-units and throughout the year monthly mean values may vary over a range of 20 to 80 N-units.</p>
5. Mediterranean	<p>Corresponds to regions in both hemispheres on fringe of desert zones, close to the sea and lying between latitudes of 30° and 40°. The climate is characterized by a fairly high temperature, which is reduced by the presence of the sea, and an almost complete absence of rain in the summer. Radio-wave propagation conditions vary considerably, particularly over the sea, where radio ducts exist for a large percentage of the time in summer.</p>
6. Continental Temperate	<p>Corresponds to regions between latitudes and 60°. Such a climate in a large land mass shows extremes of temperature and pronounced diurnal and seasonal changes in propagation conditions may be expected to occur. The western parts of continents are influenced strongly by oceans, so that temperatures here vary more moderately and rain may fall at any time during the year. In areas progressively towards the east, temperature variations increase and winter rain decreases. Propagation conditions are most favourable in the summer and there is a fairly high annual variation in these conditions. The annual mean value of N_s, is about 320 N-units and monthly mean values may vary by 20 to 40 N-units throughout the year.</p>

Table II-1. CCIR Climate Types Summary (Concluded)

CCIR Climate Type	Description
7a. Maritime Temperate, Overland	Also corresponds to regions between about 30° to 60° where prevailing unobstructed by mountains, carry moist maritime air inland. Typical of such regions are the United Kingdom, the west coast of North America and of Europe and the northwestern coastal areas of Africa. There is an annual mean value of N, of about 320 N-units, with a rather small variation of monthly mean values over the year of 20 to 30 N-units. Although the islands of Japan lie within this range of latitudes, the climate is somewhat different and shows a greater annual range of monthly mean values of N, about 60 N-units. The prevailing winds in Japan have traversed a large land mass and the terrain is rugged. Climate 6 is therefore probably more appropriate to Japan than climate 7, but duct propagation may be important in coastal and adjacent oversea areas for as much as 5 percent of the time.
7b. Maritime Temperate, Oversea	Corresponds to coastal and oversea areas regions similar to those for climate 7a. The distinction made is that a radio propagation path having both horizons on the sea is considered to be an oversea path (even though the terminals may be inland); otherwise climate 7a is considered to apply. Radio ducts are quite common in occurrence for a small fraction of the time between the United Kingdom and the European continent and along the west coasts of the United States of America and Mexico.
8. Polar	Corresponds approximately to the regions between latitudes 60° and the poles. This climate is characterized by relatively low temperatures and relatively little precipitation.

Table II-2. Locations of Data Collection for CCIR Climate Types

Climate Type	Data Collection Location
Type 1: Equatorial	Congo and Ivory Coast
Type 2: Continental Subtropical	Sudan
Type 3: Maritime Subtropical	West Coast of Africa
Type 4: Desert	Sahara
Type 5: Mediterranean	No curves available
Type 6: Continental Temperate	France, Federal Republic of Germany, and United States
Type 7a: Maritime Temperate, Overland	United Kingdom
Type 7b: Maritime Temperate, Oversea	United Kingdom
Type 8: Polar	No curves available

II.3.8 Ray-Bending for Earth-Space Paths

The CCIR reports that in the case of earth-space propagation, errors in the apparent elevation angle of a satellite due to refraction in the troposphere decreases as the satellite moves from the horizon to the zenith. Table II-3 shows the average ray-bending for propagation through the atmosphere. Elevation angle errors, , for paths of various elevation angles, , are presented. For purposes of this table, Turkey and Germany may be defined as having polar continental air and Hawaii as having maritime air.

Table II-3. Ray-Bending for Earth-Space Paths

Elevation Angle (θ)	Average Total Ray-Bending,		Day-to-Day Variation in $\Delta\theta$
	Polar Continental Air	Tropical Maritime Air	
1°	0.45°	0.65°	0.1° rms
2°	0.32°	0.47°	
4°	0.21°	0.27°	
10°	0.10°	0.14°	0.007° rms

II.4 ATTENUATION BY RAINFALL AND OTHER HYDROMETEORS

All radio frequencies are subject to the effects of hydrometeors, especially rain, which cause absorption and scattering of radio waves. Precipitation attenuation may be negligible at wavelengths greater than 10 cm (frequency less than 3 GHz) but must be considered at wavelengths less than 10 cm. It has been reported that signal attenuation in excess of free space in the range of 3 cm to 30 cm (10 - 100 GHz) is due mostly to rain as compared to other atmospheric constituents.

The CCIR has examined the characteristics of rainfall from two points of view: statistical characteristics of rainfall intensity at a point and spatial characteristics. The CCIR has also examined attenuation and scattering by hydrometeors.

II.4.1 Statistical Characteristics of Rainfall at a Point

It is suggested that experimental values of precipitation intensity be used to determine the cumulative distribution. Because experimental data are not available for some of the earth's regions and no single parameter appears to provide a satisfactory method, the CCIR proposes to continue using a method based on the concept of five rain-climate zones. As seen in Figure II-28, the zone which includes Turkey is Zone 5 except for the region on the west side of the Turkish Straits known as Thrace, which is in Zone 1. Zone 1 may also be used to characterize the rain climate of Hawaii. The figure indicates that Zone 3 applies to Germany. From this an estimate of cumulative distribution, identifying the percent of an average year for which the rainfall rate is exceeded for these zones may be found using Figure II-29. As a note of caution, it is suggested that these curves should only be used in the absence of specific information for any location. Characteristic values of the parameters for the five rain climate zones for 0.01 percent of time are given in Table II-4.

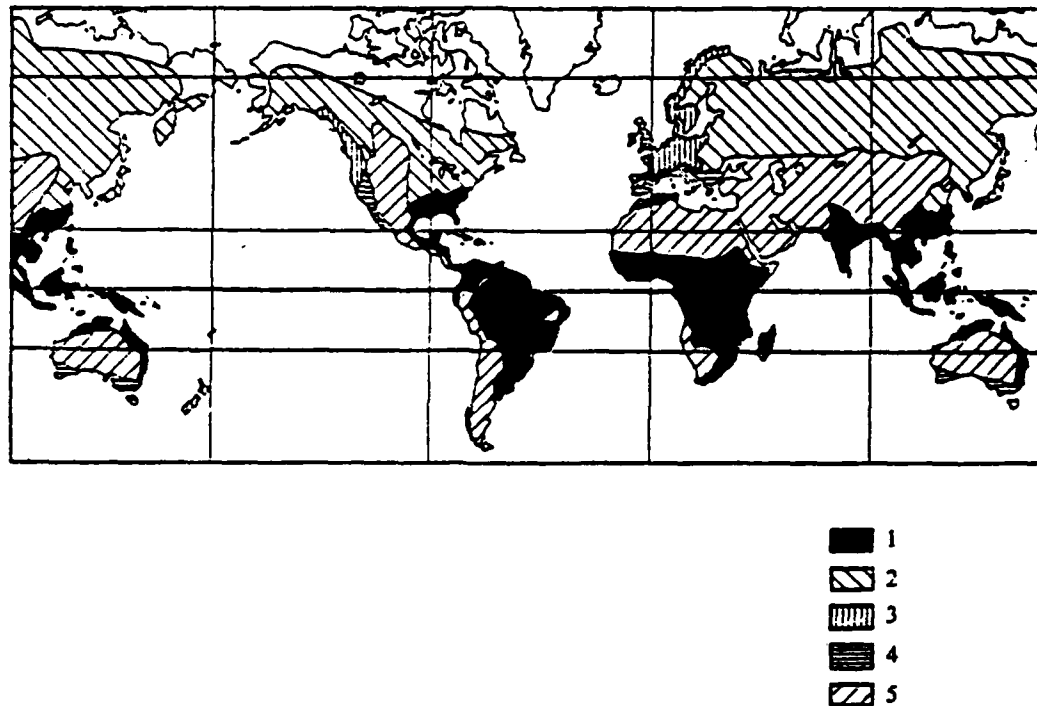


Figure II-28. Rain-Climate Zones of the CCIR

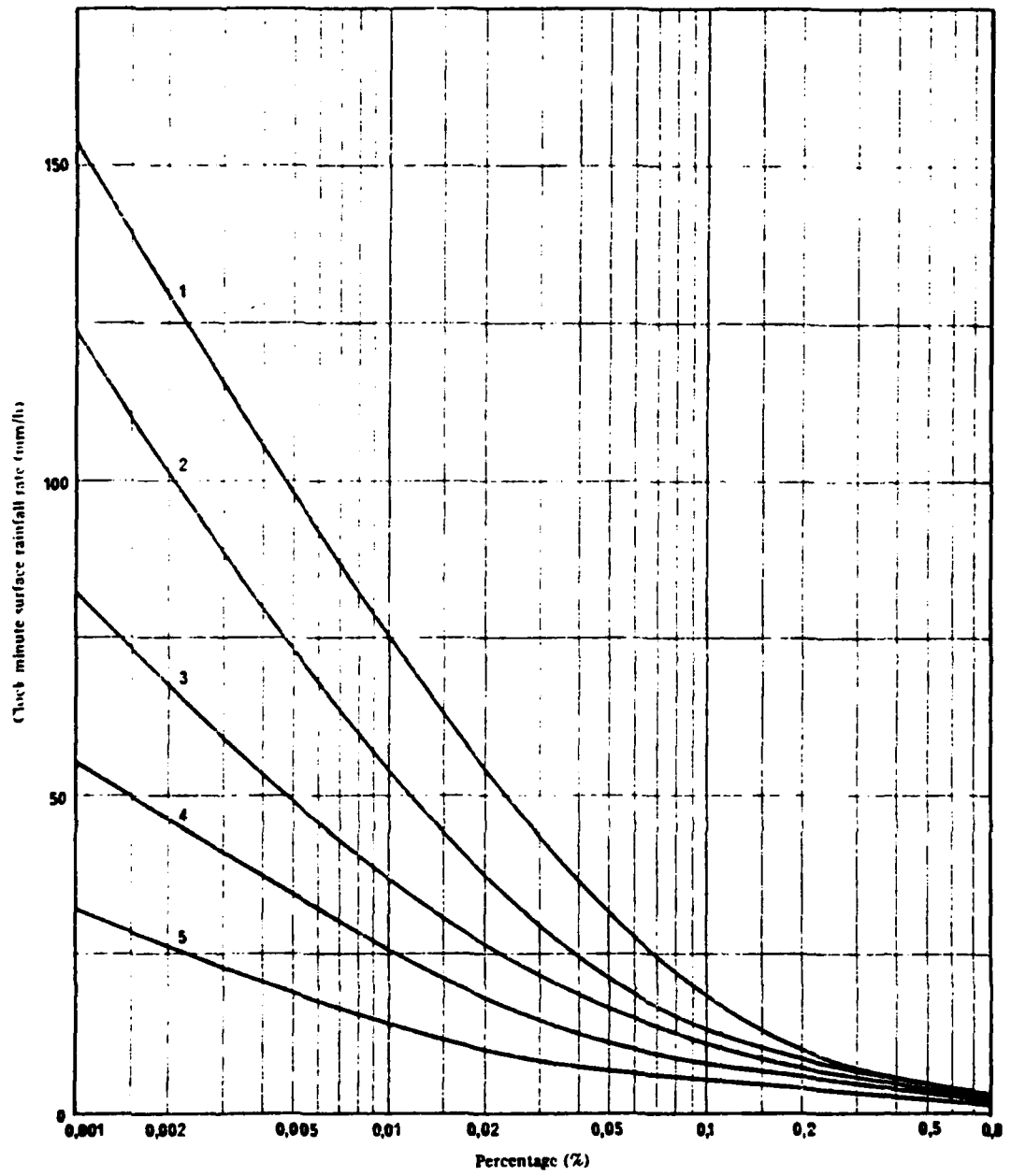


Figure II-29. Percent of Average Year Rainfall Rate Is Exceeded for Rain Climates

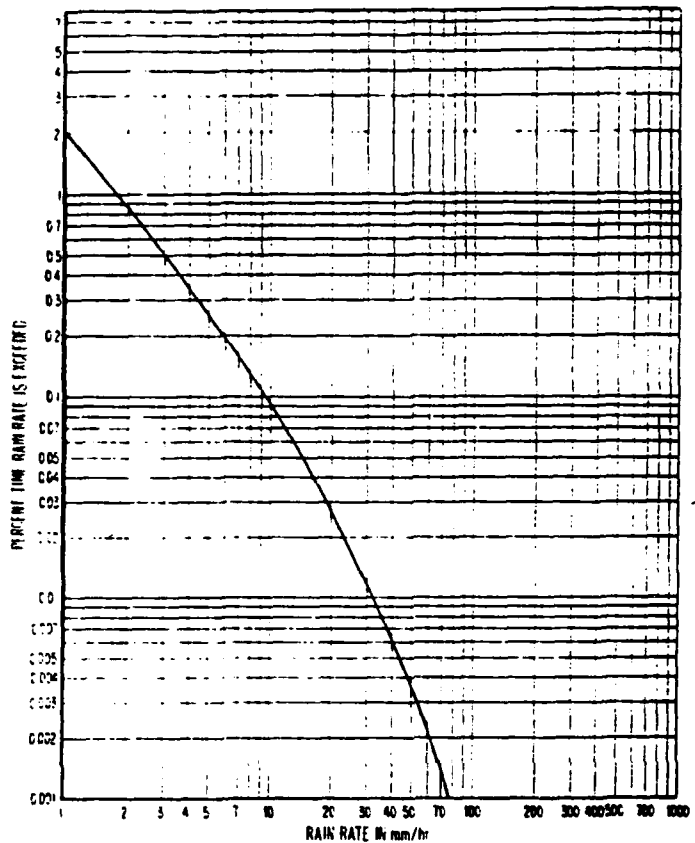
Table II-4. Characteristic Values of Parameters for CCIR Rain Climates
Zones (0.01 Percent of Time)

Parameter	Rain Climate Zones				
	1	2	3	4	5
Rainfall Rate, R (mm/hr)	75	55	37	26	14
Rain Cell Diameter, D (km)	2.5	2.8	3	3.4	4.5
Water vapour concentration, p (g/m^3)	10	5	2	2	2

C.A. Samson has provided curves of rainfall-rate distributions with data based on point rates averaged over one to five minutes, which can be assumed to represent instantaneous rates for most applications. The only stations used to collect rainfall data pertinent to this report are located in or near the area of interest in Germany. Figures II-30 through II-33 present curves from Darmstadt, Freiburg, Karlsruhe, and Koblenz.

II.4.2 Spatial Characteristics of Rainfall

Measurements made in the United States indicate that convective showers which produce heavy rainfall in temperate climates vary in size during their existence and vary considerably over short distances within a storm. It was found that these showers may reach a diameter of 15 - 20 km (9 - 12 mi.), with an average size estimated at 8 km (5 mi.). The average horizontal rain cell as a function of rain rate (mm/hr) is indicated in Figure II-34. Maximum rain-cell heights as a function of rain-climate zone and percent of time are given in Table II-5.



Darmstadt, Germany

49° 51' N, 08° 41' N

281 meters msl

Data: Rainfall rate, 5-min averages, Sept. 70 - Sept. 71

Source: Abel (1973)

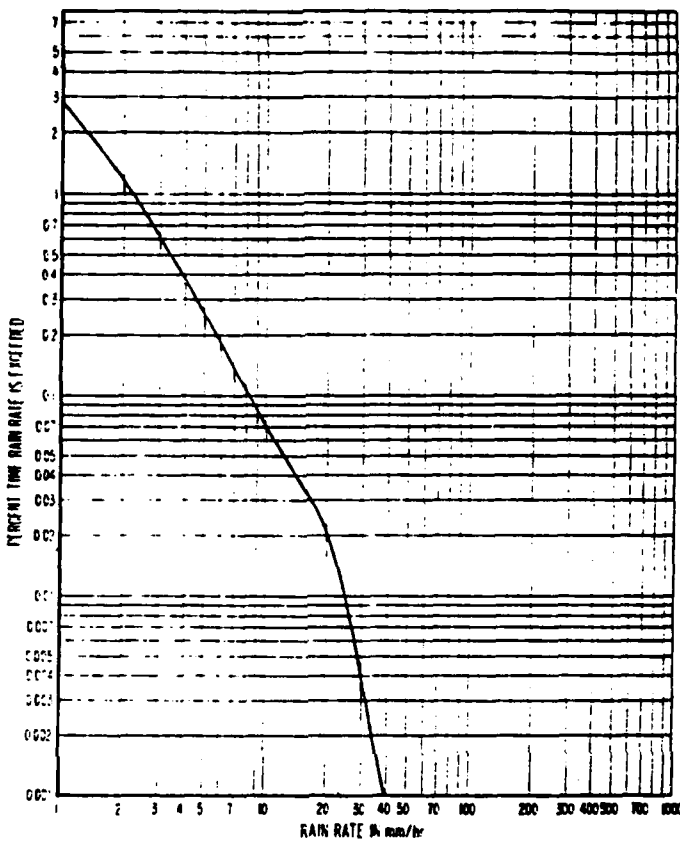
Temperature (°F): January 38/29; July 75/56

Mean Dewpoint (°F): January 29; July 54

Precipitation (inches): Annual 25.0; July 2.80; February 1.58 Days with thunderstorms 28

Located in the Rhine valley. A continental climate modified by exposure to maritime air masses from the Atlantic Ocean.

Figure II-30. Rainfall-Rate Distribution for Darmstadt, West Germany



Freiburg, Germany

49° 00' N. 07° 51' E

286 meters ms1

Data: Rainfall rate, 4-min averages, 1964 and 1965

Source: Sims and Jones (1973)

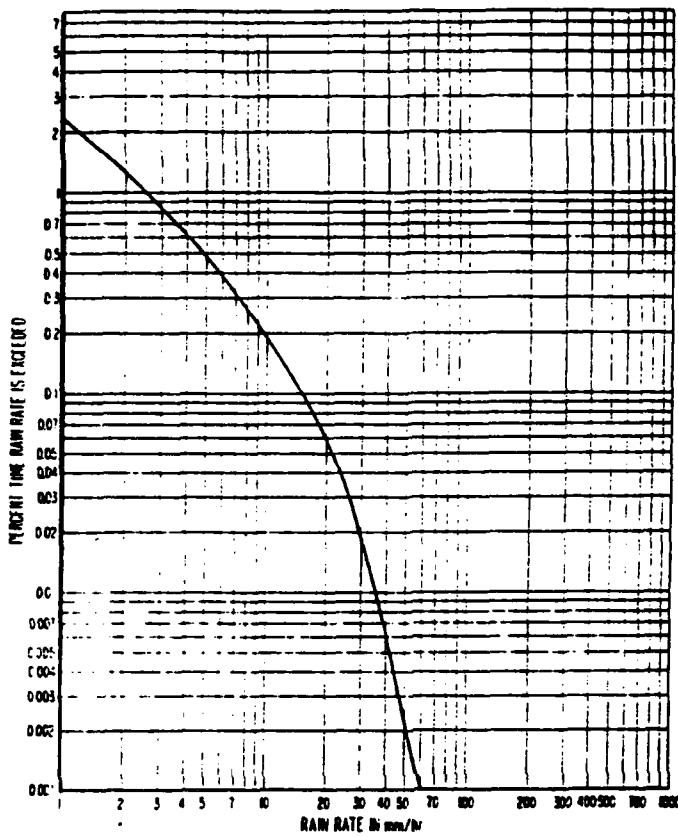
Temperature (°F): January 39/29; July 76/57

Mean Dewpoint (°F): January 29; July 55

Precipitation (inches): Annual 34.9; July 4.10; February 1.70 Test period: 26.5 (1964); 77.7 (1965) Days with thunderstorms 21

Located on the west slope of the Black Forest, 16 km east of the Rhine River. A continental climate modified by exposure to maritime air masses from the Atlantic Ocean.

Figure II-31. Rainfall-Rate Distribution for Freiburg, West Germany



Karlsruhe, Germany

49° 01' N, 08° 23' E 116 meters msl

Data: Rain rate, 2-min averages, Sept. 60 - Aug 65

Source: Zedler (1967)

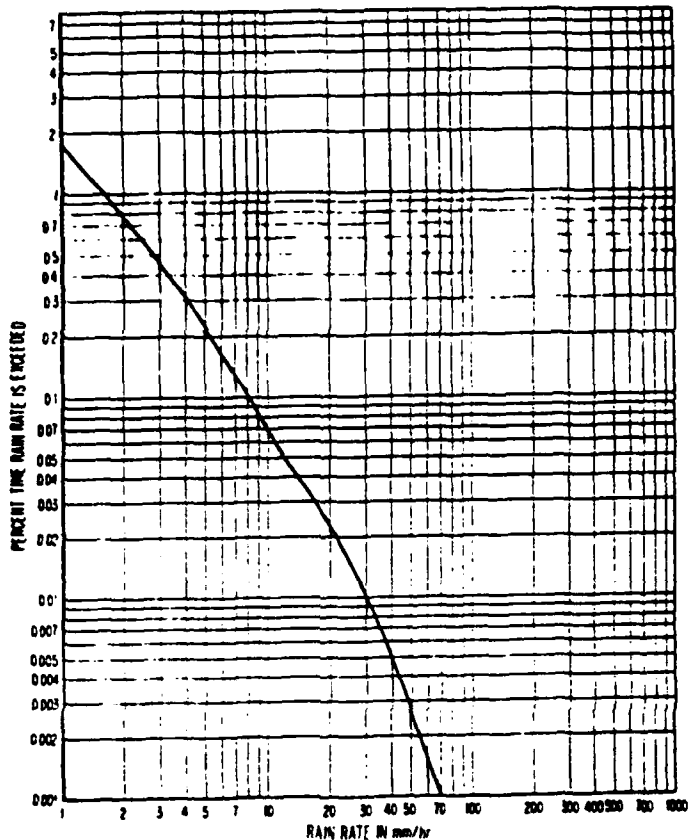
Temperature (°F): January 38/29; July 75/57

Mean Dewpoint (°F): January 29; July 55

Precipitation (inches): Annual 29.8; August 3.07; February 1.73 Test period 26.81 Days with thunderstorms 25

Located in the Rhine valley 6 km east of the river. A continental climate modified by exposure to maritime air masses from the Atlantic Ocean.

Figure II-32. Rainfall-Rate Distribution for Karlsruhe, West Germany



Koblenz, Germany

50° 21' N, 07° 36' E 97 meters msl

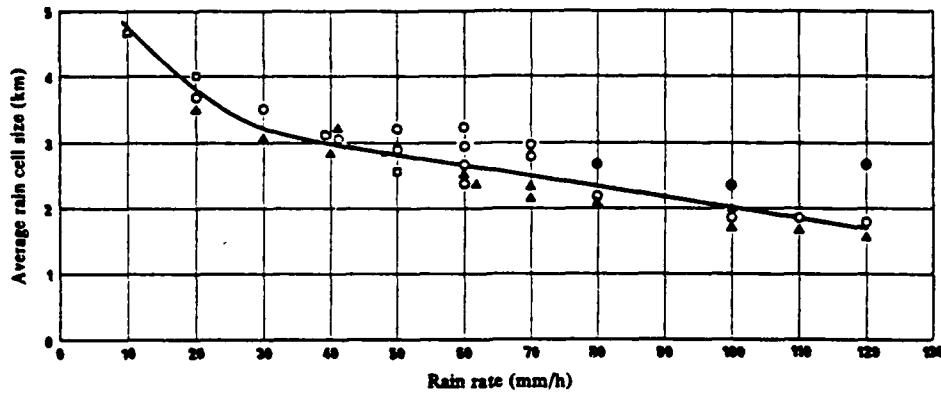
Data: Rainfall rate, 4-min averages, 1970

Source: Sims and Jones (1973)

Precipitation (inches): Annual 26.85 Test period 24.3

Located on the Rhine River at the mouth of the Mosel River. A continental climate modified by exposure to maritime air masses from the Atlantic Ocean.

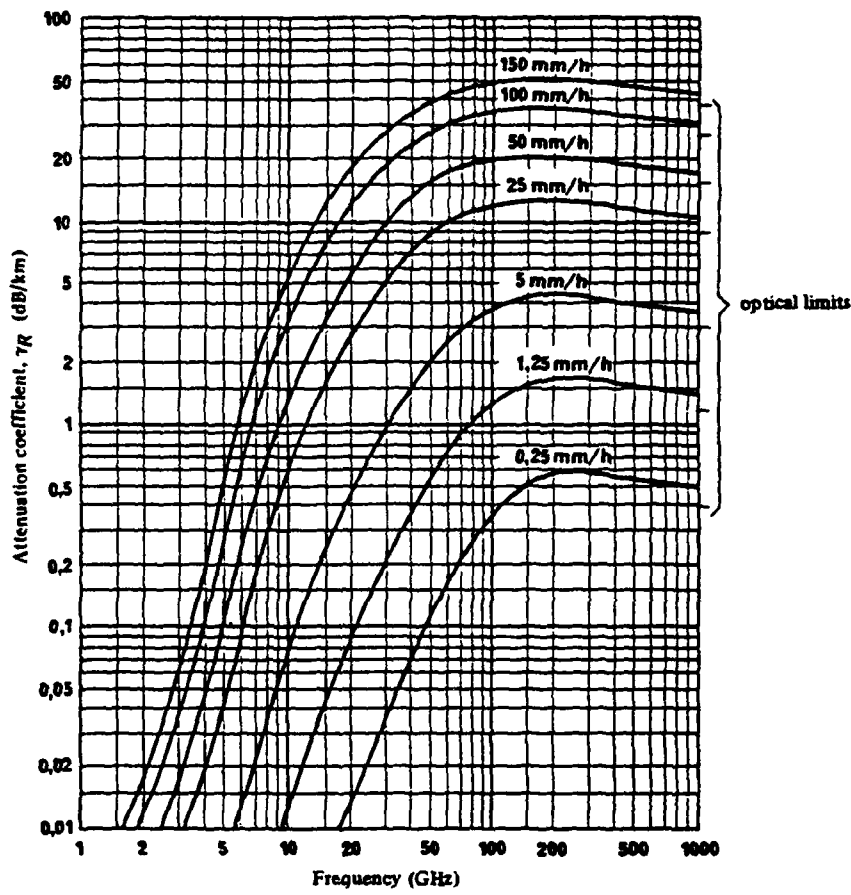
Figure II-33. Rainfall-Rate Distribution for Koblenz, West Germany



- Derived from attenuation measurements carried out in Japan (1968, 1969, 1970): Climate 2
- ▲ Derived from attenuation measurements carried out in Malaysia (1971, 1972): Climate 1
- Derived from weather radar observations carried out in Switzerland (1973): Climate 3
- Derived from rain gauge observations in France (1977): Climate 3

The measurements carried out in Japan and Malaysia are indirect, and are therefore subject to caution.

Figure II-34. Average Rain Cell Sizes



Raindrop size distribution [Laws and Parsons, 1943]
Terminal velocity of raindrops [Gunn and Kinzer, 1949]
Index of refraction of water at 20°C [Ray, 1972]

Figure II-35. Rain Attenuation Coefficient for Various Rain Rates

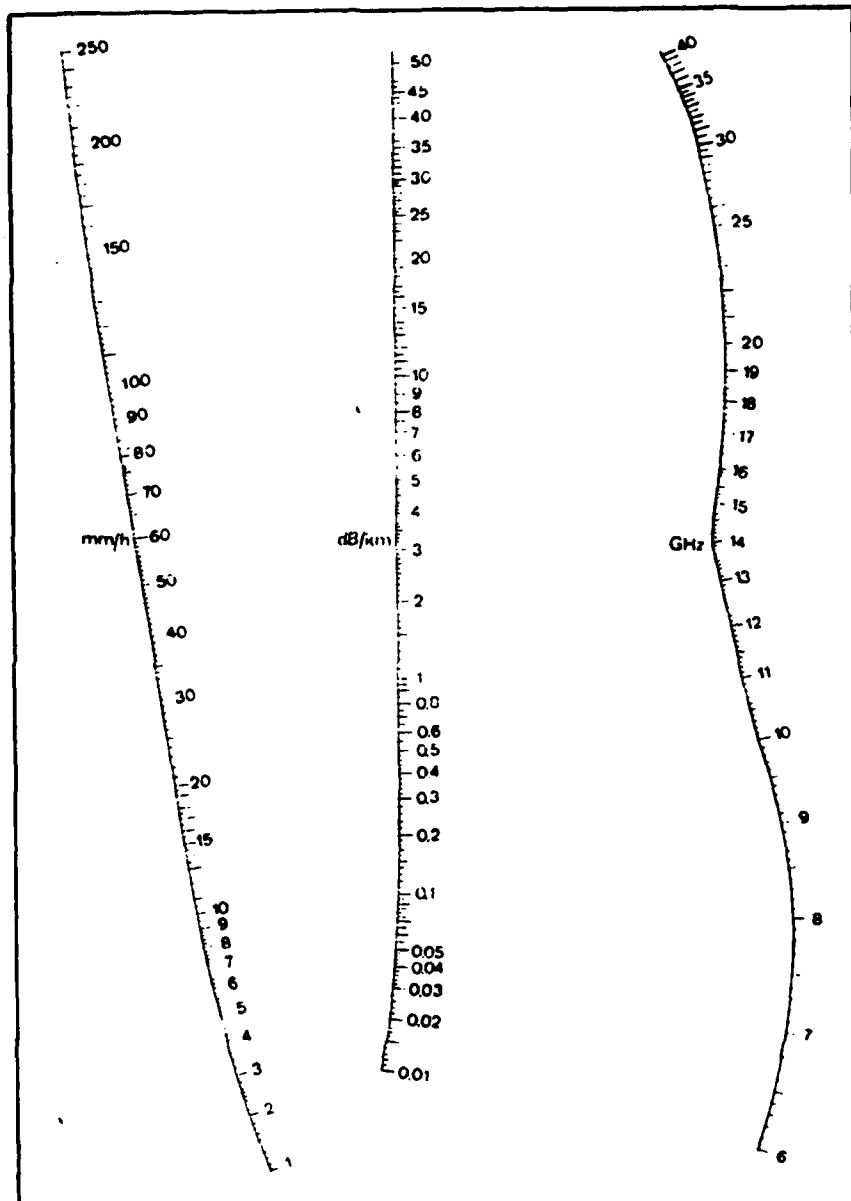
Table II-5. Maximum Rain-Cell Heights for CCIR Rain-Climates Zones

Rain Climatic Zone	Rain Cell Height (km)		
	0.001%	0.01%	0.1%
1	15	11	7
2	11	7	5
3, 4, 5	7	5	3

II.4.3 Attenuation and Scattering by Hydrometeors

The effects of hydrometeors are realized in two ways - attenuation along the propagation path and scattering of radio waves in all directions which can cause interference to other radio receivers.

Two figures are available to determine the attenuation coefficient due to rainfall, γ_R (dB/km). Figure II-35 is a logarithmic graph showing the attenuation coefficient versus frequency for various rainfall rates. The attenuation coefficient may also be found from the nomograph in Figure II-36 by placing a straightedge at the appropriate outer scales of rain rate and frequency and reading the value of attenuation coefficient from the center scale. Both figures have been developed on the basis of experimental data on raindrop size distribution (from Laws and Parsons) and on the terminal velocity of raindrops (from Gunn and Kinzer) using an empirical model for the value of refraction of water at 20°C (from Ray).



Raindrop size distribution [Laws and Persons, 1943]
 Terminal velocity of raindrops [Gunn and Kinzer, 1949]
 Index of refraction of water at 18°C [Ray, 1972]

Figure II-36. Rain Attenuation Coefficient Nomograph

For radio propagation within the troposphere, an estimate of the rain attenuation may be calculated as the product of the attenuation coefficient, γ_R (dB/km), the distance the radio wave travels through the troposphere (km), and the distance reduction coefficient. This coefficient may be found in Figure II-37 for precipitation intensities and path lengths of 50 km or less.

For earth-space paths, the attenuation coefficient, γ_R (dB/km), is multiplied by the effective propagation path length through the rainstorm, l (km), found in Figure II-38. The latter figure presents curves of effective path lengths versus elevation angle for various rain rates and was prepared from data collected in areas having temperate climates.

Three notable papers pertaining to rainfall attenuation are provided in Supplements III, IV, and V.

Although rain is the dominant hydrometeor in the attenuation of radio waves, the influence of clouds, fog, snow, and hail requires attention. The attenuation coefficient due to clouds or fog, γ_C (dB/km), may be found for small droplets generally less than 0.01 cm. It is the product of two values - the specific attenuation coefficient, K_1 (dB/km/(g/m³)), and the liquid water content of the cloud, M (g/m³). The specific attenuation coefficient may be found from Figure II-39, where it is plotted against frequency for various temperatures. It has been reported that the liquid water content, M , generally ranges from 1 to 2.5 g/m³.

The effects of snow and hail are presently not well established. It is reported that due to the difference in dielectric properties, ice clouds give attenuations up to 35 GHz of about two orders of magnitude smaller than water clouds of the same water content. At higher frequencies the attenuation may be more significant.

With rain climate and percent of time as parameters, the greatest heights at which rain scatter returns are expected to be significant are as previously indicated in Table II-5. The maximum rain scatter distances as a function of frequency and transmission loss, in dB, for 0.01 percent of the time are presented in Figures II-40 through II-42 for rain-climate zones 1, 3, and 5 respectively. These zones are relevant to Turkey, Germany, and Hawaii.

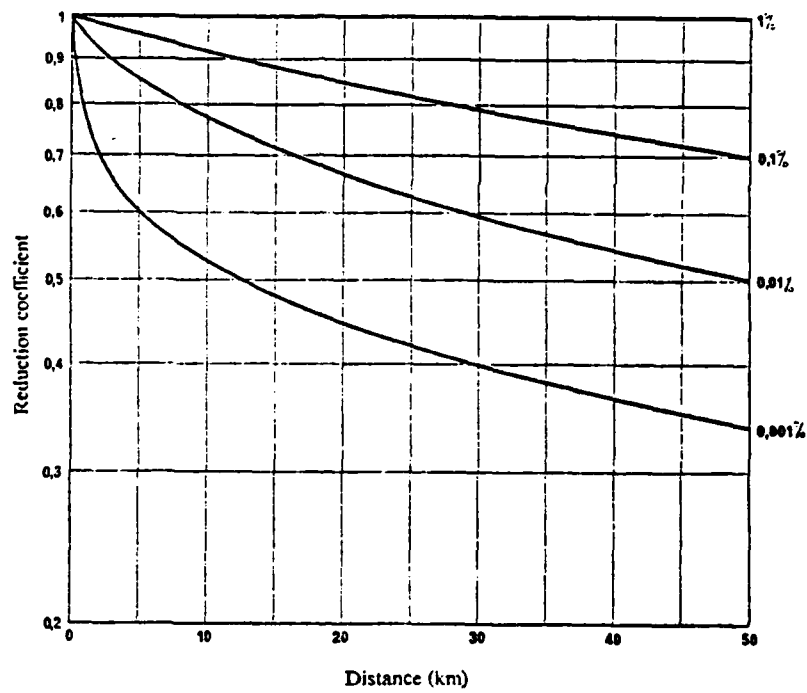


Figure II-37. Reduction Coefficient for Precipitation Intensities

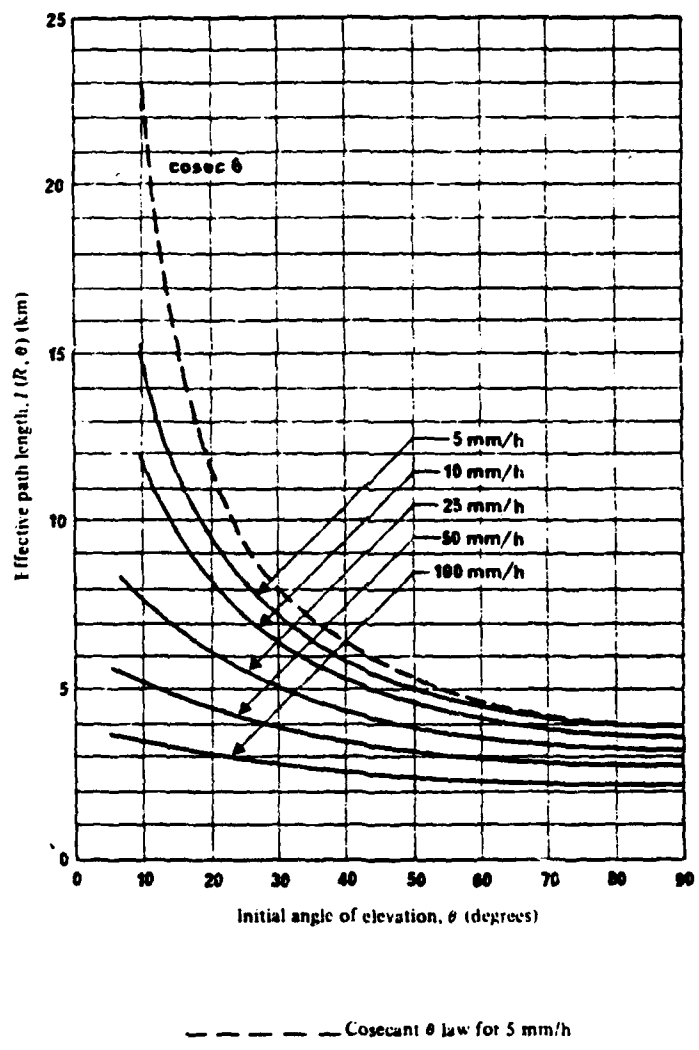


Figure II-38. Effective Path Length Through a Rainstorm

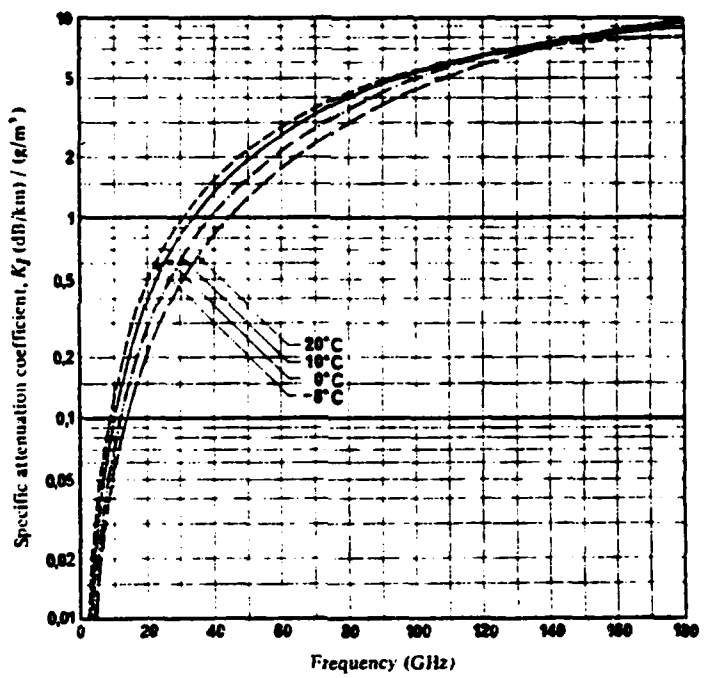
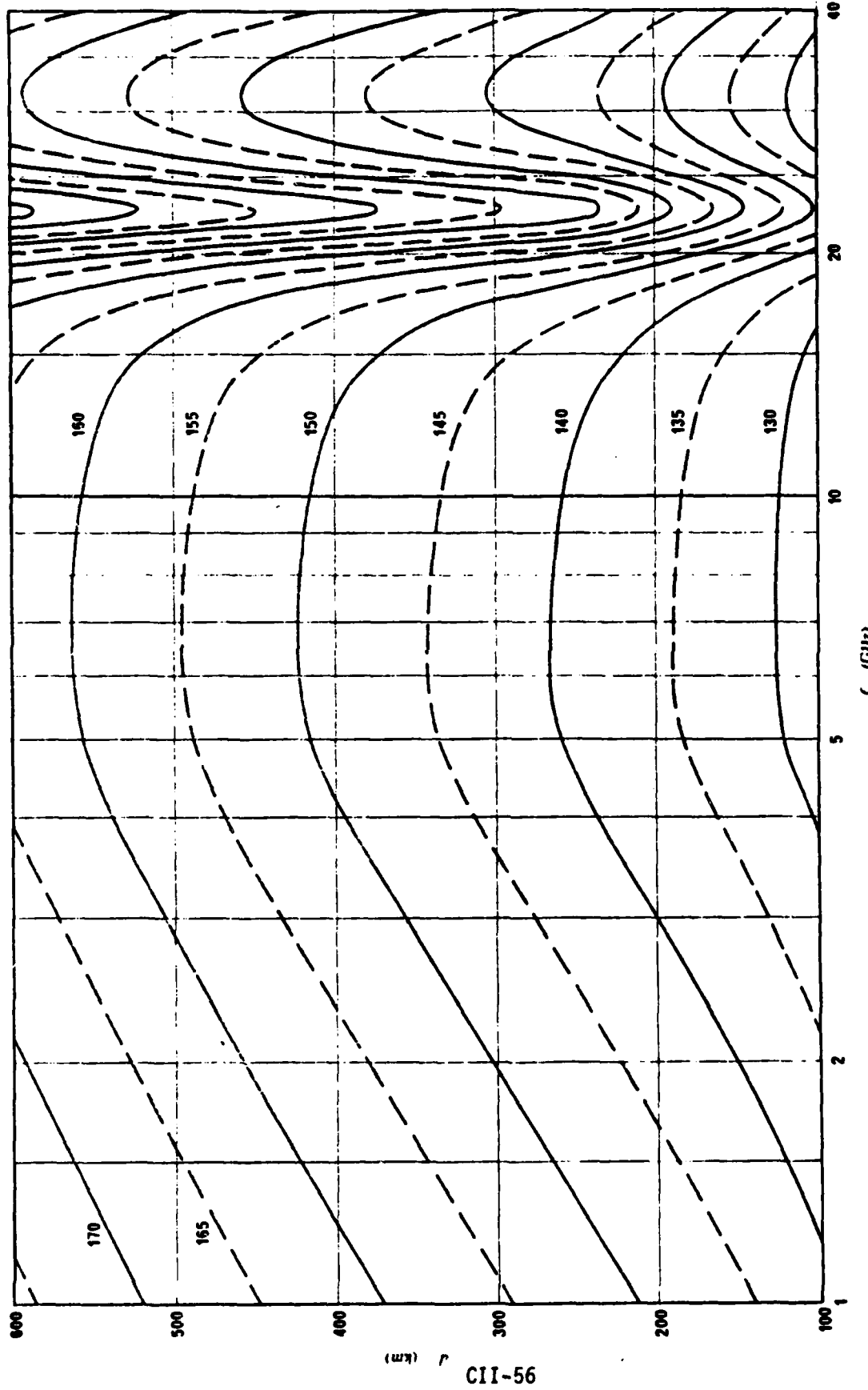


Figure II-39. Specific Attenuation Coefficient for Clouds and Fog



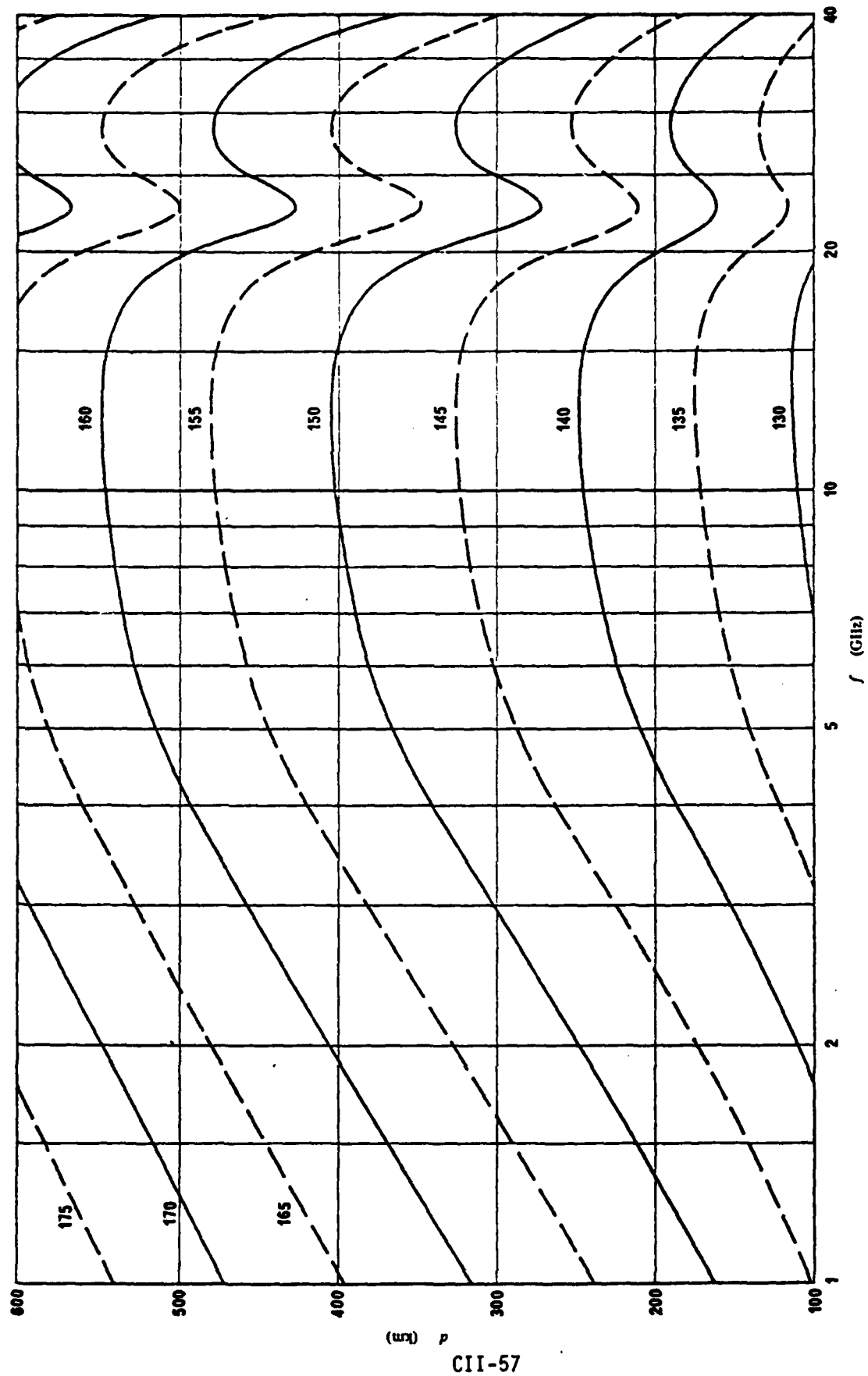


Figure II-41. Rain Scatter Distance for 0.01 Percent of Time, Rain-Climate Zone 3

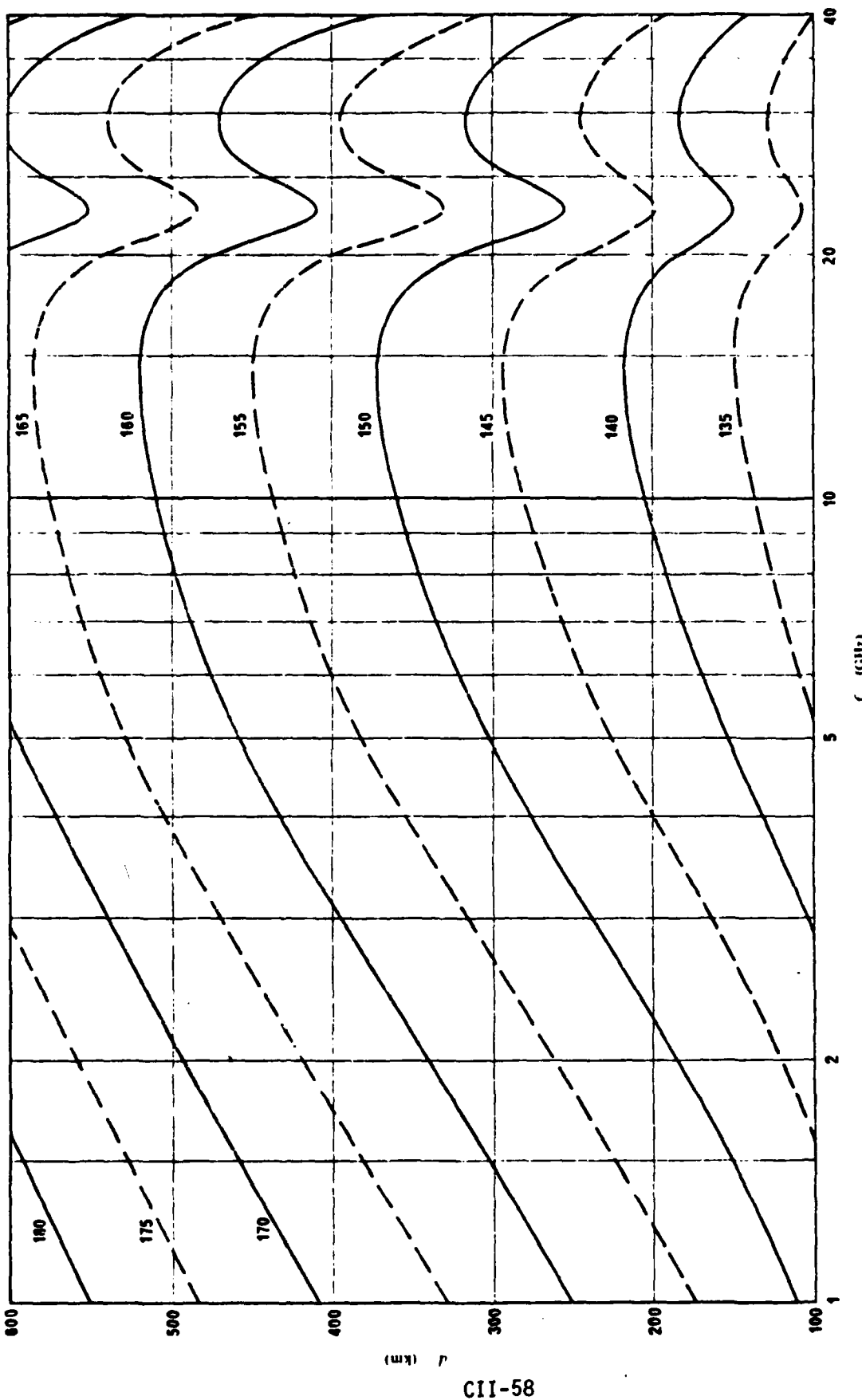


Figure II-42. Rain Scatter Distance for 0.01 Percent of Time, Rain-Climate Zone 5

CII-58

The scattering of radio waves by hydrometeors may cause a coupling between radio waves transmitted by two antennas on the ground if the two conditions that the patterns of radiation of the two antenna intercept a common volume and precipitation occurs in this volume are satisfied.

II.5 CONSIDERATIONS OF ATMOSPHERIC GASES

The atmospheric attenuation of radio waves operating at frequencies below about 10 GHz may not be significant. Absorption by both oxygen and water vapor content in the atmosphere does become significant at that frequency and above. Because of various molecular resonances, certain peaks and troughs of attenuation exist. Frequencies of 60 and 120 GHz are not recommended for long-distance propagation in the troposphere due to oxygen, and it is similarly not recommended to use 23 or 180 GHz due to water vapor except in the case of very dry air.

For LOS paths, the expression for atmospheric attenuation, A_a , (dB), may be written as

$$A_a = \left(\gamma_{oo} + \frac{\rho}{7.5} \gamma_{wo} \right) r_0 \quad (8)$$

where γ_{oo} and γ_{wo} are the absorption coefficients (dB/km) for oxygen and water vapor found in Figure II-43, ρ is the water vapor concentration (g/m^3) obtained from Figures II-44 or II-45, and r_0 is the path length (km).

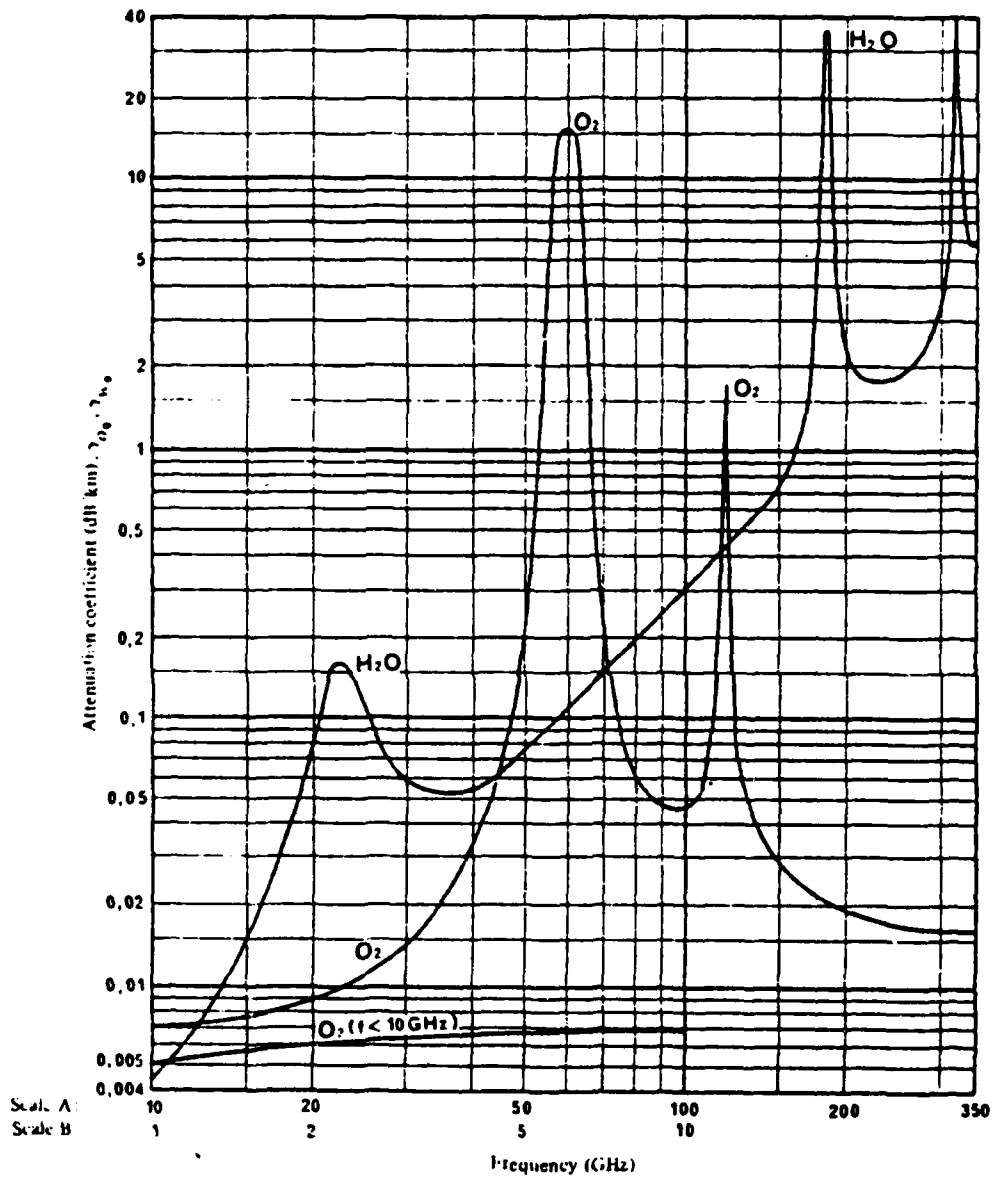
For toposcatter paths, the corresponding expression is

$$A_a = \gamma_{oo} r_o + \gamma_{ow} r_w \quad (9)$$

where r_o and r_w are the equivalent absorption path lengths (km) for oxygen and water vapor obtained from Figures II-46 and II-47 respectively, and for earth-space paths is

$$A_a = \gamma_{oo} r_{eo} + \gamma_{ow} r_{ew} \quad (10)$$

where r_{eo} and r_{ew} are the effective distances (km) of the path through the atmosphere as obtained from Figures II-48 and II-49 respectively.



Pressure: 1 atm (1013.6 mb)
 Temperature: 20°C
 Water vapour density: 7.5 g/m³

Figure II-43. Specific Attenuation Coefficient for Atmospheric Gases

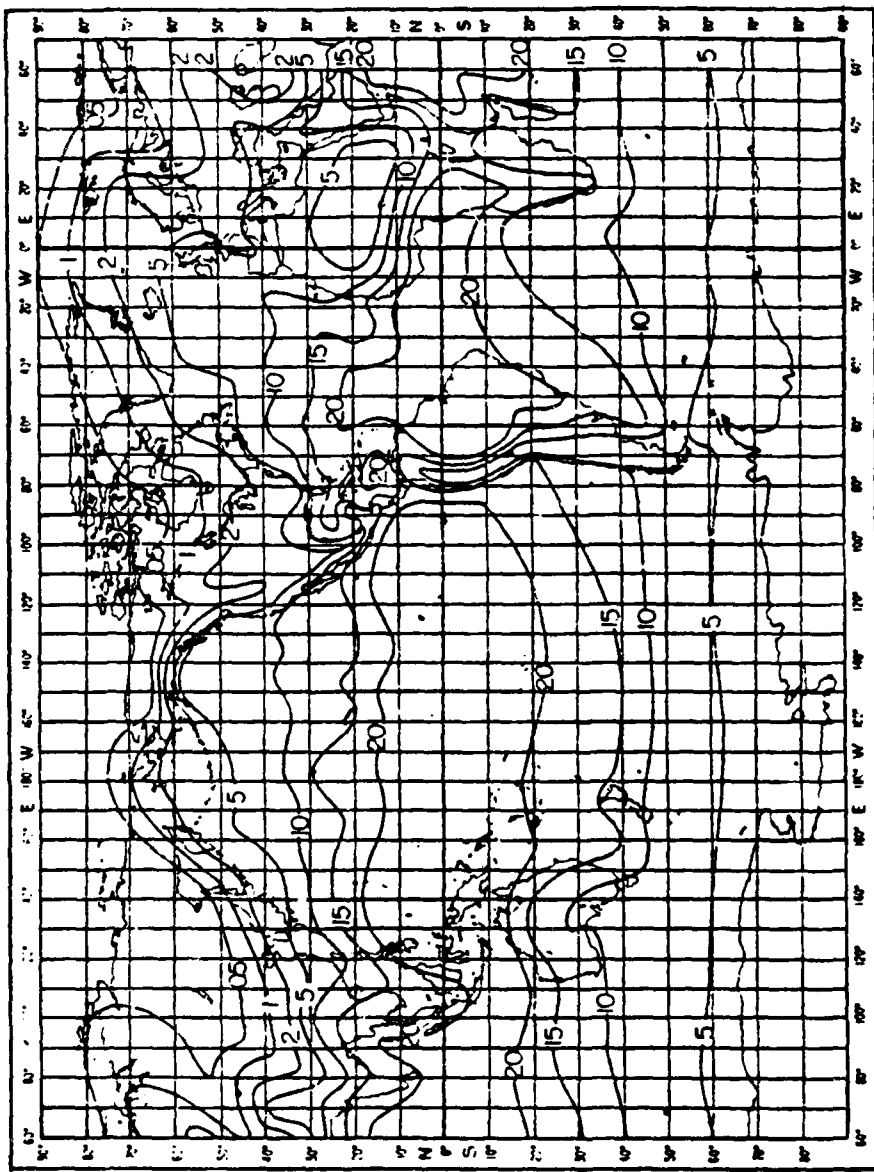


Figure II-44. Water Vapor Concentration (g/m^3), February

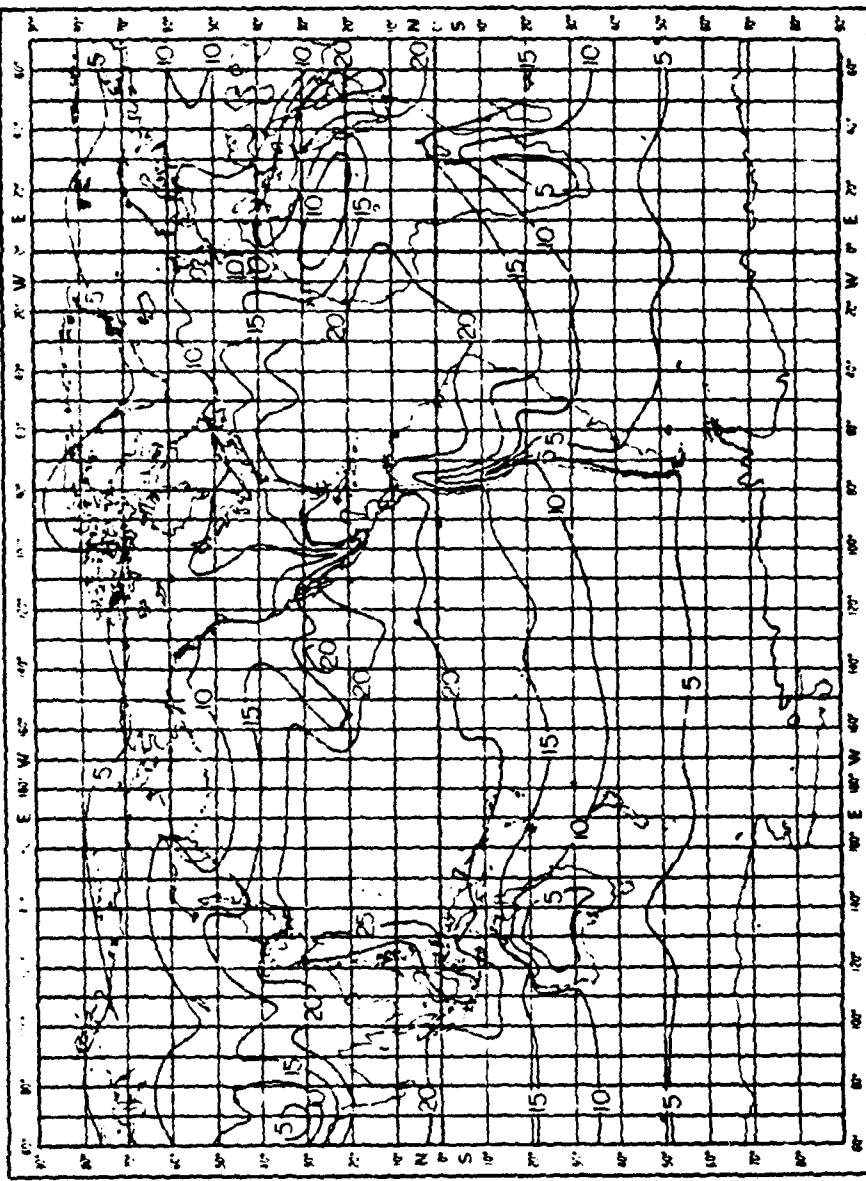


Figure 11-45. Water Vapor Concentration (g/m^3), August

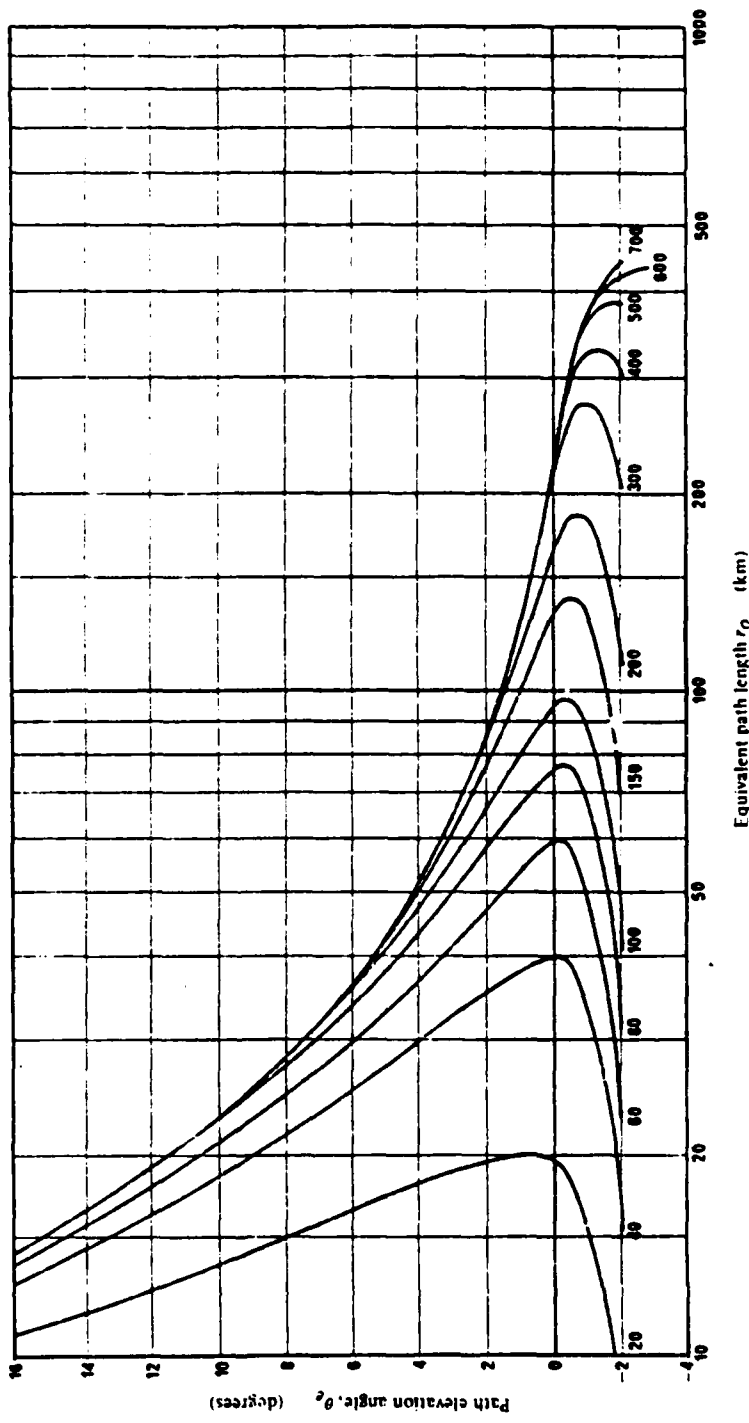


Figure II-46. Equivalent Path Length (km) for Oxygen Absorption

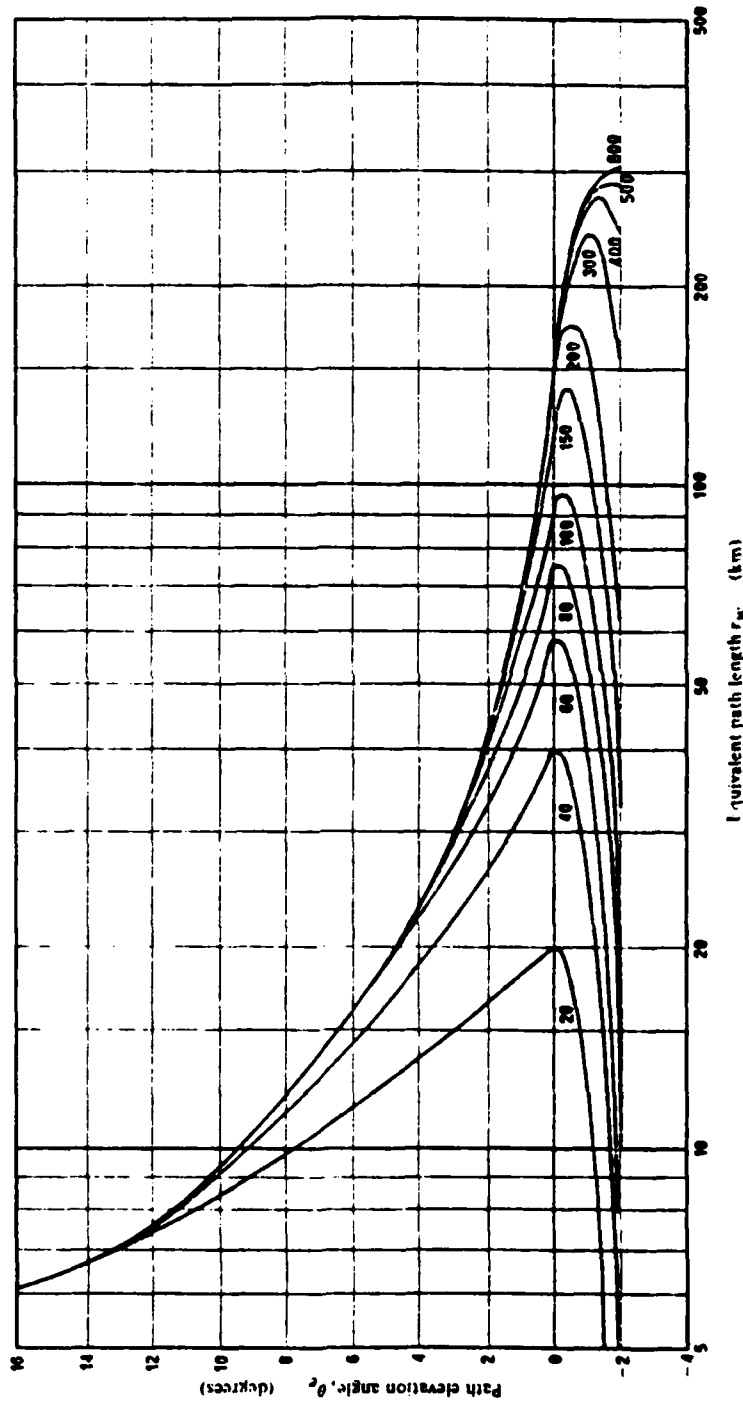


Figure 11-47. Equivalent Path Length (km) for Water Vapor Absorption

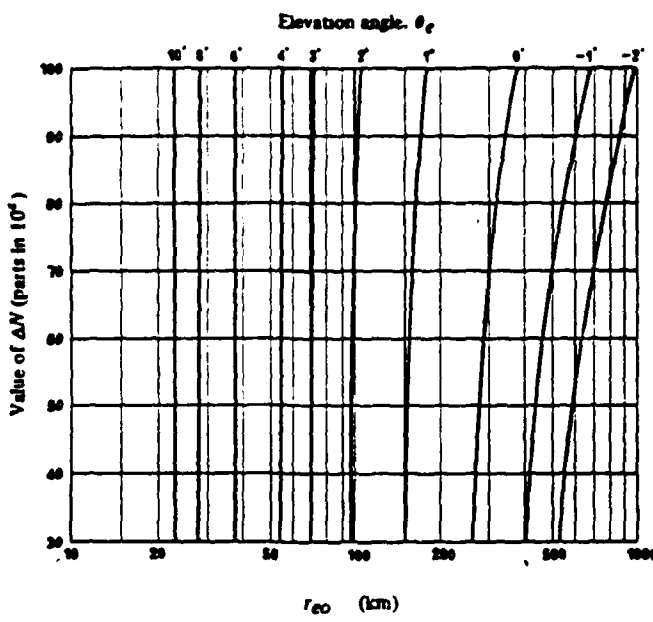


Figure II-48. Effective Path Distance (km) for Oxygen Absorption

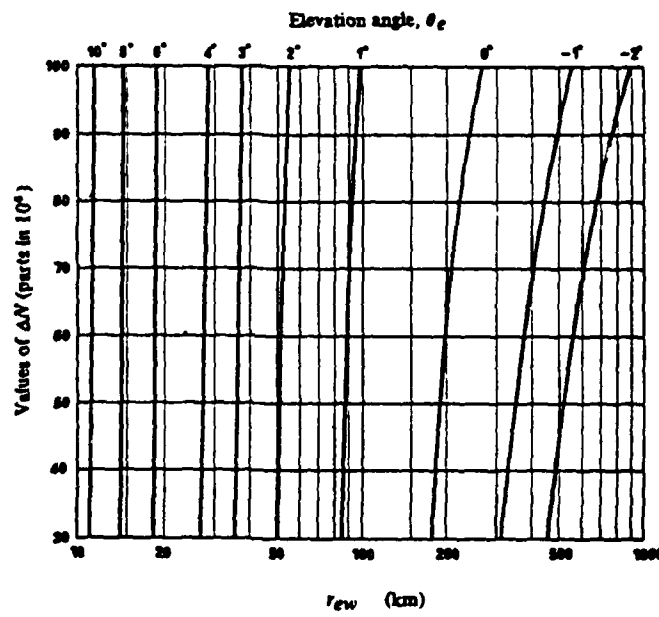
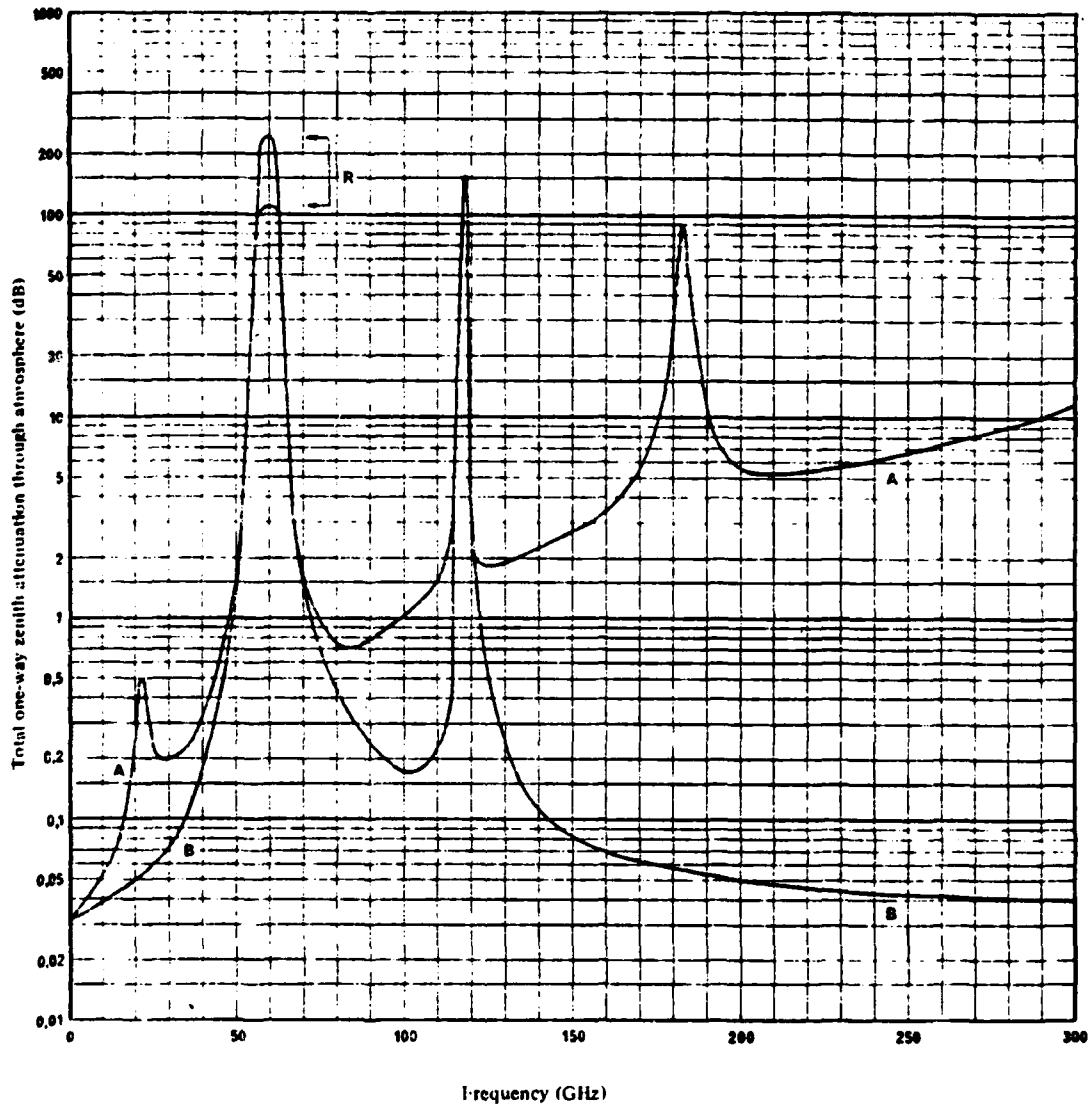


Figure II-49. Effective Path Distance (km) for Water Vapor Absorption

Figure II-50 shows an estimate of the total one-way zenith attenuation for frequencies between 1 and 300 GHz calculated for vertical radio paths through a spherically-stratified, moderately humid atmosphere. Figure II-51 shows the theoretical one-way attenuation for vertical radio paths from the indicated heights to the top of the atmosphere for a frequency range of 1 - 150 GHz and for a moderately humid atmosphere.

II.6 ATTENUATION AND USE OF THE SPECTRUM

In order to provide a general indication of the possibilities of using wavelengths of a few millimeters or less for telecommunications, Figure II-52 is presented to show the specific attenuation (dB/km) for a path near the ground as a function of frequency. For comparison, the figure gives the attenuation for three rain rates, fog, and atmospheric gases, is presented only to give an order of magnitude of attenuation.



A : 7.5 g/m³ at ground
 B : dry atmosphere (0 g/m³)
 R : range of values due to fine structure

Figure II-50. Total One-way Zenith Attenuation Through the Atmosphere

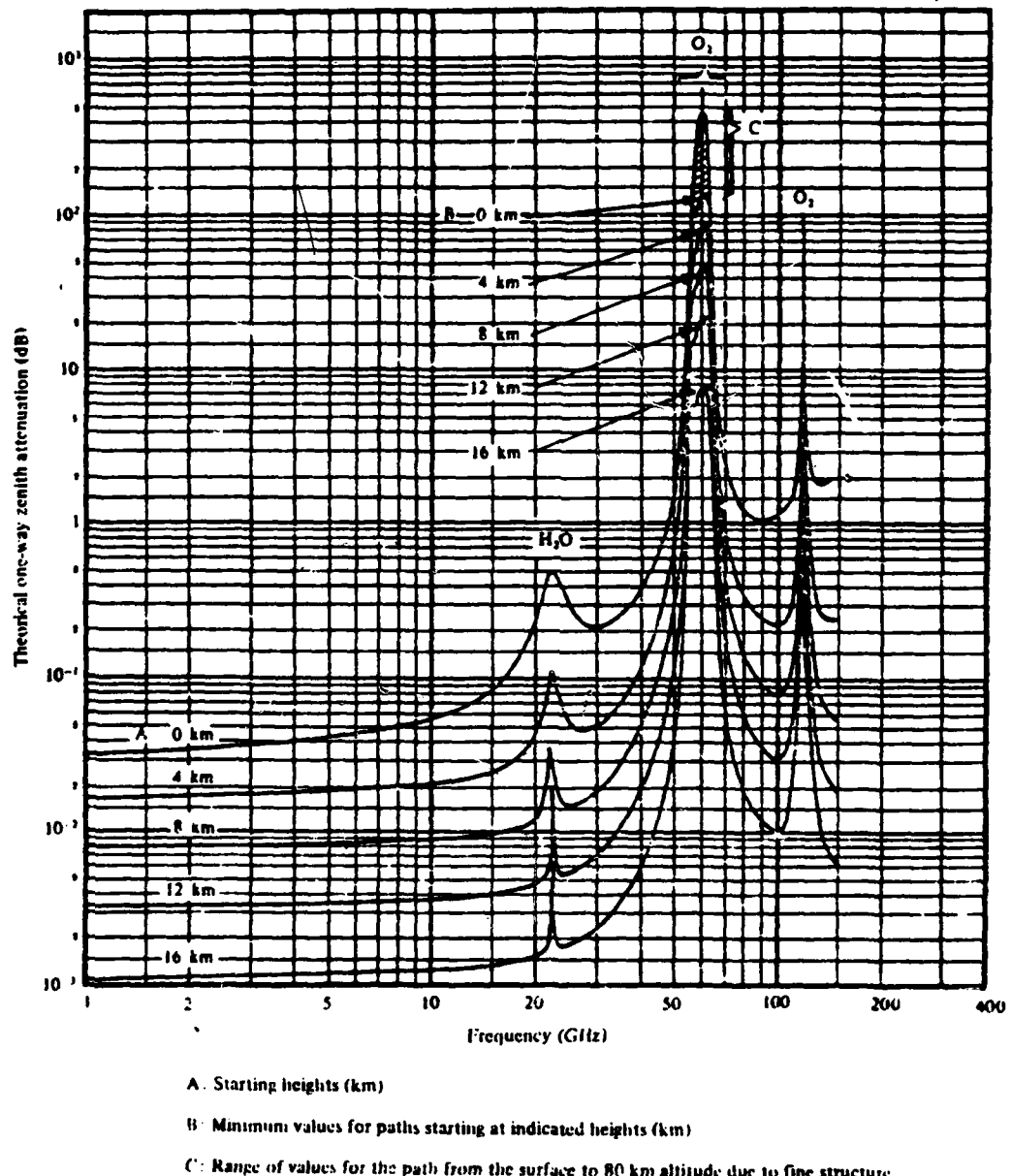


Figure II-51. Theoretical Vertical One-way Attenuation from Specified Heights to the Top of a Moderately Humid Atmosphere

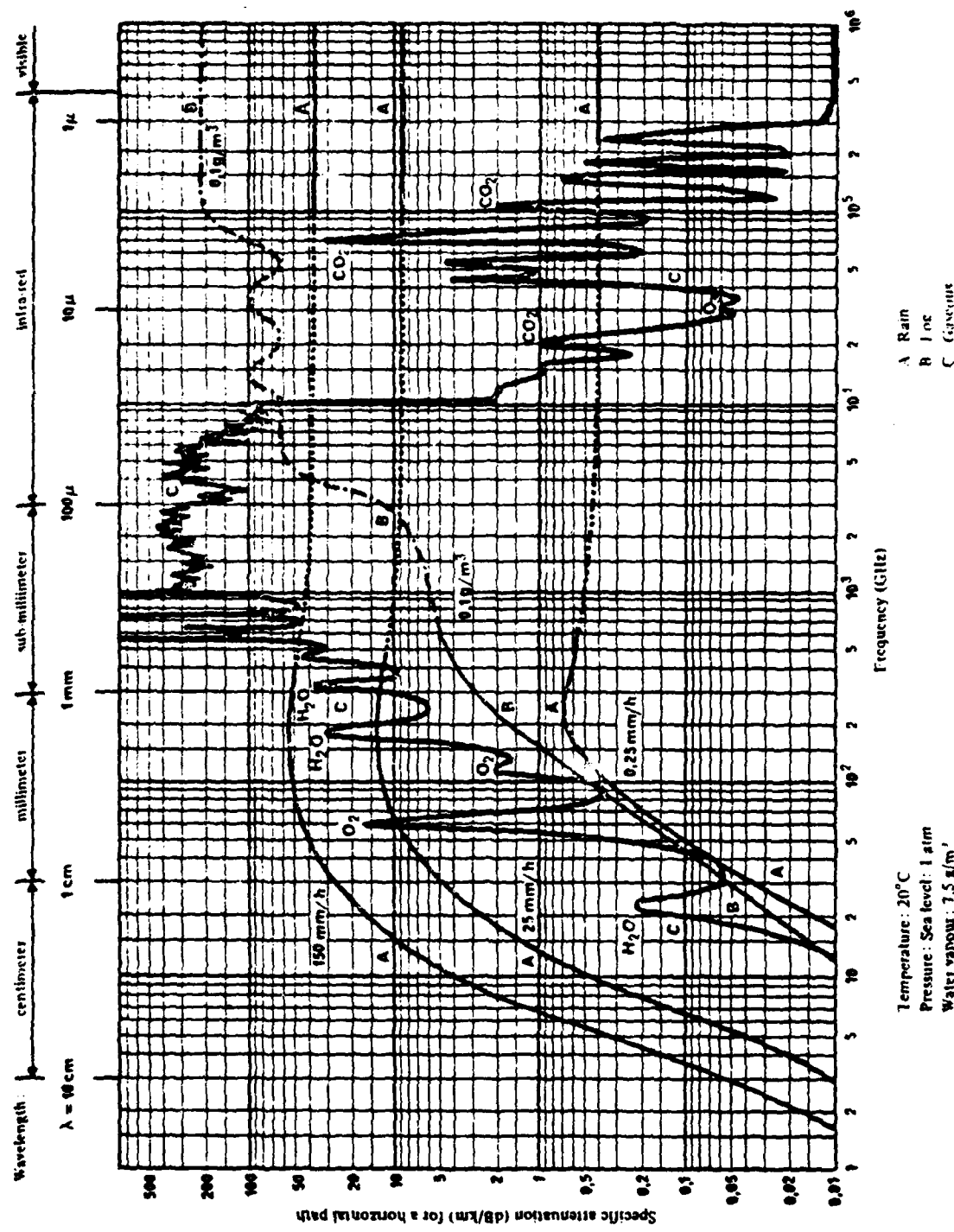


Figure 11-52. Attenuation Due to Rainfall and Gases in the Atmosphere

THIS PAGE INTENTIONALLY LEFT BLANK

CII-70

SUPPLEMENT III CUMULATIVE TIME STATISTICS
OF SURFACE - POINT RAINFALL RATE

THIS PAGE INTENTIONALLY LEFT BLANK

Cumulative Time Statistics of Surface-Point Rainfall Rates

PHILIP L. RICE AND NETTIE R. HOLMBERG

Abstract—Statistics on rainfall rates near and above the earth's surface are needed in order to estimate the percentage of time of absorption, or scattering of radio waves that affect radio system design and electro-space management. The most useful averaging time for computing such rates is on the order of 1 min or less. This paper extrapolates excessive short-duration precipitation data to provide such statistics from data routinely reported by the National Weather Service. For the 8766 h in an average year, and for a median or random location in any part of the world, the model described here estimates the fraction of time during which t -minute average rainfall rates exceed any given value.

I. INTRODUCTION

THE absorption and scattering of radio-wave energy by rain at superhigh frequency (SHF) and higher frequencies are fairly well understood [1], [2]. To estimate the percentage of time that such phenomena are important, the radio systems engineer needs predictions of the cumulative time statistics of surface rainfall rates for particular areas of interest. This paper summarizes a large sample of surface rainfall statistics. An earlier version is part of the "coordination distance" calculation procedures adopted in June 1971 by the World Administrative Radio Conference on Space Telecommunications as part of the International Radio Regulations [3].

The rainfall statistics summarized here are based upon the following:

1) average year cumulative distributions of hourly rates for the 10 years 1951 to 1960 and for a total of 63 stations, with 49 in the continental U.S. [4];

Paper approved by the Associate Editor for Radio Communications of the IEEE Communications Society for publication without oral presentation. Manuscript received May 31, 1973. This work was supported by the Office of Telecommunications, Institute for Telecommunication Sciences (OT/ITS), U.S. Department of Commerce, and NASA as part of the technical basis for a June 1971 World Administrative Radio Conference on Space Telecommunications.

The authors are with the Office of Telecommunications, Institute for Telecommunication Sciences, U.S. Department of Commerce, Boulder, Colo. 80302.

2) distributions for 15-year averages with recording intervals of 6, 12, and 24 h for 22 of these stations [5];

3) accumulations of short-duration excessive precipitation for 1951 to 1960 for recording intervals of 5, 10, 15, 20, 30, 45, 60, 80, 100, 120, and 180 min for 48 U.S. stations [6];

4) a U.S. map of the highest 5-min rates expected in a two-year period [7];

5) maximum monthly rainfall accumulations and the average annual number of thunderstorm days for the period 1931 to 1960 for 17 U.S. stations and 135 additional stations reported by the World Meteorological Organization [8], [9].

Some data that have recently become available for 1-min and 4-min recording intervals are compared with calculated values in Section III.

II. MATHEMATICAL MODEL

The statistical model is based upon the sum of individual exponential modes of rainfall rates, each with a characteristic average rate \bar{R} . According to this descriptive analysis

$$\text{rainfall} = \text{Mode 1 rain} + \text{Mode 2 rain} \quad (1)$$

where the exponential distribution chosen to describe "Mode 1 rain" corresponds to a physical analysis of thunderstorms, while "Mode 2 rain," represented by the sum of two exponential distributions, is simply all other rain. In temperate climates it appears that only convective storms associated with strong updrafts, high radar tops, hail aloft and usually with thunder can produce the high rainfall rates identified by Mode 1. Only the highest rates from excessive precipitation data were used to determine parameters for Mode 1, which is intended to represent a physical mechanism as well as a particular mathematical form.

The average annual total rainfall depth M is the sum of contributions M_1 and M_2 from the two modes:

$$M = M_1 + M_2 \text{ mm} \quad (2)$$

and the ratio of "thunderstorm rain," M_1 , to total rain M is defined as

$$\beta = M_1/M. \quad (3)$$

The number of hours of rainy t -min periods for which a surface point rainfall rate R is exceeded is the sum of contributions from the two modes:

$$T_t(R) = T_{1t}q_{1t}(R) + T_{2t}q_{2t}(R) \text{ h} \quad (4)$$

so that $T_t(R)/87.66$ is the percentage of an average year during which t -min average rainfall rates exceed R mm/h.¹ The data show that the average annual clock t -min rainfall rate for each of the modes is fairly constant. On the other hand, the total number of rainy t -min periods for each mode is relatively much more variable from year to year and between stations or climate regions. Rainfall climates defined by Barry and Chorley [10] for the United States were found to correspond very well with observed regional variations of the parameter β , defined by (3) as the ratio of "thunderstorm" or convective rainfall M_1 to the total annual rainfall M .

The average annual totals of t -min periods of Mode 1 and Mode 2 rainfall are T_{1t} and T_{2t} expressed in hours. The average annual Mode 1 and Mode 2 rainfall rates are therefore

$$\bar{R}_{1t} = M_1/T_{1t} \text{ mm/h} \quad (5)$$

$$\bar{R}_{2t} = M_2/T_{2t} \text{ mm/h}. \quad (6)$$

It should be worthwhile to note that M_1 and M_2 are not functions of t , since the amount of rainfall collected over a long period of time does not depend on the short-term recording interval t . But the total number of hours T_{1t} or T_{2t} of rainy t -min intervals (collecting at least 0.01 in or 0.254 mm of rain per interval) will depend on t .

The factors $q_{1t}(R)$ and $q_{2t}(R)$ in (4) are the complements of cumulative time probabilities. That is, each factor is the time that a rate R is exceeded by Mode 1 or Mode 2 rain, divided by the total number of hours T_{1t} or T_{2t} that there is more than 0.254 mm of rain in a t -min period.

This paper is concerned with estimating cumulative time distributions of clock-minute rates. For the more general case where $t > 1$ min, one more prediction parameter is required than the two that have been defined as M and β . This additional parameter is the number of hours D in $D/24$ rainy days. The formulas proposed here for $q_{1t}(R)$ and $q_{2t}(R)$ assume that the number of rainy days in an average year is

$$D/24 = 1 + M/8 \text{ rainy days} \quad (7)$$

where D is in hours and M is in millimeters. This relation (7) has been found good, on the average, for continental U.S. stations. For $t = 1$, the more general formulas are almost independent of D , so that

$$q_{1t}(R) = \exp(-R/\bar{R}_{1t}) \quad (8)$$

$$q_{2t}(R) = 0.35 \exp(-0.453074 R/\bar{R}_{2t}) + 0.65 \exp(-2.857143 R/\bar{R}_{2t}) \quad (9)$$

¹Following the U.S. National Weather Service, 1-h average rates begin "on the hour" and are called clock-hour rates. Extending this convention, a clock- t -min rate is $(60/t)$ times the depth of water collected in a single rain gauge during a continuous t -min period "by the clock."

and the annual average Mode 1 and Mode 2 rates \bar{R}_{1t} and \bar{R}_{2t} , are very nearly equal to 33.333 and 1.75505 mm/h, respectively, for $t = 1$. Then (4) may be written as

$$T_1(R) = M \{0.03\beta \exp(-0.03R) + 0.2(1-\beta) [\exp(-0.258R) + 1.86 \exp(-1.63R)]\} \text{ h}. \quad (10)$$

Fig. 1 shows $T_1(R)/M$ plotted versus R with the parameter β . Figs. 2 and 3 are world maps of M and β , respectively. Fig. 4 shows average year cumulative distributions $T_1(R)$ versus R for $t = 1, 5, 30, 60, 360$, and 1440 min (1 day) for $M = 1000$ mm (40 in) and $\beta = 0.125$.

When β and M are fixed, as they are for any single station, then observed long-term cumulative distributions usually show the nearly linear relationship between high values of R and low values of $T_1(R)$ that is illustrated in Fig. 1. One of these empirically determined straight lines extrapolated downwards to $R = 0$ completely determines the Mode 1 parameters β and R_{1t} .

In order to use Fig. 1 for estimating $T_1(R)$, given R , or for estimating R , given $T_1(R)$, it is necessary first to refer to Figs. 2 and 3 to obtain M and β , respectively, for the point or area of interest. If R is known, then $T_1(R)/M$ is read from Fig. 1 for the appropriate value of β , and is multiplied by M in order to estimate $T_1(R)$. If $T_1(R)$ is known, or calculated as 87.66 times the percentage of an average year for which R is exceeded, then $T_1(R)$ is first divided by M before R is read from Fig. 1 for the appropriate value of β .

The next section compares data with values of R or $R(T_1)$, read from Fig. 1 as a function of T_1/M and β , assuming that M and β are obtained from Figs. 2 and 3.

III. COMPARISON WITH DATA

Table I lists information about eight of the recording locations for which long-term cumulative distributions $T_1(R)$ and $T_4(R)$ are now available [11]-[13], and Table II compares estimated and observed values of rainfall rate R for $T_1(R)/8766$ or $T_4(R)/8766$ equal to 0.001 percent of an average year (5 min) and 0.01 percent of an average year (53 min).

Fig. 4 shows that estimates of R for $t = 1$ and $t = 4$ are nearly equal. The estimated values $R(0.001 \text{ percent})$ and $R(0.01 \text{ percent})$ in columns 5 and 7 of Table II, corresponding to the recording locations listed in Table I, were all obtained from Fig. 1, or by extrapolation of its curves. As this figure shows, all clock-minute rates above 40 mm/h are Mode 1 rates if β exceeds 0.02, or 2 percent. Accordingly, the second term of (10) may be ignored for these data, and R as a function of T_1 may be expressed explicitly as

$$R = [\ln(0.03\beta M/T_1)]/0.03 \quad (11)$$

in terms of the natural logarithm of $\beta M/T_1$. For $R > 40$ mm/h, the unique and remarkable set of data reported [11] agrees with the model (10) or (11) if $\beta = 0.035$ rather than 0.07, which is the value read from Fig. 3. There are almost 16 million min in 30 years, counting minutes when it does not rain. The highest 1-min average rainfall rate reported [11] for 1940 to 1970 at Montsouris, Paris, France is $R = 260$ mm/h. The average annual rainfall for 1940 to 1970 at St. Maur, near

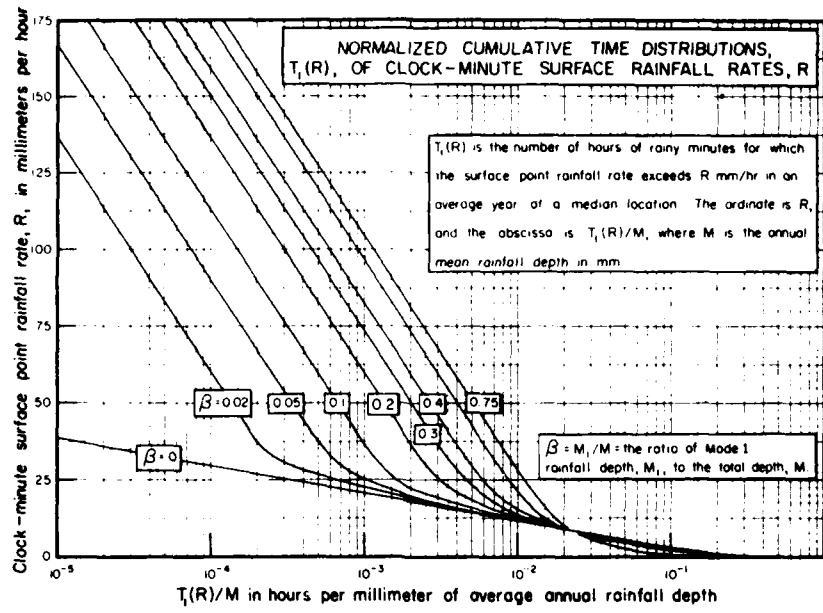


Fig. 1. Normalized cumulative time distributions.

Adapted from Miller, Albert, Meteorology, p110, C E Merrill Books, Columbus, Ohio 1966
Compare with U S Dep't of Commerce Climates of the World, p4, GPO Jan 1969

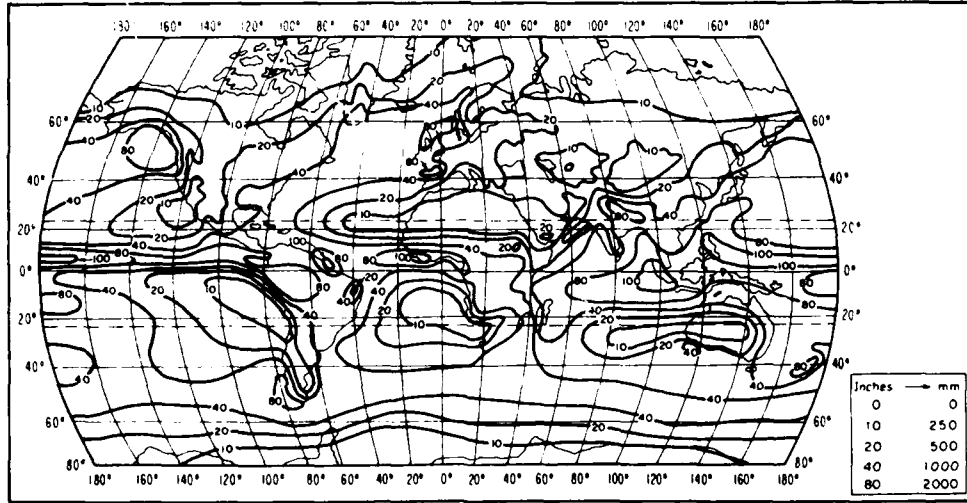


Fig. 2. Mean annual precipitation in inches (equal to $M/25.4$).

Montsouris, is $M = 644$ mm (rather than the value of 890 mm read from Fig. 2). According to (10) or (11), the calculated value of R for $M = 644$, $\beta = 0.035$, and $T_1(R) = (1/60)/30 = 1/1800$ is 237 mm/h. For $\beta = 0.07$, the calculated value is 260 mm/h, agreeing exactly with the highest observed 1-min rate. In general, a clock- t -min rate will exceed any given value R for t consecutive minutes, on the average, only once during the so-called return period

$$N_0 = (t/60)/T_1(R) \text{ years.} \quad (12)$$

For some existing radio systems this return period for critically high values of R and for $t = 1$ is often comparable to the mean time between failures of critical equipment components [14].

World record rainfall rates reported by the Air Force Cambridge Research Laboratory (AFCLR) [15] do not correspond to the median locations represented by (10) and (11). The following may be used to approximate [15, fig. 5-5]:

$$R = 2815\sqrt{t} \text{ mm/h} \quad (13)$$

for record rates and $t > 8$ min. For $t = 8$, $R = 1000$ mm/h. This is the highest rate recorded in [15, fig. 5-5] for any collection interval, including $1 < t < 8$ min.

These extremely high rates presumably correspond to rare situations involving a convergence of storm systems and storage of rain aloft, followed by a sudden decrease in updrafts. Such conditions would violate long-term conditions for a

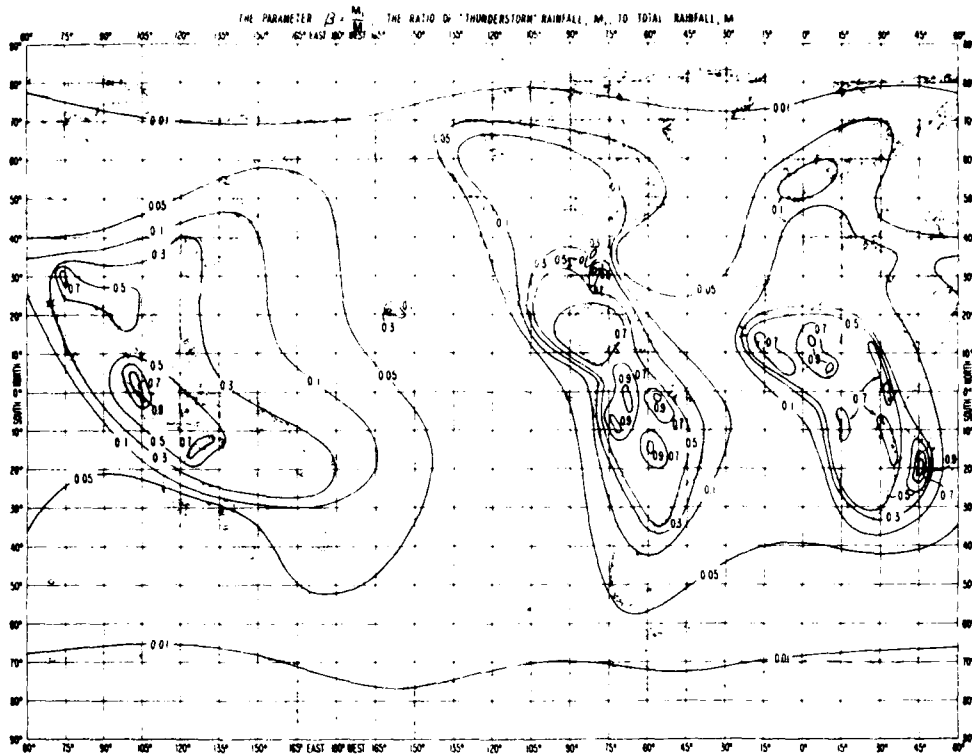


Fig. 3. The parameter β .

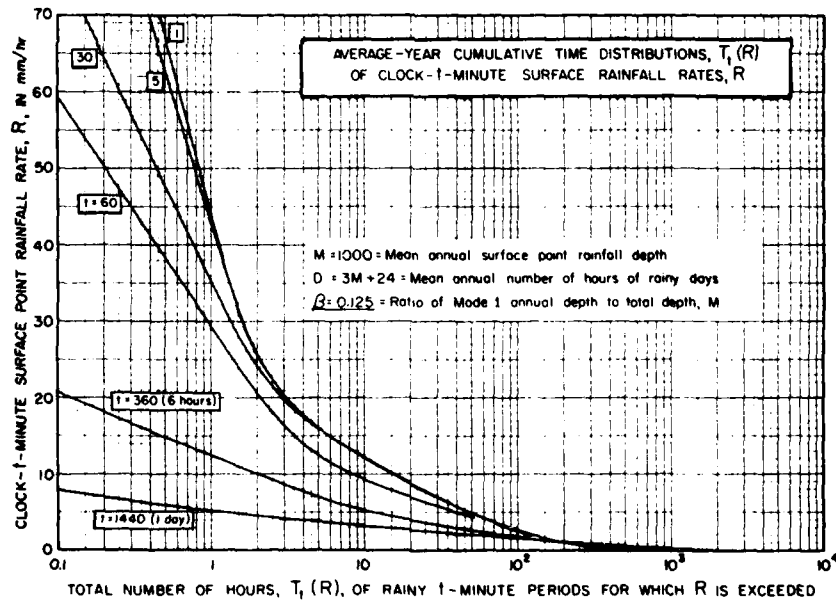


Fig. 4 Average year cumulative time distributions $T_1(R)$.

Poisson distribution of randomly light rainfall within ordinary heavy storms. The observed exponential distribution of T_1 for a fixed R , as expressed by (11), is consistent with the assumption of a Poisson distribution of durations for rates less than R [16].

The standard error of prediction associated with (11) depends upon what (11) is used for, as well as what it is based on. The root-mean-square deviation of the median observed R for the

years 1951 to 1960 and for any fixed t is 8.4 mm/h. This is calculated for the 48 U.S. stations for which excessive precipitation data were analyzed, and for all of the six collection intervals $t = 10, 15, 20, 30, 45$, and 60 min. The standard deviation of the data from year to year for $t = 30$ min and 10 randomly selected stations varies from 10 to 30 mm/h, and the corresponding pooled standard deviation is 21.5 mm/h. For the same 10 selected stations, the standard error due to

TABLE I
RAIN GAUGE LOCATIONS AND RECORDING PERIODS

1. Montsouris, Paris, France, 48.8°N, 2.5°E (30 years, 1940-1970 except 1956)	[11]
2. Franklin, N.C., 35.0°N, 83.5°W (2-1/3 years, Dec. 1960-Apr. 1962)	[12]
3. West Concord, Mass., 42.5°N, 71.3°W (2 years, 1962 and 1963)	[13]
4. Pleiku, S. Vietnam, 14.0°N, 108.0°E (1-1/2 years, 1963 and 1965)	[12]
5. DaNang, S. Vietnam, 16.1°N, 108.2°E (1 year, Jan. 1963-Feb. 1964)	[12]
6. Saigon, S. Vietnam, 10.8°N, 106.7°E (1 year, Jan. 1964-Dec. 1964)	[12]
7. Coral Gables, Miami, Fla., 25.7°N, 80.3°W (1 year, Aug. 1957-Aug. 1958)	[12]
8. Island Beach, N.J., 39.9°N, 74.1°W (1 year, May 1961-May 1962)	[12]

TABLE II
DATA AND CALCULATIONS

t (Fig. 2)	M (Fig. 2)	β (Fig. 3)	R(0.001 percent)		R(0.01 percent)	
			Estimated	Observed	Estimated	Observed
1. 1	890	0.07	103	64	30	-
2. 1	1270	0.32	164	171	88	68
3. 1	960	0.10	118	120	39	53
4. 4	1780	0.40	190	174	112	94
5. 4	1650	0.42	183	142	105	94
6. 4	2030	0.45	192	210 ^a	118	110
7. 1	1520	0.70	197	189	118	120
8. 1	1080	0.12	123	119	48	52

^aExtrapolated: for $T_4(R)/8766 = 0.002$ percent, calculated and observed values are 167 and 190 mm/h, respectively.

variations of $M_1 = \beta M$, read from Figs. 2 and 3, and then compared with values determined directly from (11) and data for R , is 11 mm/h. Then if (11) is used to estimate R for a random station year, rather than for an average year and median station (such that half of all observed values are expected to be less and half greater than the estimated R), the total standard error is

$$\sigma_R = (8.4^2 + 21.5^2 + 11^2)^{1/2} = 26 \text{ mm/h} \quad (14)$$

provided that only Mode I ($R > 40$ mm/h) is involved.

Suppose, for instance, that $M = 1000$ mm and $\beta = 0.2$ according to Figs. 2 and 3. Fig. 1 estimates that 70 mm/h will be exceeded for 60 min in an average year. Then two thirds of all rates for random station years will lie between 44 and 96 mm/h.

The electrospace planner or system engineer who is interested in an average year and a median location could hope for a standard error less than 10 mm/h if the estimates of M and β were sufficiently reliable. For any radio link, a minimum acceptable wanted-to-unwanted signal ratio is required for an acceptable grade of service. Service probability has been defined [17] as the probability that this ratio is exceeded for some minimum acceptable fraction of a given "time block," assumed here to be all of the hours of every day in an average year.

It is usually reasonable to assume that during any given minute the dominant unwanted signal in a radio system comes from a single source, either internal or external to the system. To estimate cumulative time of interference, then, one can add the numbers of minutes during which different sources and

propagation mechanisms (including diffraction, ducting, and various types of scattering) are dominant contributors to the system noise temperature. This procedure is usually realistic whenever the total time occupied by unwanted signal events is short compared to the time block during which service must be provided.

IV. CONCLUSIONS

A model for the calculation of cumulative time statistics of point rainfall in the United States has been derived from a broad data base. It provides estimates of the percentage of an average year that 1-min average surface rainfall rates exceed any given value R . Relationships between R and the volume reflectivity and absorptivity of rain make it possible to estimate the accumulated time of interference from hydrometeor scattering or absorption near the earth's surface, in terms of a given volume average of R exceeded for a given percentage of an average year [1], [2].

The methods used for the selection, interpolation, and extrapolation of available data emphasize high rain rates, as well as heavily populated areas where radio interference problems and surface rainfall data tend to be concentrated. More general interference probability estimates will require an examination of the dependence of these cumulative time statistics on area and height above the earth's surface, including specific allowances for area and height resolution, as well as regional and time resolution.

ACKNOWLEDGMENT

The authors are particularly grateful for insights into the nature of rain phenomena and sources of data supplied by F. J. Altman, Dr. P. M. Austin, Dr. R. K. Crane, Dr. D. C. Hogg, C. A. Samson, and W. I. Thompson, III, as well as for the many days of conscientious and patiently constructive criticism of earlier versions of this paper by Dr. E. L. Crow.

It is not practical to mention the hundreds of contributors to the Weather Radar Conferences and scientific journals whose studies profoundly influenced the development of the model, nor more than a few of the CCIR² workers whose quick appreciation of both its faults and its virtues were a great help. Particular thanks should go to Dr. J. A. Saxton of the United Kingdom, International Chairman of CCIR Study Group 5 (Tropospheric Propagation), P. Misme of France, Chairman of an Interim Working Party on Radio Meteorology, and to Dr. J. A. Lane of the United Kingdom and Dr. B. C. Blevins of Canada.

M. Coyle and C. Moncure of OT/ITS kept up with a tremendous volume of data analysis and computer programming over the period of a year, and H. J. Allacher is responsible for the analysis and synthesis of data for $t = 360, 720$, and 1440 min.

REFERENCES

- [1] R. K. Crane, "Propagation phenomena affecting satellite communication systems operating in the centimeter and millimeter wavelength bands," Proc. IEEE, vol. 59, pp. 173-188, Feb. 1971.

² International Radio Consultative Committee.

- [2] L. T. Gusler and D. C. Hogg, "Some calculations on coupling between satellite-communications and terrestrial radio-relay systems due to scattering by rain," *Bell Syst. Tech. J.*, vol. 49, pp. 1491-1511, 1970.
- [3] International Telecommunications Union, Final Acts of the World Administrative Radio Conference for Space Telecommunications, Geneva, Switzerland, Ann. 18 (App. 28), June 1971.
- [4] U.S. Weather Bureau, 1951 to 1961 annual reports such as Climatological Data, National Summary, Annual 1961, vol. 12, no. 13, U.S. Dep. Commerce, Asheville, N. C., 1962.
- [5] D. L. Jorgenson, W. H. Klein, and C. F. Roberts, "Conditional probabilities of precipitation amounts in the conterminous United States," U.S. Dep. Commerce, Environmental Sci. Services Administration, Weather Bureau, Office of Syst. Develop., Techniques Develop. Lab., Silver Spring, Md., ESSA Tech. Memo WBTM-TDL-18, Mar. 1969.
- [6] U.S. Dep. Commerce, "Excessive precipitation techniques," (Weather Bureau, Supt. of Documents, U.S. Government Printing Office, Washington, D.C., 1958.
- [7] R. E. Skerjanc and C. A. Samson, "Rain attenuation study for 15 GHz relay design," Fed. Aviation Administration, Washington, D.C., FAA-RD-70-21, 1970; or Nat. Tech. Inform. Service, AD-709-348, Springfield, Va.
- [8] World Meteorological Organization, Geneva, Switzerland, "Climatological normals (CLINO) for CLIMAT and CLIMAT SHIP stations for the period 1931-1960," WMO/OMM-No. 117, TP, 52, 1962.
- [9] World Meteorological Organization, Geneva, Switzerland, "World distribution of thunderstorm days, Part 2: Tables of Marine Data and World Maps," WMO/OMM-No. 21, TP, 21, 1956.
- [10] R. C. Barry and R. J. Chorley, *Atmosphere, Weather, and Climate*. New York: Holt, Rinehart and Winston, Inc., 1970, p. 205.
- [11] P. Misme, "Donnees sur le regime pluvieux de la region Parisienne," Cen. Nat. Etudes Telecommuni., Issy les Moulineux, Paris, France, Tech. Note E.S.T./A.P.H./19, 1973.
- [12] D. B. A. Jones and A. L. Sims, "Climatology of instantaneous precipitation rates," Illinois State Water Survey, Univ. Illinois, Urbana, Final Rep. on Contract F19628-69-C-0070 for U.S. Air Force Cambridge Res. Lab. (AFCRL), Bedford, Mass., Dec. 1971.
- [13] NASA, Goddard Space Flight Center, "Interference due to rain," Rep. X-750-71-211, May 1971.
- [14] R. F. White, "Some aspects of microwave system reliability, Lenkurt demodulator," presented at the Int. Conf. Commun. San Francisco, Calif., June 1970.
- [15] A. E. Cole, R. J. Donaldson, R. Dyer, A. J. Kantor, and R. A. Skrivanek, "Precipitation and clouds," in *Handbook of Geophysics and Space Environments*, Air Force Surveys in Geophysics, No. 212, Office of Aerospace Res., U.S. Air Force Cambridge Res. Lab., Bedford, Mass., AFCRL-69-0487, Nov. 1969.
- [16] W. Feller, *An Introduction to Probability Theory and Its Applications*, vol. 1 and 2, 3rd ed. New York: Wiley, 1968.
- [17] P. L. Rice, A. G. Longley, K. A. Norton, and A. P. Barsis, "Transmission loss predictions for tropospheric communication circuits," NBS Tech. Note 101, vol. I and II (revised), 1967.



Philip L. Rice (M'65) was born in Washington, D.C., on December 25, 1922. He received the B.S. degree in mathematics and physics from the Principia College, Elsah, Ill., in 1948.

In 1948 and 1949 he was employed by the firm of Raymond M. Wilmotte, Inc., Washington, D.C., consulting radio engineers. In 1950 he joined the staff of the Institute for Telecommunication Sciences of the Office of Telecommunications (formerly the Central Radio Propagation Laboratory of NBS), Boulder, Colo.

He is a member of the Systems Technology and Standards Division. He is a co-author of Technical Note 101, "Transmission loss predictions for tropospheric communication circuits," for which each author received the Department of Commerce Silver Medal. He has been an Advisor to the International Radio Consultative Committee (CCIR) since 1956 and is U.S. Chairman of CCIR Study Group 5 (Tropospheric Propagation).

Mr. Rice is a member of the IEEE Group on Antennas and Propagation, the IEEE Wave Propagation Standards Committee, the Research Society of America, and the Institute of Mathematical Statistics.

Nettie F. Holmberg was born in Seneca, N. Mex., on December 8, 1932. She received the B.S. degree from Colorado State University, Ft. Collins, in 1955, and attended graduate school there in 1961.

In 1955 she joined the U.S. Naval Ordnance Test Station working in missile research. She joined the National Bureau of Standards working first in ionospheric propagation, and later as satellite controller (Topside Sounder). Since 1968 she has been in tropospheric propagation research.

SUPPLEMENT IV ESTIMATING YEAR-TO-YEAR VARIABILITY
OF RAINFALL FOR MICROWAVE APPLICATIONS

THIS PAGE INTENTIONALLY LEFT BLANK

CIV-11

Estimating Year-to-Year Variability of Rainfall for Microwave Applications

H. T. DOUGHERTY AND E. J. DUTTON

Abstract—Recent progress is reported for extensions of the Rice-Holmberg rainfall-prediction model. This extension provides for the year-to-year variation expected for rainfall and is required to permit any useful comparison of predicted with observed rainfall (or predicted with observed microwave attenuation due to rainfall). The results are illustrated for Europe.

I. INTRODUCTION

In 1973, Rice and Holmberg [1] presented a worldwide rainfall prediction model. The model is designed specifically for telecommunication applications and consists of distributions of t -minute ($t = 1, 5, 30$, etc.) point-rainfall rates predicted from historical meteorological data. This prediction model contains three basic parameters: M , the annual rainfall in millimeters; β , the ratio of thunderstorm rain to total rain; and D , the annual number of days for which precipitation ≥ 0.25 mm. By relating D to the annual rainfall M and provid-

Paper approved by the Editor for Radio Communication of the IEEE Communications Society for publication without oral presentation. Manuscript received October 12, 1977; revised March 23, 1978.

The authors are with the Institute for Telecommunication Sciences, National Telecommunications and Information Administration, Boulder, CO 80303.

ing global maps of the two parameters M and β , Rice and Holmberg extended their rain-rate prediction worldwide. This rainfall prediction modeling was provided for an average year based upon information extracted from (for some locations) up to 30 years of climatological data. However, one of the most striking aspects of rainfall is its variability, in both space and time. The purpose of this letter is to report on progress in extending the Rice-Holmberg model by estimating the spatial and temporal (year-to-year) variability of rainfall.

II. SPATIAL VARIATION OF RAINFALL

Of course, the spatial variability has been described in a crude fashion by a division of the world into rainfall zones, based partially upon the Rice-Holmberg worldwide mapping of M and β . For example, Europe was characterized by three rainfall zones [2]. Recently more detailed mappings of the three basic parameters (M , β , and D) were developed for Europe, and rainfall zones were defined as depicted in Fig. 1 [3] [4]. Figure 2 shows their corresponding predicted ($t = 1$ min) rain-rate distributions. However, these climatological rainfall zones are geared to conditions more related to agriculture than to telecommunications. Although there tends to be some uniformity of average annual precipitation, M , throughout a zone, this is less true for β and the resulting rainfall rate. Detailed mappings of M , β , and D determined from 249 European locations permit a much more detailed presentation of the spatial variation of rainfall than does the zonal concept. This is illustrated in Fig. 3 by the contours of $t = 1$ min rainfall rate (R_1 in mm/h) expected for 0.1% of an average year in Europe. These contours were drawn from the data obtained at the 249 station locations. Figure 4 is for 0.01% of an average year; a similar mapping is available for 1.0% of an average year in Europe [3].

III. YEAR-TO-YEAR VARIATION IN RAINFALL

With the rapid extension of communication systems to EHF, both terrestrial and satellite telecommunications have experienced the impact of the year-to-year variability of rainfall and its attenuation of microwaves [6] [7]. Until very recently, however, this temporal variability had not been treated, although it can be determined from estimates of the year-to-year variation in rainfall data for rainfall zones and locations throughout the world. For example, in the process of determining rainfall distributions for the ten rainfall zones of Europe, it was necessary to also examine the monthly rainfall data for the 249 stations from 1952 through 1972. By regression analysis, it was subsequently found that the number of rainy days, D , may be expressed [3] in terms of M and β . Further, the year-to-year variation of M and β were determined for each zone and approximated by normal distributions [5].

The mathematical formulation of the Rice-Holmberg distribution is that of $T_t(R)$, the cumulative time [or the percent of time $P_t(R)$], for which a given t -minute rainfall rate R_t is exceeded during an average year. That is, $P_t(R)$ is an explicit function of R_t . As such, it can be awkward to assess the variation of R_t in terms of the variations of M and β . However, it is relatively straightforward for the inverted relationship, i.e., when $R_t(P)$ is a function of P_t . For the purposes of variational analysis only, it was therefore convenient to substantially reduce the mathematical complexity of the Rice-Holmberg distribution. The tri-exponential form of the Rice-Holmberg distribution has been approximated by three alternate exponential forms whose coefficients and



Figure 1. Ten European rainfall climatic zones.

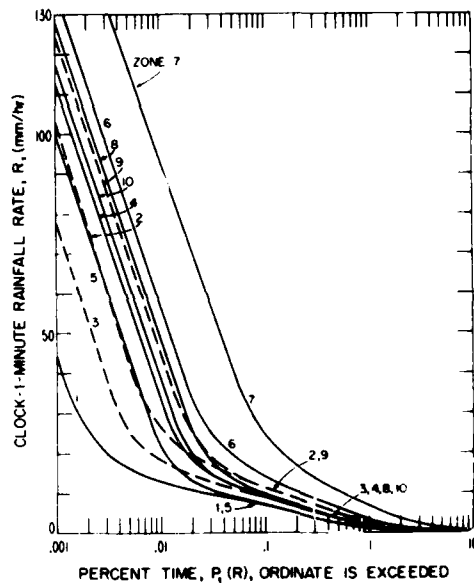


Figure 2. Estimated distribution of rainfall rates for one-minute periods, $P_1(R)$, for the European rainfall climatic zones.

powers of the variable R differ from the three ranges of R values of interest [3]. The three ranges of R are those for which the rainfall is heavy or primarily convective, very light or primarily stratiform, and moderate or mixed convective and stratiform. The associated coefficients were determined by regression analysis so that the modified form produces minimal change in predicted values and is exact for rainfall rate values of 30 mm/h or more. The standard deviation of the predicted rainfall rate at a point can therefore be expressed in terms of the average-year values and year-to-year standard deviations of M and β determined from rainfall data at stations in the vicinity of the point of interest [5].

As an example of this process, Table I lists the standard deviations $S_{R1}(P)$ for the temporal and spatial variation (year-to-year and by stations within a zone) of $t = 1$ min rainfall rates $R_1(P)$ for specified percentages $P_1(R)$ of any year and for each of the ten European zones. Note that these standard deviations range from 9 to 45% of their corresponding average-

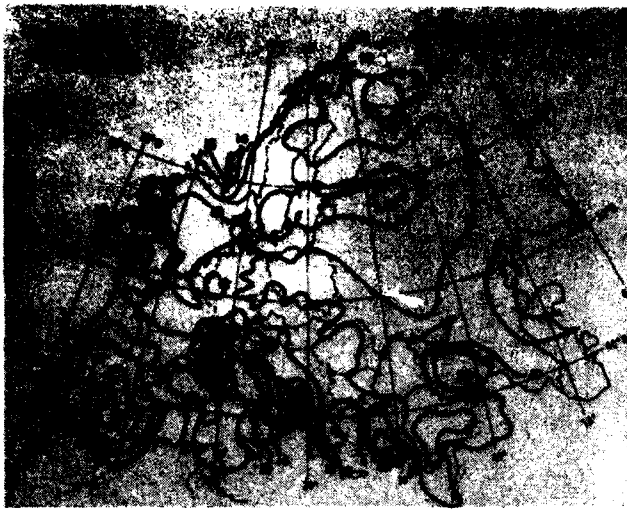


Figure 3. Spatial distribution of 1-min rainfall rates, R_1 in mm/h, expected for 0.1% of an average year in Europe.



Figure 4. Spatial distribution of 1-min rainfall rates, R_1 in mm/h, expected for 0.01% of an average year in Europe.

TABLE I
ESTIMATED DEVIATIONS $S_{R1}'(P)$, SPATIAL AND TEMPORAL, OF
 $t = 1$ MIN ZONAL RAINFALL RATES $R_1(P)$ FOR SPECIFIED
PERCENTAGES $P_1(R)$ OF ANY YEAR

European Rainfall Climatic Zone	$P_1(R) = 1\%$		$P_1(R) = 0.1\%$		$P_1(R) = 0.01\%$	
	$R_1(1\%)$ mm/hr	$S_{R1}'(1\%)$ mm/hr	$R_1(0.1\%)$ mm/hr	$S_{R1}'(0.1\%)$ mm/hr	$R_1(0.01\%)$ mm/hr	$S_{R1}'(0.01\%)$ mm/hr
1	2.3	0.2	7.1	1.8	17.3	4.3
2	3.4	0.4	10.7	3.1	27.6	7.5
3	2.8	0.3	8.6	2.8	21.6	6.5
4	2.8	0.3	10.1	3.9	33.2	11.1
5	2.3	0.2	8.2	3.0	26.6	7.8
6	4.1	0.8	14.8	6.6	56.6	17.4
7	7.8	2.9	25.4	8.5	95.6	14.9
8	3.0	0.4	11.6	5.0	48.5	15.0
9	3.4	0.4	12.3	5.0	45.5	8.2
10	2.8	0.3	10.3	3.5	38.6	10.2

year rainfall rate. For each zone, the $R_1(P)$ values for $P_1(R) = 1$, 0.1, and 0.01% are three points on the zonal distribution of rainfall rates for an average year (as in Fig. 2). We assume that the year-to-year variation is normally distributed. For each percentage $P_1(R)$, the corresponding $S_{R1}'(P)$ is proportional to the value $1.645 S_{R1}'(P)$ which must be added to and subtracted from $R_1(P)$ to determine the range within which will fall 90% of rainfall rates observed for P percent of any year at some point within the zone. From zone 4 in Table I, the rainfall rate exceeded for 0.01% of an average year, 33.2 mm/h, would correspond to a specific attenuation at 15 GHz of 1.9 dB/km [2]. For only 5% of the years would the rainfall exceed $33.2 + 1.645(11.1) \approx 51.5$ mm/h, but the specific attenuation at 15 GHz would exceed 4.5 dB/km. Although the expected 0.01% rainfall is 55% higher for 5% of the years than for the average year, the corresponding 15 GHz specific attenuation is increased by 150%. Further, the effective path length through the rainfall is likely to exceed a few kilometers [2].

As an alternative to the zonal approach, most of the spatial variation can be eliminated by determining contour maps of

the rainfall rate. For example, Figs. 3 and 4 are such determinations of the rainfall rates predicted, respectively, for 0.1 and 0.01% of an average year. Then, the corresponding standard deviations of the temporal variation can be mapped, as in Figs. 5 and 6. Actually, these temporal standard deviations also contain a slight element of spatial uncertainty, as a result of approximations in the evaluation procedure [5].

IV. CONCLUSION

The usefulness of the Rice-Holmberg rainfall prediction model has recently been extended by the detailed mappings of M , β , and D now available for Europe [3] and in preparation for the U.S.A. [5]. However, this note indicates the further development of that model by estimating the expected year-to-year variation in Europe. That is, although Figs. 1 to 4 provide the Rice-Holmberg rainfall rate predictions for an average year in Europe, Table I or Figs. 5 and 6 provide the basis for determining the confidence limits of that prediction, the intervals within which a specified percentage of observa-



Figure 5. Spatial distribution of the standard deviation, S_{R1} in mm/h for the year-to-year variation of 1-min rainfall rates expected for 0.1% of an average year.



Figure 6. Spatial distribution of the standard deviation, S_{R1} in mm/h for the year-to-year variation of 1-min rainfall rates expected for 0.01% of an average year.

tions would be expected to fall. We now finally have the means of comparing predicted and observed rainfall data. This comparison is necessary to complete the Rice-Holmberg model; i.e., to determine the prediction error, an essential ingredient of any prediction model. Similarly, we now have data for determining the year-to-year variation in microwave attenuation and in the rainfall reflectivity that is so significant for microwave interference potential [8]. That will provide the basis for a subsequent comparison of predicted and observed attenuation and reflectivity.

REFERENCES

- [1] Rice, P. L., and N. R. Holmberg, "Cumulative Time Statistics of Surface-Point Rainfall Rates", *IEEE Trans. on Communications*, COM-21, No. 10, 1131-1136, October, 1973.
- [2] CCIR, Report 563 of *Propagation In Non-Ionized Media*, Vol. V

of CCIR XIII Plenary Assembly, Geneva 1974, PB 244005, NTIS, Springfield, VA 22151.

- [3] Dutton, E. J., H. T. Dougherty, and R. F. Martin, Jr., "Prediction of European rainfall and link performance coefficients at 8 to 30 GHz", AD/A-000804 (U.S. Natl. Tech. Information Service, Springfield, VA 22151), 1974.
- [4] Goode, J. P., *Goode's World Atlas* (E. B. Espenshade, Editor), Rand McNally Co., Chicago, Ill., 1957.
- [5] Dutton, E. J., "Earth-space attenuation prediction procedures at 4 to 6 GHz", Office of Telecommunications Report, OTR 77-123, 1977.
- [6] Davies, P. G., "Radiometer measurements of atmospheric attenuation at 19 and 37 GHz along sun-earth paths", *Proc. IEE*, 120, 159-164, 1973.
- [7] Wilson, R. W., and W. L. Mammel, "Results from the three-radiometer path-diversity experiment", Conference on Propagation of Radio Waves At Frequencies Above 10 GHz, IEE Conference Publication No. 98, April, 1973.
- [8] Hubbard, R. W., J. A. Hull, P. L. Rice, and P. I. Wells, "An Experimental Study of the Temporal Statistics of Radio Signals Scattered by Rain", Office of Telecommunications Report, OTR 73-15, AD/N74-12845 (NTIS, Springfield, VA 22151), 1973.

**SUPPLEMENT V YEAR-TO-YEAR VARIABILITY OF RAINFALL
FOR MICROWAVE APPLICATIONS IN THE U.S.A.**

CV-i

THIS PAGE INTENTIONALLY LEFT BLANK

**Year-to-Year Variability of Rainfall for
Microwave Applications in the U.S.A.**

E. J. DUTTON AND H. T. DOUGHERTY

Abstract—Further extensions of the Rice-Holmberg rainfall prediction model are reported. These extensions describe the variation of rainfall with location in the U.S.A., as well as the standard deviation of their year-to-year variation. Application to the prediction of microwave signal attenuation by rainfall, and the comparison with observed data are illustrated.

I. INTRODUCTION

The prediction of microwave attenuation, etc., due to rainfall has become a concern to the telecommunications industry in the U.S.A. This results from the various impacts of rainfall (attenuation, depolarization, interference, etc.) upon terrestrial and satellite microwave system performance.

Paper approved by the Editor for Radio Communication of the IEEE Communications Society for publication without oral presentation. Manuscript received June 8, 1978; revised November 14, 1978.

The authors are with the Institute for Telecommunication Sciences, National Telecommunications and Information Administration, U.S. Department of Commerce, Boulder, CO 80303.

In 1973, Rice and Holmberg [1] presented a world-wide rainfall prediction model designed specifically for telecommunications applications. It can predict probability distributions, $P_t(R)$, of t -min duration ($t = 1, 5, 30$, etc.) point rainfall rates, R , determined from the available historical meteorological data. Since then, the model has been extended by modification, principally to accommodate the significance of chronological data on additional rainfall parameters and, to a lesser degree, to permit its inversion to determine the 1-min (approximately instantaneous) rainfall rate, $R_1(P)$, predicted for a given P percent of a year [2]-[5]. At present, the modified model still contains the three basic parameters M , D , and β . The parameters, M , the average annual rainfall in millimeters, and D , the average annual number of days for which the precipitation equals or exceeds 0.25 mm, are both determined directly from recorded data. The average annual ratio, β , of thunderstorm rain to total rain is a derived quantity determined from the data on M_m , the greatest monthly precipitation (in millimeters) observed in 30 yr, and U , the average annual number of days with thunderstorms [4]. Consequently, the resulting model is for an average year.

One of the most striking features of rainfall, however, is its variability with both location and time. This variability has already been described for Europe [3], [5]. The purpose of this letter is to describe the variation with location of rainfall rates in the U.S.A. (the conterminous U.S., Alaska, and Hawaii) for an average year and, further, to describe its temporal variation (i.e., from year-to-year).

II. VARIATION WITH LOCATION

To a degree, the spatial variation has been described in a crude fashion by the division of the world into rainfall zones, based partially upon the Rice-Holmberg worldwide mapping of M and β . For example, Europe had been characterized by three rainfall zones [6], but subsequently, more detailed mappings of the three rainfall parameters (M , β , and D) permitted the definition of 10 European rainfall zones [3]. Since then, detailed mappings of the rainfall parameters also permitted the definition of 19 rainfall zones for the U.S.A. [4].

Although these zones demonstrate the variety of rainfall conditions encountered in the U.S.A., a finer detail may be required for localized site selection. A more direct evaluation for specific locations can be obtained from a detailed mapping of the rainfall parameters themselves (M , M_m , etc.). This has now been done for the U.S.A. based upon 30 yr of meteorological data from 305 first-order U.S. Weather-Service stations [4]. The resulting mappings (M , M_m , etc.) for the U.S.A. have been incorporated into a computer program [4] for the modified Rice-Holmberg model to determine rainfall rate predictions for the U.S.A. These results are illustrated in Figures 1, 2, and 3 by the contours of $t = 1$ min rainfall rate, $R_1(P)$ in mm/h, expected for $P = 1, 0.1$, and 0.01 percent of an average year in the U.S.A. For example, Fig. 1 indicates that a rainfall rate of about $R_1(1\%) = 2.6$ mm/h would be expected for a cumulative total of 1% of an average year (87.7 h/yr) in Washington, DC. Figure 2 indicates a rainfall rate of about $R_1(0.1\%) = 14$ mm/h would be expected for a cumulative total of 0.1% of an average year (about 8.8 h/yr) in Washington, DC. Figure 3 indicates that a rainfall rate $R_1(0.01\%) = 76$ mm/h would be exceeded for a total of 0.01% of an average year (a cumulative total of about 53 min/yr) in Washington, DC.

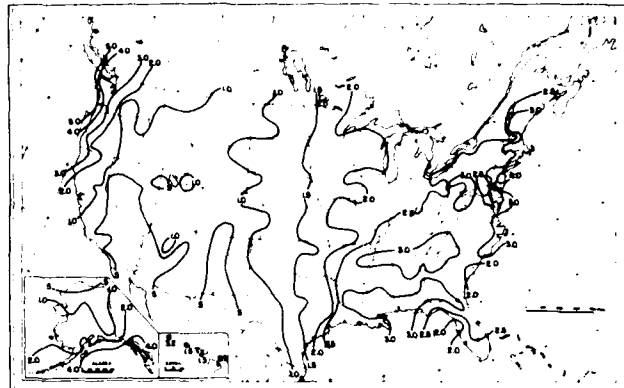


Figure 1. Contours of $R_1(1\%)$, the $t = 1$ min rainfall rates in mm/h predicted for 1.0 percent of an average year in the U.S.A.

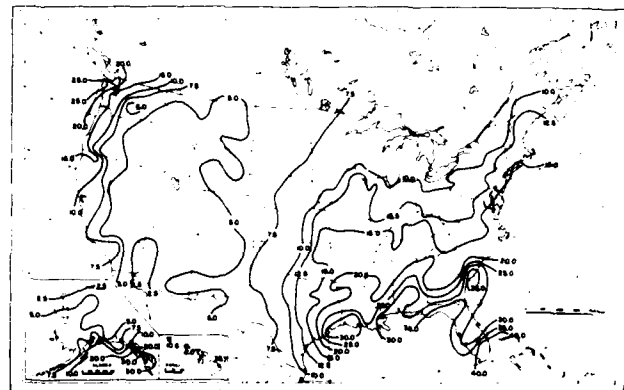


Figure 2. Contours of $R_1(0.1\%)$, the $t = 1$ min rainfall rates in mm/h predicted for 0.1 percent of an average year in the U.S.A.



Figure 3. Contours of $R_1(0.01\%)$, the $t = 1$ min rainfall rates in mm/h predicted for 0.01 percent of an average year in the U.S.A.

III. YEAR-TO-YEAR VARIABILITY

At SHF, both terrestrial and satellite operational systems have experienced a highly variable impact of rainfall on system performance. As a result, the average annual rainfall rate variation with location depicted in Figs. 1, 2, and 3 is, in

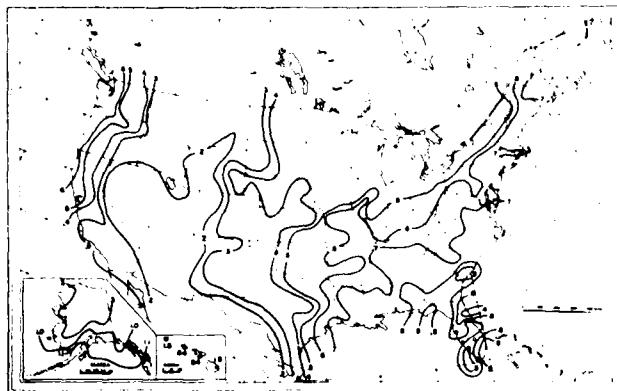


Figure 4. Contours of $S_{R1}(1\%)$, the standard deviation in mm/h of the year-to-year variation in the $t = 1$ min rainfall rate, $R_1(1\%)$, for 1 percent of all hours of a year.

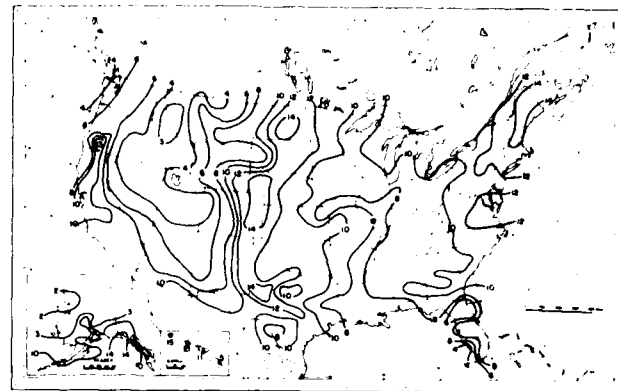


Figure 6. Contours of $S_{R1}(0.01\%)$, the standard deviation in mm/h of the year-to-year variation in the $t = 1$ min rainfall rate, $R_1(0.01\%)$, for 0.01 percent of all hours of a year.

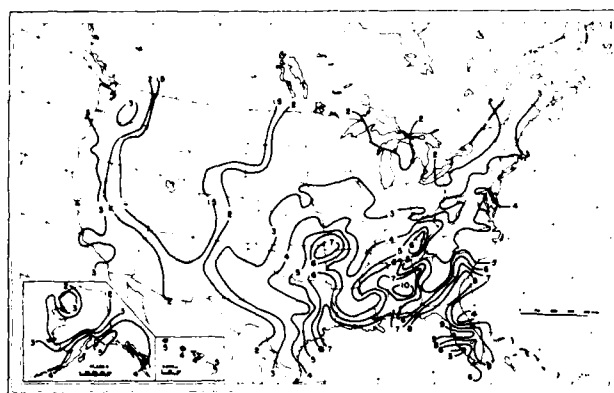


Figure 5. Contours of $S_{R1}(0.1\%)$, the standard deviation in mm/h of the year-to-year variation in the $t = 1$ min rainfall rate, $R_1(0.1\%)$, for 0.1 percent of all hours of a year.

itself, inadequate for system design and performance prediction. A further requirement is a measure of the temporal variation (the year-to-year changes) of rainfall rates, particularly at the higher rainfall rates. Therefore, we have determined standard deviations of annual rainfall rates from the 30 yr of meteorological data at the 305 U.S. Weather-Service stations. For the $t = 1$ min rainfall rate $R_1(1\%)$ that is mapped in Fig. 1, the standard deviation $S_{R1}(1\%)$ of the year-to-year variation is mapped in Fig. 4. For the rainfall rate $R_1(0.1\%)$ mapped in Fig. 2, the standard deviation $S_{R1}(0.1\%)$ of the year-to-year variation is mapped in Fig. 5. Similarly, for the rainfall rate $R_1(0.01\%)$ mapped in Fig. 3, the standard deviation $S_{R1}(0.01\%)$ is mapped in Fig. 6. At Washington, DC, for example, where $R_1(1\%) = 2.6$ mm/h, the $S_{R1}(1\%) = 0.65$ mm/h; where $R_1(0.1\%) = 14$ mm/h, the $S_{R1}(0.1\%) \approx 3.8$ mm/h; where the $R_1(0.01\%) = 76$ mm/h, the $S_{R1}(0.01\%) \approx 12$ mm/h. Actually, these temporal standard deviations also contain a slight contribution due to locational uncertainty as a result of approximations in the mapping procedures to develop contours from 305 distributed data-source locations.

By assuming a normal distribution [7] of rainfall rates, we

can add the values $\pm 1.645 S_{R1}(P)$ to the average value (such as $R_1(P)$ for any location in Figures 1, 2, or 3). This determines the range within which 90% of the rainfall rates observed at that location should fall for P percent of any year.

IV. PREDICTION AND OBSERVATION

Of course, our primary interest in rainfall is in its impact for telecommunication system performance. Recently, computer programs have been developed which incorporate the Rice-Holmberg rain prediction model, but go further to compute its impact (attenuation, reflectivity, etc.) and variance for terrestrial or satellite systems [4], [7]. These include the total atmospheric effects of the ubiquitous clear air (gaseous atmosphere), the commonly encountered non-precipitating clouds, and the much-less-frequent occurrence of storm clouds and rainfall. The computer program for an earth/satellite path [7] has been applied to the path between Rosman, NC, and ATS-6 satellite. The resulting predictions for transmission frequencies of 20 and 30 GHz, respectively, are shown in Figs. 7 and 8. In each figure, the central curve, numbered 1, is the prediction for an average year. The two curves numbered 2 are the (90%) bounds within which the annual attenuation distributions for 9 out of 10 yr are expected to fall. The pair of curves numbered 3 are the (99%) bounds within which the attenuation distributions for 99 out of 100 yr are expected to fall.

Available for comparison are the observational data recorded from the ATS-6 millimeter wave propagation experiment. That ATS-6 data report contained an extremely useful data-processing technique for combining attenuation data for part of a year and rainfall data for a full year which permitted extrapolation to an annual distribution of attenuation data [8]. The reported data curves for 20 and 30 GHz data have been superimposed upon the corresponding predictions of Figs. 7 and 8. Although this agreement between independently predicted and observed data is most gratifying, many more such comparisons will have to be made before one can determine prediction error. Note that the observational data curve falls outside the range for the predicted level for values of $P > 0.75\%$. This may be due to the observational curve being an extrapolation of attenuation due only to rainfall,

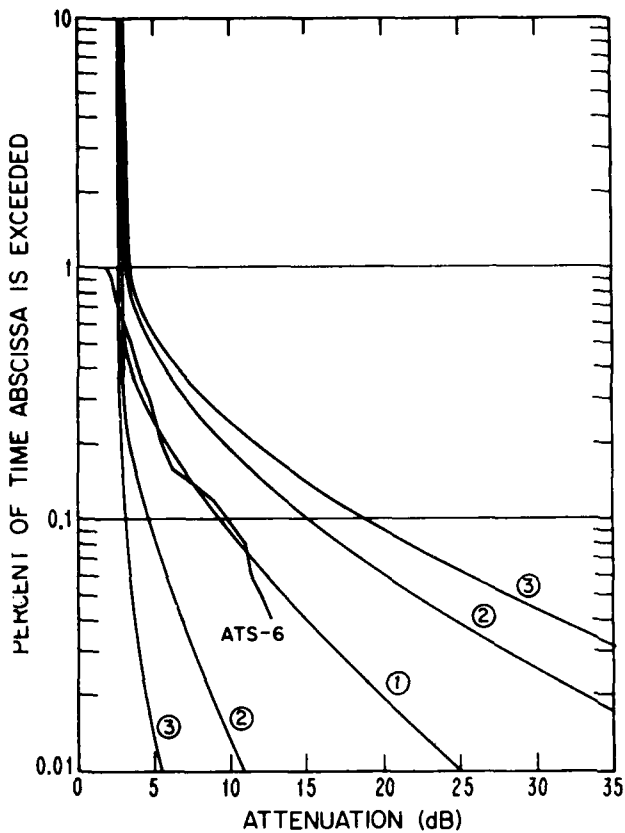


Figure 7. Comparison of the 20 GHz earth-space attenuation distributions between the ATS-6 satellite and Rosman, NC. The smooth curves are the Dutton-Dougherty predictions: 1 is for an average year, 2 are the bounds for 9 out of 10 yr, 3 are the bounds for 99 out of 100 yr. The broken-line plot is the reported ATS-6 processed observed data.

whereas the prediction curves are for attenuation due to the total atmosphere. At these frequencies, the distinction is negligible for the higher rainfall rates, but becomes noticeable for the lighter rainfall rates ($P \geq 1\%$).

V. CONCLUSION

The application of the Rice-Holmberg rainfall prediction model has been significantly advanced by the detailed mappings of its basic parameters (M , D , β , etc.) for Europe and the U.S. This short contribution indicates the further development of the model by presenting mappings of the 1-min rainfall rates in the U.S. for 1.0, 0.1, and 0.01 percent of an average year and the corresponding standard deviations of the year-to-year variation. Further, the impact upon system performance predictability has been illustrated by a prediction of earth/satellite attenuation at 20 and 30 GHz. The agreement with observational data is very encouraging, but many more such comparisons will be required before the prediction theory for atmospheric effects upon system performance may be considered as complete. One major subject required for further study is the relationship of annual rainfall to worst-month rainfall. Such predictions, made on the basis of annual characteristics, are useful and significant for the researcher or governmental system designers and operators. However, the fee and rate structure for commercial telecommunications

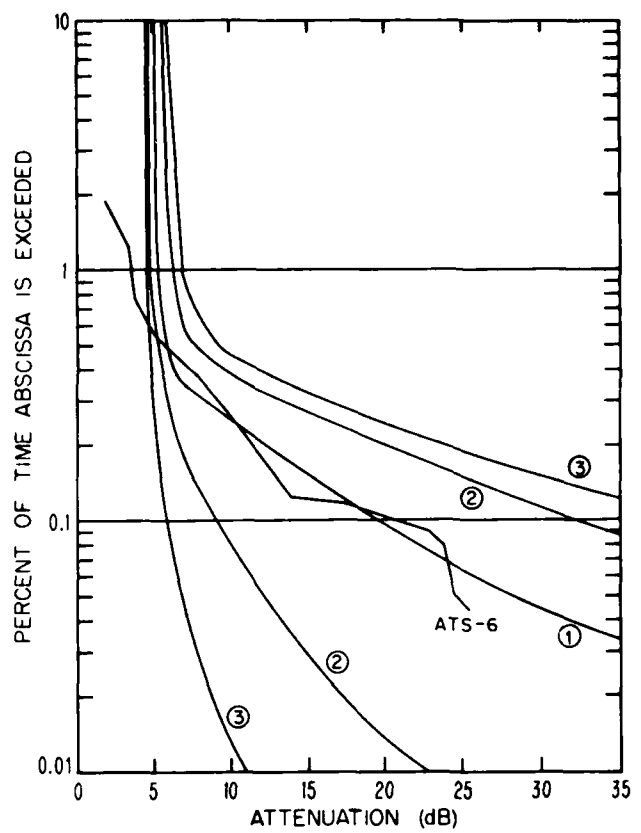


Figure 8. Comparison of the 30 GHz earth-space attenuation distributions between the ATS-6 satellite and Rosman, NC. The smooth curves are the Dutton-Dougherty predictions: 1 is for an average year, 2 are the bounds for 9 out of 10 yr, 3 is for 99 out of 100 yr. The broken-line plot is the reported ATS-6 processed observed data.

systems requires more emphasis to be placed on worst-month and other-than-annual prediction techniques [9].

REFERENCES

1. P. L. Rice and N. R. Holmberg, "Cumulative Time Statistics of Surface Point-Rainfall Rates", *IEEE Trans. on Communications*, COM-21, No. 10, 1131-1136, October 1973.
2. E. J. Dutton and H. T. Dougherty, "Modeling the Effects of Clouds and Rain Upon Satellite-to-Ground System Performance", OTR 73-5, COM 75-10950/AS (U.S. National Technical Information Service (NTIS), Springfield, VA 22151) March 1973.
3. E. J. Dutton, H. T. Dougherty, and R. F. Martin, ..., "Prediction of European Rainfall and Link Performance Coefficients at 8 to 30 GHz", AD/A-000804 (NTIS, Springfield, VA 22151), August 1974.
4. E. J. Dutton, "Prediction Variability in the U.S.A. for Microwave Terrestrial System Design", OTR 77-134 (NTIS, Springfield, VA, 22151), November 1977.
5. H. T. Dougherty and E. J. Dutton, "Estimating Year-to-Year Variability of Rainfall for Microwave Applications", *IEEE Trans. on Communications*, COM-26, No. 8, 1321-1324, August 1978.
6. "Radiometeorological Data" Report 563, Propagation In Non-Ionized Media, Vol. V of the CCIR XIII Plenary Assembly, Geneva, PB 244005 (NTIS, Springfield, VA 22151), 1975.
7. E. J. Dutton, "Earth-Space Attenuation Prediction Procedures at 4 to 16 GHz in the Conterminous United States", OTR 77-123, PB 269-228/AS (NTIS, Springfield, VA 22151), 1977.
8. "ATS-6 Millimeter Wave Propagation Experiment, Final Data Analysis Report", Report No. FIS-75-0050, Westinghouse Electric Corp., September 1975.
9. R. K. Crane and W. E. DeBrunner, "Worst-Month Statistics", *Electronics Letters*, 14, No. 2, 38-40, January 1978.

SUPPLEMENT VI PRESENT STATE AND FUTURE
OF TELECOMMUNICATIONS IN TURKEY

CVI-i

THIS PAGE INTENTIONALLY LEFT BLANK

Present State and Future of Telecommunications in Turkey

GÜNSEL BAYRAKTAR AND HÜSEYIN ABUT, MEMBER, IEEE

Abstract—The public telecommunication network of Turkey is briefly discussed in this paper. The existing telephone, telegraph, data, and other related services are summarized, and future trends in some of these services are indicated. These trends suggest that capital investments on the telecommunication services must be at least doubled in order that the standards in the country compete with those of the world averages. Finally, some of the research in communications is cited.

I. INTRODUCTION

TURKEY is a developing country of 776 000 km² with a population of 40 million, a gross national product per capita of approximately 6000 TL (equivalent of U.S. \$400) and 598 954 main telephone subscribers according to 1974 statistics [1].

The General Directorate of P.T.T. is the authority for the setting up and the operation of all public telecommunication facilities in the country. In addition to telephone and telegraph services, the necessary channels for the Turkish TV and some military networks are supplied by the P.T.T. administration. A brief overview of the present status and of the trends in the development of telecommunications in the country will be presented in the following sections.

The development rate of Turkey has been about 7–10 percent yearly during the first thirteen years of the planned development period of 1963–1995.¹ The programmed development plan forecasts that the country will reach the standards of the social welfare and industrialization of the Western European countries by the end of 1995 [2]. The importance of this last date lies in the fact that Turkey will become a full-fledged member of the European Economic Community (EEC) in 1995.² Hence, the country should accomplish her development systematically and rapidly so that the transition to membership in the EEC can be an easy one.

The existing telecommunication facilities should be increased greatly, in parallel with improvements in social and economic welfare. New services employing modern digital systems must be extensively established to catch up with the world standards. To achieve this, it has been decided in the Third Five-Year-Plan to: 1) increase the investments in telecommunications services; 2) have a national electronics in-

dustry satisfying the market demand; and 3) fulfill the demands for communication systems and devices through local sources.

II. TODAY'S TELEPHONE NETWORK

A well-established measure of the telephone services in a country is the telephone density q defined by the number of main subscribers per 100 inhabitants. Table I shows the rate of growth of the telephone services over the years 1955–1974 in Turkey [1], [3]. If we glance at the figures in the table, we see that the telephone density is increasing at a rate of about 10 percent. Since there is a commonly accepted regression between the telephone density q and the gross national product (GNP) per capita [4], [5], it would be worthwhile to compare these values with those of the world standards. Fig. 1 shows the relationships between the telephone density and GNP per capita using 1971 price indices for Turkey. In the same figure, a similar relation using the averages of 70 developed and developing member-countries of ITU for the years 1964–1968 is also plotted.

The telephone density in Turkey with a U.S. \$400 GNP in the early seventies is around 1.5 percent, whereas an average value for the developed and developing countries in 1964–1968 was above 2.1 percent. Thus, there is a gap of 0.6 percent between the national network at present and the world average of 1964–1968. This rather pronounced gap must be closed by allocating more funds to the telephone industry investments.

The network is by no means satisfying the demand. The number of people waiting for the extension of telephone services is increasing drastically every year. This trend is shown in Table II. However, the delays and shortcomings in extending services to potential customers are increasing at a smaller rate every year, which is a somewhat promising indication for future trends.

III. TELEGRAPH AND DATA SERVICES

The telegraph network is complete country-wide, interconnecting the towns and cities in Turkey. But the telex network is continually taking the place of the classical telegraph network throughout the country. There were 3950 telex terminals in 1974. During the same year, there were about 1200 potential subscribers. The ratio of potential customers to the existing ones is more than 0.3.

Data transmission facilities are not provided by the P.T.T. administration at present. The rate of growth of this service is not clear as there are no previous statistics available for reference. Nevertheless, data communication systems research is underway at a few institutions.

A very limited number of facsimile transmission networks exists among the big cities. But the customers, mainly the

Manuscript received November 13, 1975; revised January 26, 1976.

G. Bayraktar is with the Technical University of Istanbul, Istanbul, Turkey.

H. Abut is with Boğaziçi University, Bebek, Istanbul, Turkey.

¹First Five-Year Plan period: 1963–1967; Second Five-Year Plan period: 1968–1972; Third Five-Year Plan period: 1973–1977; planned development period: 1963–1995.

²Turkey has been accepted as a candidate to membership in the EEC with a 25-year transition period according to an agreement signed in 1970 in Ankara.

TABLE I
TELEPHONE DENSITY IN TURKEY OVER THE YEARS 1955-1974

Years	Number of Main Telephone Subscribers	Yearly Increase in Telephone Subscribers	Telephone Density	Yearly Increase in Telephone Density
1955	116 455	14.44	0.464	11.46
56	131 328	15.74	0.519	12.87
57	154 915	16.17	0.567	13.87
58	176 230	16.51	0.619	15.71
59	177 765	16.75	0.641	0.61
1960	180 310	16.75	0.649	0.91
61	191 267	16.75	0.665	0.16
62	199 457	16.75	0.684	0.77
63	212 183	16.75	0.697	1.07
1965	243 161	16.75	0.724	0.59
66	262 511	16.75	0.746	14.99
67	273 180	16.75	0.831	1.68
68	288 057	16.75	0.908	1.25
69	310 304	16.75	0.961	0.60
1970	318 503	16.75	1.059	10.20
71	423 172	16.75	1.172	11.45
72	471 462	16.75	1.275	4.11
73	531 367	16.75	1.385	8.67
74	598 954	16.75	1.500	8.30

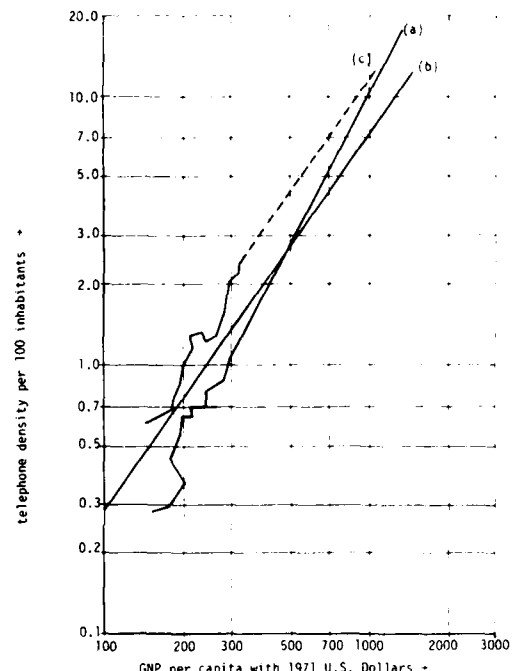


Fig. 1. Relationship of telephone density to GNP per capita. (a) Curve for the existing telephone services. (b) Curve for the average of member countries of ITU. (c) Projections of the expected potential telephone density.

press, are responsible for the total terminal equipment, leaving only the necessary channel allocation to the P.T.T. people.

The Turkish Radio and Television Organization (TRT) is using the P.T.T. radio-links, with all the necessary connections being provided by the P.T.T. servicemen.

P.T.T. renders also special network services among the various military installations of the national, NATO, and CENTO organizations.

IV. FUTURE TRENDS IN TELECOMMUNICATION SERVICES

A measure for the future trends of expectations from the telephone services is the relationship between the potential telephone density and the GNP per capita. The potential telephone density is defined by the sum of the total telephone subscribers and the customers waiting for telephone installations per 100 people for a given year. Table III shows this trend over the period 1972-1995. The expected growth in the

TABLE II
UNSATISFIED DEMANDS IN TELEPHONE SERVICES OVER THE PERIOD OF 1968-1974

Years	Number of Customers Waiting for Telephone Installations	Yearly Rate of Increase %	Ratio of Satisfied Customers and Unsatisfied Demands
1968	215 552	-----	0.75
1969	264 919	22.90	0.80
1970	329 444	24.15	0.85
1971	359 354	8.91	0.84
1972	395 927	10.00	0.84
1973	403 000	2.10	0.74
1974	408 000	1.24	0.65

TABLE III
EXPECTED DEMAND FOR TELEPHONE SERVICES FOR THE PERIOD OF 1972-1995

Years	Potential Population in millions	Potential GNP per Capita using 1971 prices U.S. \$	Potential Telephone Demand	Potential Telephone Density (%)
1972	37.6	374	870 000	2.31
1977	42.7	449	1 375 000	3.26
1982	47.9	552	2 297 000	5.00
1987	54.7	717	4 004 000	7.36
1992	60.8	1050	7 198 000	11.95
1995	65.2	1293	10 432 000	16.00

TABLE IV
EXPECTED GROWTH IN TELEX TERMINALS

Years	Number of Existing Telephone Subscribers	Number of Existing Telex Terminals	Yearly Increase in the No. of Telex Terminals %
1972	473 462	3950	-----
1977	960 000	6720	14.0
1982	1 064 000	13050	14.0
1987	3 549 000	26840	13.7
1992	6 725 000	47080	13.6
1995	9 877 000	69140	13.7

telex network is summarized in Table IV. It is clear that the number of requested telex terminals is being doubled every five years.

In order to achieve the figures given in Tables III and IV, the investments in the telecommunications industry must be, on the average, 3.4 percent of the total investments using the 1971 prices for the period of 1977-1995. However, the programmed investment allocation for the year of 1977 is only 0.357 of the GNP, or equivalent to 1.6 percent of the total capital investments. The last figure is less than half of the required amount. Therefore, a higher percentage must be allocated to this industry in the Five-Year Plans starting in 1978.

The second major and decisive factor in the future of telecommunication-services trends would be the solution of the technical personnel problem. In almost all of the developing countries, this factor is inseparable from the previous one, the increase in investment allocations in order to carry on the development plans systematically and rapidly. We feel that the technical personnel problem in Turkey is one which can be dealt with some hope of success. Once the personnel are better paid, this problem will be solved almost completely because nearly all of the technical staff employed in the telecommunication services are graduates of the national technical institutions.

The percentage of students in the electrical engineering department of Turkish universities constitutes almost 2 percent of the total higher education enrollment which is around 200 000 [6]. Since the early sixties the demand for electrical engineering studies is increasing at a much higher rate than the

capacity-increases in the schools. Therefore, every year a smaller percentage of the demand is being satisfied by means of a selection process through the Turkish Universities Entrance Examinations.

On the other hand, the staffing problem of the institutions is a stagnant one due to the underpayment of the civil servants. This, in return, has caused a considerable brain-drain to the Western European countries, U.S.A., Canada, and even Australia.

It is obvious that Turkey will need a young technical cadre available for designing, enlarging, establishing, maintaining, and managing the future telecommunication services. To fulfill these requirements, the Third Five-Year Plan includes the following suggestions to the government for taking the necessary measures: 1) to increase the number of academic staff; 2) to extend the possibilities and the capacities of the educational institutions; and 3) to end the brain-drain from the country.

V. COMMUNICATIONS RESEARCH IN TURKEY

The institutions where theoretical and experimental research is being carried out in communications are the Electronics Research Unit of the Marmara Research Institute, the P.T.T. Research Laboratories, and the electrical engineering departments of the universities.

At the Marmara Research Institute of the Turkish Scientific and Technical Research Council, 1) theoretical and experimental work on modems employing FSK and DPSK systems for the audio channels is being carried out, 2) a prototype of 32-channel PCM system for short-haul trunks is being developed, and 3) studies on digital filters are underway.

At the P.T.T. Research Laboratories, 1) development work of high channel capacity FDM equipment and high speed telegraph systems for the national network is being carried on and 2) a 24-channel VHF and a 60-channel UHF radio systems are under study.

In the universities, theoretical and experimental investigations are being carried out. Some of these projects are partially financed by the Turkish Scientific and Technical Research Council. But these funds are incomparably meager with respect to those in the developed countries, and hence the number of technical papers appearing in the international journals on the subject is very limited. The other shortcoming in research is connected with the staffing problem of the Universities. Since the departments are understaffed, the existing personnel have very limited time to divert from their daily course work to research. The authors believe that distributing more funds to fundamental research in communications holds much more promise for the future than the existing state of affairs.

VI. CONCLUSIONS

The telecommunication services in Turkey are far below the world standards. The expected rate of growth is tremendously

high but even that would not be sufficient to meet the potential demands. On the other hand, research in communications is significant. In conclusion, Turkey must allocate more funds for telecommunication investments and support more research projects in order to cope with world standards.

REFERENCES

- [1] 1974 P.T.T. Statistics, General Directorate of P.T.T., Republic of Turkey, Ankara, Turkey, 1975.
- [2] The New Strategy and Development Plan, Third Five-Years, 1973-77 (in Turkish), State Planning Organization, Republic of Turkey, publication DPT 1272, Ankara, Turkey, 1973.
- [3] E. Kinayigit, "Telephone services and Turkey" (in Turkish), P.T.T. Res. Lab. Publications, Istanbul, Turkey, 1973.
- [4] Economic Studies at the National Level in the Field of Telecommunications, ITU Publications, 1968.
- [5] S. Altay, D. Yarangümel, S. Akçaharman, and T. Tunçsav, The Estimation of Telecommunication Necessities in Turkey up to 1995 (in Turkish), General Directorate of P.T.T., Ankara, Turkey, 1975.
- [6] The Statistics of Ministry of Education-1974 (in Turkish), Republic of Turkey, Ministry of Education Publications, Ankara, Turkey, 1975.



Günsel Bayraktar received the M.S. and Ph.D. degrees in electrical engineering from the Technical University of Istanbul, Istanbul, Turkey in 1961 and 1973, respectively.

After graduation, she joined the Technical University of Istanbul and currently she is active as an Assistant Professor in the Telecommunications Department there.



Hüseyin Abut (S'70-M'74) was born in Akhisar, Turkey, on November 20, 1945. He received the B.S. degree in electrical engineering from Robert College, Istanbul, Turkey, in 1963 and the M.S. and Ph.D. degrees, both in electrical engineering, from North Carolina State University, Raleigh, in 1970 and 1972, respectively.

From 1969 to 1972 he was a Research Assistant in the Department of Electrical Engineering at NCSU, engaged in the digital source encoding team of the project THEMIS. During the period of December 1972 to October 1973 he worked for the Marmara Research Institute of the Turkish Scientific and Technical Research Council where his projects were the development of PCM and DATACOMM systems for the Turkish Post Office (P.T.T.). Since 1973 he has been an Assistant Professor of Applied Mathematics and Information Theory at Boğaziçi University (formerly Robert College) Bebek, Istanbul, Turkey. His current interests are in the areas of rate distortion functions, data communications, zero-crossing properties of digital data signals, and applied numerical analysis.

THIS PAGE INTENTIONALLY LEFT BLANK

SUPPLEMENT VII PRESENT STATE AND TRENDS OF
PUBLIC COMMUNICATIONS IN THE
FEDERAL REPUBLIC OF GERMANY

THIS PAGE INTENTIONALLY LEFT BLANK

Present State and Trends of Public Communications in the Federal Republic of Germany

RONALD DINGELDEY

Abstract—The introduction gives an account of the historical development of telecommunications in Germany (Federal Republic of Germany), the legal status of the Deutsche Bundespost, its relationship with the German telecommunication industry, and the status of the broadcasting organizations.

On the basis of the present state of the art, the future trends in switching and transmission as well as in cable and radio engineering are described.

Of special weight are the new data and telephone switching systems and the requirements for future broad-band services. Research and development are concentrated on these projects, allowance having to be made for the present state of the networks in the Federal Republic of Germany.

Manuscript received November 6, 1973.

The author is with the Fernmeldetechnisches Zentralamt (FTZ of the Deutsche Bundespost), Darmstadt, Germany.

I. INTRODUCTION

A. Historical Background

THE FORMER Deutsche Reichspost and the PTT Administrations of the individual German Länder, respectively, as the institutions responsible for public telecommunications, started at an early stage with the utilization of the technical facilities available at that time. Based on the trials made by Reis and Bell, the first telephone connections were set up in Berlin in 1877. After rapid progress in the manual telephone service the first automatic local exchange was installed at Hildesheim in 1908. A further milestone is the year 1923: in the area of Weilheim (Upper Bavaria) the first subscriber trunk

dialling (STD) network group of the world was put into operation. Here, field trials were made with automatic-call metering and coin-box telephones for STD calls. The fully automatic operation in the entire network of the Federal Republic of Germany called, however, for a transmission plan based upon four-wire through connection in all transit exchanges. The technical prerequisites were provided in 1955 by the introduction of the eight-wiper Edelmetalldrehwähler (EMD) motor switch.

As far as television is concerned, it is noteworthy that as early as 1936 television broadcasting was introduced to a limited extent on the occasion of the Olympic Games. For this purpose use was made of Nipkow's method. After an interruption caused by the war, a public television program was not emitted in the Federal Republic of Germany until 1952. The first color television broadcasts were taken up in 1967 according to the PAL system proposed by Bruch.

The former Reichspost also took an active part in the development of the Teletype service, an important step being the establishment of the public teleprinter exchange (Telex) network in 1939. The technical facilities were more or less the same as those used for telephony.

B. Legal Status of the Deutsche Bundespost in Telecommunications

The legal regulations for the setting up and operation of telecommunication installations were provided in 1892/1928 by the Telecommunication Installation Law. According to this law, the right to set up and operate telecommunication installations is granted to the Reich, today to the Federal Republic, and is, as a rule, exercised by the Minister of Posts and Telecommunications, i.e., the Deutsche Bundespost either sets up and operates the installations itself or it grants a license to do so. Certain groups of users, e.g., transportation companies, need no license for the setting up and operation of their own telecommunication equipments in connection with their own lines for the requirements of their internal service only.

As early as 1899 the Telegraph Lines Law granted the then PTT Administration the right of way, allowing free utilization of public ways for the installation of its lines. Thus it has been possible to establish an efficient public network, and lines to be used for nonpublic purposes have generally been provided out of this pool and leased by the respective user. To avoid disturbances the equipment connected to leased lines has to meet the requirements issued by the Deutsche Bundespost.

In order to prevent interference to telecommunication services caused by HF equipment, a law was enacted which allows the specification and control of admissible limits of radio interference (law concerning the operation of HF equipment). This law is also exercised by the Deutsche Bundespost.

C. Relationship Between the German Telecommunication Industry and the Deutsche Bundespost

The status of the German telecommunication industry is characterized by the allocation of specific tasks to the

Deutsche Bundespost and the industry. Thus the Administration usually leaves it to the industry to develop equipment and technical facilities. In general, there is no placing of specific development orders. The design specifications are, however, laid down by the Fernmeldetechnisches Zentralamt (FTZ) of the Deutsche Bundespost, frequently on the basis of the results of research projects carried out by the latter. In this connection allowance is made for international recommendations issued by the competent bodies. The FTZ keeps its eye on the developments carried out by the industry and influences them, if required. Thus it is ensured that the operational requirements are taken into account from the very beginning. To ensure reliable operation and reduce the number of types, the FTZ also influences the choice of components. In the case of large-size equipment field trials are performed in addition to type approval tests before final approval is given.

As far as the switching and transmission equipment is concerned, the Deutsche Bundespost asks all suppliers to provide systems of uniform design. This enables the interchange of equipment made by different manufacturers. Therefore, the industry is required to jointly specify matching interfaces for the equipment modules.

As for switching systems, an adequate allocation of tasks among the firms often helps to save unnecessary development expenses. Since the Deutsche Bundespost always wants to purchase the equipment from several manufacturers, it binds the developing firm to grant manufacturing permits.

In the field of transmission, a uniform design is requested, especially for planning reasons. Here, too, the FTZ draws up relevant specifications in cooperation with the industry. The industry is also charged with the installation of all facilities.

In order to reduce the number of cable types, so-called cable concepts have been drawn up. They resulted from discussions between the Deutsche Bundespost and the cable firms which joined to form a pooling association to clarify technical questions of common interest and to ensure a rational utilization of their capacities. This association acts as negotiator with the Deutsche Bundespost.

The reduced number of cable types and the agreement on dates for manufacturing changes are to enable an economically reasonable transition from paper-insulated to plastic-insulated cables.

The installation of long-distance cables is exclusively carried out by the Deutsche Fernkabelgesellschaft (DFKG). The Deutsche Bundespost controls the activities of the DFKG by appropriate planning measures.

D. Status of the Broadcasting Organizations

In the Federal Republic of Germany the Länder governments are responsible for the organization of broadcasting programs. For this purpose, the Länder founded nine public broadcasting corporations, viz., the Bayerischer Rundfunk, Hessischer Rundfunk, Norddeutscher Rundfunk, Radio Bremen, Süddeutscher Rundfunk, Sender Freies Berlin, Saarländischer Rundfunk, Südwestfunk,

Westdeutscher Rundfunk, and the Zweites Deutsches Fernsehen.

By federal law two organizations were set up which emit sound programs only, i.e., the Deutschlandfunk, whose programs are intended for all of Germany and the European continent, and the Deutsche Welle, whose broadcasts are emitted to the extra-European countries.

Up to the end of the Second World War in 1945, the PTT Administration was responsible for all technical matters concerning the transmission of sound and television programs. The programs were taken over at the broadcasters' studios, transmitted over adequate circuits to the transmitting stations from where they were radiated.

After the Second World War, i.e., up to the pronouncement of the Karlsruhe TV decision (decision of the Federal Constitutional Court of February 28, 1961), the Länder broadcasting organizations erected and operated the transmitting stations for the sound programs and the first television program. The Karlsruhe decision confirmed the Deutsche Bundespost's fundamental right to set up and operate broadcasting transmitters.

On account of the above-mentioned decision, the further extension and operation of the sound-broadcasting transmitter networks established up to that time—here special mention should be made of the new transmitter networks in the VHF range—and the television transmitter networks for the first TV program were left to the Länder broadcasting organizations.

From that date the Deutsche Bundespost has set up and operated the sound broadcasting transmitters of the Deutschlandfunk and the Deutsche Welle as well as the transmitters for the second and third television programs.

E. Structure of the Country and Network Configuration

The configuration of the public telecommunication network in the Federal Republic of Germany was mainly marked by the division of Germany after the war, the population density, and the economic development. At present, the network covers ten Länder and Berlin (West) with a total area of about 248 000 km². The Federal Republic of Germany more or less is a uniformly populated area with some highly developed regions of industrial concentration. A network was set up where emphasis was laid on telephony. It connects the most remote places and allows STD at both the national and international levels. For the automation of the national telephone system it was sufficient to apply a decadic numbering scheme which allows an open numbering of all local networks with four digits. For this purpose the Bundespost network was subdivided into eight central-exchange areas, the eight central exchanges being located in the cities of Berlin (West), Hamburg, Hannover, Düsseldorf, Frankfurt, Stuttgart, Munich, and Nürnberg. They are interconnected by a meshed long-distance network via cable and radio-relay links. The central-exchange area of Berlin (West) is connected with the other parts of the network via special radio-relay links. Apart from Berlin (West), each central-exchange area is according to the second digit of the

code subdivided into nine to ten main-exchange areas, a double main-exchange area being assigned to big city regions. The main exchanges belonging to these areas are connected with the superior central exchange via a star-shaped network and with adjacent main exchanges via direct routes. The second level of the hierarchy thus has a mixed structure. The network structure of the third level of the hierarchy is similar, here the third digit of the code corresponds to the nodal exchanges. A purely star-shaped network structure exists only on the fourth level, where the fourth digit of the code designates the so-called terminal exchanges which are available in each local-exchange area. Each long-distance call is initiated in a terminal exchange by the trunk prefix "O," passed on to another terminal exchange after dialing the wanted trunk code, and completed by dialing the subscriber number in the respective local-exchange area.

The configurations of the Telex and Datex networks are similar to those of the telephone network; they have, however, less network levels. The Telex network is the public Teletype network operating at 50 Bd, whereas the Datex network is a separate switched network for data and Teletype transmissions at speeds of up to 200 Bd. The public telegraph traffic is handled over the Gentex network (switched telegraph network) which comprises two levels. It is intended to computerize this network.

F. Population and Subscriber Density

Between 1960 and 1970 the population of the Federal Republic of Germany increased from 6 to 61.8 million. During the same period the number of telephone main stations rose from 3.3 to 8.8 million and the main station density from 5.9 to 14.2 stations per 100 inhabitants. In the years from 1968 to 1970 there was an extremely strong increase in the demand for telephone main stations. After the economic situation had returned to normal and the fees had been adapted to the increasing costs in 1972, the rise in the demand leveled off.

The number of main stations, the installation of which was not possible within four weeks, declined after the peak in April 1971 from 656 000 to 381 000 at the end of 1972. In the meantime, it is possible to satisfy 66 percent of all applications within three months and 75 percent within six months. The main reason for the delay in installing telephone stations is to an increasing extent to be seen in the shortage of subscriber lines. This trend is to be counteracted by effective measures such as the use of line concentrators. Shared lines make up 16.3 percent of the main stations; in accordance with the new legal provisions they are only provided for a limited period until sufficient technical facilities for main stations are available. A further reduction in the percentage of shared lines is thus to be expected.

At the end of 1972 about 10.6 million telephone main stations, 5.5 million telephone extensions, 93 000 Telex stations, and about 1000 Datex stations were operated in the Federal Republic of Germany for a population of

62.4 million. For about 10 years the annual increase in the demand for main stations will be well above one million. With a further rise in the number of population the Deutsche Bundespost expects a decline in the net demand to one million and less not before 1985. In consideration of the calculated growth rate for private telephone stations (including the shared lines of the households) and for business telephone stations the demand follows a logistic function with a saturation density of about 55 telephone main stations per 100 inhabitants. The expected annual increase in the number of Telex stations is about 7 percent.

II. SWITCHING TECHNIQUES AND TERMINAL EQUIPMENT

A. EMD Technique

In the Deutsche Bundespost telephone network the EMD technique (precious-metal motor switch) is applied in several versions. For the local traffic the direct-control two-wire system 55v and for the long-distance traffic the indirect-control four-wire system 62 are used as standard techniques. All requirements of the national and international long-distance services are met by the STD system. All routing and zoning functions are performed in the nodal exchanges of the long-distance network. By separating the functions of the long-distance traffic from those of the local traffic, the uncomplicated local system has enabled the maintenance costs in the local exchange area to be kept at a low level. For both versions of the system, test equipment is being developed which allows the data of all essential switching elements to be recorded automatically. This test equipment is mainly connected at night and runs according to a given program. It supplies information about the location and type of possible faults via output devices. This allows the transition to corrective maintenance. The quality of a connection is checked by automatic test call equipment and manual traffic observation sets. As soon as the given values are exceeded, remedial measures can be taken on the operational or the planning side.

B. Stored-Program Control-Switching System EWS

In the last decades the Deutsche Bundespost gradually automated its telephone service. With the introduction of the stored-program control-switching system EWS 1 it will be possible to extend this automation beyond the pure switching functions to the operational services. In the EWS 1 system the switching functions are controlled by a central control unit consisting of a pair of computers working in parallel for reasons of reliability. The central control units can, in turn, interwork with other data-processing systems via data circuits, take over the tasks of the operational services (e.g., telephone maintenance service), and relieve the switching system.

The efficient, programmable central control unit of the EWS 1 system allows the introduction of new subscriber facilities. Keyboard dialing will enable the subscriber

to converse with the computer system and inform the system of his wishes. Already in the phase of introduction, subscriber-controlled transfer to the absent subscriber service, abbreviated dialing, automatic alarm call service, and keyphone data transmission will be possible. Further facilities may be introduced at a later date.

In its structure the EWS 1 system is subdivided into three levels (peripheral level, partly centralized control level, central control level), which are separated by interfaces allowing the connection of various types of peripheral equipment. Through-connection of the speech channels is performed at the peripheral level which comprises mainly the switching network, including the associated control unit and the switching circuits. The exchange of signals between the EWS exchanges is effected by equipment of the partly centralized control level via common signaling channels which are separated from the speech path. The central control level is composed of the processor with the pertinent program and data stores. They also exist in pairs.

At the peripheral level it is possible that switching networks in the two-wire space-division multiplex design (for local traffic), in the four-wire space-division multiplex design (for long-distance traffic), and in the PCM time-division multiplex design are used in parallel. All switching networks receive their marker instructions from the same central control unit. Thus the system can also be introduced in rural areas if a central control unit processes both local and long-distance traffic and if small independent local exchanges have to be remotely controlled. By the use of PCM switching networks the system can also satisfy the future requirements of integrated networks.

The EWS 1 program system uses a machine-oriented language (EWS 1 assembler language). By utilizing special addressing procedures, programs and data blocks can easily be adapted to the operational requirements (enlargements, modification of facilities). A field trial with three exchanges was started in 1973. The system will be gradually integrated into the existing telephone network beginning in 1975.

C. Electronic Data Switching System and Data Transmission

The electronic data switching system (EDS), a fully electronic computer-controlled switching system, is to replace, within a decade, the existing electromechanical telegraph switching system TW 39, i.e., the entire Telex and Datex services will be integrated into the new system. At the beginning of 1973 the installation of the first EDS exchange of the future network was started.

The Telex network with almost 100 000 subscribers and a growth rate, which suggests a doubling of this figure within ten years, will provide the economic basis for higher speed data services and additional facilities which can also be realized with the EDS system. The risk of wrong planning due to uncertain forecasts on future requirements to be met by data services will thus be considerably reduced.

The switching principle is based on a code and speed transparent user-circuit-switching method in the non-synchronous division multiplex, where through connection is performed bit by bit, but only when a polarity reversal has been received. The connection of suitable line-termination units to the central unit allows an optimization of the system for the switching principle applied. In its present concept the peripheral equipment of the switching processor is adapted to the asynchronous transmission mode, i.e., it is above all suited for Telex and Datex services. According to CCITT Recommendation X.1, the signaling rates of 2.4 and 9.6 kbit/s are to be transmitted in a synchronous mode. During a period of transition the data terminal equipment operating at these speeds (it is intended to introduce these services about 1976) will obtain the clock from the data circuit-terminating unit. Code transparency is achieved by means of a scrambler which is also assigned to the data circuit-terminating equipment. In this case, the exchange does not make any differentiation between synchronous and asynchronous data. Later on, the asynchronous line-termination unit will be complemented by a synchronous line-termination unit which, in the first phase, switches envelopes for speeds of up to 48 kbit/s. Thus it will be possible to obtain a separate synchronous network parallel to the present asynchronous speed-transparent network. Both networks will, however, be integrated into one switching system.

Similar to the practice applied in the Telex and Datex services, the closed user groups will be integrated into the digital network. From the operational point of view the user groups can be compared with the present private networks, but they differ in their technical layout. Unlike the private networks, the terminations of the user groups are not interconnected by circuits separated from the public network, but by subscriber lines like all others of the general user group. At each transmission rate the general user group is that group within which all users can communicate without restriction. For instance, the general user group operating at 50 Bd is the Telex network. Terminations of a specific user group differ from those of the general user group in so far as, on account of a certain indication in the switching processor, connections are admissible only within their own group and to the general user group. But there is no access to other user groups and from the general user group.

D. Telephone Terminal Equipment

In order to satisfy the manifold wishes of the customers in the field of subscriber equipment, the Deutsche Bundespost has always strongly encouraged the initiative of private industry. Thus it has been possible to offer a wide range of products and services, especially with regard to telephone sets, private branch exchanges, and the design of accessory equipment. At present the well-tried type 61 telephone set is made available to customers in five different colors as desk and wall sets. For different

applications types 611-616 include sets with earth button, visible signal, special hook switch, and extendable equivalent network. Moreover, use is made of special-type telephone sets, e.g., with incorporated charge meter and a special key for blocking outgoing calls. A loudspeaking telephone, with voice switching for the suppression of acoustic feedback and with an electronic bell, is about to be introduced. For the future electronic switching system a push-button telephone is being developed in cooperation with the telecommunication industry. It will be operated according to the CCITT multifrequency method and will, among others, be fitted with a device preventing the confusion of poles and providing lightning protection for oscillator and transistor capsule. The Deutsche Bundespost is beginning to gather experience with different types of telephone sets with incorporated high-speed key sender to be used in private branch exchanges (PBX).

In public telephone stations the Deutsche Bundespost uses mainly coin-box telephones for the local traffic as well as for national and international subscriber dialing. In 1972 the long-distance coin-box telephone 57, also called European coin-box telephone, was introduced for subscriber dialing in Europe.

For the new electronic switching system a standard coin-box telephone with push-button dialling is under development, which is intended for worldwide connections.

About one third of all telephone stations in the Federal Republic of Germany are connected to PBX's which are available with intercommunication facilities, manual or automatic switchboards in various sizes. They may be Bundespost owned, subscriber owned, or privately owned. Within the scope of the valid regulations they may offer a number of different facilities and are thus adaptable to various requirements. The PBX's may be supplied as selector, crossbar, or relay systems. Trials are not only being made with systems equipped with electronic control of relay switching networks, but also with systems having electronic crosspoints and those with time-division multiplex switching equipment.

It is admissible to connect additional equipment, such as modems for different transmission speeds, facsimile machines, and dialing aids, to the main stations and extensions of the public telephone network.

Further development in this field is characterized by an adaptation to the continuously changing wishes of the customers, the extension of the services offered, and an easier and more convenient handling of the apparatus.

E. Data Terminal Equipment in the Telephone Network and Data Transmission

In 1965 the Deutsche Bundespost introduced data transmission in the entire telephone network. This was a necessary prerequisite for the development of remote data processing. At this time, there are more than 5700 modems connected to the public switched network. In 1972 the growth rate was about 60 percent.

Postal-owned modems for serial and transparent data

transmission in the public switched network are offered for the following speeds:

- 1) up to 200-bit/s full-duplex, according to CCITT Recommendation V.21;
- 2) up to 600/1200-bit/s half-duplex, according to CCITT Recommendation V.23;
- 3) with interchange circuits according to CCITT Recommendation V.24.

As far as data-collection systems are concerned, modems are offered for parallel data transmission with 20-40 characters/s. The new EWS 1 telephone switching system will also allow a type of simple data transmission, the so-called keyphone data transmission.

Extensive investigations indicated that data transmission in the national switched network and in most international connections is possible at even higher speeds when phase modulation is applied. Therefore, the Bundespost is going to introduce a modem operating at 2400 bit/s in the synchronous mode in conformity with CCITT Recommendation V.26, Alternative B. Additional devices such as automatic-calling units are offered for all above-mentioned modems.

In addition, for private networks point-to-point connections (leased lines) of ordinary and special quality (CCITT Recommendation M.102) are provided for approved subscriber-owned modems. Such lines allow the full utilization of the transmission capacity of the telephone channel at speeds up to 9600 bit/s. Up to now, more than 5000 telephone circuits have been leased.

Signaling rates of up to 48 to 64 kbit/s can be achieved on group links and will in future also be obtained on direct PCM connections. Efforts are being made to provide the required types of modem.

The above services complement the planned independent EDS data network which is to carry most of the future data traffic.

III. TRANSMISSION TECHNIQUES

A. Present State of Frequency-Division Multiplexing and Time-Division Multiplexing Systems

As far as time-division multiplexing (TDM) transmission systems are concerned, the PCM transmission system PCM 30 is at present used to an increasing extent on the lower network levels. This system operates at a rate of 2.048 Mbit/s and makes use largely of the latest components and circuitry (LSI, IC). From 1975 a new system generation will be available which is based on the experience gained with the present systems. This new system will be constructed according to the standard design 7R which is also applied to the carrier systems.

Moreover, a multiplex system which combines 4 × 2.048- to 8.448-Mbit/s systems (including housekeeping information) shall be made available as PCM transmission system PCM 120 beginning in 1975. A new symmetric cable was developed for this system (and also for system

PCM 480, the next higher in the hierarchy); the repeater spacing for this cable is about 4 km for PCM 120 and about 2 km for PCM 480.

Parallel to this practice-oriented planning and development, numerous other investigations are carried out, e.g., the utilization of existing symmetric and coaxial cables by medium and high-capacity PCM transmission systems (hybrid systems).

As for carrier transmission, the development of a 60-MHz system for 10 800 telephone channels or a corresponding number of video channels has recently been taken up. The first systems of this type will presumably be put into operation in 1975. The high-frequency stability of 1×10^{-8} of the fundamental oscillator required for the associated modulation stages will be ensured by a frequency-comparison network whose master oscillator must have a long-term stability of 1×10^{-9} at least. The establishment of this network has already been put in hand. In conjunction with the 60-MHz system, problems of broad-band communications (TV transmission) have also been studied. These investigations have been extended to the existing 12-MHz system (V 2700 = four-wire, 2700 channels).

By the introduction of master-group systems in conformity with CCITT Plan A and the provision of the necessary carrier equipment, the network configuration will not only become clearer but also simpler and more economical mainly at the interface between the supraregional and regional long-distance networks.

An essential feature of all German carrier systems is the application by the manufacturers of standard-design principles for all types of equipment. The development of the latest design 7R, which makes use of semiconductors and integrated circuits, has resulted in substantial simplifications and improvements in carrier transmission: reduction of the deviations of the specified overall loss by applying fully electronic level control; interchangeability of equipment made by different manufacturers; rapid fault indication by a uniform signaling method in the form of central monitoring and supervision.

In addition to these technical and operational merits, the application of the new design also yields considerable economic advantages which manifest themselves in substantial savings in space and costs. For instance, with a rack width of 600 mm, the channel capacity of 600 channels obtained with the 7R design can be quintupled as compared to the type 7 system with 120 channels. This means a reduction in costs of about 20 percent. Similar savings can also be expected for other carrier equipment.

B. Sound Program/TV Transmission Network

The Deutsche Bundespost operates extensive sound-program and television-transmission networks for the broadcasting organizations. There are wide differences in the network structures according to their application, the number and length of possible transmission links, and the state of the art at the time the network was installed.

In any case, the Deutsche Bundespost does its best to make the integration of the broadcasting networks into the remaining telecommunication network as economical as possible. In addition to the audio-frequency (AF) sound-program transmission system used for short circuits set up on quads and specially screened wires of long-distance cables, the technique of setting up sound-program channels on carrier systems has been widely adopted. Part of the 10-kHz systems have for some years been replaced by 15-kHz carrier systems. These systems are, for instance, being used in the ARD¹ network for the exchange of programs. This is a star-shaped network, its switching center (star point) being located at Frankfurt. At this point the sound-program circuits are automatically interconnected in a special IF switching matrix by means of a small computer. For the time being, this small computer is operated by personnel of the Deutsche Bundespost. At the end of this year (1973) it will, however, be connected to a large computer of the ARD, which can perform the coordinating and control functions. In future, the supervision and operation of the sound-program circuits will be considerably facilitated by the new automatic measuring set for sound-program circuits.

As far as TV transmission is concerned, large networks have been provided for the exchange of programs of the ARD, the European Broadcasting Union (EBU), and for the distribution links to the transmitters. In these networks, large distances are generally bridged by radio-relay links, whereas the shorter connections from a studio to a local switching point of the Deutsche Bundespost are established on cable links. For this purpose, use is made of the local transmission system TV 21. The future use of the 12-MHz and 60-MHz systems for all types of TV circuits is under discussion.

Since the Olympic Games in 1972 the FM TV 1300 R outside broadcast equipment, which is fully color capable, has increasingly been used for outside broadcast links to be set up at short notice.

For the operation of international TV circuits increasing use is being made of a semiconductor-equipped video switching matrix (e.g., with 10 inputs and 10 outputs) which can also be remotely controlled.

For the smooth exchange of television programs within Europe a transcoder is available for the conversion from SECAM into PAL. For the worldwide exchange of programs an electrooptical standards converter has been provided at the Raisting earth station to convert from 525-line NTSC into 625-line PAL and vice versa.

C. Cable Television

The Deutsche Bundespost considers cable television to be part of the wide field of broad-band communications. It includes not only the actual distribution of television programs, but also services which require a broader transmission band than telephony, viz., picture telephony,

¹ARD stands for *Arbeitsgemeinschaft der öffentlich-rechtlichen Rundfunkanstalten in der BRD* which is an alliance of the chartered broadcasting corporations in the Federal Republic of Germany.

picture transmission for private purposes (e.g., industrial television), and high-speed data transmission. The laying of one single cable having, for instance, one coaxial conductor for cable television and a number of screened quad units for the other broad-band services, is to allow a particularly economical construction of a broad-band network. Realistic conceptions exist already for cable television proper, for which two test networks are under construction.

The Bundespost cable television network shall be superimposed on the telephone network and have a star-shaped configuration in the local exchange area. This means the shared use of the mounting points and cable routes of the telephone network. It is, however, not intended to accommodate the interface between the Deutsche Bundespost and the subscriber in the subscriber's residence, but rather to provide only one interface for one house (premises). These plans are based on financial considerations and the fact that there is already a large number of so-called community antenna installations which are also to be used for cable television.

The experimental cable television installations are so designed as to allow the high-quality transmission of twelve television programs and a similar number of sound-broadcasting programs (in stereophonic quality) from a transmitting station (head station) to the subscriber over a distance of up to about 5 km. Since adjacent channel reception in television sets is not yet possible in the Federal Republic of Germany, a frequency range from about 40–300 MHz (Band I, Band II, Band III, the range between Bands II and III, and the range above Band III to about 300 MHz) will be required. Band II up to 104 MHz is intended to be used for sound broadcasting.

The above-mentioned experimental cable television installations are provided on the lowest network level. The technical specifications of the cable television installations are to enable the interconnection of these installations to form larger networks at a later date, possibly by making use of well-known systems (e.g., TV radio-relay links, 12-MHz or 60-MHz transmission systems). It is just this fact which is decisive for the Deutsche Bundespost. By drawing up standards for television coverage by wire, the different designs of community antennas which prevent the interconnection of these installations in a large network for technical and financial reasons will be avoided.

D. Picture Telephony

By the development of picture telephony it has for some years been possible for two people to see each other while talking together and so to enliven the conversation by facial expressions and gestures and, above all, to make it more realistic. This new facility has to be dearly paid for by a higher technical complexity than that needed for conventional telephony. The transmission of the video signal only requires a bandwidth 300 times as wide as that necessary for a speech channel proper. In order to make this new service as economical as possible, both the

Deutsche Bundespost and the potential users demanded already at an early stage to enable, in addition to the actual picture call between two persons or groups of persons, the transmission of displayed data (typewritten tests, drawings, pictures) and the connection of the picture phone to external computer and storage units (use of the picture phone as data-display device). First, general enquiries indicated that in view of these facilities the future picture telephone users will, above all, come from the sectors of industry, commerce, and transport.

The great activities displayed by the United States of America, Japan, and France in the field of videophonic communications has also induced the telecommunication industry in the Federal Republic of Germany to make further studies and efforts in this direction. Thus a development was resumed in the Federal Republic of Germany which had been initiated as early as March 1, 1936 with the first picture phone connection in the world between Berlin and Leipzig.

After a period of development which began in 1967 the first automatic picture telephone call was made between the FTZ at Darmstadt and Siemens AG in Munich over a distance of 400 km. The experimental installation operated with a frame of 50 Hz, a video bandwidth of 0.8 MHz, and had a resolution of 225 lines. The field trials showed that a face-to-face transmission and the representation of simple drawings were possible, but that the picture quality was not sufficient for the transmission of typewritten documents. For this reason, the new experimental network established in the autumn of 1973 between the Federal Ministry of Posts and Telecommunications at Bonn, the FTZ at Darmstadt, and Siemens AG in Munich will use new picture telephone equipment which corresponds to the planned international standards specifying 267 lines, a line frequency of 8 kHz, and a transmission bandwidth of 1 MHz.

In order to achieve a better picture quality, the use of broad-band transmission systems (e.g., 5 MHz and more) or special storage devices are taken into consideration. On the local network level the picture telephone signals are generally transmitted over six pairs; in each direction two of them are used for the video signal and one for the speech signal. The video signal is connected through parallel to the sound signal in a special four-wire switching network. No decision has yet been reached on the transmission mode "sound in vision" because of considerably greater expenses for the subscriber station and the test system as well as the extensive modifications to be made in the electronic switching system EWS. For long-distance picture telephone transmissions in the analog mode it is possible to use the conventional carrier systems set up on coaxial pairs and radio-relay links. The use of PCM on these two transmission media is also considered feasible. As far as switching is concerned, picture telephony is to rely on the EWS 1 system which is considered suitable for this purpose. Thus the earliest date for the introduction of this service will be 1980, since up to then the EWS 1

system will be available in a sufficient number of local networks of the eight central exchange areas.

IV. CABLE SYSTEMS

A. Present Cable Systems and Supervision Methods

To meet the Deutsche Bundespost's high demand for local cables, a concept was drawn up in 1970 which intends the use of plastic-insulated wires and plastic-sheathed [polyvinyl chloride (PVC) and polyethylene (PE)] cables in addition to the conventional type of local cable. During a longer period of transition the local cable having a lead or corrugated steel sheath and paper-insulated star-III² quads made up in layers will be replaced by a local cable with paper, foamed PE, or solid PE insulated star-III quads made up in units and having a multilayer sheath. In the case of the multilayer sheath a longitudinally feed-in overlapping aluminium foil of 0.2 mm is welded with a PE sheath without any cavities. The aluminium foil serves as a moisture carrier and as an electric screen. The five star-III quads in the basic unit are marked with the colors red (reference quad), green, grey, yellow, and white, the wires being additionally marked by rings. The maximum number of pairs for cables with 0.4-mm conductors is 2000 and that for cables with 0.6-mm conductors is 1200. The nominal line attenuation at 800 Hz is 0.91 dB/km for 0.6-mm conductors. Balancing of the capacitance unbalance is not intended for this type of cable. Normally, local cables are connected to air pressurization systems. An important feature in the supervision of cable systems was the development of the multilayer-sheathed cable providing protection against the longitudinal penetration of water. This protection, at present applied to the local cables in the distribution network, was achieved by filling the cable cavities with petroleum jelly.

In the long-distance network of the Deutsche Bundespost, the cables with star quads and styroflex air-space insulation, which, nowadays, still form part of this network, have been replaced by coaxial cables of 2.6/9.5/0.25 mm and 1.2/4.4/0.18 mm. At present, use is made of two standard types of cable, i.e., type KxFk 14f with 4 coaxial pairs of 2.6/9.5/0.25 mm and type KxFk 32c with 12 coaxial pairs of 2.5/9.5/0.25 mm.

In the regional network, the Deutsche Bundespost uses cables with different twisting elements (loaded DM³ star quads, unloaded DM star quads for carrier system Z 12 (Z 12 = two-wire, 12 channels) and coaxial pairs of 1.2/4.4/0.18 mm for carrier system V 300). Here, special mention should be made of the following cable types: KxFk 8m with 4 coaxial pairs of 2.1/4.4/0.18 mm and KxFk 9a with 6 coaxial pairs of 1.2/4.4/0.18 mm and KxFk 24f with 12 coaxial pairs of 1.2/4.4/0.18 mm.

The maximum number of telephone channels set up on cables of type KxFk 32c designed in 1971 has increased

² Star-quad twisting without phantom utilization for subscriber cables.

³ DM stands for Dieselhorst-Martin, i.e., multiple-twin twisting with phantom utilization.

to 64 800. At this time, this cable, which has a repeater spacing of 4.65 km, is used for the carrier system V 2700 up to 12 MHz. The prerequisites for an easy conversion of these cable links to the carrier system V 10 800 with a repeater spacing of 1.55 km, which can be utilized up to 60 MHz, have been given by the provision of empty underground repeater casings. By these measures the transmission capacity of the main arteries of the long-distance network approach the lower capacity limit of waveguide cables. Although the latter are being developed, their practical use by the Deutsche Bundespost is still uncertain because of economic considerations. The annual enlargement of the network by 500 line-km of coaxial cables (type KxFk 32e) provides a good basis for the high-speed data transmission to be expected in the future. The CCITT Recommendations on the electrical characteristics of coaxial pairs are observed by the Deutsche Bundespost. For instance, the admissible deviations of the characteristic impedance of coaxial pairs over a cable length and in the joints are kept so low that the cables can be mounted without considering the direction of laying. Since the inner conductor of armored, lead-sheathed coaxial cables was found to be wavy, all coaxial cables are provided with corrugated steel sheaths. This practice was adopted in 1971. As the corrugated steel sheath needs an outer PE sheath as a protection against corrosion, an 8-mm galvanized iron wire is laid approximately 20 cm above buried cables for reasons of lightning protection. In areas with extremely strong atmospheric discharges use is made of a three-layer cable sheath grounded over the entire cable length (consisting of an inner conductive layer of 2 layers of 0.2-mm copper tape, a 0.4-mm corrugated steel sheath, and an armored lead sheath as an outer conductive layer). With a view to a future integrated broad-band cable network in the Federal Republic of Germany, cables are, at present, being developed and tested which are also suitable for the transmission of television signals. This is motivated by the desire to ensure that customers in shadow regions are provided with all television programs available today and to be able to offer additional programs to interested persons. It is intended to use the cable type KxP (2.6/9.5/0.25 mm) complying with the relevant CCITT standard for cable television in the frequency range from 40 to 300 MHz on the repeater-equipped A and B levels of the broad-band networks. On the C and D levels up to the Bundespost handing-over point low-priced, metallic single-tube coaxial cables are provided. They are protected against the longitudinal penetration of water and have a line attenuation of 6 dB/100 m or 9 dB/100 m at 300 MHz.

B. New Cable for Digital Transmission

For technical and economic reasons the present-day symmetric and coaxial pair cables are not suitable for the transmission of information flows of 8 and 34 Mbit/s. Therefore, it was investigated whether the new cable

types (0.6/2.8-mm coaxial pairs; symmetric pairs and star quads with 0.9-mm conductors) are suited for PCM transmission systems (PCM 120 and PCM 480) and for analog broad-band services (up to 5 MHz). The results of the investigations of cable lengths, some of which were connected to form entire regenerative repeater sections, indicated that for an admissible bit error rate $< 10^{-6}$ and for an undisturbed transmission a far-end crosstalk value of $a_f - a \geq 28$ dB and a near-end crosstalk value of $a_n \geq 106$ dB/repeater section are required at the Nyquist frequency of the PCM system. These requirements are met by cables with 0.6/2.8-mm coaxial pairs as well as by those with symmetric twisted elements. Preference was given to the latter because of the high crosstalk attenuation in the video frequency band up to 5 MHz, its easy installation, and relatively low cable costs. With this cable five symmetric twisted elements (pairs or quads) each are combined to form one unit surrounded by a screen. This screen, which ensures a high near-end crosstalk attenuation a_n , consists of two overlapping copper foils wound counterclockwise with a plastic tape in between. Together with two additional PE threads a symmetric pair is twisted to form a "pseudoquad." Since within a unit five such pseudoquads have the same dimensions as five real high-quality star quads, the latter will be advantageous for a rational utilization of the cable cross section. The near-end crosstalk attenuation between the pairs made up as pseudoquads is the same as that between the side circuits in the adjacent star quads and is suited for transmissions by PCM system 480. Because of the coupling between the two side circuits of a quad it is only possible to use one side circuit for PCM 480 transmissions, whereas the other one is to be used for PCM system 120 or analog broad-band services (up to 5 MHz). As the costs for a unit of symmetric pairs (pseudoquads) are approximately the same as those for star quads (double the number of pairs), the Deutsche Bundespost decided to use units of high-quality star quads in cables to be provided for digital and analog broad-band transmissions. At present, an 80 pair PCM cable is being manufactured. It consists of eight units of five star quads each (0.9-mm conductor). It allows the transmission of up to 12 000 PCM telephone channels in both directions. Further cable types with 20 and 40 pairs, possibly for the branching of PCM circuits, are planned.

V. RADIO ENGINEERING

A. Sound and Television Broadcasting

In the Federal Republic of Germany about 140 AM sound broadcasting transmitters are operated in the LF, MF, and HF ranges and about 280 FM transmitters in the VHF range. About 250 basic transmitters and about 3000 fill-in stations (transposers) are set up for television purposes. The adopted standards and systems are listed in the following table.

The sound broadcasting transmitters of the Länder broadcasting organizations operating in the MF and VHF ranges supply the population in the individual Länder with three different sound programs. The HF transmitters of the Deutsche Welle give a comprehensive picture of the political, cultural, and economic life in the Federal Republic of Germany to the listeners in overseas countries. The transmitters of the Deutschlandfunk complement the number of the programs offered in the neighboring countries and the Federal Republic itself. The present television networks allow the television programs of the ARD and the Zweites Deutsches Fernsehen to be received by more than 96 percent of the population including Berlin (West) and the regional third programs by almost 94 percent.

The frequency ranges available for the transmission of broadcasting programs are fully utilized by the existing and planned sound and television broadcasting transmitter networks. Since 1960 the Deutsche Bundespost has, therefore, investigated the possibility of a terrestrial broadcast coverage in the frequency range between 11.7 and 12.5 GHz, which was equally allocated to fixed, mobile, and broadcasting services at the Administrative Radio Conference held at Geneva in 1959. For this purpose, one experimental and one test network with four television transmitters and 100 down-converters have been established in Berlin (West). At the same time, studies are being made of the possibility of distributing further sound and television programs via satellite or cable.

Standards and systems in the Federal Republic of Germany are listed below:

1. Sound broadcasting

- a) MF and LF: double sideband AM; mainly 9-kHz channel spacing.
- b) VHF: FM; ± 75 -kHz frequency deviation; pre-emphasis 50 μ s; channel spacing 300 kHz. The more recent transmitters are suitable for stereophonic transmission according to the FCC standard (pilot tone).

2. Television broadcasting

- a) Bands I and III (VHF): standard B (vestigial sideband AM for picture, FM for sound); 625 lines, vision-to-sound carrier spacing 5.5 MHz, channel spacing 7 MHz.
- b) Bands IV/V (VHF): standard G; This standard and standard B differ only in the channel spacing, which here is 8 MHz.

B. Mobile Radio Services

At present, for manually operated networks—networks A1, A2, A3, and the network for the International Rhine

Radiotelephone Service—are provided for the public land mobile service in the Federal Republic of Germany. Another network, the so-called network B, which allows STD in both directions, is under construction and is to cover the total area of the Federal Republic of Germany by around 1975. At the beginning of 1974 a one-way radio service, the so-called European Paging Service, will be opened. A selective calling system (80) is used in the A networks. Like the A networks, network B has been set up in the 2-m range. Thirty-six duplex telephone channels with a 20-kHz spacing are available for this network. The mobile stations are called on a calling channel common to all radio traffic areas on which the station in the vehicle automatically returns after a conversation. An error-detecting pulse-code method is used for the selective call and the transmission of dialing information.

The establishment of a further network with 70 channels (network C) in the 450-MHz range is scheduled for 1977. The technique will differ only slightly from that used for network B, but at present considerations are being made as to whether large calling areas can be formed for selective calling to the vehicle. Furthermore, it is being investigated as to whether it is possible to set up extremely frequency-economical cellular networks where calls can be switched over to adjacent radio traffic areas.

The International Rhine Radiotelephone Service is a mobile VHF radiotelephone service for shipping on the Rhine and on some waterways of the Rhine basin. At this time, about 5300 national and foreign ship stations take part in this service. It is based on international arrangements reached in 1970 (Regional Agreement concerning the Radiotelephone Service for the Rhine).

In order to cope with the increasing volume of traffic in the Rhine Radiotelephone Service, the channel spacing will, up to 1983, be gradually decreased from 50 kHz to 25 kHz to obtain further channels.

The selective calling system recommended by the CCIR for use in the international maritime mobile radio service was introduced at the beginning of 1973. The CEPT is going to specify a suitable coding system for dialling purposes enabling the introduction of STD in this manual service.

The European Paging Service is an international public mobile one-way radio service, whose system parameters are laid down in CEPT Recommendation T/R 6. It offers the possibility of transmitting a limited number of code signals from a telephone station to a land mobile station. In the Federal Republic of Germany about 200 000 subscribers can take part in this service. If there is a sufficient increase in the number of subscribers, this service may later on be complemented by regional paging networks.

C. Radio-Relay Systems

The radio-relay network of the Federal Republic of Germany is closely meshed. The total length of all radio-relay links is about 78 500 km, about 45 190 km being

used for carrier systems and 33 310 km for television systems. Over a length of 14 460 km it is possible to transmit simultaneously the sound signal accompanying a television signal over the same radio-relay system. A total of 1870 transmitters and receivers are operated in the 401 radio stations. In the regional and supraregional long-distance networks the various radio-relay systems are used for the simultaneous transmission of 12, 120, 300, 900 (960), or 1800 telephone calls or of the television picture—mostly together with the accompanying sound signal.

1) Most of the equipment is operated in the supraregional long-distance network. At the repeater stations the signal coming from the receiver is through connected to the following transmitter at the IF level. Demodulation and renewed modulation are not required. This equipment, which is suitable for the transmission of 300 telephone calls or more, is operated in the frequency ranges around 2, 4, and 6 GHz.

2) In the regional long-distance network, equipment for the transmission of 120 telephone calls is operated in the 7-GHz range. In the repeater stations the signal is through connected in the baseband, i.e., it is demodulated and modulated again. Transmitter and modulator form a unit as do receiver and demodulator. The final stage of the transmitter is equipped with a klystron.

At present, most of the radio-relay equipment works with tubes. The equipment of system FM 300/2600 is the first being fully transistorized. They are of a standard design which allows the interchange of units made by different manufacturers. In system FM 1800-TV/6200 a traveling-wave tube is only used in the final transmitter stage.

The television outside broadcast radio-relay equipment FM TV/13000 R was put into operation just in time for the Olympic Games held in Munich. It is also fully transistorized and works in the 13-GHz range. The equipment of all new systems is of the standard design 7R mentioned in the previous sections.

Integrated circuits will to an increasing extent be used in future equipment. Due to advances made in the field of power transistors, it will be possible to produce equipment of low power input. Improvements are also being made with regard to the power input of equipment having a traveling-wave tube in the final transmitter stage. The efficiency of the modern traveling-wave tube of German make is between 35 and 40 percent. Owing to the decreased heat dissipation, the equipment dimensions are considerably smaller.

In the coming years, new equipment will be introduced for 2700-channel working in the 6-GHz range and for 1800-channel working or TV transmissions in the 11-GHz range. These developments will be based on the latest technological knowledge. To utilize the 15- and 20-GHz ranges, it is intended to start experimental digital transmissions in the near future. In the 15-GHz range trans-

missions will at first be made at a bit rate of 8.448 Mbit/s, corresponding to 120 telephone channels. Experimental transmissions at about 34 Mbit/s corresponding to 400 telephone channels are to follow. Moreover, it is investigated how the 20-GHz range can be utilized for the transmission of signals having a very broad bandwidth. A digital radio-relay system for transmissions at about 500 Mbit/s would allow more than 7500 telephone channels to be provided on one single RF channel.

D. Communication-Satellite Services

From the very beginning, the Deutsche Bundespost has taken an active part in the commercial utilization of communication satellites. Today, three antenna installations are operated at the Raisting earth station (Upper Bavaria) within the INTELSAT system. By means of these installations, which satisfy the INTELSAT standards (figure of merit $G/T = 40.7 \text{ dB/K}$), telephone and television communications are at present established with 19 countries within the regions of the Atlantic and Indian Oceans.

At this time, another antenna installation having a figure of merit $G/T = 31.5 \text{ dB/K}$ is under construction at Raisting for the Franco-German communication-satellite project SYMPHONIE. With this installation the Deutsche Bundespost is going to take part in the test program with the SYMPHONIE satellites; the main objective of these experiments is the testing of new transmission methods for communication-satellite services. The Deutsche Bundespost also participates in the design and construction of the SYMPHONIE satellites by sending experts to the project group formed by the administrations concerned. Studies on a transponder model are made in preparation for the future experimental use of the satellites in orbit.

Further studies and investigations deal with future satellite systems. Here, special mention should be made of the project of a European communication satellite which is planned by the ESRO in cooperation with the CEPT Administrations and the EBU. By means of this satellite system, which is intended to operate in the 11-14-GHz range, it will be possible to establish telephone and television communications between major European cities from about 1980. As far as the Federal Republic of Germany is concerned, future earth stations may be located at Frankfurt, and later on at Hamburg and Munich.

In addition, further studies are made on direct TV broadcasts from satellites in the 12-GHz range. For the area of the Federal Republic of Germany planning is based on a capacity of 3-5 television channels. Parabolic-reflector antennas having a diameter of about 75 cm are to serve for reception. Such a satellite system could be implemented by about 1980. Furthermore, the Deutsche Bundespost collaborates in preparatory work for a maritime satellite system and observes the development of further projects for application satellites.



Ronald Dingeldey was born in Alsbach/Bergstraße, Germany, in 1930. He received the diploma in electrical engineering from the Darmstadt Technical University, Darmstadt, Germany, in 1955. From 1959 to 1960 he was a student at the Physical Institute at the University of Hull, Hull, Yorks., England, as a scholar of the British Council.

In the years 1956 to 1957 he participated in the preparatory service of the Deutsche Bundespost at the Frankfurt Regional Directorate. Subsequently, he was employed for four years at the Fern-

meldetechnische Zentralamt, where he was involved in studies of velocity-modulated tubes. In 1961 he became Assistant Head of the section responsible for satellite communications at the FTZ and cooperated in the Raisting project. From 1964 to 1968 he was a member of the satellite communication section of the Federal Ministry of Posts and Telecommunications, where he made preparations for the first "INTELSAT agreement." His activities at the Ministry include the years between 1968 and 1972, during which time he was the Head of the section for telephone switching and terminal instruments. In 1973 he became President of the FTZ.

Mr. Dingeldey is a member of the German Electrical Engineers' Association and has been Assistant Chairman since 1973.

SOURCE OF FIGURES FOR APPENDIX C AND SUPPLEMENTS I AND II*

<u>Figure No.</u>	<u>Source (Bibliography No.)</u>	<u>Page(s) from Source</u>
C-1	30	2
C-2	16	58
C-3	16	66
C-4	8	2
C-5	20	10-11
C-6	11	Unpaged
C-7	12	68
C-8	12	70
C-9	12	76
I-1	19	47
I-2	19	65
I-3	19	48
I-4	19	55
I-5	22	5.5
I-6	22	7.11, 7.13, 8.2
I-7	22	6.8
II-1	15	63
II-2	2	117
II-3	2	118
II-4	2	118
II-5	2	119
II-6	19	71
II-7	19	72
II-8	22	4.3
II-9	19	90
II-10	24	116
II-11	23	38
II-12	23	60
II-13	23	107
II-14	23	120
II-15	24	79
II-16	22	10.22
II-17	22	10.23
II-18	22	10.24
II-19	22	10.25
II-20	22	10.18
II-21	22	10.19
II-22	22	10.20

*Figures have been borrowed freely from the sources indicated.

SOURCE OF FIGURES (Continued)

<u>Figure No.</u>	<u>Source (Bibliography No.)</u>	<u>Page(s) from Source</u>
II-23	22	10.21
II-24	22	10.14
II-25	22	10.15
II-27	22	10.16
II-28	22	10.17
II-29	19	84
II-30	19	83
II-31	24	139
II-32	24	141
II-33	24	143
II-34	24	144
II-35	19	85
II-36	19	108
II-37	19	109
II-38	18	79
II-39	19	224
II-40	19	111
II-41	19	273
II-42	19	275
II-43	19	277
II-44	19	98
II-45	19	80
II-46	19	81
II-47	19	255
II-48	19	256
II-49	19	260
II-50	19	260
II-51	19	99
II-52	19	100
	19	101

SOURCE OF TABLES FOR APPENDIX C AND SUPPLEMENTS I AND II*

<u>Table No.</u>	<u>Source (Bibliography No.)</u>	<u>Page(s) from Source</u>
C-1	27	25-38
C-2	N/A	N/A
C-3	28	41-49
C-4	N/A	N/A
C-5	13	3
C-6	13	4
C-7	13	3
C-8	13	2
C-9	13	2
C-10	N/A	N/A
I-1	14	8
II-1	18	74-75
II-2	19	201
II-3	19	91
II-4	19	272
II-5	19	271

*Tables have been borrowed freely from the sources indicated.

THIS PAGE INTENTIONALLY LEFT BLANK

BIBLIOGRAPHY FOR APPENDIX C AND SUPPLEMENTS I AND II

1. G. Bayraktar and H. Abut, "Present State and Future of Telecommunications in Turkey", IEEE Transactions on Communications. Vol. COM-24, No. 7, July, 1976, pp 684-86.
2. B.R. Bean, et al, A World Atlas of Atmospheric Radio Refractivity. ESSA Monograph 1, Washington, D.C.: U.S. Government Printing Office, 1966.
3. B.R. Bean and E.J. Dutton, Radio Meteorology. NBS Monograph 92, Boulder, Colorado: National Bureau of Standards, 1966.
4. R. Dingeldey, "Present State and Trends of Public Communications in the Federal Republic of Germany", IEEE Transactions on Communications. Vol. COM-22, No. 9, September, 1974, pp 1456-67.
5. H.T. Dougherty and E.J. Dutton, "Estimating Year-to-Year Variability of Rainfall for Microwave Applications", IEEE Transactions on Communications. Vol. COM-26, No. 8, August, 1978, pp 1321-24.
6. E.J. Dutton and H.T. Dougherty, "Year-to-Year Variability of Rainfall for Microwave Applications in the U.S.A.", IEEE Transactions on Communications. Vol. COM-27, No. 5, May, 1979, pp 829-32.
7. Engineering Considerations for Microwave Communications Systems. San Carlos, California: GTE Lenkurt Co., Inc., 1975.
8. "Germany, Federal Republic of", Department of State Background Notes. Washington, D.C.: U.S. Government Printing Office, May, 1977, pp 1-7.
9. "Germany, Federal Republic of", Encyclopedia Britannica. 968, Vol. 8, pp 44-63.
10. "Hawaii", Encyclopedia Britannica. 1968, Vol. 8, pp 673-78.
11. "Hawaii", World Scope Encyclopedia. 1950, Vol. 5, unpaged.
12. E. Joesting, Hawaii: An Uncommon History. New York: W.W. Norton and Co., Inc., 1972.
13. Local Climatological Data, Honolulu, Hawaii. Asheville, North Carolina: National Climatic Center, 1978.

14. A.G. Longley and P.L. Rice, Prediction of Tropospheric Radio Transmission Over Irregular Terrain, A Computer Method - 1968. ESSA Tech Report ERL 79-ITS 67, Boulder, Colorado: Institute for Telecommunication Sciences, 1968.
15. E.J. McCartney, Optics of the Atmosphere: Scattering by Molecules and Particles. New York: John Wiley and Sons, Inc., 1976.
16. R.F. Nyrop, et al, Area Handbook for the Republic of Turkey. DA PAM 550-80. Washington, D.C.: U.S. Government Printing Office, 1973.
17. D.E. Parker, Design Objectives for DCS LOS Digital Radio Links. DCEC EP 27-77, Reston, Virginia: DCEC, 1977.
18. "Propagation in Non-Ionized Media." CCIR XIIIth Plenary Assembly. Vol. V, Geneva, 1974. Geneva: ITU, 1975.
19. "Propagation in Non-Ionized Media". Reports and Recommendations of the CCIR, Vol. V, XIVth Plenary Assembly, Kyoto, 1978. Geneva: ITU, 1978.
20. Rees, Goronwy. The Rhine. New York: G.P. Putnam's Sons, 1967.
21. P.L. Rice and N.R. Holmberg, "Cumulative Time Statistics of Surface-Point Rainfall Rates", IEEE Transactions on Communications. Vol. COM-21, No. 10, October, 1973, pp 1131-36.
22. P.L. Rice, and N.R. Holmberg, "Cumulative Time Statistics of Surface-Point Rainfall Rates", IEEE Transactions on Communications. Vol. COM-21, No. 10, October, 1973, pp 1131-36.
23. C.A. Samson, Refractivity Gradients in the Northern Hemisphere. OT Report 75-59, Washington, D.C.: U.S. Department of Commerce, 1975.
24. C.A. Samson, Refractivity Gradients in the Northern Hemisphere. OT Report 76-05, Washington, D.C.: U.S. Department of Commerce, 1975.
25. M.R. Shackleton, Europe: A Regional Geography. New York: Fredrick A. Praeger, Inc., 1965.
26. V. Showers, World Facts and Figures. New York: John Wiley and Sons, Inc., 1979.

27. Tables of Temperature, Relative Humidity and Precipitation for the World. M.O. 617e, London: Her Majesty's Stationary Office, 1958, pp 25-28.
28. Tables of Temperature, Relative Humidity and Precipitation for the World. London: Her Majesty's Stationary Office, 1972, pp 41-49.
29. G.T. Trewartha, An Introduction to Climate. New York: McGraw Hill Inc., 1968.
30. "Turkey", Department of State Background Notes. Washington, D.C.: U.S. Government Printing Office, January, 1976, pp 1-7.
31. "Turkey", World Scope Encyclopedia. 1950, Vol. 11, unpaged.
32. N.C. Walpole, et al, U.S. Army Area Handbook for Germany. DA PAM 550-29. Washington, D.C.: U.S. Government Printing Office, 1964.

THIS PAGE INTENTIONALLY LEFT BLANK

END